Cooperative Research Centre for Viticulture

Australian Government
Grape and Wine Research and Development Corporation

Mechanism of powdery mildew infection in grapevines



FINAL REPORT to

GRAPE AND WINE RESEARCH & DEVELOPMENT CORPORATION

Project Number: **CRV 02/07N**

Principal Investigator: **Dr Ian B. Dry**

Research Organisation: Cooperative Research Centre for Viticulture

Date: **29th June 2006**

Project Title:	Mechanism of powdery mildew infection in grapevines
CRCV Project Number:	3.1.5
Period Report Covers:	July 2002 – June 2006
Author Details:	Dr Ian Dry CSIRO Plant Industry
Postal address:	PO Box 350, Glen Osmond, SA 5064, Australia Phone: 08 83038632 Fax: 08 83038601 Mobile: Email: ian.dry@csiro.au
Date report completed:	June 2006
Publisher: ISBN OR ISSN:	Cooperative Research Centre for Viticulture

Copyright:
© Copyright in the content of this guide is owned by the Cooperative Research Centre for Viticulture.

Disclaimer:
The information contained in this report is a guide only. It is not intended to be comprehensive, nor does it constitute advice. The Cooperative Research Centre for Viticulture accepts no responsibility for the consequences of the use of this information. You should seek expert advice in order to determine whether application of any of the information provided in this guide would be useful in your circumstances.

The Cooperative Research Centre for Viticulture is a joint venture between the following core participants, working with a wide range of supporting participants.

Table of Contents

Abstract …….… 2

Executive summary ……....…. 3

Copy of Matt Hayes PhD thesis

Appendix 1: Communication

Appendix 2: Intellectual Property

Appendix 3: References

Appendix 4: Staff

Appendix 5: Publications

Appendix 6: Budget reconciliation

Abstract

This study has provided new insights into the molecular and biochemical processes associated with the powdery mildew:grapevine interaction. Our results indicate that powdery mildew infection of grapevine epidermal cells leads to the modification of specific host genes involved in carbohydrate metabolism and transport which results in increased supply of hexoses to the pathogen to support growth and development. It is not known if these changes in host gene expression are manipulated directly by the invading pathogen or are a consequence of fungal colonisation. However, there is good evidence to indicate that the plant hormone ABA has an important role in regulating these changes in host gene expression. Potentially, modification of the expression of host genes associated with carbohydrate metabolism could provide an alternative way to engineer resistance to this pathogen in grapevine.

Executive summary

Powdery mildew is the most economically important grapevine disease worldwide. Complete crop loss occurs in vineyards of unsprayed highly susceptible cultivars and frequent yield losses of 20% or more occur where fungicides are applied after the disease is well established. The effect of fungal infection of the fruit causes significant losses to both the wine and table grapes industries. Costs of disease management and yield losses in Australia are estimated at 5% the value of total grape production. Current control of the disease can only be achieved by the use of fungicides. However, powdery mildew strains resistant to DMI fungicides have recently been reported and there is world-wide pressure to reduce the use of "hard" chemicals to control plant pathogens on crops grown for human consumption. These problems could be overcome by the development of grapevine cultivars with enhanced resistance to powdery mildew.

The major focus of our CRCV research on powdery mildew resistance genes is targeted towards the isolation of resistance genes from the American grape *Muscadinia rotundifolia* (CRCV Project 3.1.1). While our research indicates that the *Run*1 gene confers complete resistance to powdery mildew isolates present in France and Australia, there can be no guarantee that new powdery mildew isolates, which are able to overcome the *Run*1 resistance, may not arise by natural mutation in the field or through accidental importation into this country. This is especially pertinent when one considers the length of time that individual vines are expected to remain in the field. Thus, the current approach of most research programs involved in developing disease resistant crops is to “pyramid” multiple resistance genes or strategies within the one plant as it is extremely unlikely that a single mutation in the pathogen would be able to overcome two different resistance mechanisms simultaneously. The aim of this project, therefore, was to provide us with a better understanding of the biochemical and genetic basis of the powdery mildew: grapevine interaction with the aim of devising alternative resistance strategies which will act in combination with the *Run*1 gene to provide long term resistance in the field.

Grapevine powdery mildew, caused by *Erysiphe necator*, is a biotrophic pathogen that forms a stable association with host cells without directly causing cell death, and take up nutrients such as sugars, amino acids etc from host epidermal cells via a feeding structure called a haustorium. There is evidence from research on other biotrophic fungal pathogens, such as rust, to suggest that pathogen infection results in changes in the expression of host genes involved in nutrient supply and transport which increases the availability of nutrients to, and hence, growth of the pathogen. It is not known if these changes in host gene expression are manipulated directly by the invading pathogen or are a consequence of fungal colonisation. This project set out to investigate whether similar processes are operating in the powdery mildew: grapevine interaction.

To identify host genes that may mediate nutrient delivery to powdery mildew infected tissues and therefore may contribute to disease susceptibility, a candidate gene approach using degenerate and RT-PCR, and a non-targeted approach using microarray analysis was instigated. In addition to genes encoding pathogenesis and stress-related proteins, microarray analysis revealed that transcript levels of a putative metal transporter and a cell wall structural protein were elevated in infected berry skin, while aquaporin water channels and genes associated with photosynthesis were generally repressed. Degenerate PCR was used to isolated new cell wall invertase, monosaccharide and amino acid transporter genes and initial RT-PCR revealed that expression of genes involved in sugar mobilisation were the most significantly modulated by powdery mildew infection.

Previously unreported hexose transporters (HTs), (*VvHT3*, *VvHT4* and *VvHT5*) and a cwINV (*VvcwINV*) were isolated from cDNA prepared from powdery mildew infected grapevine leaves. Full length clones of grapevine HTs and cwINV were obtained by RACE PCR. Heterologous expression of the three new HTs in yeast confirmed that VvHT4 and VvHT5 mediated glucose uptake, while VvHT3 did not function in the yeast system. However, transient expression of a

translational fusion of the VvHT3 protein with green florescence protein in onion epidermal cells indicated that it is targeted to the plasma membrane of plant cells.

Quantitative RT- PCR analysis of these new genes, together with previously reported grapevine HTs and cytoplasmic and vacuolar invertases, indicated that expression of *VvcwINV* and *VvHT5*, were significantly up-regulated by PM infection, while a vacuolar invertase was strongly down-regulated by PM infection. Invertase activity assays were in agreement with these findings, showing elevated sucrolytic activity in insoluble fractions and reduced sucrolytic activity in soluble fractions. These results suggest that apoplasmic phloem unloading of sucrose in the infected leaf is elevated and that *VvHT5* is induced to recover the additional hexoses from the apoplasm. Basic localisation studies indicated that *VvHT5* and *VvcwINV* are not induced specifically in powdery mildew infected leaf regions, but are induced in a more diffuse distribution within infected leaves. To determine if induction of *VvHT5* and *VvcwINV* is specific to PM infection or if other stimuli may also mediate these responses, leaves were inoculated with downy mildew or stressed by wounding. Transcript levels of *VvHT5* and *VvcwINV* were elevated by wounding and downy mildew infection, suggesting that the induction of these genes may be part of a general stress response.

To explore the signalling pathways that may underlie these responses, leaves were treated with the plant growth regulators ethylene, jasmonate and abscisic acid. Exogenous application of ethylene and methyl jasmonate only marginally affected the expression of the genes studied, however foliar application of abscisic acid (ABA) induced gene expression changes similar to those observed in response to powdery mildew infection and wounding. Promoter sequences of *VvHT3*, *VvHT4*, *VvHT5* and *VvcwINV* were isolated and analysed for the presence of regulatory elements. Compared with the promoters of VvHTs that were not induced by pathogen infection or wounding, the *VvHT5* and *VvcwINV* promoters contained numerous motifs associated with induction by ABA including ABRE, Myc and Myb binding elements.

The path of sugar loading into the mesocarp of grape berries during ripening is still poorly understood and few molecular components associated with this process have been described. Quantitative RT-PCR was used to monitor the expression of five HTs and *VvcwINV* during Cabernet sauvignon and Shiraz berry development and ripening. Of the three new HTs reported here, the expression of *VvHT3* is most consistent with a potential role in sugar loading, while *VvHT5* is induced late in this process. *VvcwINV* transcript levels were high pre-ripening and also during the later stages of ripening, therefore based on this expression pattern, a role for this enzyme during ripening is not clearly evident. These results are discussed in terms of an apoplasmic step in phloem unloading in ripening grape berries.

This study has provided new insights into the molecular and biochemical processes associated with the formation of carbohydrate sink metabolism in response to stress stimuli, and sugar delivery to grape berries during ripening. ABA-dependant pathways may mediate the stress-associated induction of *VvcwINV* and *VvHT5*, presumably to recruit additional carbohydrates to the affected organ to energise repair and defence responses. At this stage it is unknown if this response is beneficial to pathogen nutrition, however potentially, modification of host genes associated with carbohydrate sink metabolism could provide an alternative way to engineer resistance to this pathogen in grapevine.

This project was supported by the Commonwealth Cooperative Research Centres Program and conducted by the CRC for Viticulture (CRCV). Australian grapegrowers and winemakers are key stakeholders in the CRCV, contributing levies matched by the Commonwealth Government and invested by the Grape and Wine Research and Development Corporation in the Centre.The project was financially supported by the GWRDC, CRCV and CSIRO Plant Industry

Identification of host genes involved in the biotrophic interaction between grapevine and powdery mildew

by

Matthew Allan Hayes
B. Biological Science (Hons.), LaTrobe University

A thesis submitted for the degree of Doctor of Philosophy

at

The University of Adelaide,
School of Agriculture and Wine,
Discipline of Horticulture, Viticulture and Oenology

in collaboration with

CSIRO Plant Industry,
Horticulture Unit

Urrbrae, Adelaide,
January, 2006

Table of contents

Abstract ..... *VI*

Declaration ..... *IX*

Acknowledgements ..... *X*

Abbreviations ..... *XII*

Chapter 1 – General introduction *1*

1.1 Infection process of powdery mildew fungi **3**

1.2 Haustorium structure and function **5**

1.3 Host responses: compatibility and defence **10**

1.4 Host responses: amino acids and carbohydrates **13**

1.5 Carbohydrate distribution in plants **16**

1.6 Pathogen associated changes to host invertase activity **18**

1.7 Induction of sink metabolism in response to pathogens and wounding **18**

1.8 Role of plant growth regulators in biotrophic interactions **20**

1.9 Other signals in biotrophic interactions **23**

1.10 Identification of host susceptibility genes **24**

1.11 Aims of this study **26**

Chapter 2 – General Materials and Methods *28*

2.1 Materials **28**

2.1.1 Solutions, chemicals and growth media 28

2.1.2 Oligodeoxyribonucleotide primers 29

2.1.3 Bacterial and yeast strains 31

2.1.4 Grapevine tissue 32

2.1.5 *Erysiphe necator* culture and maintenance 32

2.1.6 *Plasmopara viticola* culture and maintenance 33

2.2 Methods **33**

2.2.1 Polymerase chain reaction (PCR) 34

2.2.2 Agarose gel electrophoresis 34

2.2.3 Purification of DNA from agarose gel slices 35

2.2.4 Dephosphorylation of DNA 5' termini 35

2.2.5 Purification of DNA samples following enzymatic reactions 35

2.2.6 DNA ligation 35

2.2.7 Preparation of electro-competent E. coli cells 36

2.2.8 Transformation of bacteria with recombinant plasmids 36

2.2.9 Preparation of plasmid DNA 37

2.2.10 Preparation of bacterial glycerol stocks 37

2.2.11 Preparation of DNA samples for sequencing 38

2.2.12 Preparation of total grape RNA 38

2.2.13 First-strand cDNA synthesis 39

2.2.14 Sequence analysis and manipulation 39

Chapter 3 – Isolation and identification of genes differentially expressed in powdery mildew infected grapevine tissues 35

3.1 Introduction 35

3.2 Materials and methods 36
3.2.1 Microarray analysis of powdery mildew infected berry skin 36
3.2.2 Degenerate PCR, analysis and cloning 38
3.2.3 RT-PCR analysis of selected genes in powdery mildew infected grapevine leaves 39

3.3 Results 40
3.3.1 Microarray analysis of powdery mildew infected grape berry skin 40
3.3.2 Isolation of partial length grape hexose transporter clones from powdery mildew infected leaves 43
3.3.3 Isolation of a partial length grape cell wall invertase clone from powdery mildew infected leaves 45
3.3.4 Isolation of partial length grape amino acid permease and proline transporter clones from powdery mildew infected leaves 47
3.3.5 Semi-quantitative RT-PCR analysis of selected genes in powdery mildew infected leaves 50

3.4 Discussion 52
3.4.1 Microarray analysis of powdery mildew infected berry skins 53
3.4.2 Isolation of HT, cwINV, AAP and ProT transcripts by degenerate PCR 56
3.4.3 Semi-quantitative RT-PCR analysis of selected genes in powdery mildew infected leaves 58

Chapter 4 - Isolation and functional characterisation of full length hexose transporter and cell wall invertase genes from grapevine 61

4.1 Introduction 61

4.2 Materials and methods 62
4.2.1 RACE PCR and amplification of full length cDNAs 62
4.2.2 Preparation of DNA constructs for functional characterisation of HTs in yeast 64
4.2.3 Lithium acetate yeast transformation 64
4.2.4 Functional characterisation of HTs in yeast 65
4.2.5 Analysis of GFP-fusion proteins by micro-projectile bombardment 66
4.2.6 Sequence analysis and manipulation 67

4.3 Results 68
4.3.1 Analysis of full length VvHT sequences 68
4.3.2 Functional characterisation of VvHT1, VvHT3, VvHT4 and VvHT5 in yeast 74
4.3.3 Subcellular localization of VvHT3 and VvHT4 proteins 78
4.3.4 Analysis of full length *VvcwINV* 80

4.4 Discussion 84
4.4.1 Isolation of full length *VvHT* cDNAs and functional characterisation 84
4.4.2 Isolation of a full length *VvcwINV* cDNA and bioinformatic analysis 88

Chapter 5 - Quantitative RT-PCR analysis of sugar transporters and invertases in pathogen infected and wounded grapevine tissues 90

5.1 Introduction 90

5.2 Materials and methods 92
5.2.1 *E. necator* (powdery mildew) inoculation 92
5.2.2 Powdery mildew infected and uninfected leaf regions 93
5.2.3 *Plasmopara viticola* (downy mildew) inoculation 93
5.2.4 Wounding of leaves 93
5.2.5 RNA extraction, DNase treatment and cDNA synthesis 94
5.2.6 Quantitative real-time PCR analysis 94
5.2.7 Measurement of invertase enzyme activity 95

5.3 Results **96**
5.3.1 Quantitative RT-PCR analysis of hexose and sucrose transporter expression in powdery mildew infected grapevine tissues 97
5.3.2 Quantitative RT-PCR analysis of invertase expression in powdery mildew infected grapevine tissues 100
5.3.3 Effect of powdery mildew infection on grape leaf acid invertase activity 102
5.3.4 Localisation of VvHT and invertase expression relative to powdery mildew infection sites 103
5.3.5 Changes in expression of VvHTs, SUCTs and invertases in downy mildew infected grape leaves detected by quantitative RT-PCR 104
5.3.6 Effect of wounding on VvHT and invertase expression in grape leaves 106

5.4 Discussion **108**
5.4.1 Powdery mildew infection 109
5.4.2 Specificity of powdery mildew induced transcriptional changes 112
5.4.3 Differential regulation of gene expression in response to powdery and downy mildew infection 114

Chapter 6 – Expression analysis of VvHTs and VvcwINV in grapevine carbohydrate sink tissues *117*

6.1 Introduction **117**

6.2 Materials and methods **118**
6.2.1 Grape berry ripening series 118
6.2.2 Grapevine roots 119
6.2.3 Quantitative RT-PCR analysis 119

6.3 Results **120**
6.3.1 Expression of VvHTs and *VvcwINV* in grape roots 120
6.3.2 Expression of VvHTs and *VvcwINV* during berry ripening 120

6.4 Discussion **123**
6.4.1 Expression of VvHTs and *VvcwINV* in grapevine carbohydrate sink tissues during normal growth and development 123
6.4.2 Role of *VvHT*s and *VvcwINV* in grape berry development 125

Chapter 7 - Hormonal regulation and analysis of promoters of VvHT and invertase genes *130*

7.1 Introduction **130**

7.2 Materials and Methods **131**
7.2.1 Exogenous application of ABA, ethylene and methyl jasmonate 131
7.2.2 Isolation of BAC DNA and direct sequencing 132
7.2.3 Promoter analysis 133
7.2.4 Quantitative RT-PCR analysis of ABA biosynthetic genes 133
7.2.5 Measurement of bulk leaf ABA concentration 134

7.3 Results **134**
7.3.1 Expression of VvHTs and invertases in grapevine leaves exogenously supplied with ethylene and methyl jasmonate 134
7.3.2 Expression of VvHTs and invertases in grapevine leaves exogenously supplied with ABA 135
7.3.3 Promoter analysis 137
7.3.4 Induction of ABA biosynthetic genes in mildew infected and wounded grapevine leaves 140
7.3.5 ABA concentration in powdery mildew infected grapevine leaves 143

7.4 Discussion **145**

Chapter 8 – Summary and concluding remarks *151*

Reference list *156*

Appendix 1- sequences isolated during this project *173*
Appendix 2- Expression of control genes *180*
Appendix 3- List of cDNAs on grape berry Microarray *184*

Abstract

Grapevine powdery mildew is caused by *Erysiphe necator*, an Ascomycete fungus and an obligate biotroph restricted to growth on its grapevine host. Biotrophic pathogens form a stable association with host cells without directly causing cell death, and take up nutrients from, in the case of powdery mildew (PM), host epidermal cells (Rumbolz et al., 2000). As the fungus grows, its increasing biomass becomes a strong nutrient sink capable of altering assimilate flow and storage in the host.

To identify host genes that may mediate nutrient delivery to powdery mildew infected tissues and therefore may contribute to disease susceptibility, a candidate gene approach using degenerate and RT-PCR, and a non-targeted approach using microarray analysis was instigated. Once identified, "susceptibility genes" could be targeted for manipulation to provide alternative resistance strategies based on reduced susceptibility in the future. In addition to genes encoding pathogenesis and stress related proteins, microarray analysis revealed that transcript levels of a putative metal transporter and a cell wall structural protein were elevated in infected berry skin, while aquaporin water channels and genes associated with photosynthesis were generally repressed. Degenerate PCR was used to isolated new cell wall invertase, monosaccharide and amino acid transporter genes and initial RT-PCR revealed that expression of genes involved in sugar mobilisation were the most significantly modulated by powdery mildew infection.

Previously unreported hexose transporters (HTs), (*VvHT3*, *VvHT4* and *VvHT5*) and a cwINV (*VvcwINV*) had been isolated from cDNA prepared from powdery mildew infected grapevine leaves. Full length clones of grapevine HTs and cwINV were obtained by RACE PCR. Heterologous expression of the three new

HTs in yeast confirmed that VvHT4 and VvHT5 mediated glucose uptake, while VvHT3 did not function in the yeast system. However, transient expression of a translational fusion of the VvHT3 protein with green florescence protein in onion epidermal cells indicated that it is targeted to the plasma membrane of plant cells.

Quantitative RT- PCR analysis of these new genes, together with previously reported grapevine HTs and cytoplasmic and vacuolar invertases, indicated that expression of *VvcwINV* and *VvHT5*, were significantly up-regulated by PM infection, while a vacuolar invertase was strongly down-regulated by PM infection. Invertase activity assays were in agreement with these findings, showing elevated sucrolytic activity in insoluble fractions and reduced sucrolytic activity in soluble fractions. These results suggest that apoplasmic phloem unloading of sucrose in the infected leaf is elevated and that *VvHT5* is induced to recover the additional hexoses from the apoplasm. Basic localisation studies indicated that *VvHT5* and *VvcwINV* are not induced specifically in powdery mildew infected leaf regions, but are induced in a more diffuse distribution within infected leaves.

To determine if induction of *VvHT5* and *VvcwINV* is specific to PM infection or if other stimuli may also mediate these responses, leaves were inoculated with downy mildew or stressed by wounding. Transcript levels of *VvHT5* and *VvcwINV* were elevated by wounding and downy mildew infection, suggesting that the induction of these genes may be part of a general stress response.

To explore the signalling pathways that may underlie these responses, leaves were treated with the plant growth regulators ethylene, jasmonate and abscisic acid. Exogenous application of ethylene and methyl jasmonate only marginally affected the expression of the genes studied, however foliar application of abscisic acid (ABA) induced gene expression changes similar to those observed in response to powdery mildew infection and wounding. Promoter sequences of *VvHT3*, *VvHT4*,

VvHT5 and *VvcwINV* were isolated and analysed for the presence of regulatory elements. Compared with the promoters of VvHTs that were not induced by pathogen infection or wounding, the *VvHT5* and *VvcwINV* promoters contained numerous motifs associated with induction by ABA including ABRE, Myc and Myb binding elements.

The path of sugar loading into the mesocarp of grape berries during ripening is still poorly understood and few molecular components associated with this process have been described. Quantitative RT-PCR was used to monitor the expression of five HTs and *VvcwINV* during Cabernet sauvignon and Shiraz berry development and ripening. Of the three new HTs reported here, the expression of *VvHT3* is most consistent with a potential role in sugar loading, while *VvHT5* is induced late in this process. *VvcwINV* transcript levels were high pre-ripening and also during the later stages of ripening, therefore based on this expression pattern, a role for this enzyme during ripening is not clearly evident. These results are discussed in terms of an apoplasmic step in phloem unloading in ripening grape berries.

This study has provided new insights into the molecular and biochemical processes associated with the formation of carbohydrate sink metabolism in response to stress stimuli, and sugar delivery to grape berries during ripening. ABA-dependant pathways may mediate the stress-associated induction of *VvcwINV* and *VvHT5*, presumably to recruit additional carbohydrates to the affected organ to energise repair and defence responses. At this stage it is unknown if this response is beneficial to pathogen nutrition, however potentially, modification of genes associated with carbohydrate sink metabolism could provide an alternative way to engineer resistance to this pathogen.

Declaration

This work contains no material that has been accepted for the award of any other degree or diploma in any university or other tertiary institution and to the best of my knowledge and belief, contains no material previously published or written by another person, except where due reference has been made in the text.

I give consent to this copy of my thesis, when deposited in the University Library, being available for loan and photocopying.

Matthew Hayes

January 2006

Acknowledgements

I would first like to acknowledge the late Robyn Van Heeswijck who convinced me through her enthusiasm, intelligence and warmth to move to Adelaide and commence study under her guidance. Unfortunately, after a short period of time, Robyn needed to focus on her health and was unable to continue as my supervisor, however, in the generous and composed fashion that was typical of all interaction I had with Robyn, she identified potential supervisors and continued to take an interest in my studies until her passing. Thank you Robyn, I will always be grateful for the brief time our paths crossed and wish you peace and happiness.

Due to Robyn's' advice, I was amazingly fortunate to meet Ian Dry who quickly accepted the responsibility to become my supervisor and provided me with a stimulating project. I cannot thank Ian enough for the enthusiasm, dedication and unbounded support that he has given to me during the last 3.5 years. He has been the best supervisor imaginable and has become a friend for whom I care and respect deeply. I also thank my co-supervisor, Steve Tyerman, for always taking time to discuss my work and providing physiological insights that are sometimes lacking in gene-jockey's like me.

Thanks to Claire Barker, Karina Swan and Dale Godfrey, who compose the Fungal pathology group at CSIRO in Adelaide. Claire allowed me access to and provided pertinent advice regarding working with the genomic BAC library. Karina managed to keep the powdery mildew inoculum available whenever needed and organised almost everything around the lab that myself and other staff were too busy (read lazy) to do. Many thanks to Dale who taught me how to wrestle RNA out of grapevine tissue, along with other techniques, and with whom I collaborated to perform the GFP studies and hormonal treatments. More broadly, I would like to

thank all the staff at CSIRO Plant Industry in Adelaide for being very generous with their time and resources. Specifically I would like to mention Chris Davies who donated Cabernet Sauvignon berry cDNA samples and always found time for a chat or to read drafts. Also, thanks to the administrative staff for all their efforts, especially Julie Powell who did everything in her powder to ensure I had the components necessary for my work.

I am grateful to the University of Adelaide for awarding me an Australian Post Graduate Award and the Cooperative Research Centre for Viticulture (CRCV) for providing a top-up scholarship and a generous operating budget. Peter Mansfield from the CRCV was particularly generous with his time.

I thank my family, particularly Mum and Dad, for always supporting my decisions and providing love and the financial means that have allowed me to become who I am today. Thanks to friends around Adelaide and back in Melbourne, for happy distractions and life beyond the laboratory.

Finally I want to thank my wonderful partner Rebecca Burtt who has suffered life as a PhD widow, particularly during the last 6 months, and who has shown boundless love, support and understanding during our 5 years together. I could not have done this without Rebecca and am humbled by her devotion to me.

Abbreviations

ATP	adenosine triphosphate
ATPase	adenosine triphosphatase
BLAST	basic local alignment search tool
bp	base pairs
cDNA	complementary DNA
cwINV	cell wall invertase
DNA	deoxyribonucleic acid
dNTP	deoxynucleotide triphosphate
DPI	days post-inoculation
dsDNA	double-stranded DNA
EDTA	ethylenediamine-*tetra*-acetic acid
ER	endoplasmic reticulum
EST	expressed sequence tag
FD	Faraday(s)
FW	fresh weight
g	gram(s)
g	relative centrifugal force
GFP	green fluorescent protein
h	hour(s)
HT	Hexose (monosaccharide) transporter
IPTG	*Iso*-propyl-β-D-thiogalactopyranoside
kb	kilobase pairs
L	litre(s)

LB	Luria broth
M	molar
min	minute(s)
MOPS	3-N-Morpholinopropanesulfonic acid
mRNA	messenger RNA
MPa	Mega Pascals
nINV	neutral (cytoplasmic) invertase
nt	nucleotide(s)
ORF	open reading frame
PCR	polymerase chain reaction
PM	powdery mildew
RACE	rapid amplification of cDNA ends
RNA	ribonucleic acid
rpm	revolutions per minute
RT-PCR	reverse transcription-PCR
s	second(s)
Ssynth	Sucrose synthase
SUCT	sucrose transporter
SDS	sodium dodecyl sulphate
TBE	tris-borate-EDTA
Tm	temperature of DNA disassociation (melt)
Tris	tris(hydroxymethyl)aminomethane
V	volt(s)
vINV	vacuolar invertase

Chapter 1 – General introduction

Powdery mildew is a costly and widespread fungal disease to which all commercially important European cultivars of *Vitis vinifera* are susceptible. The viticultural industry is highly dependant on the use of fungicides to manage powdery mildew. A recent report commissioned by the European Union indicated that while grapevine plantings comprised only 8% of the total crop production area in member states, grapevine cultivation accounted for approximately 70% of the total fungicide volume applied to all crops (Montgomery and Hansen, 2000). Without the use of fungicides, and particularly in mild weather conditions that favour growth of the pathogen, outright crop loss can occur (Savocchia et al., 2004).

The most heavily used fungicides in Australia are sulphur and the sterol demethylation inhibiting fungicides (DMIs). Sulphur has been in use for more than 100 years and continues to be generally effective for powdery mildew control. DMIs were first introduced in the 1970's and initially offered excellent control. However, pathogen resistance to DMIs is now widespread in North America (Erickson and Wilcox, 1997) and powdery mildew strains with reduced sensitivity to DMIs have been isolated from Australian vineyards, indicating the development of resistance to these chemicals in Australia also (Savocchia et al., 2004).

The most commonly observed symptom of powdery mildew disease is powdery white to ash-grey growth on leaf surfaces (Fig. 1.1 A). Leaf infections cause a generalised reduction in vine vigour and are a major source of inoculum for infection of young fruit, which is responsible for most of the economic losses. Uneven maturation and cracking of the fruit results in fruit rot (Ough and Berg, 1979; Fig. 1.1B). Even low levels of fruit infection reduces the quality of the final

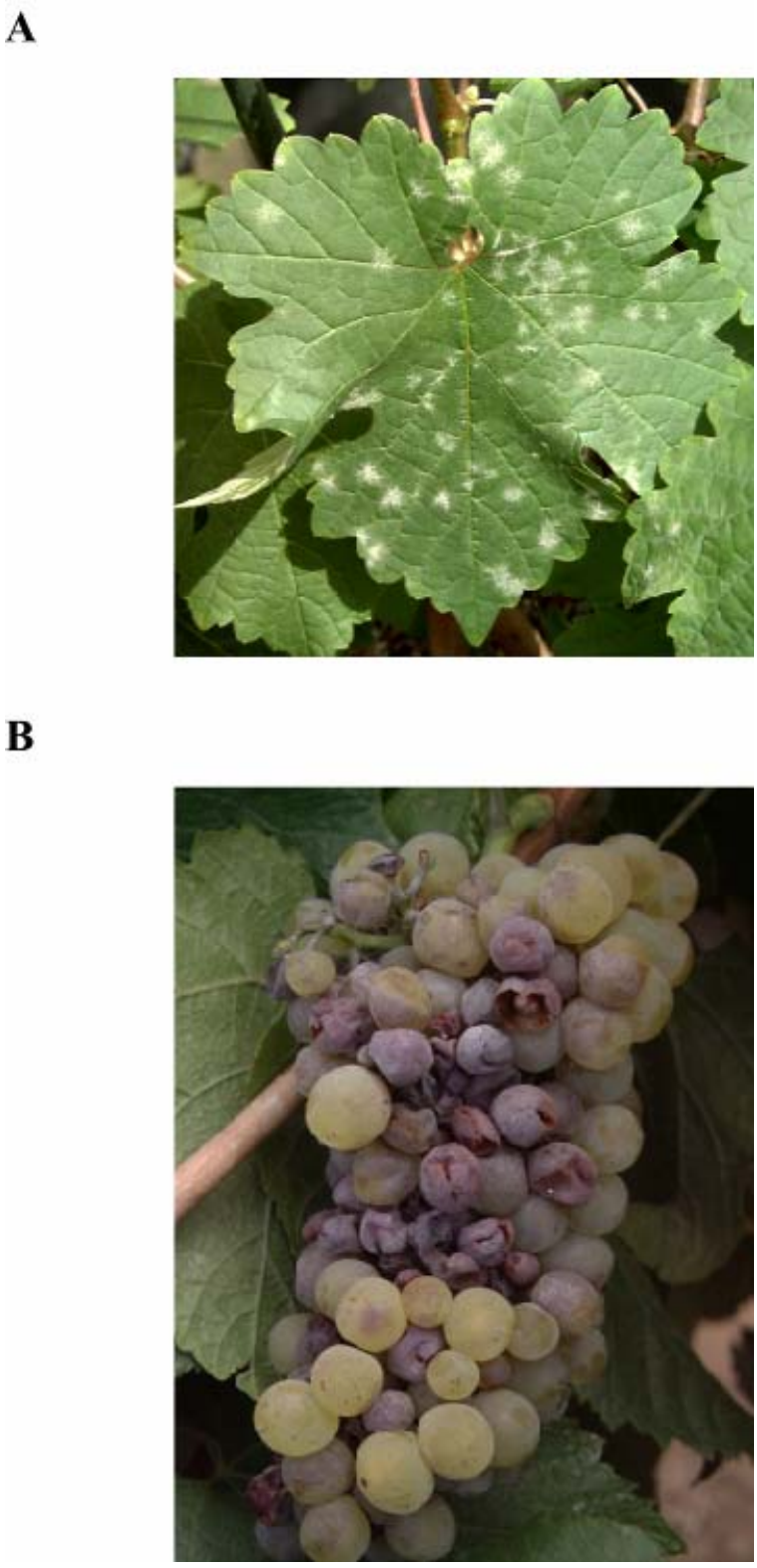


Figure 1.1. Powdery mildew infected grapevine tissues

(A) Powdery mildew colonies on the adaxial surface of an infected *V. vinifera* cv. Cabernet Sauvignon leaf. (B) Mature *V. vinifera* cv. Chardonnay bunch showing damage caused by early season powdery mildew infection

wine product by introducing negative sensory characteristics such as unpalatable flavours and aromas and an unpleasant mouth-feel (Ough and Berg, 1979; Stummer et al., 2005).

The causative agent of grapevine powdery mildew, *Erysiphe necator* (syn. *Uncinula necator*), is an Ascomycete fungus and an obligate biotroph restricted to growth on grapevine. Unlike necrotrophic pathogens such as *Botrytis cinerea* which degrade plant cells and absorb nutrients from dead tissue, biotrophic pathogens associate with host cells without directly causing host cell death and obtain all their nutrients in this manner (Rumbolz et al., 2000). Nutrient transfer from host to fungus is facilitated by the haustorium, a specialised feeding structure that develops only during plant-pathogen interaction and is formed from both fungal and host components (Rumbolz et al., 2000; Hahn and Mendgen, 2001).

1.1 Infection process of powdery mildew fungi

The infection process typical of *E. necator* is illustrated in Figures 1.2 and 1.3. Conidia are dispersed by wind or physical contact between infected and healthy plant parts. A conidium attaches to the surface of a plant tissue where it germinates and extends a primary hyphae (Fig. 1.2. A and B; Fig. 1.3. A). The primary hyphae differentiates into a lobed structure called an appressorium (Fig. 1.2 B; Fig. 1.3 B) which, via the generation of turgor pressure and enzymes that digest the cuticle and cell wall barrier, forces a penetration peg through the surface cuticle and the cell wall of the epidermal cell below. Appressoria of the wheat powdery mildew pathogen *Blumeria graminis* developes tugor pressure between 2.1 to 4.1 MPa, while appressoria of *Magnaporthe grisea* produced turgor pressure that reached eight MPa (Howard *et al*., 1991; Pryce-Jones et al., 1999). Various hydrolytic

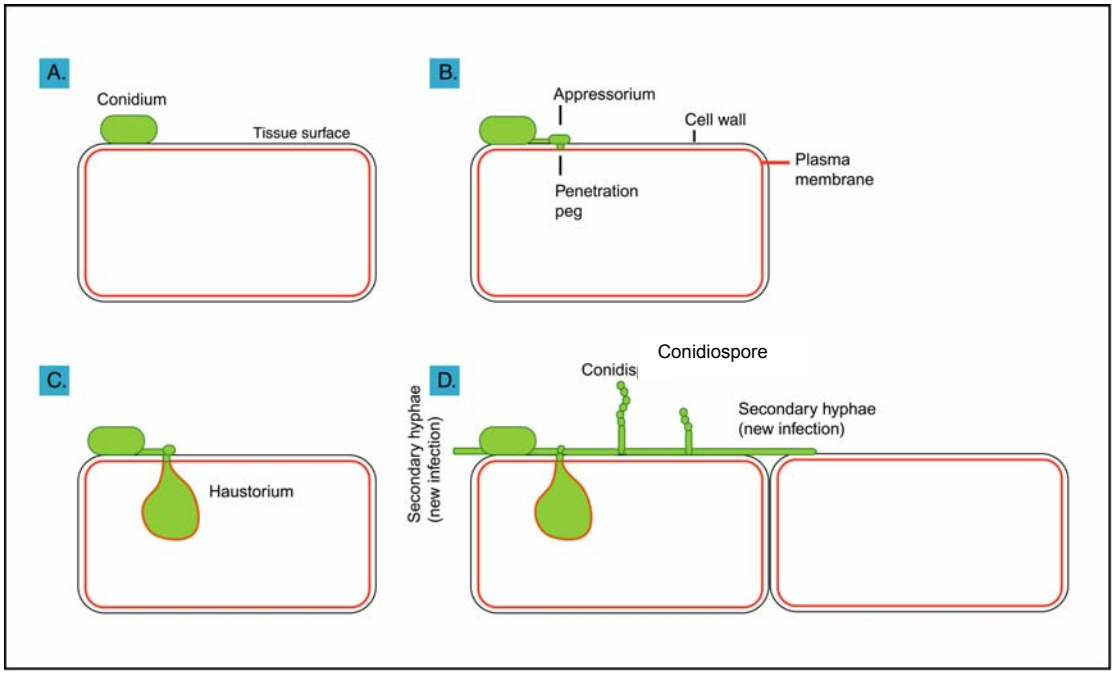


Figure 1.2. Stylised diagram of the grapevine powdery mildew infection process. For details refer to text.

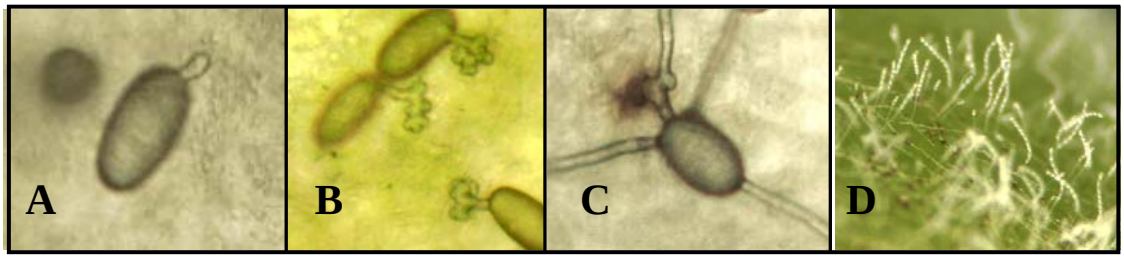


Figure 1.3. Infection structures of *E. necator* growing on *V. vinifera* leaves Cv. Chardonnay. (A): germination and hyphae extension; (B): appressorium formation; (C): secondary hyphae extension; (D): conidiophores on leaf surface. A, B, C: 40x magnification, D: 10x magnification.

enzymes have been detected in association with germinated *B. graminis* condia including esterase, protease and amylase while immunofluorescence microscopy localised cellulose enzymes to appressoria of *Trichoderma reesei* (Fric and Wolf, 1994; Pryce-Jones et al., 1999). After cuticle and cell wall penetration the fungus begins to invade into the cell but does not pierce the plasma membrane of the epidermal cell; instead the plasma membrane invaginates and expands to surround the fungal body (Fig. 1.2. C). At this point the haustorium feeding structure is complete and the fungus draws nutrients from the plant allowing continuation of the infection cycle: extension of secondary hyphae, infection of additional cells and production of conidiophores bearing new conidia (Fig. 1.2 D, Fig. 3. C and D). Germination, appressorium formation, penetration and haustorium formation occur within 24 h after inoculation and conidiophore production is observed within eight to ten days post innoculation.

1.2 Haustorium structure and function

Biotrophic fungi of several genera are pathogens of a diverse range of agriculturally important plant species. The powdery mildews (Ascomycetes), downy mildews (Oomycetes) and the rusts (Basidiomycetes) all form haustoria within host cells to gain nutrition, however the site of infection and method of host invasion differ (Voegele et al., 2001). The powdery mildews infect epidermal cells with mycelial growth on the tissue surface, therefore the haustorium is the only fungal structure inside plant tissue during these infections. The downy mildews and rusts infect mesophyll cells reached initially by penetration through stomata, with infection spreading to other mesophyll cells via intercellular mycelial growth (Green et al., 2002). Haustoria generated by members of these different genera have a range of morphologies from simple to extensively lobed in appearance, however the basic

structure and mechanism of function is presumably quite similar (Harrison, 1999). While there is a paucity of information defining the infection structures of grapevine powdery mildew, much can be inferred from data collected from the study of closely related powdery mildew haustoria of barley (*Blumeria graminis* on *Hordeum vulgare*) and pea (*Erysiphe pisi* on *Pisum sativum*), and rust haustoria (*Uromyces fabae* on *Vicia fabae*).

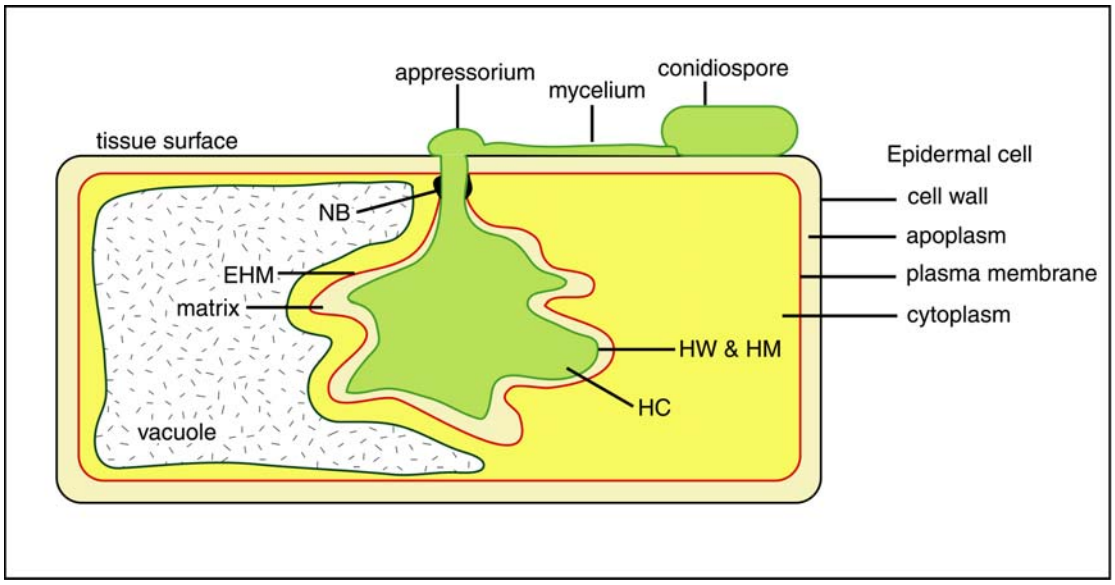


Figure 1.4. General structure of a powdery mildew haustorium. NB: neck bands; EHM: extrahaustorial membrane; HC: haustorial cytoplasm; HW: haustorial wall; HM: haustorial membrane.

A stylized diagram of a powdery mildew haustorium is shown in Figure 1.4. Haustoria are located within the cell, but are not in direct contact with the cytoplasm, because the invaginated and expanded plant plasma membrane surrounds the fungal body and isolates it from the cytoplasm. During fungal invasion, the distribution of host cell organelles becomes altered. Nuclei position shifts from the usual location at the bottom of the cell, adjacent to the mesophyll layer below, and

migrates towards the haustorium, while its volume was observed to be approximately twice that of uninfected cells (Koh et al., 2005). The endoplasmic reticulum is observed to envelop the haustorium in a mesh-like structure, while golgi, mitochondria and peroxisomes aggregate at the developing haustorium, potentially contributing to membrane synthesis and assembly for expansion of the host plasma membrane (Koh et al., 2005; Leckie et al., 1995; Aist and Bushnell, 1991). The invaginated plasma membrane of the host that surrounds the fungal body is called the extra-haustorial membrane (EHM) and it features a range of structural and compositional differences, when compared to the normal plant cell plasma membrane, that may cause altered functional properties that potentially benefit fungal nutrient acquisition (Perfect and Green, 2001). For example, antibodies raised against pea powdery mildew haustoria and pea leaf plasma membranes recognised epitopes unique to the EHM but absent from pea leaf plasma membranes, while others recognised epitopes present on leaf plasma membranes that were absent from EHM (Roberts et al., 1993). Using *Arabidopsis thaliana* lines expressing plasma membrane proteins tagged with green fluorescent protein (GFP), labelling in four lines was restricted to the host cell plasma membrane and neck band regions while completely absent from the EHM (Koh et al., 2005). Furthermore, the EHM of pea and barley powdery mildew haustoria were shown to lack the ATPase activity typical of the plasma membrane surrounding the epidermal cell cytoplasm, indicating that the membrane potential of the EHM is probably depolarised (Manners and Gay, 1982). All these observations are consistent with the hypothesis that the composition and therefore function of the EHM is distinct from the plasma membrane. Reduced ATPase activity suggests the EHM is not actively transporting nutrients but rather may be leaky, allowing deregulated solute flux into the intervening matrix between the EHM and the fungal haustorial

membrane (Fig. 1.4; Manners and Gay, 1982). The matrix is enclosed from the general apoplasm by electron dense neck bands located at the haustorial neck where the fungal and plant cell plasma membranes are fused (Koh et al., 2005). Therefore, solutes that arrive in the matrix from the host cell cytoplasm are confined to this compartment from which the fungus draws nutrients and cannot re-enter the general apoplasm (Harrison, 1999).

The fungal side of the matrix is bounded by the haustorial wall and haustorial membrane that are derived from the fungal wall and plasma membrane respectively and both appear to be differentiated from the membranes and walls associated with other fungal structures. Antibodies raised against isolated pea powdery mildew haustoria and flax rust haustoria reacted with glycoprotein and oligosaccharide epitopes on haustorial membranes and walls that were absent from other fungal structures (Green et al., 1994; Murdoch et al., 1998). Recent molecular studies on the interaction between the rust fungus *Uromyces fabae* and its broad bean host *Vicia fabae* have clearly demonstrated that the haustorial membrane, relative to the plasma membrane of other fungal structures, is uniquely differentiated to facilitate active uptake of hexoses and amino acids from the matrix into the fungal body. Screening of a cDNA library of rust fungus *in planta* induced genes (PIGs) identified putative hexose (*UfHXT1*) and amino acid (PIG2/*AAT2* and PIG27/*AAT1*) transporters and a plasma membrane H^+-ATPase (Hahn and Mendgen, 1997; Voegel et al., 2001). Detailed localisation studies demonstrated that *UfHXT1* and *AAT2* were localised specifically to the haustorial plasma membrane and, relative to other fungal membranes, high ATPase activity is a characteristic of the haustorial membrane (Struck et al., 1996; Hahn et al., 1997; Voegele et al., 2001).

The cytoplasm of the rust haustorial body does not become vacuolated like hyphae from which they differentiate and seems to be the site of biosynthetic

processes important for growth of the pathogen. Continued investigation of other rust haustorial-expressed genes has identified thiamine and mannitol biosynthetic proteins as active and localised specifically within this site but not in other fungal structures (Sohn et al., 2000; Voegele et al., 2005). Thiamine diphosphate is a cofactor of carbon and amino acid biosynthetic enzymes and a satisfactory supply of this cofactor is essential for fungal growth (Sohn et al., 2000). Specific biosynthesis of thiamine in haustoria suggests that it is either not synthesised in other fungal structures, is not available in adequate concentrations from the host or cannot be retrieved due to lack of an appropriate transporter (Sohn et al., 2000). In infected *V. fabae* leaves the concentration of mannitol increases while expression of a fungal mannitol:NADP+ 2-oxidoreductase in haustoria coincides with this accumulation (Voegele et al., 2005). Mannitol is a polyol that is not usually synthesised nor can be utilised by *V. fabae*, suggesting that its biosynthesis may be catalysed by the fungal mannitol dehydrogenase which would convert fructose obtained from the host via the haustorial expressed transporter *UfHXT1* (Voegel et al., 2001). Conversion of fructose to mannitol would potentially provide the pathogen with a carbohydrate store that is inaccessible to this host plant. Secondly, mannitol may protect the fungus from reactive oxygen species produced by the host as part of a defence response, contributing to the stability that is characteristic of biotrophic interactions (Voegele et al., 2005). These observations suggest that in addition to nutrient acquisition, haustoria play a role in biosynthetic processes essential for normal growth of the fungus.

Although only limited information is available regarding the nature and functionality of the EHM, the excellent investigations of Mendgen and co-workers provide a molecular basis for a model of haustorium function which is summarised below in the following text and Figure 1.5. The depolarisation of the EHM may

allow a deregulated flux of solutes from the host cell cytoplasm to the matrix. An electrochemical gradient across the haustorial membrane is established by H^+-ATPase activity, providing energy for active uptake of hexoses and amino acids by specific transporters localised on this membrane. Sealing of the matrix from the plant apoplasm at the haustorial neck means that solutes will not remix with apoplasmic fluids and that the electrochemical gradient across the haustorial membrane can be maintained. In the haustorial body, a mannitol dehydrogenase converts fructose into mannitol providing a carbon source that may not be utilised by the host and additionally is a factor that suppresses the host defence response. The biosynthesis of thiamine also occurs in the haustorial body, possibly because adequate amounts cannot be retrieved from the host.

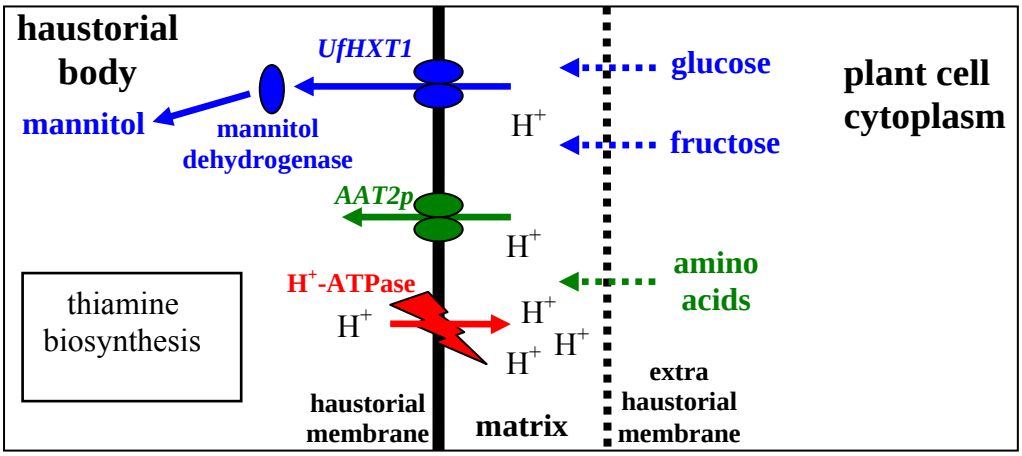


Figure 1.5. Proposed transport events and biosynthetic reactions at the haustorium interface. Refer to text above for details.

1.3 Host responses: compatibility and defence

V. vinifera is a compatible host for *E. necator* in that the pathogen is able to successfully penetrate epidermal cells and establish haustoria, enabling it to obtain sufficient nutrition to complete its asexual life cycle. However, *E. necator* is unable

to infect other plant species for example *Nicotiana tobaccum*, *Chenopodium album* and *Ricinus communis* (Boubals, 1961) that employ a range of innate defences to resist penetration and subsequent infection. These so-called 'non-host' resistance determinants may be pre-formed or induced and confer broad-spectrum resistance against the vast majority of pathogens (Heath, 2000). However, most commercially cultivated plants are susceptible to a few specific fungal pathogens that avoid or are immune to these generalised defence mechanisms, and subsequently initiate a compatible interaction with the host and establish infections.

The reasons underlying compatibility between a host plant and the few pathogens it tolerates remain obscure. Compatible pathogens may tolerate a pre-formed antimicrobial chemical produced by its host, while an incompatible pathogen may be sensitive to it (Papadopoulou et al., 1999). Host recognition and monitoring for pathogen molecules plays a part in the inducible sphere of non-host resistance responses because pathogens may lose a factor and gain susceptibility, however only to a narrow range of hosts (Kamoun et al., 1998). Furthermore, with relevance to the powdery mildews and rusts, host-specific chemical or architectural cues are perceived by a compatible fungal pathogen and influence morphogenesis of the fungal penetration organ, which initiates the whole infection process (Heath, 1976; Tsuba et al., 2002). Clearly, establishment of a compatible interaction requires a complex interplay of correctly timed cues perceived by host and pathogen, and avoidance of the non-host factors that prohibit infection by the vast majority of pathogens.

Compatible interactions are also sanctioned, or not, by 'host' resistance pathways which may be activated in subpopulations of a typically susceptible host species. Relative to the broad spectrum resistance conferred by the non-host scheme, this form of resistance is usually only effective against a single pathogen

species or race of that species. Host resistance is often controlled by single receptor-like host genes that physically interact with an avirulence factor produced by the pathogen: this interaction initiates a signal transduction cascade and activates an array of defence responses that often results in death of the infected cell via a hypersensitive response (Hammond-Kosack and Jones, 1996). This form of resistance has frequently been used by plant breeders to introduce disease resistance into otherwise susceptible cultivars. Currently, a map-based cloning approach is being used to isolate a powdery mildew resistance gene from the North American vine *Muscadinia rotundifolia*, with the eventual intention to introduce the gene into elite wine grape cultivars (Barker et al., 2005).

Although *V. vinifera* is a compatible host for *E. necator*, some typical defence responses are observed during the progression of grapevine powdery mildew disease. Expression of pathogenesis-related proteins such as chitinases and glucanases, and corresponding enzymatic activities, are induced by powdery mildew infection (Jacobs et al., 1999). In barley and *A. thaliana* infected with compatible powdery mildew fungi, induction of equivalent pathogenesis related proteins is also observed (Boyd et al., 1994; Reuber et al., 1998). Gregersen *et al*. (1997) identified additional powdery mildew induced transcripts from barley including several oxalate oxidase homologues, associated with papillae formation and penetration resistance, and putative flavonoid biosynthesis genes, which potentially contribute to phytoalexin synthesis. An oxalate oxidase gene family consisting of seven members has been identified in grapevine and two members are induced by powdery mildew infection (Godfrey and Dry, unpublished data). Ongoing analysis of this gene family is designed to determine if these genes may be used to engineer novel resistance to powdery mildew infection of grapevine. Taken together, these observations indicate that defence responses are initiated during these interactions,

but the response is not effective in halting disease progression. The defence may not be strong enough, may be too slow or may not be directed to the appropriate site at the appropriate time.

1.4 Host responses: amino acids and carbohydrates

After a pathogen has successfully avoided or suppressed all components of the plant defence network, infection is established. In the case of biotrophic fungal pathogens haustoria are formed, which retrieve nutrients from the host and allow the fungal biomass to expand and eventually reproduce via conidiospores. Several lines of evidence indicate that rust and powdery mildew infection alters amino acid composition and metabolism in host organs. Elevated lysine, proline and asparagine, and decreased glutamine levels were observed in powdery mildew infected barley leaves (Butters et al., 1985; Murray and Ayres, 1986; Jackson et al., 1995). In musk melon (*Cucumis melo* L.) infected with the powdery mildew pathogen *Sphaerotheca fuliginea*, gradual decreases in aspartic acid, glutamic acid, threonine, gamma-amino butyric acid, methionine and arginine were recorded, while cysteine and phenylalanine concentrations increased (Jindal et al., 1979). Powdery mildew infected pea leaf discs were found to have a greater capacity for amino acid uptake when compared with discs cut from uninfected leaves, and glutamine was rapidly taken up by suspensions of powdery mildew mycelia (Clarke and Hall, 1998).

Molecular studies have identified host genes involved in amino acid metabolism and transport that are induced during rust infection. For example, in rust infected broad bean, genes encoding an asparagine synthase (*VfAS1*) and an amino acid transporter (*VfAAPc*), were up regulated compared with uninfected samples (Wirsel et al., 2001). In flax infected with the rust pathogen *Melampsora lini*, *fis1*,

a gene that probably encodes a protein involved in the catabolism of proline, is strongly induced (Roberts and Pryor, 1995). Homologues of *fis1* from maize and barley are also induced by compatible rust pathogens, indicating the activity of this host gene product may serve an important role during pathogen infection (Ayliffe et al., 2002).

Changes to host carbohydrate composition and metabolism have also been observed in response to infection by biotrophic pathogens. In oak (Hewitt and Ayres, 1976), barley (Hwang and Heitefuss, 1986), pea (Aked and Hall, 1993), grapevine (Brem et al., 1986) and cucumber (Abood and Lösel, 2003) infected with compatible powdery mildew pathogens, the concentrations of glucose and fructose were found to be elevated when compared with uninfected samples, whilst sucrose concentrations declined or were unchanged. Concurrent with the rise in hexose levels of infected host tissues, net assimilation or photosynthetic activity is reduced in infected tissue. By measuring the rate of $^{14}CO_2$ fixation by grapevine leaves, Brem *et al*. (1986) showed that powdery mildew and downy mildew infection reduced net assimilation by 40% and 85% respectively. Scholes *et al*. (1994) found that the activities of three key photosynthetic enzymes; stromal fru-1,6-P_2ase, Rubisco and NADP-GAPDH, declined by approximately 50% five days after inoculation with powdery mildew in parallel with large increases in glucose, fructose and sucrose concentrations in infected tissue. The authors postulated that the high sugar levels cause a gradual decline in Calvin cycle activity which in turn inhibits photosynthetic activity.

Considered together, the dual observations of elevated carbohydrate content and reduced photosynthetic activity in diseased leaves suggests that the additional sugars may be sourced from otherwise healthy leaves or other sources and imported into the infected organ. Consistent with this idea, powdery mildew infected oak and

barley leaves showed abnormal patterns of translocation, whereby infected leaves exported less, and imported more photosynthate from uninfected healthy leaves (Hewitt and Ayres, 1976; Hwang and Heitefuss, 1986). Alternatively, in *A. thaliana* infected with white blister rust, starch was degraded from infected leaf regions in parallel with increased glucose concentrations, indicating that metabolism of carbohydrate stores may also contribute to the increased sugar levels observed in infected host tissue (Chou et al., 2000). However, starch content in uninfected leaf regions was greater than in controls, indicating that starch degradation may only occur within discreet regions and that other parts of the leaf may compensate by producing additional starch (Chou et al., 2000). In barley leaves infected with powdery mildew, total starch content increased during the period two to seven days after inoculation, indicating that infected leaves may actually contain increased levels of insoluble carbohydrate, in addition to greater amounts of soluble sugars such as glucose and fructose (Scholes et al., 1994).

The association between powdery mildew infection and increased carbohydrate content in infected tissues is further supported by studies indicating that glucose is the main carbon source transferred from the host to the fungal mycelium. Mendgen and Nass (1988) used a potentiometric fluorescent dye to estimate the membrane potential across mitochondria in haustoria of barley powdery mildew. Feeding the infected host cells with D-glucose induced an immediate reduction of fluorescence in haustorial mitochondria, indicating the D-glucose had been taken up by the haustorium. Feeding infected cells with sucrose induced a similar reaction, but the response was delayed by 20 min. Other sugars produced either smaller reductions of fluorescence or none at all. It was concluded that glucose is taken up by haustoria from host cells immediately, whereas other sugars such as sucrose, require time to be metabolised before they reach the haustorium and

mitochondria within (Mendgen and Nass, 1988). Consistent with this proposal, pea leaf disks infected with powdery mildew and mycelial suspensions acquired glucose more rapidly than fructose and sucrose, and the uptake was sensitive to chemical inhibitors of energy dependant membrane transporters (Clarke and Hall, 1998). Using asymmetrically labelled sucrose to investigate powdery mildew infected wheat, Sutton *et al*. (1999) also concluded that sucrose is hydrolysed in the host cell before being taken up by the fungus as glucose.

1.5 Carbohydrate distribution in plants

Changes to carbohydrate metabolism and translocation in host tissue infected with pathogens have been more rigorously studied than equivalent alterations to amino acid metabolism or distribution. In the following section, physiological aspects of carbohydrate distribution are discussed, however in general, the concepts also apply to amino acids (Patrick, 1997).

Plants are a mixture of autotrophic, photosynthetically active source tissues such as mature leaves, and heterotrophic sink organs such as roots, seeds and fruits. Carbohydrate assimilate synthesized in source tissues is loaded into the phloem network as sucrose in the majority of plant species, and is distributed to the various sinks where it is utilised or converted for storage. In non-leguminous plants, nitrate reductase activity in roots and leaves converts nitrate into ammonium; subsequent synthetic reactions yield amino nitrogen compounds which are also distributed by the phloem (Patrick et al., 2001). As plants develop, there are changes in both the level of supply and the numbers and sizes of sinks competing for assimilate, triggering distributive modulations to balance the carbohydrate budget. In addition to these developmental changes, exogenous factors such as environmental

conditions and pathogen challenge may retard assimilate production or apply additional carbohydrate demands, and therefore modify allocation within the plant (Roitsch et al., 2000).

Phloem unloading of sucrose at sink organs may occur within the symplasm, mediated by direct plasmodesmatal connection between the terminal sink cell cytoplasm and the end of the phloem path. Alternatively, phloem unloading may occur via efflux into the apoplasm and subsequent carrier-mediated uptake from the apoplasm by the terminal sink cells, or cells of the sink path. Apart from the relatively poorly understood control of phloem unloading mediated by the various methods of modification of plasmodesmatal conductance, metabolism and compartmentation of sucrose at the sink play delimiting roles in both routes and provide a direct connection between supply and demand (Patrick et al., 2001). Via the symplasmic path, cytoplasmic or neutral invertase (nINV) and sucrose synthase activity metabolise sucrose arriving in the sink cell cytoplasm, while uptake of sucrose into the vacuole and subsequent vacuolar invertase (vINV) activity, also contributes to the maintenance of a sucrose gradient between the sink cell cytoplasm and the phloem (Patrick, 1997). Apoplasmic unloading is driven by cell wall invertase (cwINV), which cleaves sucrose transported from the phloem to the apoplasm, thereby maintaining a sucrose gradient to support further efflux. Sucrose, and its monosaccharide cleavage products are then taken up from the apoplasm by transporters on the plasma membranes of sink cells. Thus symplasmic supply is modulated by the action of nINV, sucrose synthase and vINV, whereas apoplasmic supply is mainly regulated by cwINV and sugar transporters.

1.6 Pathogen associated changes to host invertase activity

Elevated invertase activity is commonly associated with the increased sugar concentrations observed in powdery mildew infected tissue, and most studies have concluded that the increased activities are due to invertases of host origin. Early studies on barley, grapevine and wheat reported that soluble acid invertase activity, contributed mainly by vINV forms, was elevated in powdery mildew infected tissue (Hwang and Heitefuss, 1986; Brem et al., 1986; Storr and Hall, 1992). In barley at least, most of the additional activity was confined within the mesophyll cell layer below the infected epidermis, indicating some signal is passed from the site of infection to the cells below (Scholes et al., 1994; Wright et al., 1995).

Subsequent analysis of pea leaves infected with powdery mildew showed that isolated apoplasmic fluids contained approximately 2.5 times more glucose and fructose and nearly four fold higher invertase activity than healthy leaves, indicating that most of the increase may be due to additional cwINV activity (Clarke and Hall, 1998). In powdery mildew infected wheat, all forms of invertase activity are elevated, however the biggest increase observed was in cwINV activity, consistent with the proposal that apoplasmic sucrose cleavage is an important step in sugar import to mildew infected tissues (Hall and Williams, 2000).

1.7 Induction of sink metabolism in response to pathogens and wounding

Molecular studies provide additional evidence that cwINV induction is a common element in host responses to pathogen infection and more broadly, to abiotic stresses such as wounding. In carrot storage roots, infection with the bacterial pathogen *Erwinia carotovora* strongly induced cwINV transcript one hour after inoculation before subsequently declining, while wounding induced cwINV by

a similar degree, but not until 12 hours after the wound event (Sturm and Chrispeels, 1990). Addition of fungal elicitors to suspension cultures of *Chenopodium rubrum* and tomato induced transcription of specific cwINV genes, as did mechanical wounding of source leaves of both plants (Roitsch et al., 2000). Studies on *A. thaliana* leaves infected with two different biotrophic pathogens indicated that one specific member of the cwINV gene family was induced. In leaves infected with the white blister rust pathogen *Albugo candida*, transcript levels of the cwINV *AtβFRUCT1* were found to be induced approximately ten fold, eight days after inoculation and reached levels of more than 40 fold higher than uninfected control samples 13 days after inoculation (Chou et al., 2000). Similarly, powdery mildew infected *A. thaliana* leaves displayed elevated *AtβFRUCT1* transcript levels, however only approximately four fold higher than control leaves (Fotopoulos et al., 2003).

As previously discussed, apoplasmic phloem unloading is regulated by the combined activities of cwINV, sucrose transporters and monosaccharide transporters, and genes encoding these proteins are often expressed in sink tissues. Expression of the sucrose transporter *AtSUC3* is limited to phloem cells and sink tissues such as root tips and pollen grains in *A. thaliana*. Additionally, wounding caused a strong induction of this gene within three hours and then subsequently declined (Meyer et al., 2004). Expression of the monosaccharide transporter *AtSTP4* is also induced by wounding, however by a greater amount and over a longer time period than *AtSUC3* (Truernit et al., 1996; Meyer et al., 2004). Like *AtSUC3*, *AtSTP4* expression is also usually restricted to sink organs such as roots and flowers. Fotopoulos *et al*. (2003) recently demonstrated that *AtSTP4* expression is also induced in response to powdery mildew infection in coordination with the cwINV gene *AtβFRUCT1*. Similar to the predominantly mesophyll localised induction of

invertase activity in powdery mildew infected wheat, *AtSTP4* expression was localised throughout the mesophyll and vascular tissue below areas of infected epidermis (Fotopoulos et al., 2003; Scholes et al., 1994).

In a physiological context, the induction of cwINV and sugar transporters observed in response to pathogen colonisation suggests the formation of an additional carbohydrate sink at the site of infection. cwINV and sugar transporters were also found to be induced in cells not directly infected by pathogens indicating that multiple cell layers, and potentially the whole organ, may revert to sink metabolism (Fotopoulos et al., 2003; Benhamou et al., 1991). Because wounding, in addition to pathogen infection, can induce similar gene expression modulations, it seems most likely that sink strength is increased to deliver additional carbohydrate to provide energy for defence and repair. However, in carrot storage tissues at least, the dynamics of induction of the cwINV in response to wounding and pathogen infection were quite different, suggesting that factors associated with pathogen infection may trigger more potent responses in the host (Sturm and Chrispeels, 1990). Whether or not these metabolic changes are actually beneficial for fungal nutrition has not been demonstrated.

1.8 Role of plant growth regulators in biotrophic interactions

Plants continuously interact with the biotic environment throughout their development, sanctioning some beneficial mutualistic associations, while the vast majority of pathogenic organisms are kept at bay via defence responses. Somewhere between these two outcomes is the response of plants to a select group of compatible biotrophic pathogens which manage to avoid defence responses, establish feeding sites and acquire host assimilate, which is ultimately detrimental to the plant. Plant growth regulators are thought to mediate plant-microbe interactions and many

agriculturally significant microbes, mutualistic and pathogenic alike, are capable of synthesising cytokinins and auxins, or inducing production of these regulators in infected host tissue. The pathogenesis of gall forming bacteria such as *Agrobacterium tumefaciens* and *Pseudomonas syringae* pv. s*avastanoi* is in part mediated by auxin and cytokinin biosynthetic genes encoded on specific plasmids borne by these bacteria (Jameson, 2000). Biotrophic and hemibiotrophic fungal pathogens synthesise cytokinins *in vitro* whereas necrotrophic pathogens do not, suggesting that maintenance of the biotrophic lifestyle, characterised by stable interaction between host and pathogen, may involve plant growth regulators (Murphy et al., 1997).

Elevated concentrations of plant hormones are found in infected plant tissue. During legume-rhizobia symbiosis and subsequent root nodulation that is characteristic of this association, elevated auxin and cytokinin concentrations are apparent in root cortical cells that divide and initiate nodule formation, whereas ethylene is described as a negative regulator of nodulation (Mathesius et al., 1998; Lohar et al., 2004). Interestingly, cytokinins and auxin have also been implicated in the establishment of root-knot nematode (genus *Meloidogyne*) feeding sites, also characterised by discrete regions of cell division (Lohar et al., 2004; Bird, 2004). Biotrophic and hemibiotrophic pathogens of barley, oilseed rape and apple are associated with the formation of green 'islands': infected or surrounding regions of host tissue where senescence is retarded and biosynthetic and metabolic activity is maintained (Coglan and Walters, 1990; Angra and Mandahar, 1991; Murphy et al., 1997; Cooper and Ashby, 1998). Green islands in powdery mildew and *Helminthosporium teres* I infected barley leaves contained elevated concentrations of cytokinins and polyamines, and reduced ethylene production (Coghlan and Walters, 1990; Angra and Mandahar, 1991). Furthermore, exogenous application of

cytokinins induced formation of similar zones (Angra and Mandahar, 1991). Molecular studies using *Chenopodium rubrum* suspension cultures demonstrated that cytokinins induce expression of a cwINV and a monosaccharide transporter, suggesting an induction of sink metabolism (Ehneß and Roitsch, 1997). Furthermore, a recent study by Lara *et al*. (2004) elegantly demonstrated that extracellular invertase is an essential component of cytokinin mediated delayed senescence, unequivocally proving the importance of cwINV and carbohydrate delivery in overriding usual programs of cell death.

Abscisic acid (ABA) is widely implicated in regulating responses to abiotic stresses such as drought and salinity (Zhu, 2002). More recently ABA has been found to regulate plant-microbe interactions, however the nature of its contribution to resistance and susceptibility remains unclear. Treatment of an incompatible soybean cultivar with ABA during infection with the oomycete *Phytophthora sojae* allowed the development of a compatible interaction (McDonald and Cahill, 1999). Typically, the incompatible interaction is characterised by a sharp rise in phenylalanine ammonia lyase (PAL) activity within eight h after inoculation, however this response was abolished by ABA treatment. Conversely, application of the ABA biosynthesis inhibitor norflurazon to a compatible soybean cultivar converted the interaction into an incompatible one, featuring a burst of PAL activity (McDonald and Cahill, 1999). Similar findings were observed in *A. thaliana* in response to infection by the bacterial pathogen *Pseudomonas syringae* and the downy mildew pathogen *Peronospora parasitica*. ABA application and drought stress induced susceptibility to an avirulent strain of *P. syringae*, while the ABA-deficient *A. thaliana* line *aba1-1* displayed reduced susceptibility to virulent strains of *P. parasitica* (Mohr and Cahill, 2003). These studies indicate that the endogenous ABA concentration contributes to the development of susceptibility

when plants are infected with biotrophic and other pathogens. This effect may involve down regulation of salicylic acid dependant defence pathways, as was attributed to the increased susceptibility of tomato to *Botrytis cinerea* observed after exogenous ABA application (Audenaert et al., 2002).

1.9 Other signals in biotrophic interactions

The association between legumes and Rhizobial bacteria is one of the most intensively studied plant-microbe interactions. Initiation of infection and subsequent nodule formation requires a complex procession of signals between both partners of the association, many of which are not carried by hormones. Initially, Rhizobia perceive phenolic signals such as flavonoids, secreted by legume roots, which attract bacteria and prime them for production of the various lipochitooligosaccharide symbiotic signals known as Nod factors (Long, 1996). Nod factor perception by host root cells mediates the formation of the infection thread which lines the root hair with plant derived substances such as pectins, xyloglucans and cellulose and forms a path for bacteria to invade into the root cortex where cellular division initiates nodule formation (Rae et al., 1992; Oldroyd, 2001). Although nodulation is ultimately beneficial for plant nutrition, hosts are observed to regulate the frequency of nodule initiation by means similar to the hypersensitive response observed during plant defence against many pathogens (Vasse et al., 1993).

The bacterial pathogen of bean, *Pseudomonas syringae* pv. *phaseolicola* secretes 'effector' molecules during host infection, of which three were shown to allow the bacterium to evade hypersensitive responses associated with the plant defence network (Tsiamis et al., 2000). An effector from *P. syringae* pv. *tomato* called AvrPtoB, acts as a negative regulator of programmed cell death in plants

which undermines the hosts hypersensitive response, and thus induces susceptibility to infection (Abramovitch et al., 2003). Fungal biotrophic pathogens are known to produce defence suppressing molecules, for example the soluble glucans secreted by the oomycete *Phytophthora infestans* during initial stages of infection (Doke, 1975). The tomato leaf spot fungus *Septoria lycopersici* produces tomatinase, an enzyme which degrades saponins which are antimicrobial factors and part of the preformed defence system in the host. Although tomatinase is described as a pathogenicity factor due to its role in undermining defence, the saponin degradation products were found to suppress the hypersensitive response associated with induced defence, and can therefore be considered signalling molecules (Bouarab et al., 2002).

1.10 Identification of host susceptibility genes

Host genes that contribute to susceptible pathogen interactions could be novel targets for modification to engineer resistance based on reduce susceptibility. Vogel and Somerville (2000) initiated a methane sulfonic ethyl ester mutant screen of *A. thaliana* and identified 32 lines that displayed reduced susceptibility to powdery mildew. Because the authors aimed to identify loci involved in powdery mildew susceptibility, lines which showed elevated defence activity were set aside, leaving 20 *pmr* (powdery mildew resistant) mutants. Only a few of the *pmr* loci have been mapped and cloned: *PMR5* and *PMR6* encode genes probably involved in pectin metabolism (Vogel et al., 2002; Vogel et al., 2004). Analysis of the epidermal cell walls of *pmr5* and *pmr6* plants suggested that both contained elevated pectin content, and that the pectin had altered chemical properties relative to wild type plants (Vogel et al., 2004). Contrary to the phenotype that would be predicted of plants carrying mutations in *PMR4*, the loci was found to encode a pathogen-induced callose synthase gene implicated in penetration resistance via the production

of cell wall appositions, also known as papillae (Nishimura et al., 2003). The basis of *pmr4* reduced susceptibility was found to be hyper-activation of salicylic acid defence pathways. Importantly, two of the three *PMR* genes identified up to this point do not encode proteins proposed to be involved with resistance responses, indicating that manipulation of susceptibility determinants can reduce pathogen infection. Identification of the other *PMR* genes will provide important insights into host factors involved in powdery mildew susceptibility.

Microarray analysis has also revealed novel aspects of the host response to pathogen infection. Zimmerli *et al*. (2004) monitored *A. thaliana* transcriptional responses to inoculation with compatible and incompatible powdery mildew isolates and found that overall, the responses overlapped substantially. Genes encoding putative defence factors such as a β-1, 3-glucanase like protein, a TIR-NBS class resistance protein and a thioredoxin were induced by both pathogens. However, inoculation with the incompatible pathogen *B. graminis* f. sp. *hordei* induced expression of defensin genes via a jasmonate/ethylene dependant pathway, while inoculation with two compatible pathogens did not initiate this response (Zimmerli et al., 2004). This observation is consistent with the hypothesis that compatible pathogens avoid host recognition, do not activate specific defence pathways and therefore establish disease. Commencing with microarray analysis to identify genes responsive to chitin treatment, Ramonell *et al*. (2005) identified three *A. thaliana* T-DNA mutants that were more susceptible to powdery mildew infection. Although the genes encoded at the loci probably encode proteins involved in defence responses, this investigation highlights the usefulness of microarray analysis to identify novel genes that participate in host responses to powdery mildew infection.

Candidate gene approaches have been successful in identifying genes that may contribute to the metabolic changes observed in tissue infected with various

biotrophic organisms. Examples include genes that encode proteins involved in carbohydrate and amino acid metabolism, and transporters of sugars, amino acids and phosphates (Roberts and Pryor, 1995; Chou et al., 2000; Wirsel et al., 2001; Harrison et al., 2002; Fotopoulos et al., 2003; Hoth et al., 2005). Potentially the induction of these genes in response to infection may contribute to host susceptibility.

1.11 Aims of this study

Grapevine powdery mildew is a prevalent and costly disease. Current management practices are heavily reliant on the use of fungicides which have detrimental health and overall ecological implications, and which are not compatible with the viticultural industries desire to progress towards sustainable production methods. The overall aim of this project is to investigate host (grapevine) genes that may mediate nutrient delivery to powdery mildew infected tissue and therefore can be considered susceptibility factors. Susceptibility genes could be targets for future manipulation to provide alternative disease control strategies based on reduced susceptibility rather than the introduction of traditional resistance determinants currently under investigation (Barker et al., 2005).

The specific objectives of the work described in this thesis were:

1. Identification and isolation of host genes associated with nutrient metabolism or transport that are induced by powdery mildew infection by degenerate PCR, RT-PCR and microarray analysis. In addition to enhancing current knowledge of the grapevine-powdery mildew interaction, isolation of new metabolic and transporter genes from grapevine may provide greater understanding of grape berry development.

2. Functional characterisation of novel host genes by:

    (i) sequence analysis

    (ii) heterologous expression of transporters in yeast

    (ii) determination of subcellular localisation

3. Investigation of the signalling network(s) involved in the regulation of powdery mildew responsive host genes by:

    (i) investigation of exogenous and endogenous stimuli

    (ii) isolation and analysis of promoter regions

    (iii) investigation of the hormonal regulation of these genes

Chapter 2 – General Materials and Methods

2.1 Materials

2.1.1 Solutions, chemicals and growth media

Solutions and growth media used in this project are shown in Table 2.2. All chemicals were analytical or molecular biology grade and obtained from BDH or Sigma. Solutions were prepared with nanopure or deionised water and autoclaved as necessary. Restriction endonucleases were obtained from Fermentas and Roche Diagnostics. The sources of all other supplies used in this project are indicated in the relevant methods section.

Table 2.1. Suppliers of chemicals, enzymes, growth media and other miscellaneous consumables.

Amersham Biosciences	Castle Hill, NSW, Australia
BDH	Kilsyth, Vic., Australia
Becton Dickinson (BD)	North Ryde, NSW, Australia
Bioline	Alexandria, NSW, Australia
Bio 101 Systems	distributed by Integrated Sciences
Fermentas	distributed by Quantum Scientific
Integrated Sciences	Willoughby, NSW, Australia
Invitrogen	Mount Waverley, Vic., Australia
Promega	Annandale, NSW, Australia
Qiagen	Clifton Hill, Vic., Australia
Quantum Scientific	Paddington, QLD, Australia
Roche Diagnostics	Castle Hill, NSW, Australia
Sigma-Aldrich	Castle Hill, NSW, Australia

Table 2.2. General solutions and growth media.

Solution	Composition
DNA loading dye (10x)	78% (w/v) glycerol, 0.25% (w/v) bromophenol blue, 0.25% (w/v) xylene cyanol, 10 mM EDTA
RNA loading dye (5x)	90% (v/v) deionised formamide, 10% DNA loading dye (10x))
DNSA-reagent	1% (w/v) 3,5-dinitrosalicylic acid, 0.5M KOH, 1M K/Na-tartrate
LB (liquid growth media)	1% (w/v) bacto-tryptone, 0.5% (w/v) yeast extract, 1% (w/v) NaCl pH 7.0
LB agar (solid growth media)	1% (w/v) bacto-tryptone, 0.5% (w/v) yeast extract, 1% (w/v) NaCl, 1.2% (w/v) bacto-agar, pH 7.0
Murashige and Skoog (MS) salts	4.33 g MS basal salt mixture (complete) L^{-1}
RNA extraction buffer	5 M sodium perchlorate, 0.3 M TrisHCl (pH 8.3), 1% (w/v) SDS, 1% (v/v) β-mercaptoethanol, 8.5% (w/v) PVPP, 2% (w/v) PEG 4000
RNA extraction buffer (modified)	5 M sodium perchlorate, 0.3 M TrisHCl (pH 8.3), 1% (w/v) SDS, 1% (v/v) β-mercaptoethanol
5 x SSC	750 mM NaCl, 75 mM tri-sodium citrate, pH 7.0
STET buffer	8% (w/v) sucrose, 5% (w/v) triton X-100, 50 mM EDTA (pH8.0), 50 mM Tris (pH8.0)
TBE buffer	90 mM Tris-HCl, 90 mM borate, 2 mM EDTA, (pH 8.3)
TE buffer (pH 7.6)	10 mM Tris-HCl (pH 7.6), 1 mM EDTA (pH 8.0)
YT1	10 mM Tris-HCl (pH 8.0), 1 mM EDTA (pH 8.0), 100 mM lithium accetate
YT2	10 mM Tris-HCl (pH 8.0), 1 mM EDTA (pH 8.0), 100 mM lithium accetate, 45% (v/v) PEG-4000
YPM (Liquid yeast media)	1% (w/v) yeast extract, 2% (w/v) peptone, 2% (w/v) maltose
YPM agar (Solid yeast media)	1% (w/v) yeast extract, 2% (w/v) peptone, 2% (w/v) maltose, 1.2% (w/v) bacto-agar
Uracil drop out media	0.17% (w/v) Difco yeast nitrogen base without amino acids (BD), 0.5 % (w/v) ammonium sulfate, 0.08% (w/v) CSM -uracil (Bio101 systems), 2% (w/v) maltose
Uracil drop out media agar	0.17% (w/v) Difco yeast nitrogen base w/o amino acids (BD), 0.5% (w/v) ammonium sulfate, 0.08% (w/v) CSM-uracil (Bio101 systems), 2% (w/v) maltose, 1.2% (w/v) bacto-agar

2.1.2 Oligodeoxyribonucleotide primers

All oligodeoxyribonucleotide primers were obtained from GeneWorks (Hindmarsh, SA, Australia) and their sequences are shown in Table 2.3. Degenerate oligodeoxyribonucleotide primers were designed with the assistance of CODEHOP: Consensus-Degenerate Hybrid Oligonucleotide Primers (Rose *et al.* 1998; http://blocks.fhcrc.org/blocks/codehop.html/). All other primers were designed

manually and with the assistance of Oligo Calculator (http://mbcf.dfci.harvard.edu/docs/oligocalc.html) to estimate Tm.

Table 2.3. Oligonucleotide primers used in this study. Underlined sequences correspond to specific restriction enzyme sites.
Mixed base codes: R(AG) Y(CT) K(GT) S(GC) W(AT) H(ACT) B(GCT) V(AGC) D(AGT) N(AGCT)
I(deoxyinosine)

Primer	Description	Sequence (5'-3')
AAPDEGF1	Degenerate PCR	CAGTTACCGGAAAGAGGAACTAYACNTAYAT
AAPDEGR1	Degenerate PCR	GTGGGGACTTAACGGTATCYTGDATYTC
AAPF1	Quantitative RT-PCR	GGAGGACAGTTGGAGTGGA
AAPR1	Quantitative RT-PCR	CCAACACAACCGCATAGGAC
AAP	5' RACE PCR	GGCCACGCGTCGAACTAGTACGGGIIGGGIIGGGIIG
B26	3' RACE PCR	GACTCGAGTCGACATCGATTTTTTTTTTTTTTTTT
BQ794584 fwd	Quantitative RT-PCR	CTATGGCTTCTTCGCCTTTG
BQ794584 rev	Quantitative RT-PCR	AGTCCACATCCCTTCTCCAC
BQ794584rev.2	5' RACE PCR	ATGTCAGTTAGACCAGCTCCAT
BQ794584rev.3	5' RACE PCR	GACAATGCAGCCAGCATAAAC
BQ794584FLF	Clone full length cDNA	GTGAATTCAAAAACATGGAAACTGAGCTG
BQ794584FLR	Clone full length cDNA	CACTCGAGCTTCCTCTATGAAGCC
CWINVDEGF1	Degenerate PCR	AAATACCGGAATGTGGGARTGYCC
CWINVDEGR1	Degenerate PCR	AAGCGAAAGTCATCAGTCCRAANGGNCC
CWINV fwd	Quantitative RT-PCR	ATGAATCATCTAGYGTGGAGCAC
CWINV rev	Quantitative RT-PCR	CTTAAACGATATCTCCACATCTGC
CWINVrace fwd	3' RACE PCR	GTGCATCAGTAAAAGGTGGG
CWINVrace rev	5' RACE PCR	GTATCCTTCTCACGGTTGTAGC
CWINVrace rev	5' RACE PCR	TCCAATCGTGTAGTAGTCATGC
CWINVFL fwd	Clone full length cDNA	GTGAATTCAAAGCCATCATGGCCAC
CWINVFL rev	Clone full length cDNA	GTCAAGCTTCACTCACAACTCTACATAC
CWINVBS 1	Promoter sequencing	GATCATTCATCCAGTTCTTGCG
CWINVBS 2	Promoter sequencing	GGGATTGGCCAAAAAGCTCC
CWINVBS3	Promoter sequencing	GAAAATAAACACTGCAAGTGTGCC
CWINVBS4	Promoter sequencing	CAGAGGAATCTTGGAAAATTTGTCAG
GIN1fwd	Quantitative RT-PCR	CCATCTCCATCCCATCGTAACC
GIN1rev	Quantitative RT-PCR	GGCTATCCAAGTTTCCAACCAACC
GIN2fwd	Quantitative RT-PCR	GAGCACAGTTCCAGTAATCAAAGG
GIN2rev	Quantitative RT-PCR	GTGAGGCGTAGTTTTAGGACTCC
HT1 fwd	Quantitative RT-PCR	TCGGAGTGGATGGAGAACCTTG
HT1 rev	Quantitative RT-PCR	GACATCACCACCACAAAGAAGGC
HT1FL fwd	Clone full length cDNA	CTGGATCCATGCCGGCTGTCGGAGGC
HT1FL rev	Clone full length cDNA	GACTCGAGTCATACATTCTTAACAGGGTAGTTTTCC
HT2 fwd	Quantitative RT-PCR	GTTGCCGTCAACTTCGCAAC
HT2 rev	Quantitative RT-PCR	GAAGGAATTTAGCTATGGCAGAG
HTDEGF1	Degenerate PCR	TCCACTGTACCTGTCCGARATGGCNCC
HTDEGR1	Degenerate PCR	TCCCAGTGGTCCCCANSWCCA
HT3 fwd	Quantitative RT-PCR	TAATCGAACGGGGATCAAG
HT3 rev	Quantitative RT-PCR	CCCCCAGAAATCAATAAAACTC
HT3race fwd	3' RACE PCR	GCTAGTGAGCCTGCAAACTCA
HT3race rev	5' RACE PCR	ATGAGGGGAGCTTTGCAGTT
HT3race rev	5' RACE PCR	TCCCCGTCGTAGTTGCTAAC
HT3FL fwd	Clone full length cDNA	GTAGAATTCAGAAGAGGAACTATGGAGG
HT3FL rev	Clone full length cDNA	TCAAGCTTGGCTCATGATAGGAGC
HT3GFP fwd	Translational fusion to GFP	GCTCGAGGAAGAAGAGGAACTATGGAG
HT3GFP rev	Translational fusion to GFP	CTCTAGAGCTGCCTAGCTTTGTCTTTTCAC
HT3BS1	Promoter sequencing	GTCATTGTACTTGCAGTAGTGG
HT3BS2	Promoter sequencing	GTCATAGCCGAAAATTGCACCC
HT3BS3	Promoter sequencing	CTGCTATGTCTGCATTCCTCC

Table 2.3. (continued).

Primer	Description	Sequence (5'-3')
HT4 fwd	Quantitative RT-PCR	CCTACTTTGTCGACAGAGTAGACG
HT4 rev	Quantitative RT-PCR	GGAGGCCATACCAACTACG
HT4race fwd	3' RACE PCR	GGTAGGAGGAATATTGGCAGC
HT4race rev	5' RACE PCR	AGCCAATGCTAGAGAAACTCG
HT4race rev	5' RACE PCR	TAATAAGGTTAGCTGATAGAGCC
HT4FL fwd	Clone full length cDNA	GTAGAATTCAGAGCCATGGCAGTG
HT4FL rev	Clone full length cDNA	ACAAGCTTAGAGGAGGATGCTGTTG
HT4GFP rev	Translational fusion to GFP	CGTCTAGAGGCTGTCTCCATTTTAGG
HT4BS 1	Promoter sequencing	AGGGAGGATGTGAATGAGGTC
HT4BS2	Promoter sequencing	CCATGGCTTGTTACTGCAATTCC
HT4BS3	Promoter sequencing	GAAACAAAATCGCATTTATACCATTGC
HT5 fwd	Quantitative RT-PCR	GTCGCTTGGAAGAAGGAAAG
HT5 rev	Quantitative RT-PCR	CCTACTTTGTCGACAGAGTAGACG
HT5race fwd	3' RACE PCR	GGTAATTGCAATCATACTAGGCAT
HT5race rev	5' RACE PCR	CCAGCCAACCCCAATGATAC
HT5race rev	5' RACE PCR	TAGTGACGTTAAGTTGGAACAGT
HT5FL fwd	Clone full length cDNA	CTGAATTCCATCATGCCTGCTGGA
HT5FL rev	Clone full length cDNA	ACAAGCTTTCCCTCCCCATACAC
HT5BS 1	Promoter sequencing	CTGTAGCCCTTGGTTGTCG
HT5BS2	Promoter sequencing	GATGTCACCACCTACAAAGTCC
HT5BS3	Promoter sequencing	GATGTCACCACCTACAAAGTCC
HT5BS4	Promoter sequencing	GTCAGAGTTGATGGCATCGAG
HT5BS5	Promoter sequencing	GGTCATTCAACTAAAATAGATAAAACAATCC
PhT1F	Quantitative RT-PCR	CTTTGCAGGTGGACATTGAG
PhT1R	Quantitative RT-PCR	GAGCAATAAGCGTTTGCGC
PhT2F	Quantitative RT-PCR	AGATATGTCTAAAGTTCTCCACCTT
PhT2R	Quantitative RT-PCR	CTGCAGAGGGCTATGAGAGT
PIP1A fwd	Quantitative RT-PCR	TCCTGTTCTGGCACCTCTTC
PIP1A rev	Quantitative RT-PCR	CCTGAATGACCCAAGAGCC
ProTDEGF1	Degenerate PCR	ATACTCCGGTACCATTATGGTNCCNYT
ProTDEGR1	Degenerate PCR	TCGTACATTGGGGAAGCRAADATRTG
ProTF1	Quantitative RT-PCR	CAGGAACAGAAGCAAGCAAGG
ProTR1	Quantitative RT-PCR	AACCAAACTGGACCAGAGAC
SP6	Screening & sequencing	TTAGGTGACACTATAGAATACTC
SUC11 fwd	Quantitative RT-PCR	AAACCAAATGAAGGGCAGAA
SUC11 rev	Quantitative RT-PCR	TCAGTGCAGCAATCACAACA
SUC12 fwd	Quantitative RT-PCR	CGGATTGGATGGGTAGAGAA
SUC12 rev	Quantitative RT-PCR	CATGCAGGCAAACACAATAAA
SUC27 fwd	Quantitative RT-PCR	GGGGCTGATGCTGAACTCT
SUC27 rev	Quantitative RT-PCR	AAGCCAGAGCAAATGGAATG
TC11451fwd	Quantitative RT-PCR	GATGCAGAGAAGAGGCTCGC
TC11451rev	Quantitative RT-PCR	CCGTCCAGTTTTGCTGAGGTC
TC11207fwd	Quantitative RT-PCR	GCCAGAATACTATGATGGAAAGCTC
TC11207rev	Quantitative RT-PCR	CCGAATACAGAATACAAACTACCTGC
TIP3 fwd	Quantitative RT-PCR	GTATGCCACAGCAGTGGATCC
TIP3 rev	Quantitative RT-PCR	GAAGATGTGATCGTAGATGATGGC
TC7206fwd	Quantitative RT-PCR	CGAAATGGGCGGTTCATAGGC
TC7206rev	Quantitative RT-PCR	CCACCATGCTCTTCCTCGTG
UBQ fwd	Quantitative RT-PCR	AGTAGATGACTGGATTGGAGGT
UBQ rev	Quantitative RT-PCR	GAGTATCAAAACAAAAGCATCG
T7	Clone screening, sequence	GTAATACGACTCACTATAGGG

2.1.3 Bacterial and yeast strains

Escherichia coli strain XL1-Blue (Stratagene; Cedar Creek, TX) was used for all cloning procedures. Yeast strain *EBY.VW4000* (Wierkzork *et al*., 1999) was used for heterologous expression of putative HTs.

2.1.4 Grapevine tissue

The various grapevine tissues used in this study were sampled from the Coombe vineyard and from potted glasshouse vines on the Waite Campus of Adelaide University (Adelaide, South Australia, latitude 34° 56' south, longitude 138° 36' east). Grapevines were propagated from dormant Cabernet Sauvignon and Chardonnay cuttings obtained from the Riverland Vine Improvement Committee (Monash, South Australia), stored at 4ºC before use. To strike, the base of each cutting was cut and scored, dipped in Clonex Hormone Rooting Gel (Growth Technology, Western Australia) and transferred to pots containing potting mix of sand : composted pine bark (1:2 v/v) supplemented with 1 g L^{-1} ferrous sulphate and 4 g L^{-1} Osmocote slow release fertilizer (Yates, Australia). Pots were incubated on a 25°C heat-bed containing Perlite for three weeks following striking and watered lightly at two-day intervals. During this period rooting and bud-burst occurred, and pots were transferred to temperature-controlled glasshouses with a minimum air temperature of 23ºC and a maximum temperature of 25ºC. Each pot was irrigated with a single drip emitter with two irrigations per day.

2.1.5 *Erysiphe necator* culture and maintenance

E. necator was maintained on a detached leaf inoculation system as previously reported (Donald et al., 2002) with some modifications. Young, glossy *V. vinifera* leaves, typically 3 to 8 cm in diameter, were sterilised for 3 min in 50% (v/v) Milton Solution (Procter and Gamble, NSW, Australia) containing 0.01% (v/v) Tween 20 with gentle agitation, followed by four times in sterile water. Sterilised leaves were laid on to four sterile toothpicks placed across the surface of agar plates containing 1% (w/v) agar and 400µl L^{-1} Pimaricin (Sigma) and petioles embedded in the agar with tweezers. Spores from powdery mildew-infected leaves were applied

to leaves prepared as above by vigorously tapping the infected leaf above the recipient leaf allowing spores to fall onto the surface. Plates were sealed with Parafilm and incubated at 24.5°C under a 16 h light and 8 h dark cycle. Leaves were examined for sporulation after 8 d using a Stemi 2000 microscope (Zeiss, North Ryde, Australia).

2.1.6 *Plasmopara viticola* culture and maintenance

P. viticola was maintained on glasshouse-grown potted vines. Infected leaves (7 to 10 DPI) were removed and incubated upside down on moist filter paper in large petri dishes overnight at 22°C to facilitate sporulation. To collect spores, leaves were placed in a 50 ml Falcon tube containing 5 mL water and agitated to displace the spores and a haemocytometer used to estimate the spore concentration. The spore solution was diluted to a concentration of 1 $x10^6$ spores per ml before being sprayed on the abaxial surface of leaves on glasshouse-grown potted vines. Inoculated leaves were enclosed in plastic bags overnight to maintain humidity.

2.2 Methods

This section outlines general methods used throughout this project and are essentially as described by Sambrook and Russell (2001) or according to the manufacturer's instructions. Methods significantly modified from their published form are outlined. Other methods specific to experiments carried out in one chapter only are outlined in the materials and methods section of the relevant chapter.

2.2.1 Polymerase chain reaction (PCR)

Typical components of a PCR reaction were as follows: DNA template (cDNA 2 µl, genomic DNA 10 ng), oligonucleotide primers (200-500 nM), 1× PCR buffer (Bioline), 200 µM dATP, dCTP, dGTP, and dTTP (Invitrogen), 1.5 µM $MgCl_2$, and 1 unit of recombinant BioTaq Red DNA polymerase (Bioline), in a 20 µl reaction volume.

For amplification of full-length cDNAs for functional characterisation and for sub cellular localization (Chapter 4), Platinum Taq DNA Polymerase High Fidelity (Invitrogen) was used according to the manufacturer's instructions and with supplied buffer. Thermal cycling generally consisted of: 3 min at 95°C (one cycle); 30 s at 94°C, 30 s at 52-57°C, 30 - 90 s at 72°C (30-40 cycles); 7 min at 72°C (1 cycle).

2.2.2 Agarose gel electrophoresis

EasyCast horizontal minigel tanks (OWL Scientific Inc., Cambridge, UK) were used for electrophoresis of DNA. Agarose gels, 0.7-2.0% (w/v) were prepared with TBE buffer (Table 2.1), and contained 0.5 µg ml^{-1} (w/v) ethidium bromide. Before application to wells, DNA loading dye (Table 2.1) was added to each sample to a final concentration of 2×. Gels were electrophoresed at approximately 100 V in TBE running buffer before being visualized and photographed using a short wavelength UV transilluminator.

Electrophoresis of RNA was essentially the same as that described for DNA except that gel tanks, trays, and combs were treated with 0.2 M NaOH for approximately 1 h prior to use, an RNA loading dye (Table 2.1) was added and each

sample was heated at 65°C for five min and then chilled on ice for two min before loading into wells.

2.2.3 Purification of DNA from agarose gel slices

Purification of specific DNA species from agarose gels after visualization with ethidium bromide was achieved using a QIAquick Gel Extraction Kit (Qiagen) according to the manufacturer's instructions.

2.2.4 Dephosphorylation of DNA 5' termini

The 5' phosphate groups were removed from restricted vector DNA fragments prior to ligation with insert DNA fragments using calf intestinal alkaline phosphatase (Roche). The enzyme was inactivated by addition of 20 mM EDTA and incubation at 65°C for 15 min.

2.2.5 Purification of DNA samples following enzymatic reactions

Extraction of DNA samples after restriction enzyme digestion (Section 2.2.1), PCR (Section 2.2.4) and dephosphorylation (Section 2.2.5) reactions was achieved using a QIAquick PCR Purification Kit (Qiagen).

2.2.6 DNA ligation

Purified PCR products were ligated into the T-tailed vectors pGEM T-Easy (Promega) or pDRIVE (Qiagen) using the pGEM T-Easy Vector System I (Promega) and the PCR Cloning Kit (Qiagen) according to the manufacturer's instructions.

All other ligations were carried out in 10 µl reaction volumes containing an insert: vector ratio of approximately 6:1, 10 units of T4 DNA ligase (Fermentas) in the supplied buffer and incubated overnight at 16°C.

2.2.7 Preparation of electro-competent E. coli cells

LB (500 ml) was inoculated with a five ml overnight culture of XL1-Blue and grown at 37°C with vigorous shaking to an optical density (OD_{600}) of 0.5. Cells were chilled on ice for 10 min and centrifuged for 15 min at 4°C at 5000 *g*. The cells were resuspended in 500 ml of sterile ice-cold water and centrifuged again. The cells were washed and centrifuged again with 250 ml sterile ice-cold water and resuspended in 10ml of sterile ice-cold 10% (v/v) glycerol. The cells were transferred to a new 50 ml falcon tube and centrifuged again. The cells were finally resuspended in 2 ml of ice-cold glycerol. Aliquots of 40 µl were placed into ice-cold eppendorf tubes, snap-frozen in liquid nitrogen, and stored at -80°C.

2.2.8 Transformation of bacteria with recombinant plasmids

Electro-competent *E. coli* XL1-Blue were transformed by electroporation using a Gene-Pulser apparatus (Bio-Rad, CA, USA). Approximately 10 ng of plasmid or 1 µl ligation reaction was mixed with a 40 µl aliquot of cells and transferred to an ice-cold electroporation cuvette (path length = 1mm; Invitrogen). This was then given a single pulse in the Gene-Pulser (1.8 kV, 125 µFD, 200 Ohms), and immediately resuspended in 600 µl of LB (Table 2.1). After incubation at 37°C for 1 h to allow expression of antibiotic-resistance genes, the transformed cells were spread on 1.2% LB agar plates (Table 2.1) with appropriate antibiotic selection and incubated at 37°C overnight.

2.2.9 Preparation of plasmid DNA

High quality plasmid DNA for vector preparation, DNA sequencing, yeast transformation and for transient expression in onion cells was prepared from 1-5 ml of overnight culture using a QIAprep Spin Miniprep Kit (Qiagen) according to the manufacturers instructions. Large-scale (20-50 ml cultures) preparation of plasmid DNA was achieved using a Plasmid Midi Kit (Qiagen).

For general screening purposes, plasmid DNA was prepared using a miniprep boiling method (Holmes and Quigley, 1981). Briefly, 1 ml of overnight culture was centrifuged at 16,000 *g* for 1 min at room temperature. The supernatant was discarded and the pellet resuspended in 350 µl STET (Table 2.1) buffer. After adding 12.5 µl of 20 mg ml^{-1} lysozyme, the cells were placed in boiling water for one min and centrifuged at 16,000 *g* for 20 min. The pellet was removed with a sterile toothpick and 40 µl of 3 M sodium acetate and 220 µl isopropanol added to the supernatant. This mixture was centrifuged at 16,100 *g* for 10 min. The resulting pellet was washed with 70% (v/v) ethanol, dried briefly under vacuum, and resuspended in 50 µl of sterile water.

2.2.10 Preparation of bacterial glycerol stocks

Bacterial glycerol stocks were prepared by adding 1 volume of 40% (v/v) sterile glycerol to overnight culture, snap-freezing in liquid nitrogen, and storing at -80°C.

2.2.11 Preparation of DNA samples for sequencing

DNA sequencing reactions were carried out using an ABI PRISM BigDye Terminator Cycle Sequencing Ready Reaction Kit (PE Applied Biosystems, Norwalk, CT, USA) according to the manufacturer's instructions using plasmid DNA prepared with the QIAprep Spin Miniprep Kit (Qiagen). Extension products were precipitated by adding 80 µl of 75% (v/v) isopropanol, incubating for 20 min at room temperature, and centrifuging at 16,000*g* for 20 min. After discarding the supernatant and adding another 250 µl of 75% (v/v) isopropanol, the tubes were centrifuged at 16,000*g* for 5 min. The samples were then aspirated, dried under vacuum for 15 min, and sent to the Institute of Medical and Veterinary Science (Adelaide, Australia) for analysis.

2.2.12 Preparation of total grape RNA

Total RNA was isolated from grape tissues using a sodium perchlorate method (Rezaian and Krake, 1987) with modifications. Plant material (0.5 to 4 g FW), was ground in liquid nitrogen in a mortar and pestle, the powder added to 20 ml of RNA extraction buffer (Table 2.2) and mixed by shaking at 200 rpm on an orbital shaker at room temperature for 30 min. The homogenate was then centrifuged at 80 *g* for 10 min at 4°C through a crude separation apparatus consisting of a 20 ml disposable syringe plugged with approximately 2 cm^3 of silane-treated glass wool (Alltech, Baulkam Hills, NSW, Australia) wrapped in Miracloth (Calbiochem, Croydon, Vic., Australia) and secured into a 250 ml centrifuge tube (Corning, Acton, USA). Modified extraction buffer (Table 2.2), was added to the crude separation apparatus and centrifuged as before. The combined eluate was mixed with 2.5 vol of cold absolute ethanol and stored at -20°C

overnight. The precipitate was pelleted via centrifugation at 10,000 *g* for 20 min at 4°C and the resulting pellet was dried under vacuum and resuspended in 1 mL of TE Buffer (Table 2.1) containing 0.2% (v/v) *β*-mercaptoethanol. The suspension was extracted 3 times with an equal volume of phenol:chloroform:isoamyl alcohol (25:24:1 v/v) and once with an equal volume of chloroform:isoamyl alcohol (24:1 v/v). The upper aqueous phase was retained, mixed with 2.5 vol of cold absolute ethanol and 0.1 vol of 3 M sodium acetate (pH 5.2) and then stored at -20°C overnight to precipitate RNA. The RNA precipitate was pelleted at 16,000 *g* for 10 min at 4°C, dried under vacuum, rinsed with cold 70% (v/v) ethanol and resuspended in 50 to 200 µl of sterile water. RNA was quantified spectrophotometrically and integrity checked by agarose gel electrophoresis.

2.2.13 First-strand cDNA synthesis

Before reverse transcription, 100 µg of total RNA was further purified and DNase treated using an RNeasy Mini Kit (Qiagen) and an RNase-Free DNase Set (Qiagen) according to the manufacturer's instructions. DNase-treated RNA (2 µg) was reverse transcribed using the SuperScript III First-Strand Synthesis System for RT-PCR (Invitrogen) using the Oligo $(dT)_{20}$ primer according to the manufacturer's instructions. Before use in RT-PCR experiments, cDNA reactions were diluted 10-fold to 200 µl with 10 mM Tris-HCl, pH 7.6.

2.2.14 Sequence analysis and manipulation

DNA sequences were analysed using various basic local alignment search tools (BLAST) served at the National Centre for Biotechnology Information (NCBI) website (http://www.ncbi.nlm.nih.gov/BLAST/) and the GCG WebAngis Wisconsin

software package operated by the Australian National Genomic Information Service (http://www.angis.org.au/). Multiple sequence alignments were drawn by Pile Up or ClustalW (both served at ANGIS) and displayed and further manipulated using GeneDoc (www.psc.edu/biomed/genedoc). Potential signal peptides of deduced amino acid sequences were mapped using SignalP v. 3.0 (http://www.cbs.dtu.dk/services/SignalP/). Transmembrane domains and membrane topology was predicted using TMHMM v 2.0 (http://www.cbs.dtu.dk/services/TMHMM; Krogh et al., 2001) and theoretical isoelectric points were calculated using Iep, also served at ANGIS (http://www.angis.org.au/).

Chapter 3 – Isolation and identification of genes differentially expressed in powdery mildew infected grapevine tissues

3.1 Introduction

Biotrophic pathogens, such as powdery mildew, form a stable association with host epidermal cells to acquire nutrients from the host plant. Nutrient transfer from plant to fungus is facilitated by a specialised structure called the haustorium, a biotrophic interface that develops only during this interaction, formed from fungal and host components (Hahn & Mendgen, 2001). As the fungus grows, its increasing biomass becomes a strong nutrient sink capable of altering assimilate flow and storage in the host (Brem et al., 1986; Murray & Ayres, 1986; Jackson et al., 1995; Clarke and Hall, 1998). Two approaches were initiated to identify grapevine genes that are responsive to powdery mildew infection and may mediate these changes.

To identify differentially expressed grapevine transcripts, a grape microarray was screened with probes generated from powdery mildew infected Chardonnay berry skin and probes produced from healthy uninfected berry skin. This array consists of approximately 1,200 ESTs isolated from grape berries spotted in duplicate, allowing calculation of the standard error of expression of each gene via comparison of these technical replicates. Microarray analyses of powdery mildew infected *A. thaliana* and wheat have identified previously unreported host genes that are induced by infection with these pathogens (Zimmerli et al., 2004; Ramonell et al., 2005). By using microarray analysis to compare gene expression in powdery

mildew infected and healthy grapevine tissue samples, novel powdery mildew responsive grapevines genes may be identified.

Molecular studies in broad bean and *A. thaliana* have identified host carbohydrate and amino acid transporters, and metabolic enzymes that are induced in response to infection with biotrophic fungal pathogens (Wirsel et al., 2001; Fotopoulos et al., 2003). Specifically in powdery mildew infected grapevine leaves, hexose concentrations and invertase activity were increased, while net assimilation was repressed, suggesting additional carbohydrate is imported to the infection site (Brem et al., 1986). Based on these published observations a second screening approach was initiated to target genes that may contribute to these metabolic changes. To isolate new grapevine and powdery mildew responsive transcripts a degenerate PCR cloning approach using cDNA prepared from powdery mildew infected leaves as template was employed. It should be noted that at the time this project commenced, the sequences of only two grapevine HTs (*VvHT1* and *VvHT2*; Fillion et al., 1999) and two vacuolar invertases (vINVs) (GIN1 and GIN2; Davies and Robinson, 1996) had been reported.

3.2 Materials and methods

3.2.1 Microarray analysis of powdery mildew infected berry skin

The *V. vinifera* cDNA microarray slide (kindly donated by Dr Mark R. Thomas, CSIRO Plant Industry, Adelaide, Australia) contained 1,220 unique sequences, (now part of the grapevine Unigene set at http://www.ncbi.nlm.nih.gov/) plus 12 non-*V. Vinifera* control sequences. All genes were printed in duplicate within the array and are subsequently referred to as technical replicates. Total RNA was extracted as described (Section 2.2.12) from healthy and powdery mildew

infected Chardonnay berry skins collected 10 DPI, and then treated with DNase using the RNase free DNase Set (Qiagen) in combination with the RNeasy mini kit (Qiagen). Microarray probes were prepared from the total RNA using a method modified from Schenk *et al*. (2000). RNA (60 µg) was reverse transcribed using Superscript II (Invitrogen) with an oligo(dT) 23mer anchored primer (Invitrogen) at 42°C for one h. The cDNA was treated with 2 U of RNase H (Invitrogen) at 37°C for 30 min and then purified and concentrated to 8 µl in TE (pH 8.0) using YM-30 Microcon centrifugal columns (Millipore). Half of the resulting concentrate was used for each labelling reaction as described in Schenk *et al*. (2000) except that 10 U of Klenow enzyme was used for each labelling reaction. Probes produced from total RNA extracted from powdery mildew infected berry skins were labelled with Cyanine 5 and probes prepared from RNA extracted from healthy Chardonnay berry skins were labelled with Cyanine 3.

Cyanine 5-labelled probe was combined with an equal amount of Cyanine 3-labelled probe, the mix purified and concentrated using YM-30 Microcon columns, and then resuspended with 10 µg single stranded salmon sperm DNA in 25 µl hybridization solution (25% (w/v) formamide, 5x SSC, 0.1% (w/v) SDS). After heat denaturation at 65°C for 5 min, the denatured probe was added to the array and hybridized overnight in a sealed hybridization chamber at 42°C. After hybridization, slides were washed with 0.1x SSC, 0.1% SDS, and then rinsed in 0.1x SSC and water, and finally dried by centrifugation.

The microarray slides were scanned using a GenePix Scanner 4000A (Molecular Devices Corporation, Sunnyvale, Ca., USA) to measure the fluorescence intensity at 635 nm and 532 nm of each spot. The fluorescence intensity was corrected using local background measurements surrounding each spot using

GenPixPro Version 3 (Molecular Devices Corporation). A GenePixPro *gpr* file, which included all fluorescent intensity measurements, was generated for the array and this file was imported into GeneSpring Version 5 (Agilent Technologies, Forest Hill, Vic., Australia) for statistical analysis to determine which genes were differentially expressed between the powdery mildew infected and healthy samples. The fluorescent intensity values were adjusted using the values obtained for 10 negative control sequences and corrected for dye incorporation biases using Intensity Dependent Normalisation of 100% of the data. When the value of intensity at 532 nm was less than 10, the data point was removed from the analysis. The ratio of normalised Cyanine 5: Cyanine 3 intensity was calculated for each gene, and values greater than 2 or less than -2 were considered to be differentially expressed.

3.2.2 Degenerate PCR, analysis and cloning

HT, cwINV, ProT and AAP degenerate PCR products were PCR amplified (Section 2.2.) from cDNA prepared from total RNA extracted from powdery mildew infected grapevine leaves using BioTaq Red DNA polymerase (Bioline) and the PCR conditions as described (Section 2.2.) Degenerate primer sequences are listed in Table 2.3.

Amplified products were cloned using the pGEM T-Easy Vector System I (Promega) and transformed into XL1-Blue (Stratagene). To screen transformants, inserts were amplified using SP6 and T7 primers which bind left and right of the pGEM T-Easy polylinker, and these products subsequently restricted with *Rsa*I. Analysis of the restriction pattern of individual transformants allowed identification of different insert species which were then DNA sequenced as described (Section 2.2.11).

3.2.3 RT-PCR analysis of selected genes in powdery mildew infected grapevine leaves

Expression analysis was done by real-time PCR using a SYBR green method on a Rotor-Gene 3000 thermal cycler (Corbett Research, Mortlake, Australia). Reactions were run in triplicate and each 15 µl reaction contained: 333 nM of each primer, 3 µl of diluted cDNA (Section 2.2.15), 1 x ABsolute^{TM} QPCR SYBR$^{®}$ Green ROX Mix (Integrated Sciences) and water. The thermal cycling conditions used were 95°C for 15 min followed by 40 cycles of: 95°C for 30 s, 56°C or 58°C for 30 s, and 72°C for 30 s, followed by a melt cycle of 1°C increments from 55 to 96°C. All primer pairs amplified a single product of the expected size and sequence, which was confirmed by melt-curve analysis, agarose gel electrophoresis and DNA sequencing. A set of standards, consisting of isolated PCR product from each primer pair diluted in a 10 fold dilution series (usually 10^{-4} to 10^{-8} dilutions), was used to draw a standard curve from which the target concentration, corresponding to each primer pair, was estimated in each cDNA sample analysed. The concentration of actin was used to normalise the target concentration in each sample. To calculate the change in gene expression, a ratio of normalised target concentration in powdery mildew infected leaves to the target concentration in control leaves was made (infected:control). For negative changes the opposite ratio was calculated. This method was used to estimate the difference in target concentration in powdery mildew infected leaves compared with control leaves to determine if any selected genes are induced or repressed by powdery mildew infection. The change in gene expression does not reflect the level of expression of each gene relative to the others tested. Primer sequences are listed in Table 2.3.

For this analysis, control and powdery mildew infected detached Cabernet Sauvignon leaves were prepared as described (Section 2.1.5). RNA was prepared (Section 2.2.12) from control and infected leaves two days after detachment and inoculation and cDNA synthesised (Section 2.2.13). Under the conditions used, more than 90% of powdery mildew conidia germinate and have established haustoria, as indicated by secondary mycelial extension, within 24 h. At the time sampled, considerable mycelial coverage of the leaf surface was observed using a Stemi 2000 microscope (Zeiss).

3.3 Results

3.3.1 Microarray analysis of powdery mildew infected grape berry skin

RNA was extracted from healthy control and powdery mildew infected (collected 10 DPI) Chardonnay berry skins and Cy3 (control) and Cy5 (infected) labeled probes synthesized. Microarray analysis indicated that 75 (6.1%) of the transcripts on the *V. vinifera* cDNA microarray grape array were differentially expressed more than two fold in powdery mildew-infected berry skins compared with uninfected control samples (Table 3.1). Thirty five of these transcripts were up regulated in response to powdery mildew infection. The largest class of differentially expressed transcripts, which comprised approximately 60% of the up regulated genes, encode typical pathogenesis related and other stress responsive proteins. Members of this class accounted for 17 of the 20 most strongly up regulated transcripts in the powdery mildew infected sample. A group of seven transcripts encoding cell wall and structural proteins such as expansin and peptidylprolyl isomerase homologues were generally down regulated in the infected sample. However, *GRIP 13* (AJ237983), a grape berry ripening-induced gene

Table 3.1. Powdery mildew induced changes to gene expression in grape berry skins determined by microarray analysis. Probes from powdery mildew infected berry skin were labelled with Cy5 and control probes were labelled with Cy3. The array consisted of 1,225 ESTs isolated from grape berries. The array was scanned using a GenePix Scanner 4000A and GenPixPro Version 3 software. Data were analysed using GeneSpring Version 5.

Rank	EST ID	Normalised Ratio LogCy5:LogCy3	StdDev	Best blast match or description
Pathogenesis and stress related				
+1	1414	10.20	0.20	PR-13 cDNA
+2	1432	10.19	0.04	Germin-like gene (VvGLP3)
+3	1422	10.11	0.14	(Y109920) PR5-type Thaumatin-like protein (VvTL2)
+4	1429	9.13	0.90	Stilbene synthase
+5	1433	8.04	2.22	Germin-like gene (VvGLP4)
+6	1417	7.89	0.27	(AF053750) PR2-type basic glucanase (VvGlub)
+7	1430	7.64	0.06	Germin-like gene (VvGLP1)
+8	1412	7.26	0.06	Prl-7 cDNA
+9	1416	7.14	0.17	(U68144) PR2-type basic glucanase (VvGlua)
+10	1415	6.01	0.35	Prl-5 cDNA
+11	1421	5.49	0.60	(Z68123) PR3-type ClassIII basic chitinase (VvChi3)
+12	1413	5.30	0.37	Prl-4 cDNA
+13	1406	4.51	0.90	(AF003007) thaumatin-like protein
+15	1121	4.42	0.44	GLUCAN ENDO-1,3-BETA-GLUCOSIDASE PRECURSOR
+18	1407	3.82	0.46	(AF061329) VVPR-4A cDNA PR-4 type protein
+19	185	3.37	0.13	(X94995) naringenin-chalcone synthase [Juglans nigra x Juglans regia]
+20	1410	3.33	0.21	chalcone isomerase
+28	549	2.67	0.12	(AJ236913) metallothionein-like protein [Elaeis guineensis]
+33	1431	2.29	0.21	Germin-like gene (VvGLP2)
-12	1066	-3.64	0.83	(ABB02395) temperature-induced lipocalin, Vitis vinifera
Cell wall and structural proteins				
+14	1441	4.45	0.21	(AJ237983) Grip 13, Cell wall associated
-24	814	-2.75	0.25	(AAC27459) cellulase, Arabidopsis thaliana
-19	1102	-3.01	0.29	(BAD09075) putative fiber protein Fb14, Oryza sativa
-14	1367	-3.20	0.77	(AAC27459) cellulase (EC 3.2.1.4) F16B22.6 - Arabidopsis thaliana
-7	1453	-3.91	0.71	Expansin 3 (Exp3-4)
-6	1112	-4.08	0.26	(AB015468) peptidylprolyl isomerase [Arabidopsis thaliana]
-2	1246	-5.31	0.26	(AF248055) proline-rich protein [Glycine max]

Rank	EST ID	Normalised Ratio LogCy5:LogCy3	StdDev	Best blast match or description
Membrane channels and transporters				
+17	1265	3.91	0.61	(AAS00691) metal-nicotianamine transporter YSL1 [Arabidopsis thaliana]
+23	526	3.22	0.23	(AF200713) inwardly rectifying potassium channel Kir7.1 [Cavia porcellus]
+24	33	3.10	0.74	(Z70524) PDR5-like ABC transporter [Spirodela polyrrhiza]
-29	1375	-2.60	0.47	(AP002818) putative peptide transporter-like protein [Oryza sativa]
-20	1042	-2.98	0.62	(AAF80557) plasma membrane aquaporin, Vitis vinifera
-4	710	-4.22	0.31	(AF271660) putative aquaporin TIP3 [Vitis berlandieri x Vitis rupestris]
General metabolism				
+16	740	4.14	0.53	(AC004473) Arabidopsis thaliana Similar to red-1 (related to thioredoxin)
+26	314	2.92	0.26	(S71580) GLUTAMINE SYNTHETASE CYTOSOLIC ISOZYME 2
-25	756	-2.73	0.66	(AF044204) lipid transfer protein precursor - upland cotton
-3	1292	-4.63	0.00	cryptogene protein G4 - Leishmania tarentolae (strain LEM125)
Secondary metabolism				
+30	393	2.56	0.39	(AJ238754) phenylalanine-ammonia lyase [Citrus clementina x Citrus reticulata]
+35	510	2.23	0.00	(AF194174) alcohol dehydrogenase 2 [Vitis vinifera]
-35	755	-2.28	0.06	(AC015446) Similar to Allinase [Arabidopsis thaliana]
-15	385	-3.12	0.73	(AAB87126) mannose-1-phosphate guanylyltransferase, Arabidopsis thaliana
Photosynthesis				
-38	1220	-2.16	0.10	(AF139468) photosystem I reaction center subunit III [Vigna radiata]
-30	650	-2.55	0.35	(AF139470) chlorophyll a/b-binding protein CP24 precursor [Vigna radiata]
-18	1154	-3.04	0.48	(AB012639) light harvesting chlorophyll a/b-binding protein [Nicotiana sylvestris]
-16	71	-3.08	0.24	(CAD37939) photosystem I subunit O, Arabidopsis thaliana
-11	1293	-3.76	0.17	(CAB44683) cytochrome P450 homolog F23K16.110 - Arabidopsis thaliana

Rank	EST ID	Normalised Ratio LogCy5:LogCy3	StdDev	Best blast match or description
Transcription factors				
+21	538	3.28	0.07	(AJ237992) putative ripening-related bZIP protein [Vitis vinifera]
+22	476	3.23	0.39	(AF200322) putative glycine-rich RNA binding protein 3 [Catharanthus roseus]
+31	290	2.50	0.13	(AAM65129) putative DNA-binding protein [Arabidopsis thaliana]
-33	1215	-2.34	0.18	(AAA23712) transcription activator of D-serine dehydratase - Escherichia coli
Protein turnover				
+25	213	3.07	0.44	(AB033601) polyubiquitin [Cucumis melo]
+29	607	2.65	0.44	(M62431) nonstructural protein; putative helicase/protease
+32	246	2.45	0.16	(U66264) ubiquitin [Nicotiana tabacum]
-27	1322	-2.68	0.25	(AAT08675) ubiquitin-conjugating enzyme, Hyacinthus orientalis
Heat shock proteins				
-34	265	-2.30	0.29	(AAB63310) small heat-shock protein class I, 18.6K - common sunflower
-21	570	-2.95	0.40	(U13949) AtHSP101 HEAT SHOCK PROTEIN 101, Arabidopsis thaliana
-13	548	-3.34	0.08	(AJ297951) p23 co-chaperone [Arabidopsis thaliana]
Hormone signalling and development				
-31	1274	-2.53	0.14	(AF136539) YABBY2 [Arabidopsis thaliana]
-28	1007	-2.65	0.26	S-ADENOSYLMETHIONINE SYNTHETASE 1 (ethylene production)
-26	634	-2.71	0.48	(T09782) 3-HYDROXY-3-METHYLGLUTARYL-COENZYME A REDUCTASE 1
Unknown or miscellaneous				
+27	397	2.73	0.39	(D84126) leptin receptor(short cytoplasmic form) [Rattus norvegicus]
+34	558	2.24	0.25	(AAC17693) hypothetical protein, Caenorhabditis elegans
-40	324	-2.13	0.03	(CAB36531) hypothetical protein F10M23.190 - Arabidopsis thaliana
-37	281	-2.21	0.15	(AAD18971) ct565 hypothetical protein - Chlamydia pneumoniae
-36	833	-2.27	0.25	No match

Rank	EST ID	Normalised Ratio LogCy5:LogCy3	StdDev	Best blast match or description
Unknown or miscellaneous (continued)				
-32	176	-2.44	0.22	(CAA99759) hypothetical protein SENU1, senescence up-regulated - tomato
-23	1321	-2.75	0.20	(AAC49369) (U34333) proline-rich 14 kDa protein, kidney bean
-22	1200	-2.91	0.03	(AF228877) unknown [Strongylocentrotus purpuratus]
-17	1319	-3.04	0.00	conserved hypothetical protein CP1049, Chlamydophila pneumoniae
-10	1342	-3.77	0.90	(AF090446) unknown [Zea mays]
-9	1223	-3.88	0.23	(CAA49341) ADR11-2 protein - soybean auxin down regulated (X69640)
-5	421	-4.10	0.31	No match
-1	540	-5.53	0.00	(A38958) TRANSLATIONALLY CONTROLLED TUMOR PROTEIN HOMOLOG

proposed to be involved with cell wall modification was 4.45 times more highly expressed in the infected berry skin than in the control sample. *GRIP 55* (AJ237992), another grape ripening induced gene which encodes a bZIP transcription factor, was also elevated in the powdery mildew infected berry skins.

Grape genes encoding membrane channels and transporters were also differentially expressed in response to powdery mildew infection. Thus, a putative tonoplast aquaporin (AF271660) and one plasma membrane aquaporin (AAF80557) were down regulated in the powdery mildew infected sample whereas a metal-nicotianamide YSL transporter homologue (CF403181), an inwardly rectifying potassium channel homologue (CV179380), and an ABC transporter homologue

(CF403138), were induced more than three fold in the infected berry skins. Transcript levels of five photosynthesis related genes and three heat shock proteins were significantly reduced in powdery mildew-infected grape berry skin compared to control samples. Expression of individual members of other functional classes of genes did not change in a consistent manner. A complete list of the ESTs on the array can be found in the Appendix section.

3.3.2 Isolation of partial length grape hexose transporter clones from powdery mildew infected leaves

Multiple sequence alignments of plant HT peptide sequences identified a number of absolutely conserved regions within this family. Using CODEHOP (Rose et al., 1998), a pair of degenerate primers were designed (Table 2.3) to the plant HT family at the conserved residues 'SEMAP' (HTDEGF1) and 'WSWGP' (HTDEGR1) as indicated in Figure 3.1 A.

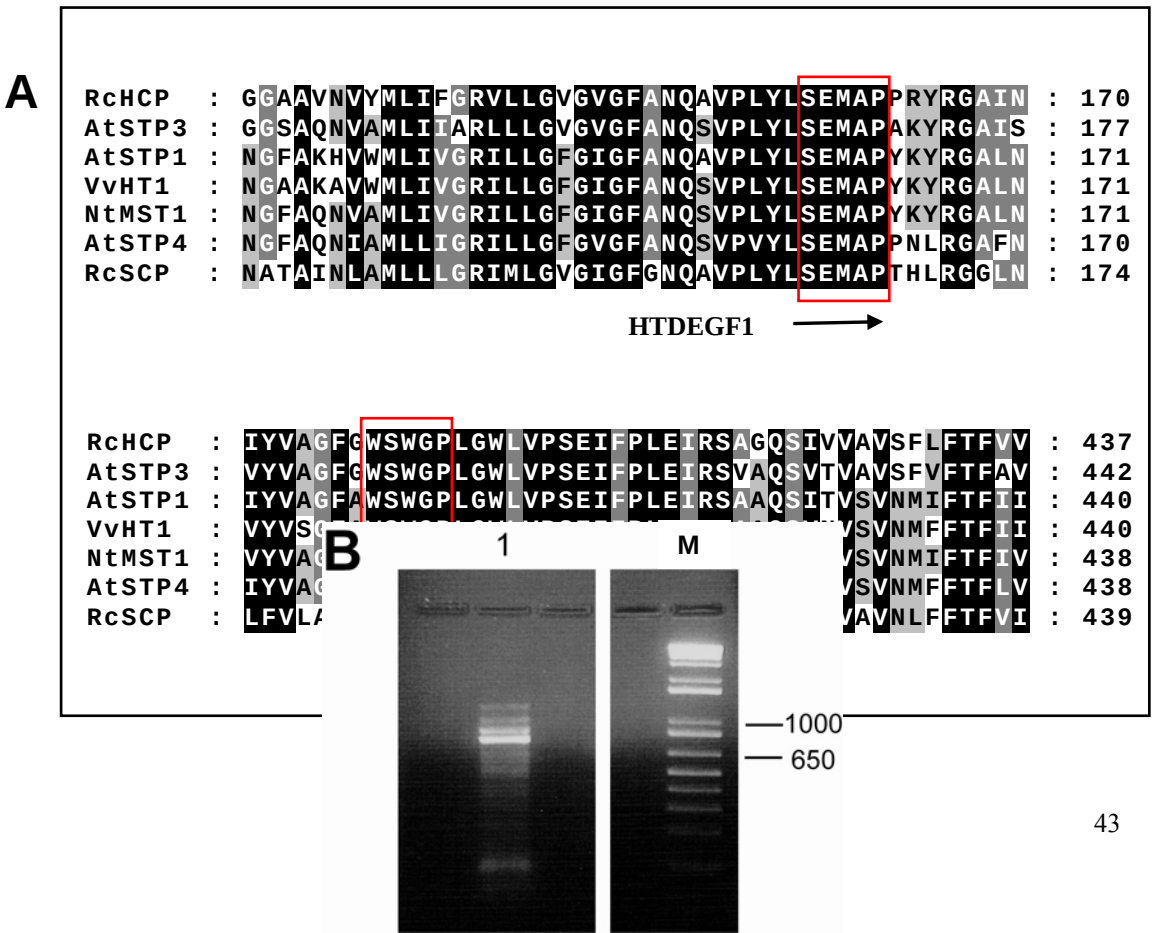


Table 3.2. Homology between predicted translation products of grapevine degenerate HT clones and previously reported plant HT peptides. The percentage identity and similarity (in brackets) between protein sequences as determined by the BestFit algorithm. Bolded values indicate the highest BestFit values. Database accession numbers of the sequences used in the comparison are: VvHT1 (CAA70777), VvHT2 (AY663846), AtSTP7 (AJ344331), AtSTP13 (AJ344338), RcHex6 (AAA79857), AtSTP4 (BAB01308).

	VvHT4	**VvHT5**	**VvHT1**	**VvHT2**	**AtSTP7**	**AtSPT13**	**RcHex6**	**AtSTP4**
VvHT3	61 (74)	56 (73)	56 (66)	53 (64)	**80 (87)**	61 (74)	52 (65)	55 (66)
VvHT4		51 (64)	57 (66)	56 (66)	53 (64)	57 (67)	**80 (89)**	56 (67)
VvHT5			58 (68)	53 (63)	55 (70)	**84 (91)**	50 (64)	52 (65)
VvHT1				57 (56)	57 (66)	61 (69)	58 (70)	59 (69)
VvHT2					52 (62)	54 (64)	54 (65)	53 (65)
AtSTP7						62 (73)	57 (69)	56 (67)
AtSPT13							56 (67)	55 (67)
RcHex6								59 (67)

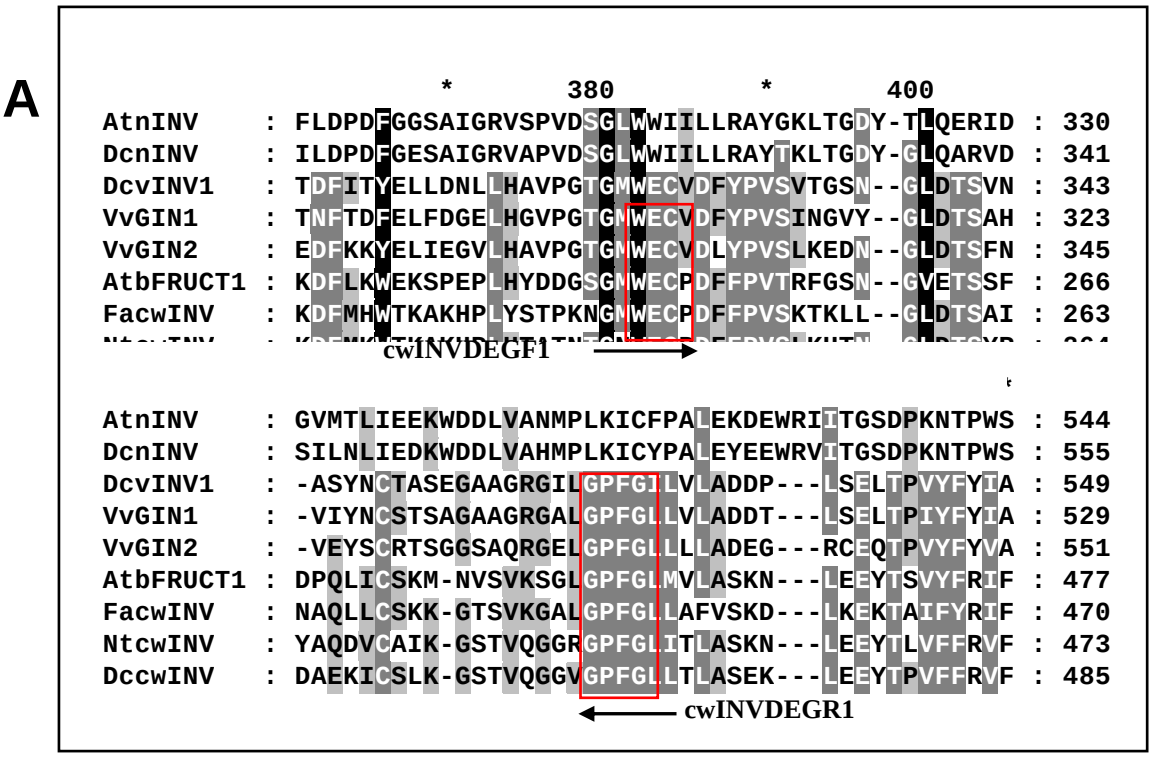
PCR using the HT degenerate primers HTDEGF1, HTDEGR1 and cDNA template prepared from RNA isolated from powdery mildew infected leaves, amplified two major products around the expected size of 750 bp and other products of different sizes in less abundance (Fig. 3.1 B). Products of the expected size were cloned, inserts amplified using SP6 and T7 primers and these products fingerprinted using *Rsa*I, a restriction enzyme with a four base-pair recognition site, to detect sequence differences. After representative clones of each species were sequenced and analysed using Blast and BestFit analysis, three different HT-like sequences

were obtained. The predicted peptides encoded by the three partial length grape HT degenerate products were observed to share 80-84% amino acid identity with HT proteins from *A. thaliana* and *Ricinus communis* (Table 3.2) and were designated as *VvHT3*, *VvHT4* and *VvHT5*. These three VvHT sequences share approximately 60% amino acid identity with each other and with the previously reported grapevine sequences *VvHT1* (CAA70777) and *VvHT2* (AY663846) (Table 3.2).

3.3.3 Isolation of a partial length grape cell wall invertase clone from powdery mildew infected leaves

Multiple sequence alignment of cwINV protein sequences identified a number of absolutely conserved regions within this family, however many motifs are also present in vINV protein sequences. In order to avoid amplification of the highly expressed grape vINV genes *GIN1* and *GIN2* (Davies and Robinson, 1996), the cwINVDEGF1 degenerate primer targeted the motif 'WECP' that is conserved within the cwINV family but which is substituted with 'WECV' in vacuolar invertase forms (Fig. 3.2 A). The reverse degenerate primer, cwINVDEGR1, targeted the motif 'GPFG' which is common to both cwINV and vINV forms. The nINV family of cytoplasmic-localised proteins is not homologous at these targeted motifs.

Amplification with cwINV degenerate primer combination cwINVDEGF1 / cwINVDEGR1 produced a single, clean band of approximately the expected size of 650 bp from powdery mildew infected leaf cDNA (Fig. 3.2 B). Cloning and sequencing indicated that degenerate PCR targeting the cwINV family had amplified a single species with homology to the targeted family.



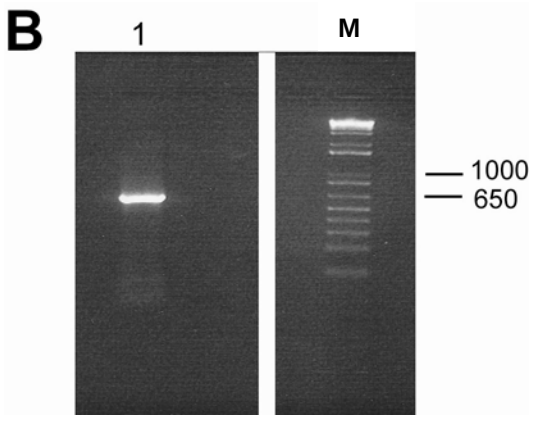


Figure 3.2. Degenerate PCR targeting grapevine cell wall invertase (cwINV). (A) Conserved motifs targeted by degenerate primers. (B) Amplification products generated by PCR using these primers with cDNA template prepared from powdery mildew infected grapevine leaves. Lane 1: degenerate PCR product, M: DNA size markers, in bp. ClustalW was used to make the multiple sequence alignment, only part of which is shown. Accession numbers of the sequences used in the alignment are: AtnINV (AAP40464), DcnINV (CAA76145), DcvINV (P80065), VvGIN1 (AAB47171), VvGIN2 (AAB47172), AtbFRUCT1 (CAA52620), FacwINV (AAD10959), DccwINV (AAA03516), NtcwINV (X81834). Primer sequences are in Table 2.3.

Table 3.3. Homology between the predicted translation product of the grapevine cwINV degenerate clone, two previously reported plant cwINV proteins and the two grapevine vacuolar invertase proteins (VvGIN1 and VvGIN2). The percentage identity and similarity (in brackets) between protein sequences as determined by the BestFit algorithm. Database accession numbers of the sequences used in the comparison are: AtcwINV (NP_566464), BvcwINV (CAB95010), VvGIN1 (AAB47171), VvGIN2 (AAB47172).

	AtcwINV	**BvcwINV**	**VvGIN1**	**VvGIN2**
VvcwINV	65 (75)	69 (74)	46 (54)	48 (53)
AtcwINV		66 (74)	42 (51)	45 (52)
BvcwINV			44 (54)	44 (53)
VvGIN1				62 (70)

Blast analysis and local alignment using BestFit of the predicted peptide encoded by the cwINV degenerate product indicated that it shares approximately 75% amino acid similarity with cwINV sequences from *A. thaliana* (NP_566464) and *Beta vulgaris* (CAB95010) and less than 55% amino acid similarity with the grapevine vINVs GIN1 and GIN2 (Table 3.3).

3.3.4 Isolation of partial length grape amino acid permease and proline transporter clones from powdery mildew infected leaves

Alignment of plant proline transporter (ProT) and amino acid permease (AAP) protein sequences identified conserved regions within these peptide families. Forward and reverse degenerate primers were designed with the assistance of CODEHOP to two of these motifs within each family. In AAPs the conserved peptides targeted were “TYMD” by the forward primer AAPDEGF1 and “EIQD” by the reverse primer AAPDEGR1 (Figure 3.3 A). In ProTs the motifs targeted were

A

```
StAAP1 : FSFITYFTSTLLADCYRSPGPISGKRNYTYMDVVRSHLGGVKVTLCGIAQY :  83
AtAAP1 : FSFITYFTSTMLADCYRAPDPVTGKRNYTYMDVVRSYLGGRKVQLCGVAQY : 129
AtAAP2 : FSLVTLYSSTLLSDCYRTGDAVSGKRNYTYMDAVRSILGGFKFKICGLIQY : 138
RcAAP1 : FSLVTYYTSTLLSACYRSGDPVNGKRNYTYMDAVRTNLGGAKVKLCGFVQY :  67
RcAAP2 : FSLVTYYTSTLLSACYRSGDPVNGKRNYTYMDAVRTNLGGAKVKLCGFVQY : 131
AtAAP3 : FSAVTYFTSSLLAACYRSGDPISGKRNYTYMDAVRSNLGGVKVTLCGIVQY : 122
RcAAP3 : FSLVTYYTSTLLSACYRTGDPVNGKRNYTYMDAVRSNLGGAKFKICGYVQY : 110
AtAAP5 : FSFVTFYTSTLLCSCYRSGDSVTGKRNYTYMDAIHSNLGGIKVKVCGVVQY : 120
                                          AAPDEGF1

StAAP1 : TGVVVGV-----DVSGTEKVWRSFQAIGDIAFAYAYSTVLIEIQDTLK-SS : 228
AtAAP1 : TGTAVGV-----DVTAAQKIWRSFQAVGDIAFAYAYATVLIEIQDTLR-SS : 273
AtAAP2 : TGISIGT------VTQTQKIWRTFQALGDIAFAYSYSVVLIEIQDTVR-SP : 281
RcAAP1 : TGISIGA-----NVTPTQKIWRSFQALGDIAFAYSYSIILIEIQDTVR-SP : 211
RcAAP2 : TGISIGA-----NVTPTQKIWRSFQALGDIAFAYSYSIILIEIQDTVR-SP : 275
AtAAP3 : TGISIGA------VTETQKIWRTFQALGDIAFAYSYSIILIEIQDTVK-SP : 265
RcAAP3 : TGISIGT------VTETQKIWRSFQALGDIAFAYSYSLILIEIQDTIR-SP : 255
AtAAP5 : TGVTVGTVTLSGTVTSSQKIWRTFQSLGNIAFAYSYSMILIEIQDTVK-SP : 269
                                          AAPDEGR1
```

B

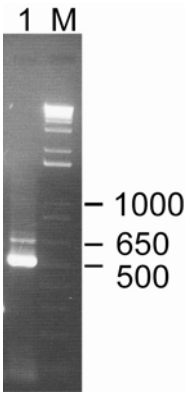


Figure 3.3. Degenerate PCR targeting the grapevine amino acid permease (AAP) gene family. (A) Conserved motifs targeted by degenerate primers. (B) Amplification products generated by PCR using these primers with cDNA template prepared from powdery mildew infected grapevine leaves. Lane 1: degenerate PCR product, M: DNA size markers, in bp. ClustalW was used to make the multiple sequence alignment (A), only part of which is shown. Accession numbers of the sequences used in the alignment are: StAAP1 (CAA70968.2), AtAAP1 (AAB87674), AtAAP2 (CAA50672), RcAAP1 (ABA96629), RcAAP2 (CAA07563), AtAAP3 (CAA54630), RcAAP3 (CAA10608), AtAAP5 (CAA54632). Primer sequences are in Table 2.3.

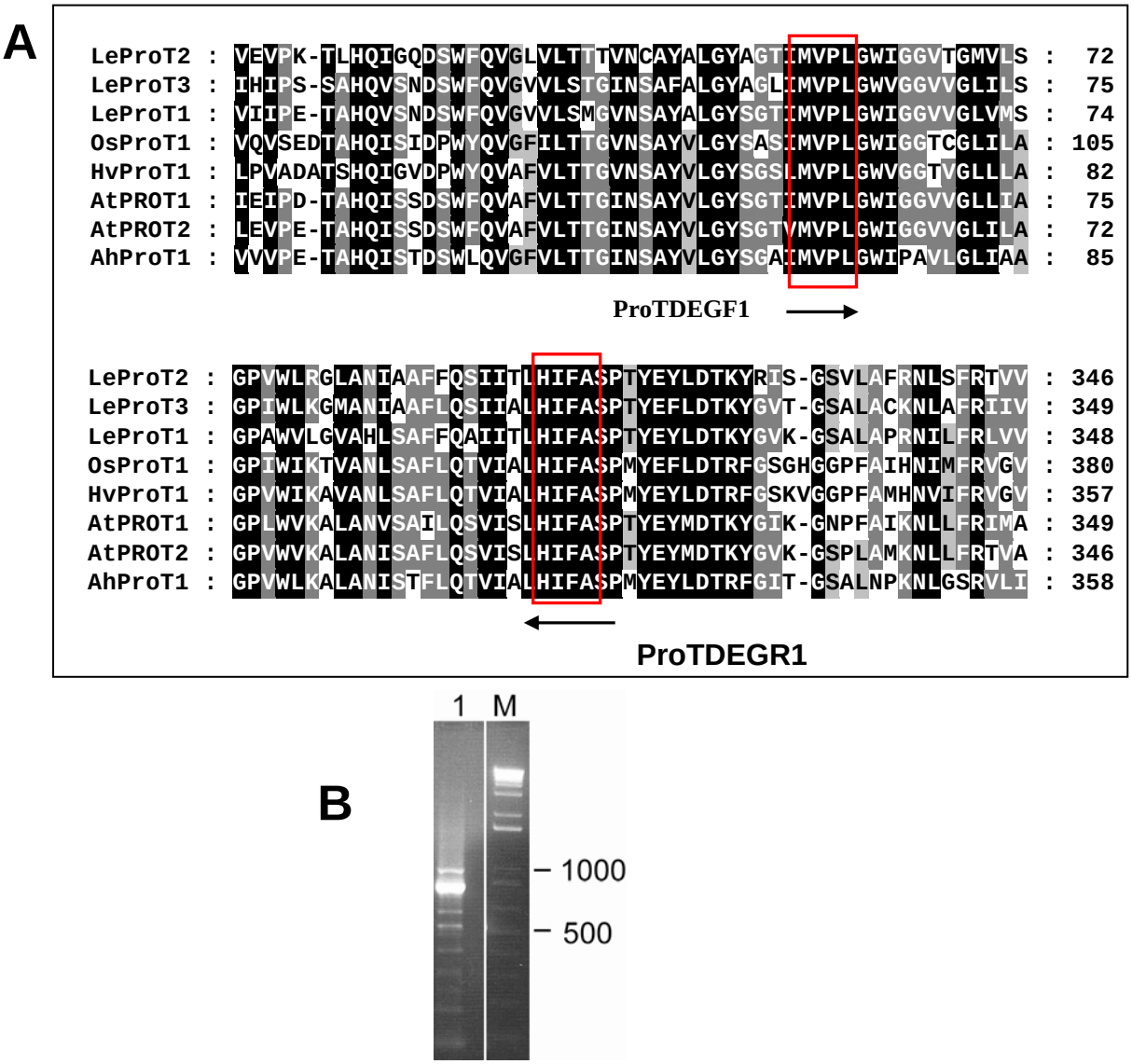


Figure 3.4. Degenerate PCR targeting the grapevine proline transporter (ProT) gene family. (A) Conserved motifs targeted by degenerate primers. (B) Amplification products generated by PCR using these primers with cDNA template prepared from powdery mildew infected grapevine leaves. Lane 1: degenerate PCR product, M: DNA size markers, in bp. ClustalW was used to make the multiple sequence alignment (A), only part of which is shown. Accession numbers of the sequences used in the alignment are: LeProT2 (AAD25161), LeProT3 (AAD25162), LeProT1 (AAD25160), OsProT1 (BAA93437), HvProT1 (BAB69951), AtProT1 (AAB95274), AtProT2 (CAA65053), AhProT1 (AAF7897); Primer sequences are in Table 2.3.

"MVPL" by the forward primer ProTDEGF1 and "FQFT" by the reverse primer ProTDEGR1 (Figure 3.4 A).

PCR with AAP and ProT degenerate primers amplified products of the expected sizes of approximately 520 bp (Fig. 3.3 B) and 850 bp (Fig. 3.4 B) respectively, which were cloned and transformants screened using *Rsa*I fingerprinting as described previously. After sequencing, degenerate PCR targeting AAP and ProT families were found to have amplified a single species with homology to the targeted families. Blast analysis revealed that the AAP and ProT partial sequences encode predicted peptides that share 92% and 89% identity with RcAAP2 (CAA07563) from *Ricinus communis* and AtProT1 (AAB95274) from *A. thaliana* respectively (data not shown).

3.3.5 Semi-quantitative RT-PCR analysis of selected genes in powdery mildew infected leaves

To determine if any of the genes isolated by degenerate PCR were induced during powdery mildew infection, gene-specific primers were designed to each of the partial cDNAs, and to sequences of previously reported HTs (VvHT1 and VvHT2), SUCTs (SUC11, SUC12, SUC27) and vINVs (GIN1 and GIN2). Primers were also designed to two partial grape sequences homologous to plant phosphate transporters, *VvPi1* (AY463369) and *VvPi2* (AY463367) which had been recently cloned in the CSIRO Plant Industry laboratory (Malone and Dry, unpublished data). Additionally, in early 2003 a grapevine EST sequence database became publicly accessible at http://www.tigr.org/tigr-scripts/tgi/T_index.cgi?species=grape. Primers were designed based on grape EST sequences homologous to three neutral (cytoplasmic) invertases (nINVs) (TC7206, TC11451 and TC11207) and two

Table 3.4. Semi quantative RT-PCR analysis of changes in gene expression in response to powdery mildew infection. Detached leaves were inoculated with powdery mildew and sampled two days later. Change in gene expression is the ratio, infected : control expression (induction), or the ratio, control : infected expression (repression). All values were normalised by the level of actin expression in each sample and each value is the average of three replicates. * indicates the gene was isolated in this study.

	Transcript	Accession number	Change transcript amount (fold)
Hexose transporters	VvHT1	CAA70777	1.6
	VvHT2	AY663846	2.17
	VvHT3	*	-1.13
	VvHT4	*	1.5
	VvHT5	*	7.1
Sucrose transporters	VvSUC11	AAF08329	-1.13
	VvSUC12	AAF08330	1.2
	VvSUC27	AAF08331	2.48
Invertases	VvcwINV	*	12.8
	VvGIN1	AAB47171	-1.5
	VvGIN2	AAB47172	2.47
	TC7206	TC7206	2.02
	TC11451	TC11451	1.7
	TC11207	TC11207	1.2
Sucrose synthases	TC4408	TC4408	1.6
	TC5103	TC5103	-1.3
Phosphate transporters	VvPi1	AY463369	-2.6
	VvPi2	AY463367	3
Amino acid transporters	VvAAP	*	1.1
	VvProT	*	1.82

sucrose synthases (SSynth) (TC4408 and TC5103). Semi-quantitative real-time PCR using a Sybr green method was used to measure abundance of the selected transcripts in cDNA prepared from control and powdery mildew infected detached Cabernet Sauvignon leaves sampled two days after detachment and inoculation. The housekeeping gene actin was used as the reference for normalisation of the samples being compared. After normalisation using actin, the ratio of infected:control expression was calculated for each transcript to determine the fold-change in transcript abundance (Table 3.4). Negative changes were calculated using the opposite ratio.

Transcripts of *VvHT5* and *VvcwINV* were 7.1 and 12.8 fold more abundant in powdery mildew infected leaves compared to control samples, respectively (Table 3.4). Expression of the four other putative HTs did not change significantly, but tended to be higher in the infected sample. Similarly, expression of the other invertase forms did not change significantly and, with the exception of the vINV *GIN1*, transcript levels of each tended to be elevated in the powdery mildew infected sample. The putative grapevine phosphate transporters responded differentially to powdery mildew infection with one induced 2.6 fold and one repressed three fold compared to the control, whereas transcript levels of the ProT and AAP degenerate clones were not significantly different in the samples measured.

3.4 Discussion

The general aim of this project is to identify and characterise host genes that might contribute to the metabolic changes observed in powdery mildew infected tissue and thus mediate nutrient delivery to the site of infection. To achieve this goal, two approaches were instigated. Firstly, a general, non-targeted analysis of

gene expression in powdery mildew infected berry skins was conducted using a grapevine microarray consisting of 1,225 ESTs isolated from grape berries at various stages of development. Secondly, based on evidence that indicates changes to carbohydrate and amino acid metabolism in host tissue are associated with powdery mildew infection, a candidate gene approach was initiated using degenerate PCR was used to isolated new grapevine transcripts encoding putative HT, cwINV, AAP and ProT proteins. Subsequent RT-PCR analysis was then used to determine if the abundance of any of these transcripts changed in powdery mildew infected leaves, relative to controls. Additionally, RT-PCR was used to measure expression of previously reported HTs, SUCTs, vINVs and ESTs homologous to nINV and SSynth in powdery mildew infected leaves.

3.4.1 Microarray analysis of powdery mildew infected berry skins

The microarray screen indicated that 75, or 6.1% of the total 1,225 ESTs comprising the array, were differentially expressed (Table 3.1). The largest and most strongly up regulated group encode typical PR and stress induced proteins. Enhanced expression of pathogenesis-related proteins such as chitinases, glucanases and thaumatins has been previously reported in grapevine and in *A. thaliana* infected with powdery mildew, and is taken in the current study as molecular evidence of a host defence response to fungal pathogenesis (Jacobs et al., 1999; Boyd et al., 1994; Reuber et al., 1998). Expression of the secondary metabolism gene phenylalanine-ammonia lyase (PAL) was also increased by PM infection of grape, and elevated PAL expression and enzyme activity in response to pathogen infection is another typical host defence response (McDonald and Cahill, 1999). Recent microarray analysis of *A. thaliana* responses to inoculation with the powdery mildew species

Erysiphe cichoracearum reported induction of a few defence genes only, however in this study probes were prepared from samples collected only 24 h after inoculation, therefore infection and probably host defence responses may have only just commenced (Zimmerli et al., 2004).

Only 3 of the 20 most strongly induced genes do not encode pathogenesis related proteins. Transcripts of *GRIP 13* were 4.45 fold more abundant in powdery mildew infected samples compared to controls and it was the 14th most induced transcript. *Grip 13* encodes a proline rich cell wall associated protein proposed to be involved in cell wall modification and repair during the ripening phase of berry development (Davies and Robinson, 2000). Considering that cell wall penetration is required for powdery mildew infection, the induction of GRIP 13 may be associated with defence and repair in response to this injury.

A member of the ubiquitous thioredoxin gene family (CF403952) was also up-regulated more than 4 fold and was the 16th most strongly induced gene in powdery mildew infected grape berries, relative to controls. In addition to a protective role against oxidative damage, specific thioredoxins have been implicated in the host response to exogenous stress stimuli. For example, expression of a thioredoxin from *A. thaliana*, *AtTRXh5*, is strongly and rapidly induced in response to pathogen infection and wounding while another related gene did not respond (Laloi et al., 2004).

Interestingly, a putative metal-nicotianamine transporter, or YSL homologue, was identified by the microarray to be induced 3.9 fold in response to powdery mildew infection and was the 17th most strongly induced gene. The *Arabidopsis* genome contains a family of eight YSL proteins and two of these have been shown to transport iron and copper complexed with nicotianamine (DiDonato

et al., 2004). YSLs are expressed in vascular associated cells of roots, leaves and shoots (DiDonato et al., 2004) indicating that nicotianamine-complexed metals are transported throughout plants. Microarray analysis showed that *YSL3* from *A. thaliana* was down regulated in root-knot nematode infected roots (Hammes et al., 2005), however no other data regarding the expression of this family of transporters in response to pathogen infection is currently available. YSL peptides are grouped within the oligopeptide transporter (OPT) family, and expression of another grapevine OPT homologue was repressed in the powdery mildew infected berry skins approximately 2.6 fold compared with controls. The array study of Hammes *et al*. (2005) reported that expression of two additional OPT genes declined during root-knot nematode infection, however the identity of these genes is not available.

Grapevine aquaporins, one homologous to tonoplast membrane intrinsic proteins (TIP) and one homologous to plasma membrane intrinsic proteins (PIP), were observed to be down regulated in powdery mildew infected grapevine tissue (Table 3.1). A family of at least 8 TIP and PIP aquaporins have been identified in grapevine (Baiges et al., 2001). Specific members are expressed in most grapevine tissues and some are developmentally regulated (Baiges et al., 2001; Picaud et al., 2003). Recent studies indicate that expression of two PIPs are up regulated in water stressed grapevine roots and homologues from other plant species are differentially responsive to stress stimuli (Vandeleur and Tyerman, unpublished data). Individual TIPs and PIPs expressed in *A. thaliana* roots were down or up regulated in response to treatment with 100 mM NaCl, drought and exogenous ABA application (Boursiac et al., 2005; Jang et al., 2004). In tomato, expression of *LeAqp2* is induced within 6 h after inoculation with an incompatible pathogen while expression of *TRAMP*, a closely related gene, was not altered (Werner et al., 2001). Specific aquaporins have

also been shown to be strongly induced in the Rhizobial, arbuscular mycorrhizal and root-knot nematode biotrophic interfaces, further indicating that individual members of the aquaporin gene family are regulated by diverse stimuli (Miao and Werma, 1993; Roussel et al., 1997; Opperman et al., 1994).

Genes associated with photosynthesis were down regulated in the powdery mildew infected berry skins (Table 3.1). At the developmental stage when these berries were sampled, they are green and photsynthetically active and have not yet proceeded into the ripening phase where colour development and sugar accumulation occurs. Reduced activity of key photosynthetic enzymes was measured in barley leaves infected with powdery mildew, while net CO_2 fixation declined in powdery mildew infected grapevine leaves by approximately 50% (Scholes et al., 1994; Brem et al., 1986). Scholes *et al*. (1994) suggested that elevated sugar levels associated with pathogen infection may cause a gradual decline in the Calvin cycle which, in turn, inhibits photosynthetic activity.

3.4.2 Isolation of HT, cwINV, AAP and ProT transcripts by degenerate PCR

Using a degenerate PCR approach new grapevine transcripts that encode putative HT, cwINV, AAP and ProT proteins were isolated. Fillion *et al*. (1999) had previously reported two grapevine HT sequences: *VvHT1* and *VvHT2*. In the current study, three new partial sequences homologous to plant HT peptides were isolated (*VvHT3, VvHT4, VvHT5*), indicating that a family with at least five HT genes is encoded in the grapevine genome: in *A. thaliana* the STP family contains approximately 12 members (Büttner and Sauer, 2000). The TIGR grape gene index (http://www.tigr.org/tigr-scripts/tgi/T_index.cgi?species=grape) contains one EST identical to *VvHT3* (TC47882), however ESTs of *VvHT4* and *VvHT5* were not

identified in the database. Obviously, isolation of the full length cDNAs of *VvHT3*, *VvHT4* and *VvHT5*, and subsequent analysis, will establish if these transcripts do encode functional HT proteins.

Degenerate cloning targeting the cwINV family isolated one transcript homologous to each group, and other non-related sequences. Blast and BestFit analysis of the predicted peptide encoded by cwINV showed that it shares most homology with cwINV peptides from other plant species and considerably less with vINV peptides such as those reported by Davies and Robinson (1996). The TIGR grape gene index contains one EST (TC42830) that shares 96% amino acid identity with the predicted peptide encoded by the cwINV degenerate clone.

As was observed with the cwINV degenerate cloning, one sequence homologous to the AAP and ProT families were isolated amongst other unrelated transcripts. The TIGR grape gene index contains at least four ESTs homologous to the AAP family (TC39577; CF213995; CB342010, CB344631), although none shares more than 60% identity with the predicted AAP peptide encoded by the sequence isolated by degenerate PCR, indicating this clone represents a different form. Furthermore, this suggests there are multiple AAP genes in grapevine, which is consistent with the multi-member AAP family identified in *A. thaliana* (Fischer et al., 1998). In contrast, the TIGR index contains two ESTs identical to the putative ProT partial cDNA isolated by degenerate PCR, but no other sequences that encode peptides that are homologous to ProT proteins.

There are several possible scenarios that would explain why only one sequence belonging to the cwINV, AAP and ProT families were isolated while three HT sequences were identified. Firstly, the species amplified may be the most prevalent forms of the targeted families represented in the template cDNA and

therefore other species may have been amplified at a relatively low frequency. This seems a likely explanation for the ProT and cwINV clones because only one member of these families is found on the TIGR EST database. Alternatively, despite designing the cwINV, AAP and ProT degenerate primers to include the majority of nucleotide possibilities at the conserved motifs targeted, these primers may have some innate bias towards the forms amplified and therefore may not have primed amplification of other related species as efficiently.

3.4.3 Semi-quantitative RT-PCR analysis of selected genes in powdery mildew infected leaves

Semi-quantitative RT-PCR was used to measure the change in abundance of 20 selected transcripts in cDNA prepared from powdery mildew infected leaves compared with cDNA prepared from uninfected control leaves. The largest changes observed were 12.8 fold and 7.1 fold increases in *VvcwINV* and *VvHT5* transcripts in the infected sample, respectively. Both genes are previously unreported in grapevine, however in other plants species, pathogen infection and other stress stimuli are known to induce expression of homologous genes. For example, the expression or enzyme activity of cwINV from *Daucus carota*, *Pisum sativum*, *C. rubrum* and *A. thaliana* is observed to increase in response to infection by a diverse range of pathogen species, and the carrot and *C. rubrum* homologues are also induced by wounding (Sturm and Chrispeels, 1990; Clarke and Hall, 1998; Roitsch et al., 2000; Chou et al., 2000). The two previously reported HTs from grapevine, *VvHT1* and *VvHT2* are developmentally regulated during grape berry ripening, however their expression pattern in pathogen infected or other stressed tissues has not been documented (Fillion et al., 1999; Vignault et al., 2005). The family of

approximately 12 HTs from *A. thaliana* (called STPs for Sugar Transport Proteins) contains two pathogen or wound induced members, *AtSTP4* and *AtSTP3*. *AtSTP4* is rapidly and strongly induced by wounding while *AtSTP3* responds more slowly and by a smaller amount (Truernit et al., 1996; Büttner et al., 2000). A recent study of powdery mildew infected leaves showed that expression of *AtSTP4* and one of four cwINV genes, *AtβFRUCT1*, are co-ordinately induced (Fotopoulos et al., 2003). The proposed physiological significance of the induction of cwINV and HTs in response to pathogen infection suggests the formation of a new carbohydrate sink via elevated phloem unloading of sucrose (Patrick, 1997). Additional carbohydrate may provide energy for host defence or repair, or in terms of the biotrophic interface, increased availability of carbohydrate for pathogen nutrition (Truernit et al., 1996; Fotopoulos et al., 2003). In grapevine leaves infected with powdery mildew, the specific induction of one of eight sucrose cleaving enzymes and one of five HTs indicates that these particular genes contain unique qualities that mediate this responsiveness, or that the localisation of the gene products may be of particular significance during infection.

The other significant change identified by RT-PCR analysis was the differential response of the host phosphate transporters *VvPi1* and *VvPi2*. In leaves, *VvPi1* is constitutively expressed while *VvPi2* expression increases during leaf expansion (J. Malone and I.B. Dry, unpublished data). Interestingly, powdery mildew infection strongly repressed *VvPi1* expression and simultaneously elevated *VvPi2* transcript levels. Expression of specific phosphate transporters from *Medicago truncatula* were also repressed or up-regulated in response to infection with Arbuscular Mycorrhizal (AM) fungi (Liu et al., 1998; Harrison et al., 2002). These fungi associate with a diverse range of plant species and contribute to plant

phosphorus nutrition in exchange for reduced carbon in a mutualistic relationship. *MtPT1* and *MtPT2* are down regulated during the development of the association while *MtPT4* is expressed exclusively in AM infected cells (Liu et al., 1998; Harrison et al., 2002). Furthermore, MtPT4 protein co-localises with the peri-arbuscular membrane, consistent with a role in retrieving fungal released phosphate (Harrison et al., 2002).

Chapter 4 - Isolation and functional characterisation of full length hexose transporter and cell wall invertase genes from grapevine

4.1 Introduction

In *A. thaliana*, rice and tomato, molecular studies and genome sequencing have established that monosaccharide transporters are encoded by multi-member gene families (Büttner and Sauer, 2000; Gear et al., 2000; Toyofuku et al., 2000). In the plant kingdom, the best characterised family is from *A. thaliana*: it contains 14 members which are differentially expressed in response to spatial, temporal and exogenous cues, but are predominantly expressed in sink organs such as roots and reproductive structures (Büttner and Sauer, 2000). All plant monosaccharide transporters characterised range in size from approximately 510 to 560 amino acids and hydrophobicity profiles indicate the presence of 12 membrane-spanning domains with a large cytoplasm-located loop between domains six and seven (Büttner and Sauer, 2000). Using the yeast heterologous expression system, the function of HTs from a range of plant species has been successfully demonstrated. In yeast, plant HT function is sensitive to external pH and the addition of proton ionophores, consistent with proton-symport energetics (Boorer et al., 1992; Gear et al., 2000). Most plant HTs appear to have a strong preference for glucose as substrate, but are capable of transporting other monosaccharides such as fructose, galactose and mannose at lower rates (Weber et al., 1997; Scholz-Starke et al., 2003).

At the commencement of this project, two putative grapevine monosaccharide transporters (*VvHT1* and *VvHT2*) had been reported by Fillion *et al*.

(1999) and more recently, *VvHT1* has been demonstrated to be functional by heterologous expression in yeast (Vignault et al., 2005). In Chapter 3, three partial length cDNAs homologous to plant monosaccharide transporters were cloned from powdery mildew infected leaves. In this chapter, the isolation of full length *VvHT* cDNAs is described and the function and sub-cellular localization of the encoded proteins analysed.

Plant invertases are also encoded by multi-member gene families and their expression and activity is subject to extensive regulation (Tymowska-Lalanne and Kreis, 1998). The encoded proteins are localized to three cellular compartments: the vacuole, cytoplasm and apoplasm, where they catalyse the hydrolysis of sucrose into the hexose monomers, glucose and fructose. In grapevine, Davies and Robinson (1996) reported the isolation of two vacuolar (vINV) isoforms from grapevine, *GIN1* and *GIN2*, however a cell wall invertase (cwINV) has not been previously reported. In Chapter 3, a partial cwINV clone was isolated from powdery mildew infected leaves and in this Chapter the cloning and analysis of a full length cwINV clone is described.

4.2 Materials and methods

4.2.1 RACE PCR and amplification of full length cDNAs

After cloning and sequencing of partial cDNA fragments (Section 3.3.2), full-length cDNA sequences and clones were obtained using RACE PCR techniques (Frohman et al., 1988). For amplification of 3' cDNA ends, target cDNA was amplified using 25 ng of a target-specific forward primer and 25 ng of the oligodT-adapter B26 primer, using grapevine leaf cDNA as template. All target specific

primers were designed to produce approximately 100 nt overlaps with the partial cDNA fragments from Chapter 3 to facilitate unambiguous alignment.

For amplification of 5' cDNA ends, first-strand cDNA was synthesized using 25 ng of a target-specific reverse primer, 1 µg of DNase-treated total RNA and the SuperScript III First-Strand Synthesis System for RT-PCR (Invitrogen) according to the manufacturer's instructions. The cDNA was then purified using the QIAquick PCR purification kit (Qiagen) and resuspended in a final volume of 20 µl. Half of the cDNA reaction was treated with 1 µl of Terminal deoxynucleotide transferase (TdT; Invitrogen) in the buffer supplied and supplemented with 200µM dCTP to add homopolymeric tails of dCTP to the 3'-ends of the cDNAs. C-tailed cDNAs were purified again using the QIAquick PCR purification kit and resuspended in a final volume of 20 µl. Target molecules were amplified from 2 µl of C-tailed cDNA using 25 ng of the AAP (Oligo-dG^{14}) forward primer, which anneals to the homopolymeric tail at the 3'-ends of the cDNAs, and 25 ng of a target-specific reverse primer.

For both 3' and 5' RACE, standard PCR techniques (Section 2.2.1) using 1 unit of recombinant BioTaq Red DNA polymerase (Bioline) were used to amplify the targets. Target DNA was cloned into pGEM T-Easy or pDRIVE vectors and sequenced using T7 and SP6 primers (Table 2.3) as described in Chapter 2.

The RACE sequences were aligned with the degenerate products isolated in Chapter 3 manually using GeneDoc (www.psc.edu/biomed/genedoc) and ORFs and translation products predicted using ORF Finder (http://bioinformatics.org/sms/orf_find.html). After sequence coverage of complete mRNA molecules, new oligonucleotide primers were designed incorporating the predicted initiation and termination codons. Using these primers, full-length cDNAs

were amplified from grapevine powdery mildew infected leaf cDNA with HiFi *Taq* High Fidelity DNA polymerase (Invitrogen) in the buffers supplied and according to the protocols of the manufacturer. These products were cloned into pGEM T-Easy or pDRIVE vectors as described in Chapter 2. All oliognucleotide primers are listed in Table 2.3.

4.2.2 Preparation of DNA constructs for functional characterisation of HTs in yeast

The yeast expression vector p426Met25 (Mumberg et al., 1994), which contains the *URA3* gene for uracil prototrophy and the Met25 promoter for constitutive expression of a trans-gene, was used for heterologous expression of grapevine HTs. Full length cDNAs of *VvHT3*, *VvHT4* and *VvHT5* were sub-cloned from pGEM T-Easy or pDRIVE vectors into p426Met25 via *EcoR*I and *Hind*III restriction sites designed into the forward and reverse primers respectively. After PCR amplification and cloning into pGEM T-Easy, the *VvHT1* full length cDNA was subcloned into p426Met25 via *Bam*HI and *Eco*RI sites designed into the primers. Primer sequences are listed in Table 2.3.

4.2.3 Lithium acetate yeast transformation

Yeast cultures, in 5 ml of YPM, were incubated at 30°C overnight with shaking. The following day, 50 ml of YPM was inoculated with the overnight culture to an OD_{600} of 0.2 - 0.3 and grown at 30°C with shaking for 4 h. Cells were pelleted by centrifugation at 1000 *g* for 5 min, resuspended in 20 ml sterile water, pelleted again, and resuspended in 1.5 ml of YT1. For transformation, 200 ng of

plasmid DNA, 100 µg of denatured salmon sperm DNA, 100 µl of resuspended cells and 600 µl of YT2 were mixed in microcentrifuge tubes. After vortexing, tubes were incubated at 30°C with gentle shaking for 30 min. A 70 µl volume of DMSO was added and the tubes mixed by gentle inversion and incubated at 42°C for 15 min. After cooling on ice for 2 min, cells were pelleted at 16,000 *g* for 15 s and resuspended in 0.4 ml TE buffer. Aliquots of 200 µl of transformation mix was spread on 90 mm plates, and incubated at 30°C for 2 days.

4.2.4 Functional characterisation of HTs in yeast

After selection for uracil prototrophy on minimal media uracil drop-out plates, 5 ml cultures of transformants of strain *EBY.VW4000* carrying p426Met25-*VvHT1*, p426Met25-*VvHT3*, p426Met25-*VvHT4*, p426Met25-*VvHT5* and p426Met25 vector alone, were grown in uracil drop-out media (Table 2.2) overnight at 30°C with shaking. The following day, 100 ml of uracil drop-out medium was inoculated with the overnight culture to an OD_{600} of 0.2 - 0.3 and grown at 30°C with shaking for 4 h or until an OD_{600} of 1.0 - 1.2 was reached. Cells were pelleted by centrifugation, washed twice with 25mM $NaHPO_4/NaH_2PO_4$ (pH 5.0) and resuspended in this buffer at a final concentration of 10 OD_{600} units per ml.

For each measurement, one OD_{600} unit (100 µl) of cell suspension was incubated at 30°C on a shaking water bath for 2 min prior to addition of 100 µl of D-[U-^{14}C]glucose (specific activity: 185 KBq µmol^{-1}; Amersham Biosciences) at the specified concentration in 25mM $NaHPO_4/NaH_2PO_4$ (pH 5.0) and incubated for 30 min. Duplicate samples of 100 µl were pipetted directly into 10ml cold water, filtered onto GF/C filters (Whatman, #1822021) followed by two washes with 15ml

cold water. Filters were removed, placed into scintillant and incorporation of radioactivity determined using a Beckman LS3801 liquid scintillation counter. For competitor and inhibitor studies, D-[U-^{14}C]glucose concentration was 100μM, competing sugars were at 500μM and CCCP was at 50μM. Transport activity was determined per FW of yeast cells.

4.2.5 Analysis of GFP-fusion proteins by micro-projectile bombardment

The pART7 vector (Gleave, 1992) was modified to produce pART7-C'gfp which contains the full length *GFP* ORF (lacking the start codon) downstream of the multiple cloning site (T. Franks, unpublished results), and used to transiently express VvHT3:GFP and VvHT4:GFP fusion proteins in onion epidermal strips. Full length *VvHT3* and *VvHT4* cDNAs were amplified using primers HT3GFPfwd/HT3GFPrev, HT4FLfwd/HT4GFPrev with HiFi *Taq* High Fidelity DNA polymerase and cloned into pART7-C'gfp using *Xho*I and *Xba*I (VvHT3:GFP) or *Eco*RI and *Xba*I (VvHT4:GFP) sites within the primers (Table 2.3). Also used in this experiment was pART7-ATG:GFP (T. Franks, unpublished results) which expresses free GFP. The localization of GFP fusion proteins was determined by bombardment of GFP constructs into onion epidermal strips and subsequent visualization using confocal microscopy.

The internal surface of onion epidermal peels were placed facing up on agar plates containing Murashige and Skoog (MS) Salt Mixture (Invitrogen) and bombarded with the vectors. For four shots, 400 μg of gold particles in 100 μl ethanol were vortexed for 2 min, spun down for 10 s in a microfuge, drained, washed twice with sterile water, and resuspended in 25 μl of 40% glycerol. While gently vortexing, 4 μl of the plasmid solutions (400 ng μl^{-1}), 10 μl of cold 0.1 M

spermidine and 25 µl 2.5 M $CaCl_2$ were added drop-wise and this mixture incubated on ice for 10 min. The particles were spun down, washed with 70% ethanol, resuspended in 24 µl cold absolute ethanol and 6 µl aliquots were placed onto sterile filter holders. After sterilising the gun chamber with 70% (v/v) ethanol, plates containing onion strips on MS media were placed inside, covered with a sterile mesh, and bombarded with a pressure of 650 kPa after evacuating the chamber to 90 kPa. After bombardment, tissue was stored in the dark for 48 h and GFP fluorescence visualised using a Bio-Rad Radiance 2100 Confocal Laser Scanning Microscope System (The Hanson Institute Detmold Family Trust Cell Imaging Centre, Institute for Medical and Veterinary Science, Adelaide, Australia). The excitation wavelength used for GFP detection was 488nm.

4.2.6 Sequence analysis and manipulation

DNA sequences were analysed using various basic local alignment search tools (BLAST) served at the National Centre for Biotechnology Information (NCBI) website (http://www.ncbi.nlm.nih.gov/BLAST/) and the GCG WebAngis Wisconsin software package operated by the Australian National Genomic Information Service (http://www.angis.org.au/). Multiple sequence alignments were drawn by Pile Up or ClustalW (both served at ANGIS), displayed and further manipulated using GeneDoc (www.psc.edu/biomed/genedoc) and after RACE sequences were joined, open reading frames (ORFs) were predicted using ORF Finder (http://bioinformatics.org/sms/orf_find.html). Cellular location and potential signal peptides of deduced amino acid sequences were predicted using PSORT (http://psort.nibb.ac.jp/form.html; Nakai and Horton, 1999), WoLFPSORT (http://wolfpsort.seq.cbrc.jp/; Horton, Park, Obayashi and Nakai, manuscript in

preparation), PLOC (http://www.genome.jp/SIT/plocdir/; Park and Kinehisa, 2003), SignalP 3.0 (http://www.cbs.dtu.dk/services/SignalP/; Bendtsen et al. 2004), IPSORT (http://hc.ims.u-tokyo.ac.jp/iPSORT/; Bannai et al., 2002) and ChloroP (http://www.cbs.dtu.dk/services/ChloroP/; Emanuelsson et al., 1999). Transmembrane helices were mapped using TMHMM Server v.2.0 (http://www.cbs.dtu.dk/services/TMHMM/ ; Krogh et al. 2001) and theoretical isoelectric points were calculated using Iep, served at ANGIS (http://www.angis.org.au/).

4.3 Results

4.3.1 Analysis of full length VvHT sequences

Based on the sequences of the partial clones isolated in section 3.3.2, RACE PCR methods were used to isolated full length cDNAs of *VvHT3*, *VvHT4* and *VvHT5*. The target specific oligos used to amplify 5' and 3' cDNA ends, primed products with approximately 100 bp sequence overlap with the partial clones. Over these overlapping regions, RACE and degenerate clones were observed to share 100% sequence identity and therefore concluded to be fragments from the same transcript (data not shown). These sequences were joined and ORFs predicted using ORF Finder, which identified a single ORF in each sequence between 5' and 3' untranslated regions. New primers were designed to incorporate predicted start and stop codons and these used to amplify full length cDNAs using a high fidelity polymerase. The sequences of full length *VvHT3*, *VvHT4* and *VvHT5* cDNAs were

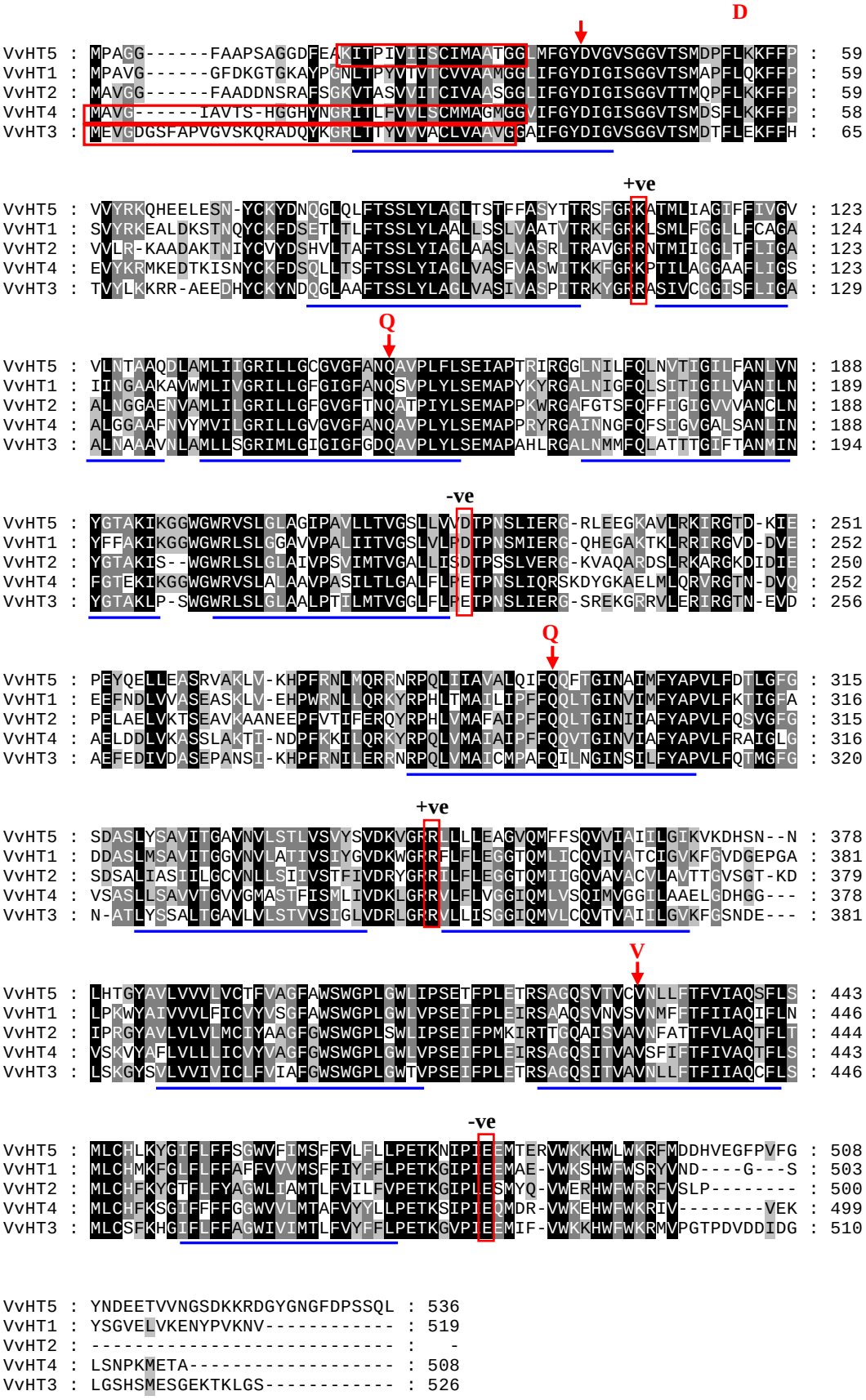

D
+ve
Q
-ve
Q
+ve
V
-ve

Figure 4.1. Amino acid sequence alignment of putative grapevine hexose transporters. The full length sequence of *VvHT3*, *VvHT4* and *VvHT5* were cloned by RACE PCR and the ORF and amino acid sequence was predicted using ORF Finder. Signal peptides are marked with horizontal red boxes, conserved and functionally important residues are marked with arrows, and conserved charged residues are marked with vertical red boxes. Residues predicted to form transmembrane helices are underlined with a blue line. The alignment was made with ClustalX (Thompson et al., 1997). The accession numbers used in the alignment are *VvHT1* (CAA70777), *VvHT2* (AY663846).

found to be identical to the full length sequence obtained by joining the initial partial and RACE cDNA clones.

The predicted ORFs of *VvHT3*, *VvHT4* and *VvHT5* encode peptides of 508, 526 and 536 amino acids respectively (Fig. 4.1) which share approximately 60% amino acid identity with predicted peptides of the previously reported grapevine HT genes *VvHT1* and *VvHT2* (Table 4.1). Most of the homology between the VvHT peptides is located within discrete regions predicted to form twelve transmembrane helices in these proteins (Fig. 4.1 and Fig. 4.2). All three VvHT predicted proteins also show the presence of an approximate 60 amino acid cytoplasmic-exposed loop between transmembrane helices six and seven (Fig. 4.2; residues 220 to 290) which is another typical secondary structural element of plant HTs (Büttner and Sauer, 2000). According to SignalP 3.0, VvHT3 and VvHT4 peptides contain predicted *N*-terminal sorting signals: VvHT3 has an uncleaved signal anchor while VvHT4 has a signal peptide cleaved between resides 32 and 33 (Fig. 4.1). SignalP analysis suggested VvHT5 does not contain a *N*-terminal sorting signal, however it is homologous to VvHT3 around the signal peptide cleavage site predicted by SignalP. Conserved charged residues and other functionally important residues (Will et al.,

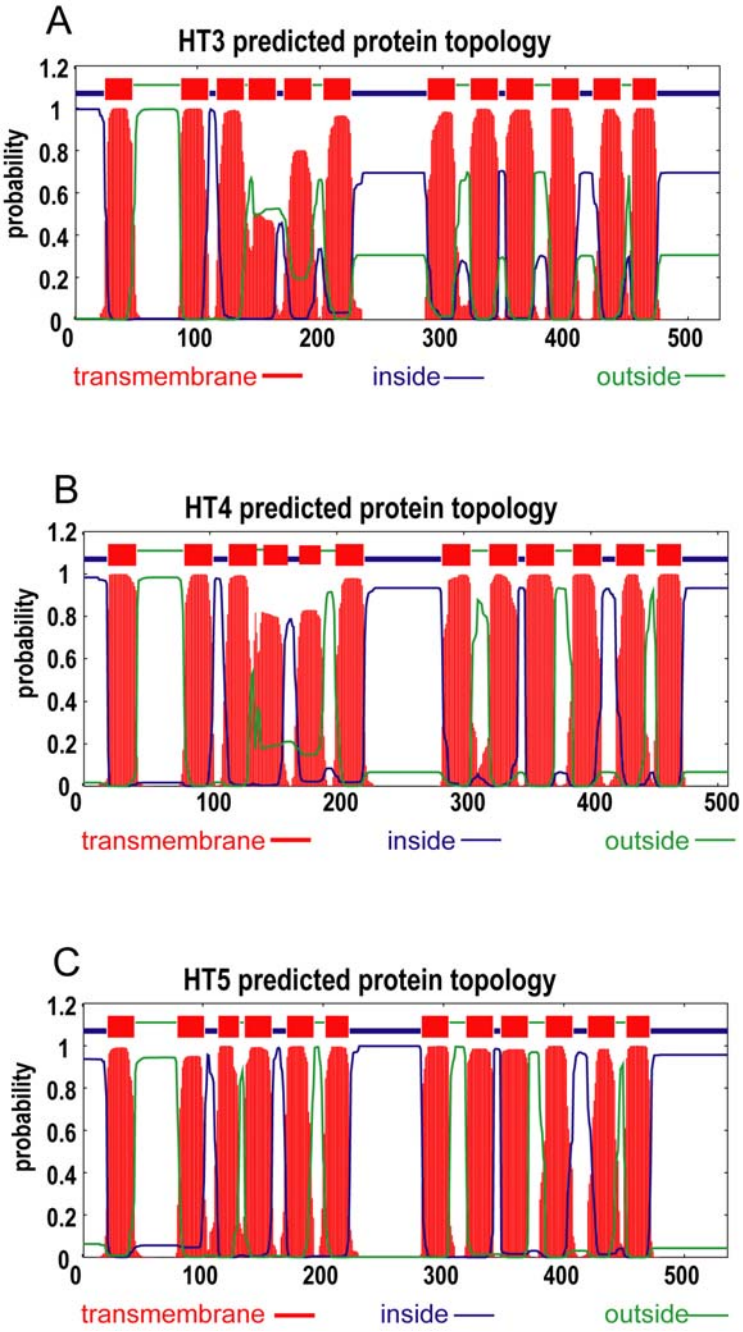


Figure 4.2. Protein topology predicted for VvHT3 (A), VvHT4 (B) and VvHT5 (C) indicates the presence of 12 transmembrane helices and a large cytoplasm-located loop between helices six and seven. THMMH Server v. 2.0 (Krogh et al., 2001) was used to predict transmembrane helices and location of intervening loops.

Table 4.1. Homology between plant hexose transporters. The accssion numbers of the sequecnes used can be found in Figure 4.3. Bolded numbers indicate sequences with the highest level of homology with VvHT3, VvHT4 and VvHT5. The percentage identity and similarity (in brackets) as determined by the Gap algorithm are shown.

	VvHT2	VvHT3	VvHT4	VvHT5	VvHT6	AtSTP1	AtSTP4	AtSTP7	AtSTP8	AtSTP13	CkHUP1	LeHT2	MtST1	NtMST1	RcHex6
VvHT1	57 (66)	56 (64)	58 (66)	58 (68)	26 (35)	83 (88)	62 (72)	56 (64)	51 (63)	59 (67)	46 (56)	57 (67)	82 (87)	81 (87)	57 (67)
VvHT2		53 (64)	56 (66)	53 (63)	25 (35)	57 (66)	53 (65)	52 (62)	48 (60)	54 (64)	43 (53)	52 (63)	56 (65)	56 (67)	54 (65)
VvHT3			58 (67)	56 (68)	24 (32)	56 (65)	54 (64)	**78 (84)**	51 (61)	59 (69)	47 (56)	59 (69)	54 (65)	59 (69)	56 (67)
VvHT4				56 (68)	24 (33)	57 (66)	57 (67)	56 (66)	50 (60)	57 (66)	45 (56)	58 (68)	58 (66)	60 (68)	**80 (88)**
VvHT5					25 (35)	57 (67)	57 (64)	59 (71)	57 (66)	**84 (89)**	47 (57)	**83 (88)**	59 (68)	56 (68)	56 (66)
VvHT6						26 (36)	24 (35)	26 (36)	26 (36)	26 (36)	25 (33)	23 (34)	24 (34)	26 (36)	24 (33)
AtSTP1							62 (71)	56 (65)	51 (64)	58 (66)	46 (56)	55 (65)	80 (85)	80 (85)	58 (67)
AtSTP4								55 (66)	50 (61)	54 (65)	45 (55)	53 (64)	62 (71)	63 (72)	58 (67)
AtSTP7									51 (62)	61 (72)	48 (58)	60 (72)	55 (65)	57 (68)	56 (67)
AtSTP8										58 (67)	47 (58)	60 (68)	51 (62)	53 (66)	50 (60)
AtSTP13											48 (57)	82 (87)	60 (68)	59 (69)	54 (65)
CkHUP1												50 (61)	47 (57)	46 (58)	47 (57)
LeHT2													57 (66)	57 (67)	56 (66)
MtST1														80 (86.	58 (66)
NtMST1															59 (68)

1994) are also present in the grapevine HT peptides and these map to various transmembrane helices and cytoplasm-located loops (Fig. 4.1).

A sixth putative HT sequence from grapevine, *VvHT6* (AAX47312) has also recently appeared on the GenBank database. This transcript encodes a predicted ORF of 740 amino acids, suggested to form 11 transmembrane helices with an approximate 250 amino acid insertion between transmembrane helices six and seven (data not shown). On either side of this insertion, VvHT6 shares significant homology with the other putative grapevine HTs, however overall it is only 30% homologous with these peptides. VvHT6 is homologous to sequences from *A. thaliana* (AAM19835) and rice (XP_464773) however no putative HTs of this type have been functionally demonstrated.

In phylogenetic analysis the grapevine sequences fall into different nodes, indicating that they share more homology with sequences from other plant species than with those from grapevine (Fig. 4.3). VvHT3 shares approximately 80% amino acid identity with AtSTP7 (CAB80698) from *A. thaliana* while VvHT4 shares approximately 80% amino acid identity with RcHex6 (AAA79857; Weig et al., 1994) from *R. communis* (Table 4.1). VvHT5 is most homologous to AtSTP13 (CAC69074) and LeHT2 (AJ132224; Gear et al., 2000) from *A. thaliana* and *Lycopersicon esculentum* respectively. Interestingly, *VvHT1* groups in a node

containing the first HTs isolated from *A. thaliana* (AtSTP1; Sauer et al., 1990), *Medicago truncatula* (Harrison, 1996), *Vicia faba* (VfSTP1; Weber et al., 1997) and *Nicotiana tabacum* (NtMST1; Sauer and Stadler, 1993), while *VvHT2* and *VvHT6* are separated from the other sequences analysed.

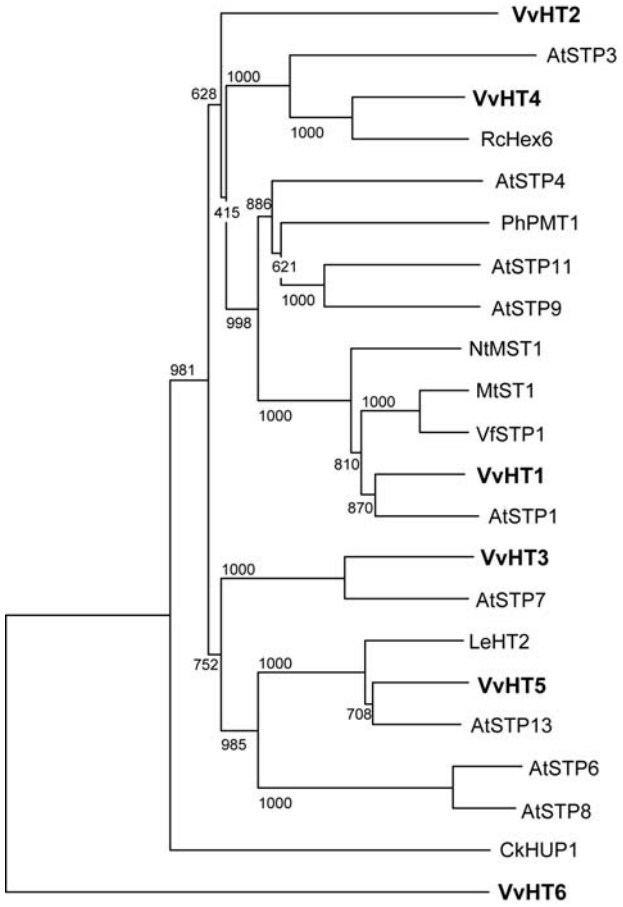


Figure 4.3. Phylogenetic analysis of monosaccharide transporter like sequences from grapevine and other plant species. Multiple sequence alignment was made with ClustalX (Thompson et al., 1997) and phylogenetic analysis was done by the parsimony method with Protpars (Felsenstein, 1989) using VvHT6 as the outgroup. Bootstrap analysis was performed with ClustalX (Thompson et al., 1997), and values shown at internal nodes indicate the occurance of these nodes in 1000 replicates. Database accession numbers of the sequences used are: VvHT6 (AAX47312), VvHT2 (AY663846), AtSTP3 (AJ012399), RcHex6 (AAA79857), AtSTP4 (AB025631), PhPMT1 (AF061106), AtSTP11 (AJ001664), AtSTP9 (AJ001662), NtMST1 (X66856), MtST1 (U38351), VfSTP1 (Z93775), VvHT1 (CAA70777), AtSTP1 (AC007259), AtSTP7 CAB80698), LeHT2 (AJ132224), AtSTP6 (AJ001659), AtSTP13 (CAC69074), AtSTP8 (AF077407), CkHUP1 (X55349).

4.3.2 Functional characterisation of VvHT1, VvHT3, VvHT4 and VvHT5 in yeast

Analysis of the full length sequences of *VvHT3*, *VvHT4* and *VvHT5* suggested that they encode HTs. To demonstrate functionality, each was expressed in the hexose transport-impaired *Saccharomyces cerevisiae* mutant *EBY.VW4000* (Wiezorke et al., 1999) and the rate of D-[U-^{14}C]glucose transport measured. This strain has a very low rate of hexose uptake due to concurrent knockout of 20 endogenous transporter genes, and has been used in recent studies to functionally characterise monosaccharide transporters (Scholz-Starke et al., 2003; Vignault et al., 2005). The functionality of VvHT1 was also tested in this system, and *EBY.VW4000* expressing empty vector was used as a measure of the innate rate of glucose uptake by this strain.

Yeast expressing VvHT1, VvHT4 and VvHT5 accumulated radio-labelled glucose at faster rates than the empty vector control, indicating that they were functional glucose transporters (Fig. 4.4A). In yeast, VvHT1 facilitated the highest rate of glucose transport, estimated to be in excess of 1 μmol min^{-1} g FW^{-1} (Fig. 4.4 A). The rates of glucose transport mediated by VvHT4 and VvHT5 were approximately 10 and 20 fold less than VvHT1 respectively, or approximately 0.1 μmol min^{-1} g FW^{-1} for VvHT4 and 0.04 μmol min^{-1} g FW^{-1} for VvHT5. Glucose uptake into yeast facilitated by VvHT1, VvHT4 and VvHT5 was also sensitive to the pH of the external medium, with uptake rates significantly higher at pH 5.0 than at pH7.0 (Fig. 4.4 B, C and D).

Yeast expressing VvHT3 accumulated radio-labelled glucose at a similar rate to the empty vector control, indicating that VvHT3 was not functioning as a hexose transporter. Even after re-sequencing of the VvHT3 construct, repeat transformation

of yeast and finally re-synthesis of the expression construct and transformation, functionality was not observed.

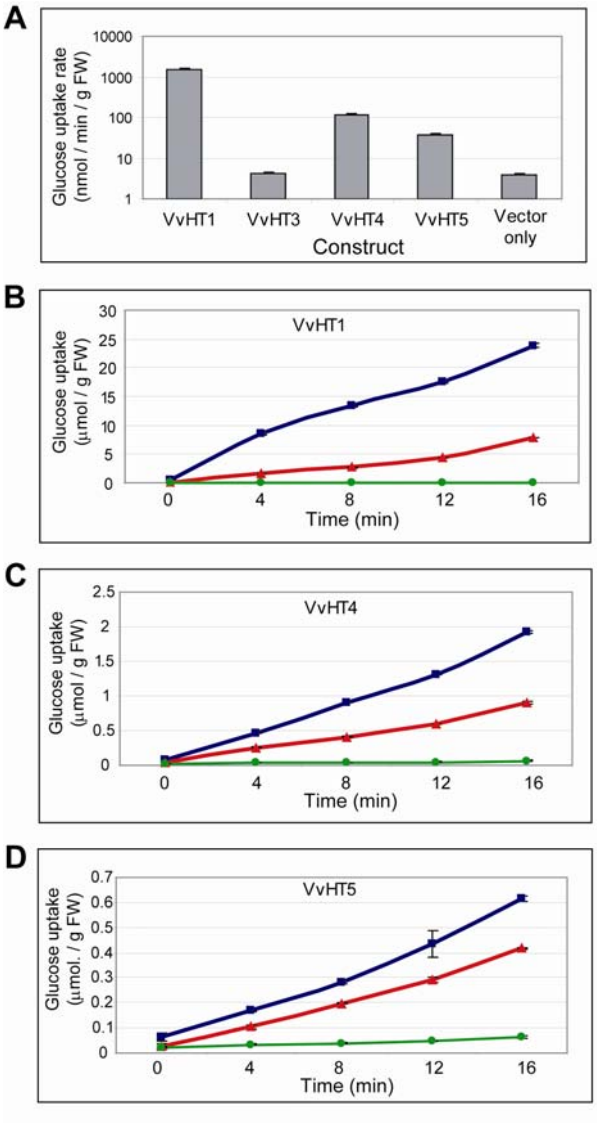


Figure 4.4. Glucose uptake assays in yeast. (A) Relative rates of glucose uptake in yeast expressing grapevine HTs (Note: log scale). (B) Effect of pH on glucose uptake in yeast expressing grapevine HTs. Glucose uptake was measured using 200 µM [^{14}C]-D-glucose in phosphate buffer pH 5.0 (A) or pH as indicated (B, C and D). Yeast strain *EBYVW4000* was transformed with expression constructs containing *VvHT1*, *VvHT3*, *VvHT4* and *VvHT5* ORFs, or empty vector only as a control. Data are means of one transformant tested in duplicate and are representative of two transformants tested. Error bars represent standard errors. ▬ pH 5.0, ▬ pH 7.0, vector only control ▬ .

Each of the functional transporters exhibited concentration-dependant rates of D-[U-^{14}C] glucose uptake (Fig. 4.5 A, C, E). The Lineweaver-Burk double-reciprocal plot of the data displayed a linear relationship, indicating that the glucose transport mediated by these proteins conforms to typical Michaelis-Menten kinetics (Fig. 4.5 B, D, F). Of the three hexose transporters analysed, VvHT1 had the highest affinity for glucose with an estimated K_m for glucose of 67 μM (+/-12.2). VvHT4 and VvHT5 displayed lower affinities for glucose with K_m's of 137 μM (+/-25.5) and 89 μM (+/-12.1) respectively.

To test if VvHT1, VvHT4 and VvHT5 may have affinity for, and therefore potentially transport other sugars, the rate of D-[U-^{14}C]glucose transport was measured in the presence of fructose, galactose, mannose and sucrose supplied at five-fold higher concentrations in an uptake competition assay (Fig. 4.6). Glucose transport by yeast expressing VvHT1 was inhibited more than 60% and 50% by galactose and mannose respectively, and these values were significantly different to controls at the 95% confidence level, as calculated with the student's t-Test. Glucose transport mediated by VvHT4-expressing yeast was slightly inhibited by galactose and mannose, however the students t-Test indicated these values were not significantly different from controls at the 90% confidence level. In contrast, glucose transport facilitated by VvHT5 was not significantly inhibited in the presence of galactose and mannose but was reduced approximately 25% by fructose, significantly different from controls at the 90% confidence level.

The effect of the proton ionophore cyanide *m*-chlorophenylhydrazone (CCCP) on glucose uptake was also tested. CCCP addition ablated transport activity in all yeast lines tested (Fig. 4.6), indicating that a pH gradient across the plasma membrane is essential for VvHT1, VvHT4 and VvHT5 mediated glucose uptake.

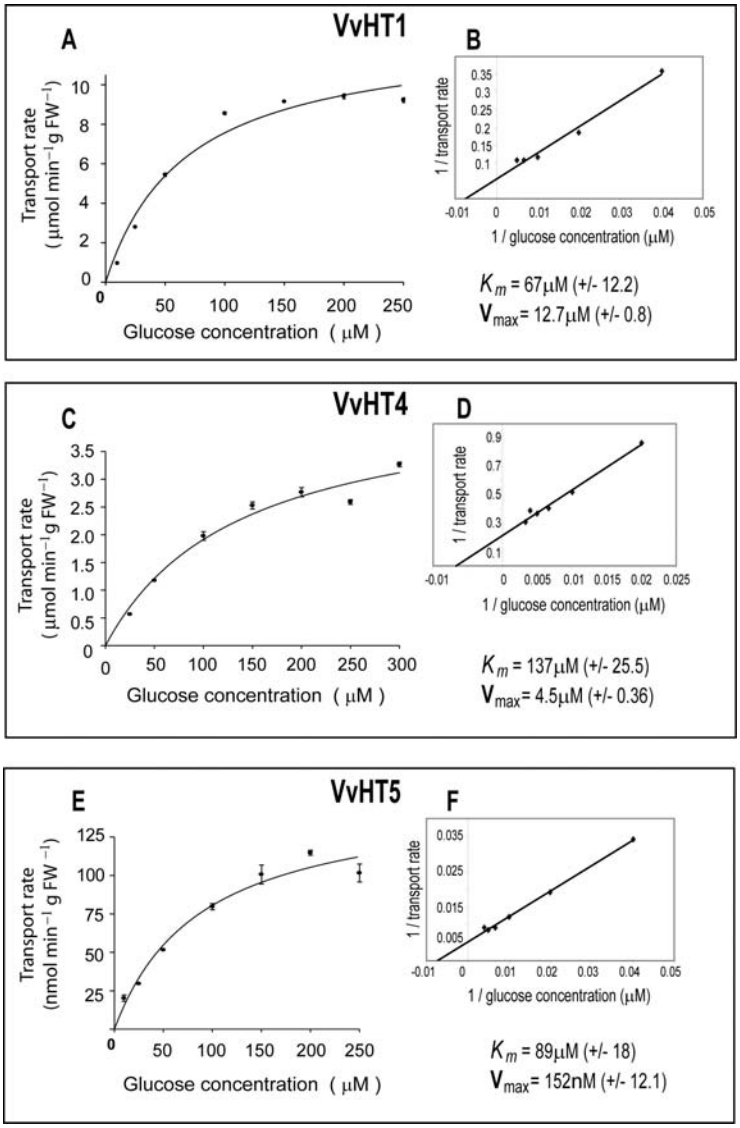


Figure 4.5. Concentration-dependant [^{14}C]-D-glucose uptake by yeast strain *EBY.VW4000* expressing grapevine hexose transporters. (A and B): VvHT1, Michaelis-Menton curve (A), double reciprocal plot (B) and estimate of Km and Vmax.
(C and D): VvHT4, Michaelis-Menton curve (C), double reciprocal plot (D) and estimate of Km and Vmax.
(E and F): VvHT5, Michaelis-Menton curve (E), double reciprocal plot (F) and estimate of Km and Vmax.
Uptake was determined in phosphate buffer pH 5.0. Data are means of one transformant tested in duplicate and are representative of two transformants tested. Error bars represent standard errors. FW= fresh weight.

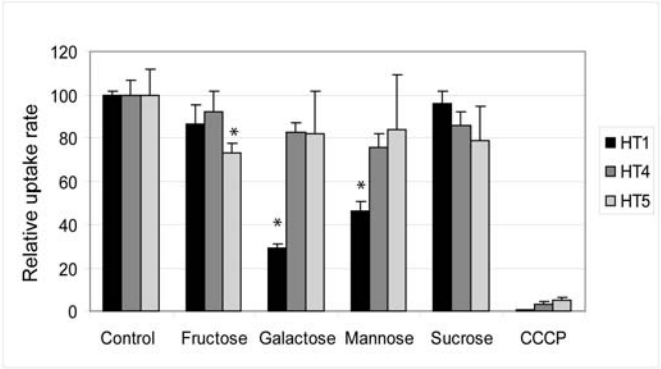


Figure 4.6. Substrate specificity of grapevine hexose transporters. Competitive inhibition of C-glucose uptake by yeast expressing VvHT1, VvHT4 and VvHT5. C-glucose was supplied at 100 mM, competing sugars were supplied at 500 mM and CCCP was supplied at 50 mM. Values are expressed as the percentage of the control without competing sugar and are means of two transformants. Asterix indicates signifcant differences at 90% confidence level. Error bars are standard deviations.

4.3.3 Subcellular localization of VvHT3 and VvHT4 proteins

To be functional in the yeast heterologous expression system, transporters must be targeted to the plasma membrane. To try and gain further information regarding the subcellular localization of VvHT3, which would provide additional information regarding its function and physiological role *in planta*, additional bioinformatic analysis was made. PSORT suggested that VvHT3 may be targeted to the chloroplast or the plasma membrane, while WoLFPSORT and PLOC predicted it is directed to the plasma membrane (Table 4.2). Analysis for potential *N-terminal* sorting signals was more unclear. ChloroP suggested that VvHT3 peptide does not contain a chloroplast transit peptide, while SignalP v 3.0 suggested it may contain an uncleaved signal anchor. Conversely, iPSORT did not detect an *N-terminal* sorting signal in the VvHT3 peptide. The ambiguous results from these bioinformatic analyses were not restricted to VvHT3: WoLFPSORT suggested VvHT4 may be localized to the vacuole membrane, whereas VvHT1 and VvHT4 were predicted by

all three programs to be localized to the plasma membrane. Analysis for *N-terminal* sorting sequences were also unclear, in that the three programs used gave conflicting results.

Table 4.2. Subcellular localisation and *N*-terminal sorting sequences in *VvHT1*, *VvHT3*, *VvHT4* and *VvHT5* peptides, predicted using various bioinformatic tools.

	VvHT1	VvHT3	VvHT4	VvHT5
Subcellular localisation				
PSORT [a]	PM	Chloroplast/PM	PM	PM
Wolf PSORT [b]	PM	PM	PM/Vac	PM
PLOC [c]	PM	PM	PM	PM
N-terminal sorting sequences				
SignalP v 3.0 [d]	Signal anchor	Signal anchor	Signal peptide	Non secretory
iPSORT [e]	Mitochnondrial	No signal	Chloroplast	Chloroplast
ChloroP 1.1 [f]	not present	not present	not present	not present

[a] Nakai and Horton (1999). Predicts subcellular location of proteins.

[b] Updated version of PSORT (Horton, Park, Obayashi and Nakai, in preparation).

[c] Park and Kinehisa (2003). Predicts subcellular location of proteins.

[d] Bendtsen *et al.* (2003). Predicts presence of *N*-terminal sorting sequences and cleavage sites.

[e] Bannai *et al.* (2002). Predicts presence of *N*-terminal sorting sequences.

[f] Emanuelsson *et al.* (1999). Predicts presence of chloroplast transit peptides.

To directly investigate the subcellular localization of VvHT3, the full length cDNA was cloned upstream and in-frame with GFP and downstream of the CaMV 35S promoter. As an example of likely plasma membrane targeting, a C-terminal GFP fusion construct with *VvHT4* was also prepared. The fusion proteins VvHT3:GFP and VvHT4:GFP, together with a native GFP construct, were transiently expressed in onion epidermal cells following biolistic delivery of vector DNA and cellular localization analysed by confocal microscopy.

Free GFP was found to be distributed in both the cytoplasm and nucleus of bombarded onion cells (Fig. 4.7 A). In contrast, VvHT4:GFP and VvHT3:GFP were localized exclusively to the periphery of bombarded cells (Fig. 4.7 B, C and D). Careful analysis of serial optical-sections of both VvHT4:GFP and VvHT3:GFP bombarded cells, established that these fusion proteins were only associated with the cell periphery and were never observed around the inner edge of nuclei, suggesting a likely plasma membrane localization (data not shown).

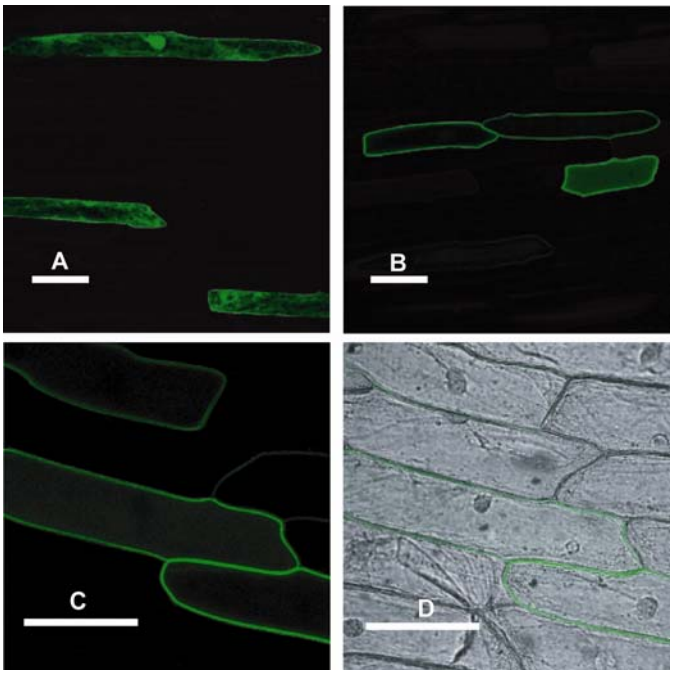


Figure 4.7. Analysis of the cellular targeting of VvHT3:GFP and VvHT4:GFP fusion proteins in onion epidermal cells. GFP alone (A), VvHT4:GFP (B) and VvHT3:GFP (C and D) were expressed in onion epidermal cells using the CaMV 35S promoter following biolistic delivery of vector DNA. VvHT4:GFP was a positive control for plasma membrane localisation. Cells were analysed for GFP fluorescence (A, B and C) by confocal microscopy and false colour applied. Differential phase contrast (DIC) and GFP fluorescence image were merged (D). Bar = 100 mm.

4.3.4 Analysis of full length *VvcwINV*

Using the sequence of the partial cwINV clone isolated in section 3.3.3 by degenerate PCR, RACE PCR methods were used to isolate a full length cDNA. Target specific oligos for 5' and 3' RACE were designed to amplify products with approximately 100 bp sequence overlap with the partial clone isolated earlier. Over the overlapping regions, RACE and degenerate clones shared 100% sequence identity and were concluded to be fragments from the same transcript (data not shown). These sequences were joined, ORFs predicted using ORF Finder, new primers designed incorporating predicted start and stop codons and these used to

amplify a full length cDNA using a high fidelity polymerase. The sequence of full length *VvcwINV* was identical to the full length sequence obtained by joining the initial and RACE cDNA clones (data not shown).

The full length grapevine *VvcwINV* ORF is predicted to encode a peptide of 576 amino acids and contains the proposed active site and other motifs characteristic of invertase enzymes (Fig. 4.8). The first motif, DPNG, is conserved in all invertase isoforms. The second, WECPDFFPV, contains a Cysteine considered important for sucrose catalysis along side other conserved residues (Sturm and Chrispeels 1990). In vINV peptides, this motif is typically WECVDF/LYPV, with the substitution of Valine for Proline characteristic of vINV isoforms (Roitsch et al., 1995). Grapevine VvcwINV shares between 55 - 69% amino acid identity with cwINV sequences from other plant species, less than 50% identity with vINV sequences and only low identity with neutral invertase (nINV) isoforms (Table 4.3).

Phylogenetic analysis of invertase peptides shows that VvcwINV forms a distinct group with cwINV and fructan exohydrolase (FEH) peptides from a range of plant species (Fig. 4.9). Vacuolar INV and nINV sequences group in separate branches. FEH and cwINV sequences share considerable homology and these functionally distinct enzymes cannot be separated for function based on sequence comparison alone. FEH have acidic theoretical isoelectric point (pI) values whilst true VvcwINV have basic pI values (De Conninck et al., 2005). The theoretical pI of VvcwINV, as estimated using the computer program IeP, is 9.7, well within the basic range, suggesting that it does encode a cwINV enzyme and is the first isolated from grapevine (Fig. 4.10 A).

The predicted translation product of *VvcwINV* contains a signal peptide that is predicted to target the protein for secretion to the extracellular space. The signal

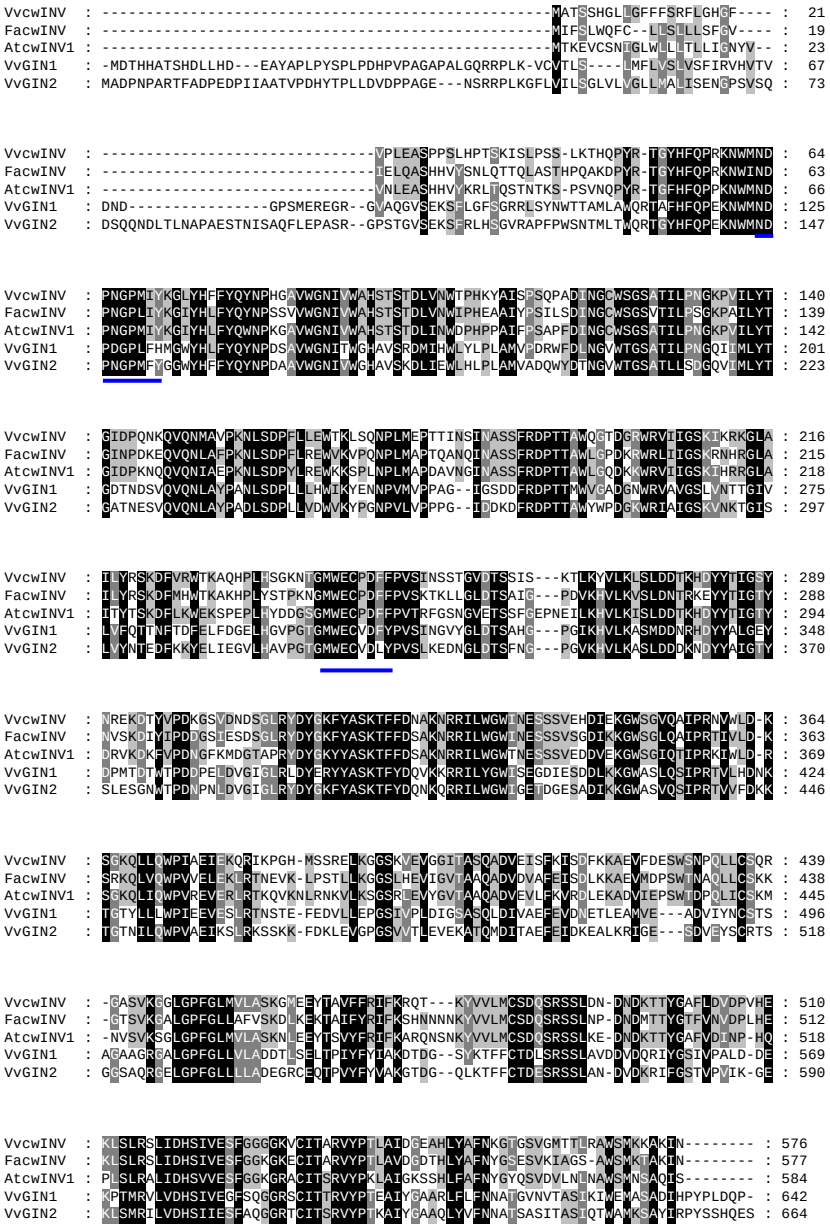


Figure 4.8. Alignment of the full length predicted peptide encoded by *VvcwINV* with grapevine vacuolar invertases (*VvGIN1* and *VvGIN2*) and cwINVs from other plants species. Underlined motifs are conserved in all invertase sequences. Full length *VvcwINV* was cloned by RACE PCR and the ORF and amino acid sequence was predicted using ORF Finder. The alignment was made with ClustalX (Thompson et al., 1997). The accession numbers used are: FacwINV (AF000521), AtcwINV1 (X74514), VvGIN1 (AAB47171), VvGIN2 (AAB47172).

peptide, predicted using SignalP v.3.0, is 26 amino acids in length and contains a prevalence of hydrophobic residues (Met, Ala, Leu, Phe, Val, Trp and

Pro), characteristic of the signal peptides encoded by cwINV sequences from other plants (Fig. 4.10 B). The grapevine VvcwINV signal peptide is predicted to be cleaved inside a motif that is found in cwINV peptides from several plant species which is located approximately 25 residues after the start Methionine.

Table 4.3. Homology between plant invertase peptide sequences. The accession numbers used can be found in Figure 5.8. The percentage identity and similarity (in brackets) as determined by the Gap algorithm are shown. cwINV for cell wall invertase, vINV for vacuolar invertse and nINV for neutral invertase.

	FacwINV	ZmcwINV	AtcwINV1	NtcwINV	VvGIN1	VvGIN2	DcvINV	AtnINV	DcnINV
VvcwINV	69 (74)	55 (62)	66 (73)	57 (63)	46 (53)	47 (54)	47 (56)	14 (29)	50(50)
FacwINV		55 (62)	65 (73)	59 (66)	44 (52)	46 (53)	47 (55)	14 (29)	43 (43)
ZmcwINV			54 (61)	59 (66)	44 (51)	46 (53)	47 (55)	27 (33)	43 (43)
AtcwINV1				60 (68)	44 (51)	45 (52)	47 (55)	43 (52)	42(42)
NtcwINV					43 (51)	45 (52)	45 (52)	25 (33)	16 (33)
VvGIN1						62 (70)	68 (73)	32 (41)	8 (8)
VvGIN2							63 (70)	43 (43)	20(20)
DcvINV								21 (26)	17 (20)
AtnINV									53 (64)

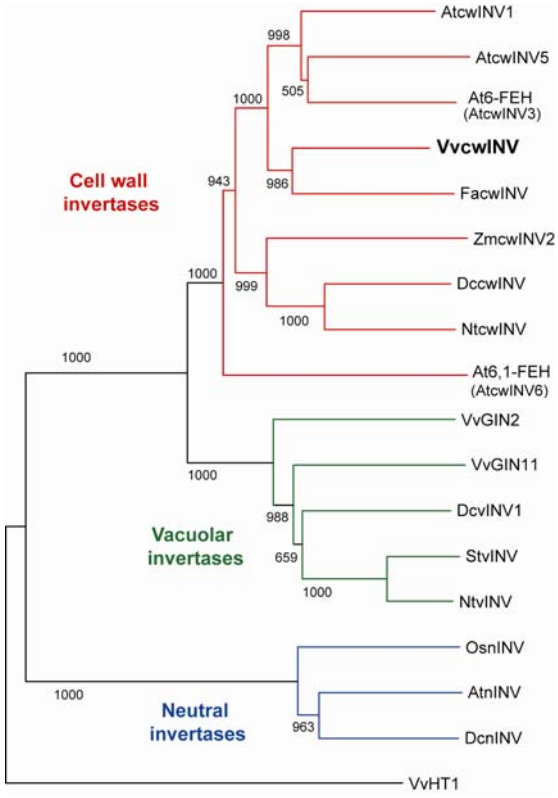


Figure 4.9. Phylogenetic analysis of the predicted amino acid sequences of invertases from grapevine and other plant species. Multiple sequence alignment was made with ClustalX (Thompson et al., 1997) and phylogenetic analysis was done by the parsimony method with Protpars (Felsenstein, 1989) using VvHT1 as the outgroup. Bootstrap analysis was performed with ClustalX (Thompson et al., 1997), and values shown at internal nodes indicate the occurance of these nodes in 1000 replicates. cwINV for cell wall

invertase, vINV for vacuolar invertase and nINV for neutral invertase. Database accession numbers of the sequences used are: VvHT1 (CAA70777), AtcwINV1 (X74514), AtcwINV5 (AP001307), AtcwINV3 (AB029310), FacwINV (AF000521), ZmcwINV2 (AF050128), DccwINV (M58362), NtcwINV (X81834), AtcwINV6 (Ay060553), VvGIN2 (AAB47172), VvGIN1 (AAB47171), DcvINV1 (P80065), StvINV (AAQ17074), NtvINV (CAC83577), OsnINV (BAD53496), AtnINV (AAP40464), DcnINV (CAA76145).

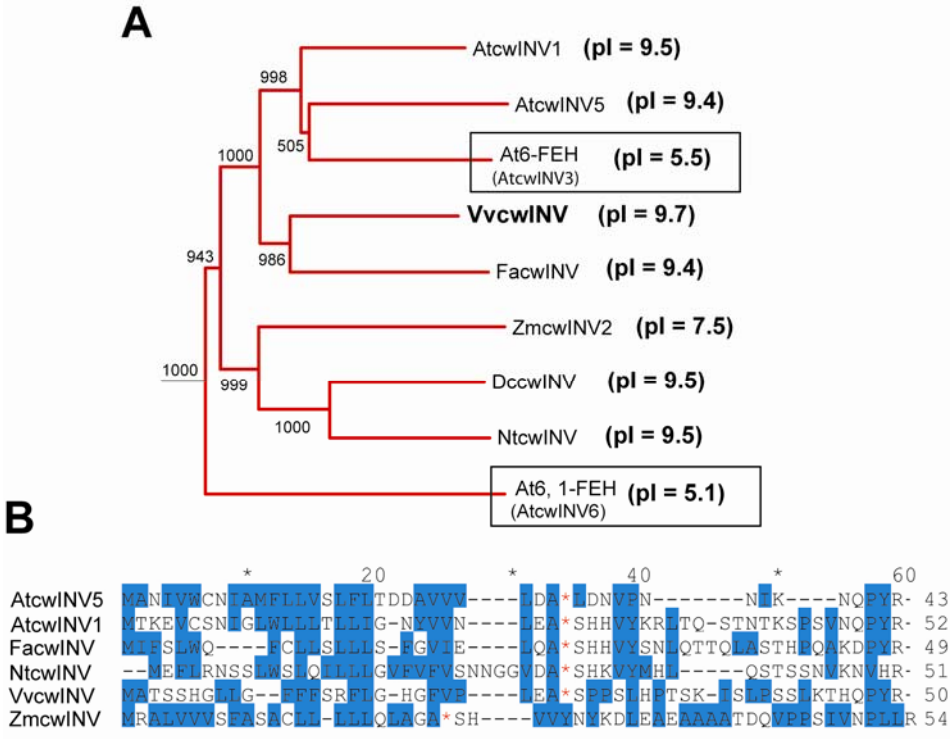


Figure 4.10. (A) The cwINV sub-tree from the phylogenetic analysis preseneted in Figure 4.9. The theoretical isoelectric point (pI) is indicated in brackets and was calculated using the computer program IeP. Fructan exohydrolases from *A. thaliana* are boxed. The accession numbers used can be found in Figure 4.9. (B) Alignment of the first fifty amino acids of cwINV peptide sequences. Hydrophobic non-polar residues are highlighted in blue and predicted signal peptide cleaveage sites are indicated by red asterix. Hydrophobic residues were identified using GeneDoc (Nicholas et al., 1997) and signal peptide cleavage sites were mapped with SignalP v. 3.0 (Bendtsen et al., 2004).

4.4 Discussion

4.4.1 Isolation of full length *VvHT* cDNAs and functional characterisation

In this chapter, full length cDNAs of each of the three partial HT cDNAs isolated in section 3.3.1 were cloned, analysed and functionally tested by expression

in yeast. The inferred peptide products of the three *VvHT* cDNAs are predicted to form secondary structures with 12 transmembrane helices and a large cytoplasmic loop located between helices six and seven. All plant HTs isolated to date have this secondary structure in common and this is a typical feature of members of the major facilitator superfamily (MFS) of uniporter, symporter and antiporter proteins (Büttner and Sauer, 2000). Functionally important conserved residues identified by site-directed mutagenesis and K_m mutant screening of a monosaccharide transporter from *Chlorella kessleri* (CkHUP1) are also present in predicted translation products of *VvHT3*, *VvHT4* and *VvHT5* (Fig. 4.1; Will et al., 1994). The full length sequences isolated in the current study share approximately 60% amino acid identity with the other grapevine HTs excluding *VvHT6*, but up to 80 % identity with HTs from other plant species (Table 4.1). This suggests that the evolutionary ancestors of plants already had several HT genes, theoretically allowing differential regulation and cell-specific monosaccharide uptake, as observed in the higher plants of today (Büttner and Sauer, 2000).

To demonstrate functionality of VvHT3, VvHT4 and VvHT5, each was expressed in a hexose transport-impaired yeast strain (*EBY.VW4000*; Wiezorke et al., 1999) and the rate of D-[U-^{14}C]glucose transport measured. Initially, a complementation assay was employed, however yeast expressing VvHT3, VvHT4 and VvHT5 did not exhibit enhanced growth rates on glucose media indicating that these transporters did not enable sufficient glucose transport to support yeast growth (M. Hayes and I.B. Dry, unpublished data). Subsequently it was decided to attempt a more sensitive assay to determine if these transporters did mediate glucose uptake. Using radio-labelled glucose, yeast expressing VvHT4, VvHT5 and VvHT1 (Fillion et al., 1999) accumulated glucose at faster rates than yeast transformed with the

empty vector suggesting they are functional glucose transporters, however, VvHT3 did not increase this rate and is therefore not functional in yeast. Glucose transport facilitated by VvHT4, VvHT5 and VvHT1 was sensitive to external pH (Fig. 4.4) and the proton ionophore CCCP (Fig. 4.6), indicating that these transporters are energized by the plasma membrane electrochemical gradient and therefore are likely to be H^+/glucose symporters.

VvHT4 shares 80% amino acid identity with RcHex6, one of six putative HT sequences isolated from *R. communis*, however, RcHex6 has not been further investigated (Weig et al., 1994). Phylogenetic analysis (Fig 4.3) grouped VvHT4 and RcHex6 with a third transporter, AtSTP3, which shares 65% amino acid identity (74% similarity) with VvHT4. Of the three grapevine HTs examined, VvHT4 had the lowest affinity for glucose (K_m 137 μM; Fig. 4.5 C). Functional characterisation of AtSTP3 in yeast indicated that this transporter also has a low affinity for glucose, however in this case, the estimated K_m for glucose was 2 mM, approximately 20 fold higher than the K_m of VvHT4 and far higher than the K_m range of 15-80 μM estimated for other plant HTs (Büttner et al., 2000; Büttner and Sauer, 2000). Thus, despite the significant homology between AtSTP3 and VvHT4 peptides, there are major functional differences suggesting that substrate affinity may be determined by a few important amino acid residues. This idea is supported by mutational analysis of CkHUP1, where mutation of amino acids at positions D44, Q179, Q298 and V433 increased K_m values by 10 to 500 fold (Will et al., 1994). It should also be noted that these particular residues are conserved in AtSTP3 and all other functionally determined plant HTs, (including VvHT1, VvHT4 and VvHT5; Fig. 4.1), which suggests there may be additional amino acid residues that determine substrate affinity that have not yet been identified.

VvHT5 is most closely related to the hexose transporters AtSTP13 and LeHT2 (Fig. 4.3) and shares approximately 80% amino acid identity with these peptides (Table 4.1). When expressed in yeast, VvHT5 mediated glucose uptake with a K_m for glucose of 89 μM (Fig. 4.5 E), similar to the K_m estimated for RcHex3 (80 μM) but almost double the K_m estimated for its close homologue LeHT2 (Weig et al., 1994; Gear et al., 2000). The rate of glucose uptake facilitated by VvHT5 was reduced in competition with fructose suggesting glucose and fructose may be potential substrates for this transporter. Initial studies using [^{14}C]fructose indicated that VvHT5 can transport fructose, but at less than half the rate observed for glucose (data not shown).

VvHT1 was the first HT isolated from grapevine (Fillion et al., 1999) and shares more than 80% amino acid identity with AtSTP1, MtST1 and NtMST1, the first HTs isolated from *A. thaliana*, *M. truncatula*, and *N. tabacum* respectively. VvHT1 also mediated glucose transport in yeast with a K_m for glucose of 67 μM (Fig. 4.5 A), which is in close agreement with the report of Vignault *et al*. (2005) where the K_m of VvHT1 was estimated at 70 μM. In competition assays, galactose and mannose strongly inhibited uptake of radio-labelled glucose suggesting they may also be substrates for VvHT1. Vignault *et al*. (2005) also observed this inhibition in competition assays, however expression of VvHT1 only marginally increased the rate of radio-labelled mannose uptake relative to untransformed yeast cells, suggesting that mannose may compete for the active site in VvHT1, but may not transported.

Despite numerous attempts, and observation of all HT-associated hallmarks in the predicted peptide of *VvHT3*, glucose transport activity was never observed in yeast. Bioinformatic analysis of VvHT3 using several software prediction tools

gave ambiguous predictions of its subcellular targeting. However, VvHT3:GFP fusion proteins were localized to the plasma membrane of onion epidermal cells indicating that, at least in plant cells, VvHT3 is targeted to the plasma membrane, and additionally suggesting that targeting problems in yeast may not explain its non-functionality. However, the localisation of VvHT3 in yeast was not determined, therefore it is possible that aberrant targeting may have prevented functionality in this particular heterologous expression system.

The likelihood that a particular HT will function in yeast is unpredictable due to numerous potential problems (N. Sauer, personal communication). It is possible that VvHT3 might facilitate transport of a substrate other than glucose, although all functionally defined plant HTs transport glucose to some degree (Büttner and Sauer, 2000). Alternatively, improper protein folding or a low rate of translation or transcription may have impeded the functional activity of VvHT3 in yeast, however these possibilities were not investigated.

4.4.2 Isolation of a full length *VvcwINV* cDNA and bioinformatic analysis

RACE PCR was also successfully used to obtain the full length cDNA sequence of a grapevine cwINV, the first reported from this plant species. The predicted ORF of *VvcwINV* displays a number of features typical of cwINV enzymes isolated from other plants including an isoform specific active site motif (Sturm and Chrispeels, 1990; Roitsch et al., 1995), a high theoretical pI value (Fig. 4.10A) and a predicted N-terminal signal peptide (Fig. 4.10 B).

Phylogenetic analysis grouped VvcwINV with functionally characterised cwINV peptides and with two functionally distinct fructan exohydrolase (FEH) enzymes from *A. thaliana* (Fig. 4.10 A). Although sequence homology alone is

insufficient to determine if *VvcwINV* encodes a true invertase enzyme, the theoretical pI value can be used to distinguish between cwINV and FEH peptides and thus provide additional evidence (De Conninck et al., 2005). True cwINV enzymes have high pI values whereas FEH enzymes (and vINV isoforms) have low, acidic pI values. VvcwINV was estimated to have a high pI value, suggesting it is a cwINV enzyme and not an FEH.

The first 26 residues encoded by the grapevine cwINV peptide were predicted by Signal P v. 3.0 (Bendtsen et al., 2004) to function as a signal peptide that directs the protein for secretion to the cell wall space. The N-terminal signal sequence of cwINV peptides from grapevine and other plants feature a run of approximately ten hydrophobic residues and a conserved motif that marks the peptidase cleavage site (Fig. 4.10 B; Bendtsen et al., 2004).

Chapter 5 - Quantitative RT-PCR analysis of sugar transporters and invertases in pathogen infected and wounded grapevine tissues

5.1 Introduction

Investigations on powdery mildew infected grapevine and barley leaves have described elevated soluble carbohydrate concentrations, increased invertase activity and decreased assimilation or photosynthetic activity (Brem et al., 1986; Scholes et al., 1994). Investigators have proposed that additional sugars are probably imported from adjacent non-infected and otherwise healthy leaves due to increased phloem unloading mediated, in part, by the elevated invertase activity. More recently, studies employing molecular biology techniques have shown that pathogen infection and wounding elevates expression of specific cwINV and HT genes suggesting that apoplasmic phloem unloading of sucrose is enhanced by these biotic and abiotic stress stimuli (Truernit et al., 1996; Roitsch et al., 2000; Fotopoulos et al., 2003).

In Chapter 3, semi-quantitative RT-PCR analysis indicated that transcript levels of *VvHT5* and *VvcwINV* were elevated 12.8 and 7.1 fold respectively, in powdery mildew infected leaves relative to controls. These leaves were detached from vines, a subset inoculated with spores and incubated for two days under conditions that facilitate maximal infection rates and therefore would be expected to produce a strong host response. To confirm that the gene expression changes reported in Chapter 3 were due to powdery mildew infection and were not an artefact of detachment from the plant and subsequent incubation, expression of sugar transporters and invertases was measured in three additional powdery mildew infected samples and controls. Leaf samples from cv. Cabernet Sauvignon and cv.

Chardonnay vines grown under glasshouse conditions, and berry skin samples from cv. Chardonnay vines grown in a local vineyard were assessed.

The experimental procedures and analysis method were improved from Chapter 3 to yield more informative and robust data by following the quantitative RT-PCR strategy described by Muller *et al*. (2002). In addition to quantifying differences in transcript amounts of a single gene in several cDNA samples, as achieved in Chapter 3, this method can estimate transcript abundance of one gene relative to the abundance of another. This additional layer of information is of importance when quantifying transcript levels of several members of a gene family that may be expressed within the same tissue, as may be the case with the sugar transporter and invertase gene families. Furthermore, this method incorporates vigorous statistical analysis to estimate means and standard errors ensuring validity of the final data.

The specificity of powdery mildew-associated gene expression responses was investigated in several ways. Firstly, transcript levels were measured in discrete powdery mildew infected regions and compared to levels observed in uninfected areas of the same leaf. This comparison was made to determine if gene expression changes were restricted to infected leaf regions as a preliminary experiment to indicate if more time consuming localisation studies by *in situ* hybridisation may be justified. Secondly, to establish if powdery mildew induced gene expression changes were specific to this pathogen or if they may be part of a more general response, the expression of sugar transporters and invertases was monitored in downy mildew infected and wounded leaves. Like powdery mildew, downy mildew is a biotrophic pathogen, however, it infects mesophyll cells while powdery mildew infection is restricted to the epidermis. Wounding was tested as it is an abiotic

stimulus which has been shown in *A. thaliana* and carrot to induce expression of sugar transporters and invertases, reflecting responses observed in pathogen infected tissue (Sturm and Chrispeels, 1990; Truernit et al., 1996; Fotopoulos et al., 2003; Meyer et al., 2004).

5.2 Materials and methods

5.2.1 *E. necator* (powdery mildew) inoculation

E. necator spores grown on detached leaves (section 2.1.5) were transferred to leaves of glasshouse grown *V. vinifera* cultivars Cabernet Sauvignon and Chardonnay using a fine paintbrush. Powdery mildew infected leaves were sampled eight to 10 days after inoculation. Healthy control leaves were sampled from vines grown in a separate glasshouse compartment but maintained under identical temperature and irrigation conditions. Healthy and powdery mildew infected leaves were of similar developmental ages and always sampled at the same time of day.

Young Chardonnay bunches consisting of berries two to four days post flowering were tagged and inoculated with *E. necator* spores grown on detached leaves and suspended in water at a concentration of 1×10^6 spores per ml. Berries were visually inspected for infection and severely infected and healthy berries sampled two weeks after inoculation. Berry skin, seeds and pulp were separated by hand and stored at -80^{o}C before RNA extraction.

5.2.2 Powdery mildew infected and uninfected leaf regions

Discrete powdery mildew infected regions of Cabernet Sauvignon leaves were excised from uninfected leaf areas using a scalpel and these infected regions and the remaining leaf tissue were stored at -80^{o}C until RNA was extracted as described previously. Microscopic observation using a Stemi 2000 microscope (Zeiss, North Ryde, Australia) was used to view leaf surfaces to establish that areas beyond the excised powdery mildew colonies were free of surface mycelia.

5.2.3 *Plasmopara viticola* (downy mildew) inoculation

P. viticola was maintained as described (section 2.1.6). A spore solution containing 1 x10^{6} spores per ml was sprayed on to the abaxial surface of fully expanded leaves on glasshouse-grown potted vines. Inoculated leaves and water-sprayed controls were enclosed in plastic bags overnight to maintain humidity and infected and control leaves sampled 10 DPI and stored at -80°C before RNA was extracted.

5.2.4 Wounding of leaves

The adaxial surface of glasshouse-grown Cabernet Sauvignon leaves were gently rubbed with fine sandpaper and two control and two wounded leaves sampled at 0, 1, 2, 4, 8 and 24 h post-wounding. Leaves were immediately frozen in liquid nitrogen and stored at -80°C before RNA was extracted independently from each leaf.

5.2.5 RNA extraction, DNase treatment and cDNA synthesis

Total RNA was extracted following the method of Rezaian and Krake (1987) and DNase treated as described (section 2.2.12). RNA (2 μg) was reverse transcribed using the SuperScript III First-Strand Synthesis System for RT-PCR (Invitrogen) as described (section 2.2.13).

5.2.6 Quantitative real-time PCR analysis

Expression analysis was carried out by real-time PCR using a SYBR green method on a Rotor-Gene 3000 (Corbett Research, Mortlake, Australia) thermal cycler. Each 15 μl PCR reaction contained: 330 nM of each primer, 3 μl of diluted cDNA (Section 2.2.15), 1 x ABsolute^{TM} QPCR SYBR$^{®}$ Green ROX Mix (Integrated Sciences) and water. The thermal cycling conditions used were 95°C for 15 min followed by 40 cycles of: 95°C for 30 s, 56°C or 58°C for 30 s, and 72°C for 30 s, followed by a melt cycle of 1°C increments from 55 to 96°C. All primer pairs amplified a single product of the expected size and sequence, which was confirmed by melt-curve analysis, agarose gel electrophoresis (section 2.2.2) and DNA sequencing (Section 2.2.11). After testing the suitability of actin (TC45156), ubiquitin (TC38636) and β-tubulin (TC39826) for use as reference genes, actin was selected for normalisation of all pathogen infected and wounded comparisons, while β-ubiquitin expression was used as the reference for the analysis of the grape berry developmental series (see Chapter 6). The expression of each target gene was calculated relative to the expression of actin in each cDNA tested using Rotor-Gene 6.0 software (Corbett Research, Mortlake, Australia) to calculate CT values, observe melt profiles and to measure primer pair amplification efficiencies. Q-Gene software (Muller et al., 2002) was used to calculate the mean normalized expression

level (and the standard error) of each gene in each cDNA tested relative to actin using method two (Equation 3 in Table 2; Muller et al., 2002). The expression of genes belonging to a single gene family were analysed together to produce data representative of the relative expression of these genes. For example, the expression of five hexose transporters were analysed as a group, and six invertases were analysed as a separate group. All primer sequences are described in Table 2.3. The un-normalized expression of actin in pathogen infected and wounded samples is shown in Appenidx 2, Figures A2.1 through A2.4.

5.2.7 Measurement of invertase enzyme activity

Invertase was extracted from grape leaves and enzyme activity measured using the method of Ruffner *et al*. (1995), with some modifications from Tang *et al*. (1996). Briefly, 0.5 g tissue was ground under liquid nitrogen, 1.8 ml of extraction buffer added (0.25 M MES, 20 mM cysteine/HCl, 20 mM DTT, 3 mM EDTA, 5% (w/v) PEG 4000, pH 6.5) followed by further grinding. The semi-thawed slurry was transferred to a 2ml microcentrifuge tube and centrifuged at 10,500 rpm for 10min at 4°C. The supernatant was collected and stored on ice and used as the soluble invertase extract. The pellet was washed three times by resuspending in 1.8 ml ice-cold extraction buffer and subsequent centrifugation as above, before finally resuspending in 1ml acetate buffer (0.2 M Na acetate, 0.2 M acetic acid, pH 4).

To measure invertase activity, 50 µl of cell wall pellet suspension or soluble extract was mixed with 200 µl acetate buffer (pH 4) and 200 µl 0.225 M sucrose and incubated on a rotating wheel for 40 min at 30°C. To stop the reaction, 500 µl of DNSA-reagent (1% (w/v) 3,5-dinitrosalicylic acid, 0.5M KOH, 1M K/Na-tartrate) was added and this mixture placed in a boiling water bath for 10min and then on ice

for 5min. Before the insoluble extract was boiled, tissue debris was removed by centrifugation at 13,000 rpm for 3 min and the supernatant decanted to a new tube and then boiled. Absorbance was read at 560 nm. Protein concentration in extracts was determined using a D_C protein assay kit (Biorad) according to the manufacturer's instructions using bovine serum albumin standards (Fermentas) to make a standard curve.

5.3 Results

Semi-quantitative RT-PCR analysis in Chapter 3 indicated that expression of *VvHT5* and *VvcwINV* is up regulated by powdery mildew infection. To confirm and extend these observations, sugar transporter and invertase transcript levels were measured using a quantitative RT-PCR analysis in additional powdery and downy mildew infected samples, and in leaves wounded with sandpaper.

Selection of a reference gene to normalise the cDNAs being compared is a critical component of any quantitative RT-PCR analysis. In this study ubiquitin (TC38636) and actin (TC45156) transcripts were selected as reference genes after also testing β-tubulin (TC39826). The expression of actin was the most stable of the three candidates in the pathogen infection and wounded treatments and was selected as the reference for these comparisons. Microarray analysis (section 3.3.1; Table 3.1) indicated that transcript levels of ubiquitin were 2.45 fold higher in powdery mildew infected berry skin than control samples. However, actin was found to be more variable when comparing tissues at different developmental stages or from different organs, therefore, ubiquitin was used for comparisons across grape berry developmental series' and for comparing gene expression in different organs

(Chapter 6). β-Tubulin was not a good candidate as it was expressed at a relatively low level and gave inconsistent results. The sequences were obtained from the TIGR Grape Gene Index (http://www.tigr.org/tigr-scripts/tgi/T_index.cgi?species=grape).

5.3.1 Quantitative RT-PCR analysis of hexose and sucrose transporter expression in powdery mildew infected grapevine tissues

Glasshouse-grown Chardonnay and Cabernet Sauvignon grapevine leaves were inoculated with powdery mildew and control (healthy) and infected leaves collected 10 DPI. Additionally, young field-grown Chardonnay berries approximately seven days after flowering were inoculated with powdery mildew and control and infected berries collected 14 DPI. Total RNA was extracted from these samples, genomic DNA removed by DNase treatment and the expression of *VvHT1* and *VvHT2* (Fillion et al., 1999), and *VvHT3*, *VvHT4* and *VvHT5* (Chapter 3) measured using quantitative RT-PCR.

Similar changes to HT transcript levels were observed in powdery mildew infected leaves of Cabernet Sauvignon and Chardonnay, when compared with controls (Fig. 5.1 A and B). In healthy grapevine leaves, a low level of constitutive expression of all *VvHT* genes was observed with *VvHT1* having the highest expression. However, in powdery mildew infected leaf samples, *VvHT*5 transcript levels were strongly elevated by approximately 12 fold and 20 fold, relative to controls, in Cabernet Sauvignon and Chardonnay leaves respectively (Fig. 5.1 A & B). *VvHT1* was also induced in response to powdery mildew infection but to a much smaller degree, approximately 3-4 fold compared to healthy leaves. In contrast, the

expression of *VvHT2* and *VvHT3* and *VvHT4* showed little or no response to PM infection.

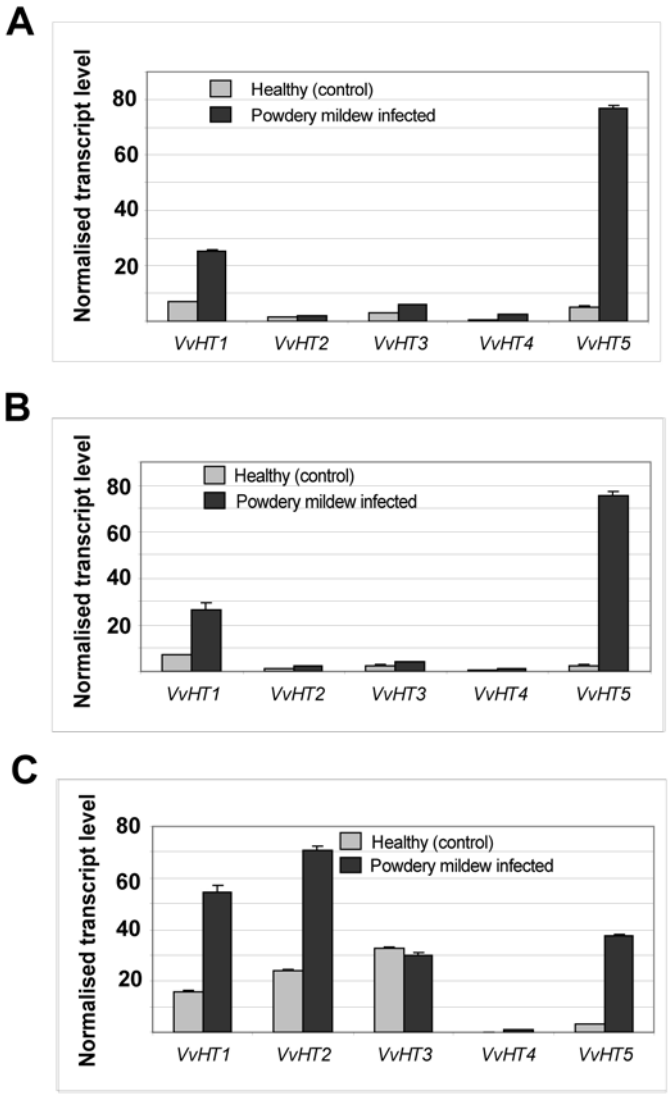


Figure 5.1. Quantitative RT-PCR analysis of HT expression in powdery mildew infected grape tissues.
(A) Cabernet Sauvignon leaves
(B) Chardonnay leaves
(C) Chardonnay berry skin

All values were normalised to the expression of actin and each is the average of one sample tested in triplicate. Analysis was performed using the method of (Muller et al., 2002) which allows comparison of expression level between the genes in each figure. Error bars represent the standard error, primer sequences are in Table 2.3.

A somewhat different *VvHT* expression pattern was observed in Chardonnay berry skin samples (Fig. 5.1 C). In the skin of healthy berries, *VvHT1*, *VvHT2* and *VvHT*3 were expressed considerably more than *VvHT4* and *VvHT5*. As in leaves, powdery mildew infection of Chardonnay berries resulted in a marked increase of *VvHT5* transcript levels in skin tissue (~12 fold) and a lower induction of *VvHT1* (~ 3 fold). However, *VvHT2* expression was also up regulated by approximately 3 fold and was therefore the most highly expressed *VvHT* gene in infected berry skin. As was observed in grapevine leaves, *VvHT4* was the least expressed of the VvHTs.

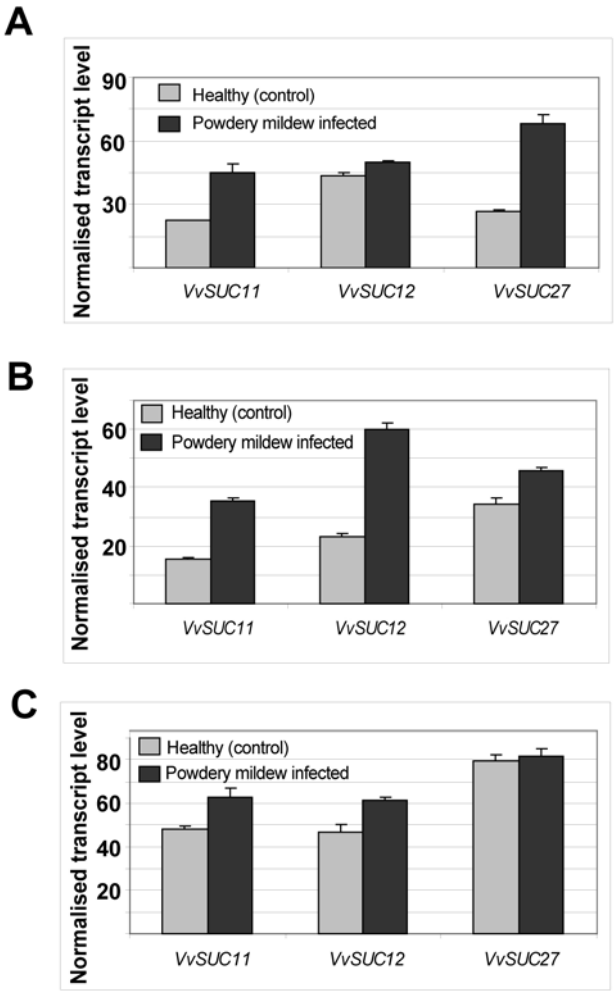


Figure 5.2. Quantitative RT-PCR analysis of sucrose transporter expression in powdery mildew infected grapevine tissues.
(A) Cabernet Sauvignon leaves
(B) Chardonnay leaves
(C) Chardonnay berry skin

All values were normalised to the expression of actin and each is the average of one sample tested in triplicate. Analysis was performed using the method of (Muller et al., 2002) which allows comparison of expression level between the genes in each figure. Error bars represent the standard error, primer sequences are in Table 2.3.

The expression of three sucrose transporters reported by Davies *et al*. (1999) was also monitored in powdery mildew infected and control leaf and berry samples (Fig. 5.2 A-C). It can be seen that while there was a general trend for the expression of these sucrose transporter genes to be up regulated in response to powdery mildew infection, the size of the response was much smaller than observed for *VvHT1* and especially *VvHT5*, and no common trend was apparent between the different samples.

5.3.2 Quantitative RT-PCR analysis of invertase expression in powdery mildew infected grapevine tissues

Transcript levels of *VvcwINV* were measured in the powdery mildew infected and control samples described above and compared with levels of two vacuolar invertases, (*VvGIN1* and *VvGIN2;* Davies and Robinson, 1996) and three grape ESTs (TC7206, TC11451, TC11207; retrieved from the TIGR Grape Gene Index) which share between 84% and 87% identity with nINV homologues from carrot (CAA76146) and *A. thaliana* (CAB45447). With the exception of TC11207 which is expressed at a low level in the samples measured, all of the invertase genes investigated were constitutively expressed in healthy leaves of both grape cultivars examined. The only major difference was that in healthy Cabernet Sauvignon leaves, *VvGIN1* transcript levels were significantly higher compared with transcript levels of the other invertases tested, while in Chardonnay, this difference was smaller (Fig. 5.3 A and B). In the powdery mildew infected Cabernet Sauvignon

and Chardonnay leaf samples, *VvcwINV* expression was elevated more than 9 and 4 fold respectively. In contrast, transcript levels of *VvGIN1* were strongly reduced more than 10 fold in both leaf samples. Also worth noting, expression of TC7206, one of three nINV-homologous ESTs was up regulated approximately 3 fold in powdery mildew infected leaf samples from both cultivars. To summarise, in the powdery mildew infected leaf samples *VvcwINV* transcripts are significantly more abundant than any of the other invertase transcripts measured.

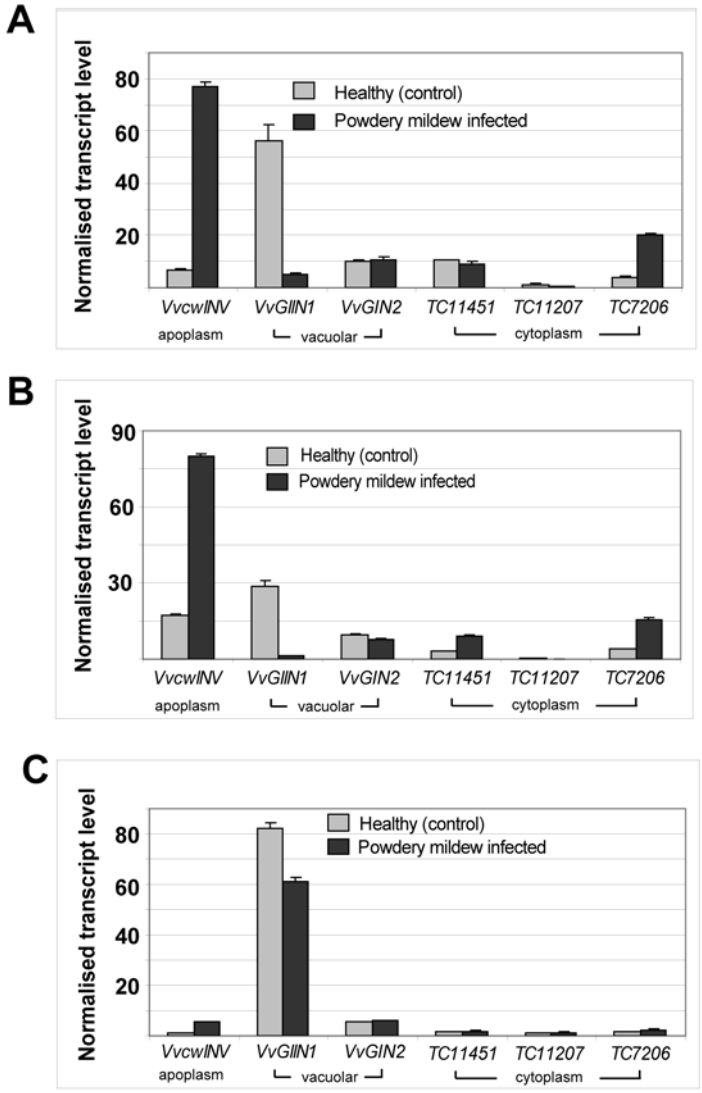


Figure 5.3. Quantitative RT-PCR analysis of invertase expression in powdery mildew infected leaves and berry skin.
(A) Cabernet Sauvignon leaves
(B) Chardonnay leaves
(C) Chardonnay berry skin

All values were normalised to the expression of actin and each is the average of one sample tested in triplicate. Analysis was performed using the method of (Muller et al., 2002) which allows comparison of expression level between the genes in each figure. TC numbers correspond to sequences on the TIGR grape gene index. Error bars represent the standard error, primer sequences are in Table 2.3.

As observed in the leaf samples, *VvGIN1* showed the highest levels of gene expression in healthy Chardonnay berry skin (Fig. 5.3 C). However, in contrast to the response of powdery mildew infected leaf samples, *VvGIN1* expression was only slightly reduced in the powdery mildew infected berry skin sample. Furthermore, while *VvcwINV* was induced approximately 4 fold in the powdery mildew infected sample, the level of *VvcwINV* expression was approximately 10 fold less than the amount of *VvGIN1* transcripts in the powdery mildew infected sample. The other invertase transcripts quantified were expressed at relatively low levels in Chardonnay berries and were not significantly altered by powdery mildew infection.

5.3.3 Effect of powdery mildew infection on grape leaf acid invertase activity

The relative sucrolytic activity of soluble and insoluble extracts obtained from healthy and powdery mildew infected leaves are shown in Figure 5.4. The rate of sucrose hydrolysis is expressed on a h^{-1} g FW^{-1} basis to allow comparison with previous reports of invertase activity in grapevine tissues (Ruffner et al., 1990). In the buffer (pH 4) used for the assay, *VvcwINV* activity is measured in the insoluble pellet suspension and mainly vINV activity contributes to the soluble sucrolytic activity. In the healthy Cabernet Sauvignon leaf samples, the average rate of invertase activity in the soluble fraction was 82.5 μmol sucrose hydrolysed h^{-1} g FW^{-1} while in the insoluble pellet suspension the average rate of invertase activity was 23.9 μmol sucrose hydrolysed h^{-1} g FW^{-1} or approximately 3.5 fold less. These rates

are similar to those published by Ruffner *et al*. (1990) where soluble and cell wall associated activities were approximately 72 and 25 µmol sucrose hydrolysed h^{-1} g FW^{-1} respectively. In contrast, in powdery mildew infected leaf samples, the soluble activity was decreased by 55% to 45.9 µmoles sucrose hydrolysed h^{-1} g FW^{-1} while the insoluble invertase activity was found to be increased by 2.5-fold to 61.6 µmol sucrose hydrolysed h^{-1} g FW^{-1} which is in agreement with the observed increase in *VvcwINV* transcript levels (Fig. 5.3 A).

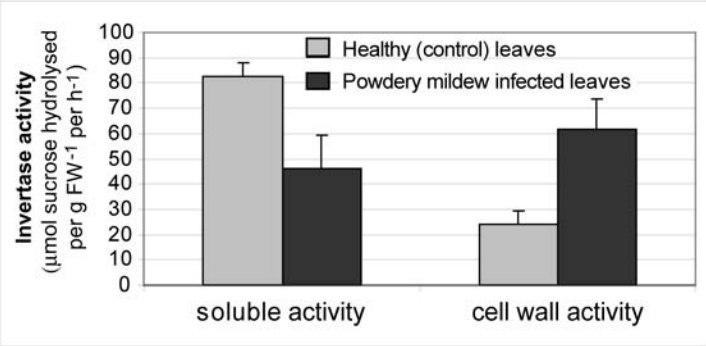


Figure 5.4. Acid invertase activity assays on soluble (vINV) and insoluble (cwINV) extracts from healthy and powdery mildew infected leaves. Invertase assays were performed in 0.1M accetate buffer, pH4.0. The values plotted are the averages of two independant extractions of 0.5 g leaves, each extraction tested in triplicate. Error bars represent one standard deviation.

5.3.4 Localisation of VvHT and invertase expression relative to powdery mildew infection sites

To investigate if powdery mildew induced gene expression changes were restricted to infected leaf regions and therefore may be specific to infected cells, transcript levels of *VvHT1*, *VvHT5*, *VvcwINV* and *VvGIN1* were measured in discrete powdery mildew infected regions and compared to levels observed in uninfected areas of the same leaf. As an infection-specific positive control, expression of a powdery mildew induced grapevine germin-like protein homologue (*VvGLP3*; AY298727) was measured in these samples. Unpublished RT-PCR analysis and

localisation studies using transgenic *A. thaliana* plants expressing the GUS reporter gene under control of the *VvGLP3* promoter indicate that expression of this gene is induced specifically in powdery mildew infected epidermal cells (D. Godfrey and I. B. Dry, manuscript in preparation). Relative to uninfected leaf regions, *VvGLP3* transcript levels were more than five fold higher in powdery mildew infected areas, consistent with previous data regarding its specificity (Fig. 5.5). In contrast, *VvHT1*, *VvHT5*, *VvcwINV* and *VvGIN1* transcript levels were reasonably similar in infected areas and in uninfected regions indicating that powdery mildew induced expression of these genes is not highly specific for the infection site.

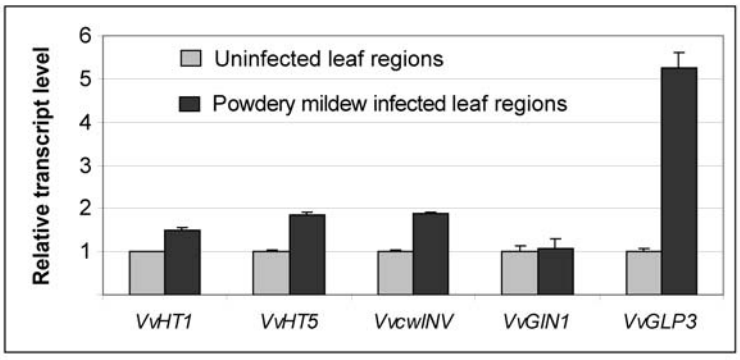


Figure 5.5. Localisation of transcripts of powdery mildew responsive genes by semi-quantitative RT-PCR. cDNA was synthesised from powdery mildew infected leaf regions and from uninfected areas of the same leaf. The ratio of transcript levels in infected areas : uninfected areas was caluclated using semi-quantative RT-PCR. All values were normalised to the expression of actin and each is the average of one sample tested in triplicate. Error bars represent the standard error, primer sequences are in Table 2.3.

5.3.5 Changes in expression of VvHTs, SUCTs and invertases in downy mildew infected grape leaves detected by quantitative RT-PCR

Leaves were inoculated with grapevine downy mildew (*P. viticola*) by spray application to the under dermis of fully expanded leaves. Control and infected leaves were sampled 10 days post inoculation. Leaf age was matched by size and node position. Relative transcript levels of VvHT genes in control leaves were similar to those observed in Figure 5.1 A with *VvHT1*, *VvHT3* and *VvHT5* expressed

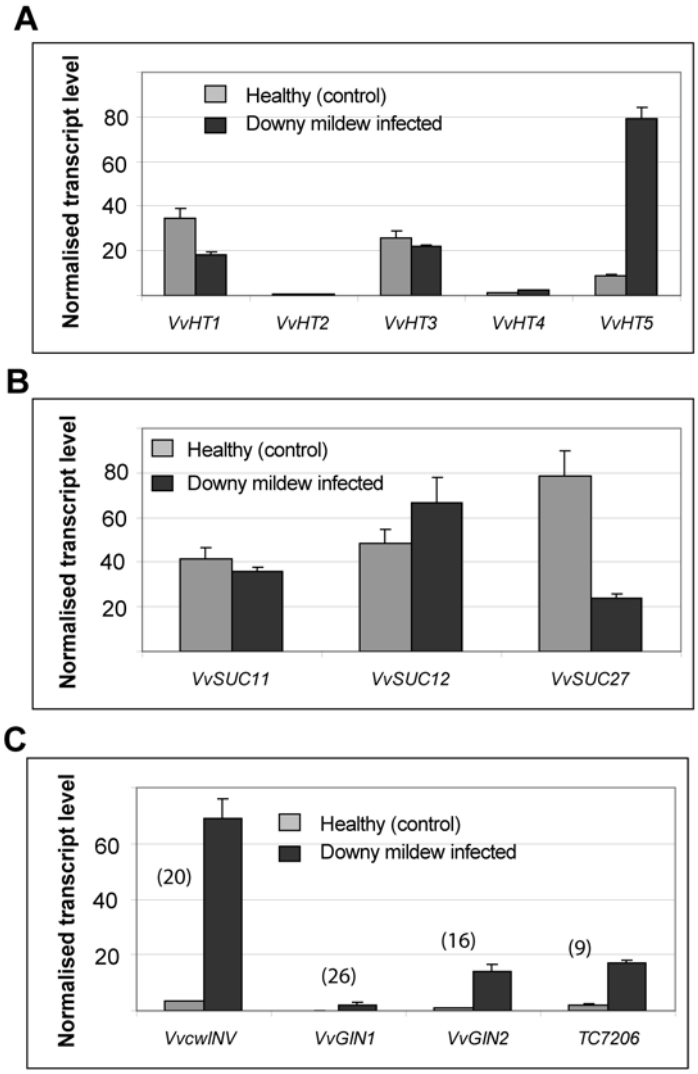


Figure 5.6. Quantitative RT-PCR analysis of HTs (A), sucrose transporters (B) and invertases (c) downy mildew infected Cabernet Sauvignon leaves. All values were normalised to the expression of actin, each value is the average of three replicates and are representative of two infected and control samples tested. Numbers in brackets are the fold change in expression between the control and infected samples. Analysis was performed using the method of (Muller et al., 2002) which allows comparison of expression level between the genes in each figure. Error bars represent the standard error, primer sequences are in Table 2.3.

more than *VvHT2* and *VvHT4* (Fig. 5.6 A). In downy mildew infected samples, transcript levels of *VvHT*5 increased more than 6-fold relative to the control sample and became the most highly expressed *VvHT* in the downy mildew infected leaf by approximately 4 fold. Expression of the other *VvHT*s was only moderately affected

or not altered by downy mildew infection. Interestingly, while expression of *VvHT1* was induced approximately 4 fold in powdery mildew infected leaves (Fig. 5.1A), it was slightly repressed in response to downy mildew infection (Fig. 5.6 A). Expression of the sucrose transporter genes *VvSUC11* and *VvSUC12* in the downy mildew sample was not significantly different from the control sample, however, *VvSUC27* transcript levels were approximately three fold lower in infected samples (Fig. 5.6 B).

Invertase transcript levels were very low in downy mildew control samples in comparison to the levels observed in powdery mildew control samples (Fig. 5.3). In downy mildew infected samples, expression of all invertase genes examined was dramatically elevated (Fig. 5.6 C). *VvcwINV* transcript levels increased by more than 20 fold, *VvGIN1* and *VvGIN2* expression was enhanced 26 fold and 16 fold respectively, while the nINV EST homologue TC7206 was induced 9 fold. However compared to the level of *VvcwINV* expression in downy mildew infected samples, these transcript levels were relatively low.

5.3.6 Effect of wounding on VvHT and invertase expression in grape leaves

Leaves were wounded by abrasion of the upper surface with sandpaper and wounded and control leaves collected at 1 h, 2 h, 4 h, 8 h and 24 h after the wound event. Two wounded and two control leaves of similar age, (as defined by node position and size), were collected at each time point. Quantitative RT-PCR analysis revealed that both *VvHT5* and *VvHT1* were significantly induced within 1-2 h following the wounding treatment (Fig. 5.7 A). *VvHT5* transcript levels were approximately 4 fold higher than controls 1 h after wounding and approximately 10 fold higher after 2 h. Expression levels then appeared to gradually decline over the

next 4-24 h but remained significantly higher than in control leaves during this period. The response of *VvHT1* to the wounding treatment was more transient and less pronounced than *VvHT5*. Expression was elevated approximately 2 fold compared to control leaves 2 h after wounding and had declined back to control levels within 8 h after wounding. There were no significant differences in *VvHT4* transcript levels between the wounded and control samples. *VvHT*2 which was expressed at a relatively low level, was slightly but consistently down regulated in the 2 h, 4 h and 8 h wounded samples. Similarly, transcript levels of *VvHT*3 were also lower than controls in the 2 h, 4 h and 8 h wounded samples.

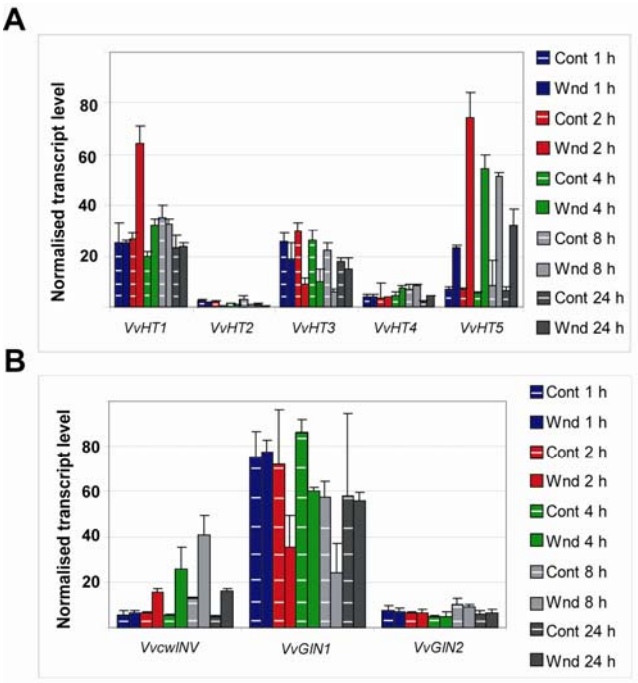


Figure 5.7. Quantitative RT-PCR analysis of VvHTs (A) and invertases (B) in wounded Cabernet Sauvignon leaves over a 24 h time period. All values were normalised to the expression of actin and each is the average of two biological replicates tested in triplicate. Analysis was performed using the method of (Muller et al., 2002) which allows comparison of expression level between the genes in each figure. Cont = control, Wnd = wounded. Error bars represent the standard error, primer sequences are in Table 2.3.

Transcript levels of *VvcwINV* were also higher in wounded samples compared to controls, but the timing of induction was delayed relative to *VvHT5*

(Fig. 5.7 B). *VvcwINV* expression was not elevated in the 1 h wounded sample but gradually increased over the 2 h, 4 h and 8 h period. Transcripts of *VvcwINV* were still considerably higher than controls in the 24 h wounded sample. *VvGIN1* expression appeared to be repressed in the 2 h, 4 h and 8 h wounded leaves compared to controls, but returned to the control level after 24 h. In contrast, *VvGIN2* transcript levels were not significantly different in control and wounded samples.

5.4 Discussion

Invertase, and sucrose and monosaccharide transporter activities, contribute to carbohydrate sink metabolism and the genes that encode these proteins are regulated by numerous endogenous and exogenous cues. Infection with fungal pathogens such as powdery or downy mildew elicits alterations to normal host carbohydrate distribution which result in elevated soluble carbohydrate concentrations and repressed photosynthetic activity (Brem et al., 1986; Scholes et al., 1994 Abood and Losel, 2003). A candidate gene approach was commenced to identify new grapevine genes that may mediate these carbohydrate changes. Based on a review of literature concerning host responses to biotrophic pathogen infection, the monosaccharide and cwINV gene families were targeted. In Chapters 3 and 4, cDNAs encoding three new HTs and a new cwINV were isolated from cDNA prepared from powdery mildew infected leaves, while preliminary RT-PCR analysis suggested *VvHT5* and *VvcwINV* transcript levels are elevated in infected leaves, compared to controls. To confirm and extend these observations, quantitative RT-PCR methods have been used to measure invertase and sugar transporter gene expression in additional powdery mildew infected samples, and in downy mildew

infected and wounded leaves. Together, these studies indicate that expression of specific invertase and sugar transporter genes are induced in pathogen infected and wounded tissues.

5.4.1 Powdery mildew infection

Gene expression studies carried out on leaves from two different grapevine cultivars showed that powdery mildew infection was accompanied by a strong increase of *VvcwINV* transcripts and reduced expression of the vacuolar invertase *VvGIN1* (Fig 5.3). *VvcwINV* expression was also enhanced in infected berry skin, however, relative to *VvGIN1* expression, this gene was expressed at a low level. As *VvcwINV* was cloned as part of this study, there is no pre-existing data concerning the expression of this gene in grapevine. However, previous research on carrot (Sturm and Chrispeels, 1990), *A. thaliana* (Chou et al., 2000; Fotopoulos et al., 2003) and *C. rubrum* (Roitsch et al., 2000), has shown that exogenous stimuli such as pathogen infection and wounding can elevate cwINV transcript levels and activity. *VvGIN1* is one of two vINV genes cloned from grape berries by Davies and Robinson (1996) who showed that *VvGIN1* transcript levels are much higher than *VvGIN2* levels in expanding leaves and in berries. The quantitative RT-PCR analysis presented in this chapter is consistent with these observations.

Although the magnitude of the changes to soluble and insoluble invertase enzyme activity were not as large as those observed in *VvcwINV* and *VvGIN1* gene expression, enzyme assays were in agreement with the transcriptional analysis, indicating that infected leaves contained reduced vINV activity and approximately two fold increased cwINV activity (Fig. 5.4). In reference to the soluble enzyme, the apparent stability of grapevine vacuolar invertase activity may underlie the

discrepancy between gene expression and enzyme activity, because in grape berries soluble acid activity remains strong six weeks after expression of *VvGIN1* and *VvGIN2* has stopped (Davies and Robinson, 1996).

Initial studies on powdery mildew infected barley, grapevine and pea leaves concluded that acid invertase activity was elevated compared with healthy tissue, however, these investigations did not examine the potential contribution of cell wall associated forms to the elevated sucrolytic activities observed (Hwang and Heitefuss, 1986; Brem et al., 1986; Storr and Hall, 1992). By measuring invertase activity in apoplasmic washing fluids prepared from control and powdery mildew infected pea leaves, Clarke and Hall (1998) demonstrated that extracts from infected leaves contained nearly four fold more invertase activity and also, higher concentrations of glucose and fructose. Fotopoulos *et al*. (2003) also observed a similar increase in cell wall associated invertase activity and gene expression in powdery mildew infected *A. thaliana* leaves. According to Hall and Williams (2000), all forms of invertase activity are elevated in powdery mildew infected wheat, however the biggest increase is observed in cwINV activity. Thus, the results obtained in the current study support previous observations indicating an important role for apoplasmic sucrose cleavage in the establishment of powdery mildew infection.

In coordination with the powdery mildew induced elevation of *VvcwINV* expression and enzyme activity, was increased expression of specific grapevine monosaccharide transporters. Of the five studied, expression of *VvHT5* and *VvHT1* was significantly enhanced in powdery mildew infected leaves while the other three transporters did not respond. In berry skin, expression of *VvHT1* and *VvHT5* was also higher than controls, however, transcript levels of *VvHT2* were also greater,

suggesting some tissue specific responses to infection (Fig. 5.1 C). The enhanced expression of a subset of *VvHT* genes in response to powdery mildew infection is in agreement with studies in *A. thaliana*, where expression of two members of the STP family is elevated by powdery mildew infection. *AtSTP4* transcript levels were strongly elevated while expression of *AtSTP3* was increased by a relatively small amount (Fotopoulos et al., 2003).

Elevated expression of *VvHT5*, *VvHT1* and *VvcwINV*, and increased cwINV activity may have significant effects on carbohydrate distribution in the host. Apoplasmic phloem unloading of sucrose is driven by cwINV activity which cleaves sucrose desorbed from the phloem to the apoplasm, thereby maintaining a sucrose gradient to support further efflux (Patrick, 1997). Sucrose and the hexose cleavage products are then taken up from the apoplasm by sucrose and monosaccharide transporters localised on the plasma membranes of sink cells. In light of these physiological roles, increased *VvcwINV* activity would increase apoplasmic phloem unloading of sucrose, and also reduce phloem loading of sucrose produced in the infected tissue, while elevated *VvHT5* and *VvHT1* expression would enhance the monosaccharide uptake capacity of sink cells. Powdery mildew infected grapevine leaves showed elevated sucrose, glucose and fructose concentrations when compared with healthy control leaves, and because photosynthetic ^{14}C-fixation was reduced, it is likely that the additional sugars are the result of enhanced import (Brem et al., 1986). Coordinate induction of cwINV and HT expression was correlated with elevated glucose and sucrose uptake capacity in *C. rubrum* suspension cultures treated with cytokinins and in powdery mildew infected *A. thaliana* leaves, suggesting a direct link between cwINV and HT expression in sink tissues and the rate of sugar import (Ehneß and Roitsch 1997; Fotopoulos et al., 2003).

Furthermore, additional cwINV activity can delay leaf senescence and inhibit activation of usual cell death programs (Lara et al., 2004), which in terms of biotrophic fungi, would prolong the viability of the host-pathogen association by providing a continued supply of nutrients.

Reduced vINV expression and activity may also mediate changes to carbohydrate allocation via regulation of the symplasmic path of phloem unloading. In addition to regulation by plasmodesmatal conductance, symplasmic unloading is controlled by sucrolytic activity and sucrose compartmentation at the sink cells (Patrick, 1997). The powdery mildew associated reduction in vINV expression and activity, in terms of sink physiology, implies reduced vacuolar compartmentation of sucrose at the sink cells which may in turn retard the symplasmic unloading of sucrose at the sink tissue. However, sucrose hydrolysing enzymes localised in the cytoplasm such as nINVs and sucrose synthases, also regulate the rate of symplasmic unloading (Patrick, 1997). Therefore, without investigation of these alternative sucrolytic possibilities, a diagnosis of the activity of the symplasmic route in powdery mildew infected leaves cannot be established.

5.4.2 Specificity of powdery mildew induced transcriptional changes

The broad aim of this project was to isolate and characterise grapevine transporter or metabolic genes induced by powdery mildew infection. To establish if these genes might be good targets for modification to form the basis of alternative resistance to powdery mildew via reduced susceptibility, the specificity of powdery mildew-associated induction of *VvHT1*, *VvHT5* and *VvcwINV* was explored. Firstly, the spatial specificity was investigated by quantitative RT-PCR. Transcript levels of *VvHT1*, *VvHT5* and *VvcwINV* were less than 2 fold higher in powdery mildew

infected leaf regions compared with uninfected areas of the same leaf, suggesting that expression of these genes is modulated in cells remote from infection sites (Fig. 5.5). This observation is in agreement with previous studies on powdery mildew infected leaves. Using transgenic *A. thaliana* plants expressing the glucuronidase reporter gene under control of the *AtSTP4* promoter, Fotopoulos *et al*. (2003) showed that this promoter drives expression in the mesophyll and vasculature in cells not in direct contact with the infected epidermis. Furthermore, in powdery mildew infected barley leaves, the additional invertase activity was predominantly associated with the mesophyll cell layer and not specifically with infected epidermal cells (Scholes et al., 1994). Due to the lack of spatial specificity indicated by the results presented in Figure 5.5, additional localisation studies were not performed.

To determine if other exogenous stimuli might elicit the powdery mildew-associated responses discussed above, expression of invertases and sugar transporters was measured in downy mildew infected and in wounded grapevine leaves. Quantitative RT-PCR analysis of *VvHT1*, *VvHT5* and *VvcwINV* indicated that expression of these genes was elevated by downy mildew infection (Fig. 5.6) and by wounding (Fig. 5.7), indicating that biotic and abiotic stimuli may elicit a common signal in the host that up regulates expression of these genes. Taken together, these observations are consistent with the hypothesis that induction of *VvHT1*, *VvHT5* and *VvcwINV* expression represents a generalised stress response that may be important to provide energy for repair and the initiation of defence mechanisms in the host. In terms of biotrophic pathogens such as powdery and downy mildew fungi, additional carbohydrate import to infected organs may also contribute to pathogen nutrition and may extend the host-pathogen association by repression of senescence (Lara et al., 2004).

Overall, sucrose transporters were not responsive to pathogen infection, however, their response to wounding was not investigated. At least one sucrose transporter from *A. thaliana*, (*AtSUC3*), is strongly and rapidly induced by wounding (Meyer et al., 2004). This suggests that in pathogen infected tissue, when phloem unloading of sucrose occurs via the apoplasm, sucrose is rapidly hydrolysed to hexoses which are subsequently retrieved by *VvHT*s.

5.4.3 Differential regulation of gene expression in response to powdery and downy mildew infection

Of the invertase transcripts measured in powdery mildew infected tissues, only *VvcwINV* expression was significantly elevated by powdery mildew infection, while in contrast, downy mildew infection elevated expression of all invertase genes tested (Fig 5.6). As powdery mildew infection is limited to the epidermis and downy mildew infects mesophyll cells, these contrasting host responses may relate to distinctive properties of the specific cell types infected. For example, epidermal cells contain predominantly anticlinal positioned plasmodesmata and therefore relatively little symplasmic interconnection with the cell layers below, suggesting that the epidermal cell layer forms an isolated symplasmic domain (Vasil'ev, 1999; Ma and Peterson, 2001). In contrast, downy mildew infects the mesophyll which is comprised of phototrophic cells symplasmically integrated with the phloem via plasmodesmatal connection (Haupt et al., 2001; Blackman and Overall, 2001). The induction of vacuolar (*VvGIN1* & *VvGIN2*) and cytoplasmic (TC7206) invertase genes, as observed in response to downy mildew infection, may alter the source-sink status of infected cells and mediate symplasmic unloading of sucrose at infected cells and reduce phloem loading (Patrick, 1997).

Alternatively, the differential responsiveness of invertase gene expression to powdery and downy mildew infection may be associated with differences in the metabolic status and age of leaves used for powdery and downy mildew inoculations. Powdery mildew studies used expanding leaves, approximately two weeks post emergence, in which transcript levels of invertase genes were considerably higher than in the fully expanded mature leaves used for the downy mildew expression analysis (compare healthy control levels in Fig. 5.3 and 5.6). The decrease in vacuolar invertase expression during leaf development is consistent with observations by Davies and Robinson (1996) who showed that expression of *VvGIN*1 and *VvGIN2*, and soluble acid invertase enzyme activity, declined sharply once leaves had fully matured. Koch (2004) suggested that invertase activity mediates sink formation and expansion while the developmental transition to mature status is marked by a shift from invertase to sucrose synthase cleavage paths. Thus, in mature leaves downy mildew infection may cause leaf metabolism to revert from a mature carbohydrate "source" status to an importing "sink" state characteristic of younger growing tissues. This metabolic environment would presumably provide energy for host defences and repair, and may favour nutrient delivery to and acquisition by the pathogen.

Another notable difference in the response of carbohydrate metabolism genes between powdery and downy mildew infection was the expression of the sucrose transporter *VvSUC27* which was repressed in downy mildew infected leaves (Fig. 5.6) but appeared to increase slightly in response to powdery mildew infection. Again, this differential response may reflect the different site of infection or the age of the leaves tested as discussed in relation to *VvGIN1* expression. Additionally, if *VvSUC27* has a role in phloem loading, its down regulation may be associated with

reduced carbohydrate export and elevated soluble carbohydrate concentrations observed in leaves infected with fungal pathogens (Hewitt and Ayres, 1976; Brem et al., 1986; Hwang and Heitefuss, 1986). Consistent with this proposal is the finding that antisense repression of *NtSUT1* in tobacco leaves led to an accumulation of soluble carbohydrates and reduced export of fixed $^{14}CO_2$ (Burkle et al., 1998). Relative to the other two reported grapevine sucrose transporters, the expression profile of *VvSUC27* is quite different. During berry development, Vv*SUC27* expression is limited to the green phase which precedes the period of rapid sugar import while *VvSUC11* and *VvSUC12* expression is elevated during the sugar accumulation phase (Davies et al., 1999). Furthermore, *VvSUC27* is expressed more highly in mature leaves than in young leaves, but is also strongly expressed in roots, indicating expression in sink and source tissues (Davies et al., 1999). Phloem localised ZmSUT1 from maize was recently shown to mediate both sucrose efflux and uptake dependant on the direction of the sucrose gradient and membrane potential, providing a physiological explanation for the role of sucrose transporters in source and sink tissues (Carpaneto et al., 2005).

Chapter 6 – Expression analysis of VvHTs and *VvcwINV* in grapevine carbohydrate sink tissues

6.1 Introduction

Plants are an assortment of photosynthetically active source organs and heterotrophic sink tissues. Mature leaves produce carbohydrate in surplus of their needs and export it to organs that obtain all, or at least part of their carbohydrate requirements by importation. Variation in supply and demand is a function of the normal life cycle of the plant. Leaves initiate as carbohydrate importers and mature into net exporters. Roots and other sites of vegetative growth require a constant supply of carbohydrate, while other sink tissues such as reproductive organs, tubers and fruit exert demand during tightly regulated periods of development. Additionally, exogenous biotic or abiotic stimuli can influence supply and demand for carbohydrate, contributing further complexity to the problem of establishing a dynamic equilibrium between source and sink organs (Chou et al., 2000).

In Chapter 5, pathogen infection and wounding of grapevine leaves was observed to co-ordinately induce expression of *VvcwINV*, *VvHT1* and *VvHT5* and to repress expression of *VvGIN1*. The aim of the experiments described in this Chapter were to investigate the potential involvement of these stress induced hexose transporter and invertase genes in carbohydrate metabolism associated with sugar importing (sink) tissues of grapevine during normal growth and development. In particular, the research focussed on the regulation of expression of these genes in roots and in ripening berries.

Sugar import into grape berries is of considerable commercial significance because during wine making fermentation of sugar by yeasts produces alcohol and

augments the flavour and aroma profile of the final wine product. Grape berry development can be essentially divided into two stages. During the first phase, imported carbohydrate is utilized for several processes including seed development, cell proliferation and expansion, and the synthesis of organic acids (Davies and Robinson, 1996). The inception of the second or "ripening" phase, between 8-14 weeks after flowering, is termed véraison. After véraison berries accumulate sugar, soften, and in the case of red varieties, accumulate anthocyanins (Davies and Robinson, 1996). During ripening, imported carbohydrate is loaded into the vacuoles of berry pericarp cells which expand significantly in size and, at ripeness, contain approximately 1 M glucose and fructose concentrations (Vignault et al., 2005). Previous studies have identified vINVs, HTs and SUCTs expressed during various stages of grape berry ripening (Davies and Robinson, 1996; Davies et al., 1999; Fillion et al., 1999; Terrier et al., 2005). In this context, the expression of *VvHT1*, *VvHT2*, *VvHT3*, *VvHT4*, *VvHT5* and *VvcwINV* was examined in ripening V. Vinifera cv. Cabernet Sauvignon and cv. Shiraz berries sampled at two week intervals.

6.2 Materials and methods

6.2.1 Grape berry ripening series

The Shiraz berry series was collected from the Coombe vineyard at the Waite Campus of Adelaide University (Adelaide, South Australia, latitude 34° 56' south, longitude 138° 36' east) during the 2002/2003 growing season. Flowering was defined as the date on which 50 % of flowers within an individual bunch had undergone capfall. All subsequent samplings were conducted at two week intervals

after this date. Berries were skinned and deseeded before RNA extraction of the sugar-loading pulp cells and cDNA synthesis as described in sections 2.2.12 and 2.2.13. Sugar concentration of a subset (12 berries) of sampled berries was estimated by the total soluble solids determined with a refractometer (Reichart, Vienna). The Cabernet Sauvignon berry cDNAs and associated developmental data were kindly provided by Dr Chris Davies (CSIRO Plant Industry, Adelaide).

6.2.2 Grapevine roots

Young roots were removed from glasshouse-grown Cabernet Sauvignon plants, soil removed by gentle washing and the roots frozen in liquid nitrogen and then RNA extracted and cDNA synthesized as described in sections 2.2.12 and 2.2.13.

6.2.3 Quantitative RT-PCR analysis

Quantitative RT-PCR was conducted according to the methods outlined in section 5.2.6 using ubiquitin (TC38636) instead of actin as the reference gene for normalization. The level of actin expression was found to be more stable than ubiquitin in pathogen infected and wounded samples, however in grape berry developmental series ubiquitin was more stable than actin (M. Hayes and C. Davies, unpublished data). The un-normalized expression of ubiqutin during Cabernet Sauvignon and Shiraz berry development is shown in Appenidx 2, Figure A2.5 and Figure A.2.6.

6.3 Results

6.3.1 Expression of VvHTs and *VvcwINV* in grape roots

The expression of *VvHT*s and *VvcwINV* was also examined in roots, to investigate if these genes contribute to the importation of carbohydrate into this sink tissue. *VvHT5* was found to be the most highly expressed HT of those examined in roots (Fig. 6.1). It was expressed approximately 8 fold more than *VvHT3* and more than 50 fold more than *VvHT1* and *VvHT4*. *VvcwINV* was also strongly expressed in roots.

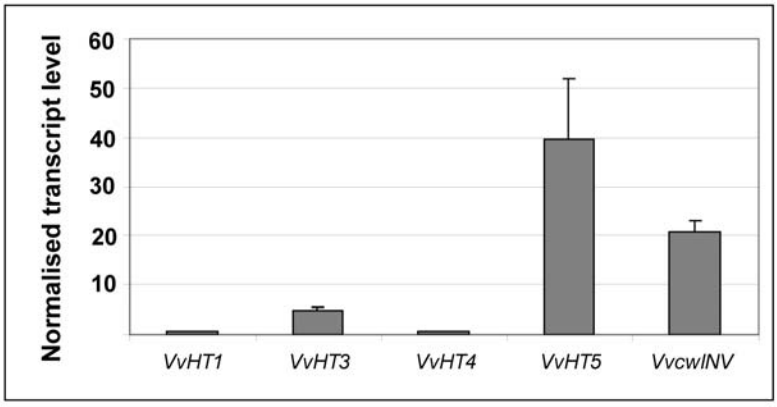


Figure 6.1. Quantitative RT-PCR analysis of HTs and cwINV in Shiraz roots. Values are relative to the expression of ubiquitin and the analysis performed allows comparison of expression level of genes within the figure (Muller et al., 2002). Data are the mean of one sample tested in triplicate. Error bars are the standard error, primer sequences are described in Table 2.3.

6.3.2 Expression of VvHTs and *VvcwINV* during berry ripening

The expression of *VvHT1*, *VvHT2*, *VvHT3*, *VvHT4*, *VvHT5* and *VvcwINV* was measured across ripening in Cabernet Sauvignon and Shiraz berries sampled at two week intervals to investigate if these genes may contribute to the accumulation of sugar that occurs during berry ripening.

Figure 6.2 shows changes in the weight and sugar concentration of Shiraz and Cabernet Sauvignon berries sampled over the growing season. At ripeness,

Shiraz berries weighed approximately 1.2 g, almost double the weight of Cabernet Sauvignon berries. Both cultivars commence a rapid increase in sugar concentration at 8 weeks post flowering which continues to increase to almost 25% total soluble solids after 14 weeks. Berries are usually considered ripe and are harvested between 22 - 25% (w/v) total soluble solids.

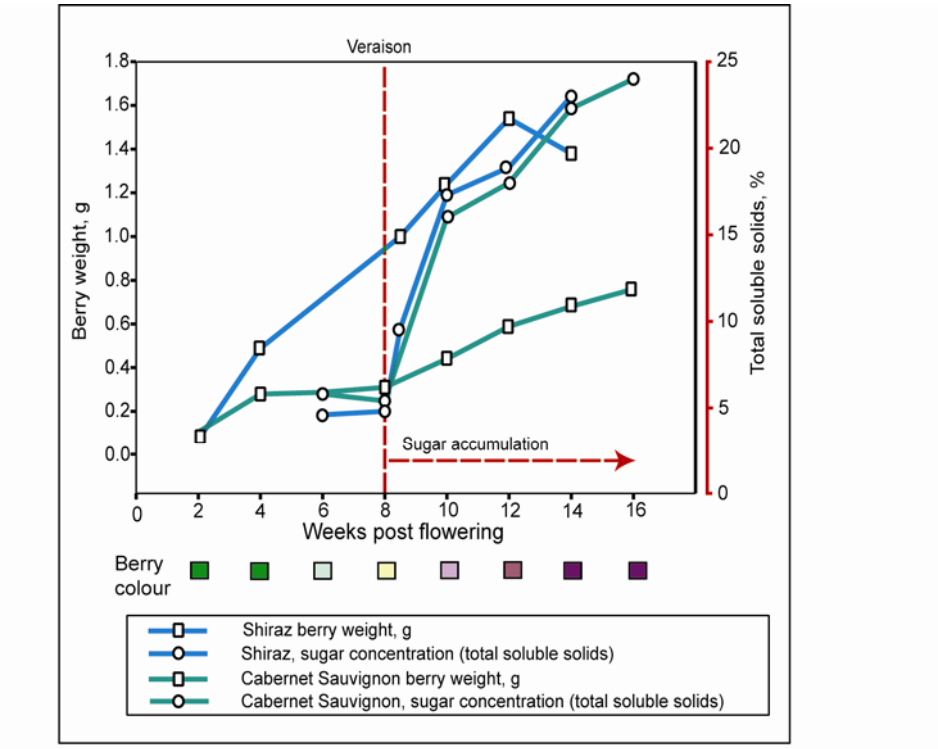


Figure 6.2. Weight and sugar concentration of Shiraz and Cabernet Sauvignon grape berries sampled over development until ripeness. Sugar concentration was measured using a refractometer to estimate total soluble solids. All values are means of multiple berries tested. Veraison marks the inception of ripening.

Figure 6.3 shows that *VvHT1*, *VvHT2* and *VvHT3* were much more highly expressed than *VvHT4* and *VvHT5* in berries of both Shiraz and Cabernet Sauvignon across the developmental period. In Shiraz, *VvHT1* was expressed more highly pre-véraison than post-véraison (Fig. 6.3 A). This trend was also observed in Cabernet Sauvignon berries (Fig. 6.3 B), however, a second increase in the amount of *VvHT1* transcript post-véraison was apparent in this cultivar whereas in Shiraz *VvHT1* expression declined sharply after the 6 weeks post flowering sample.

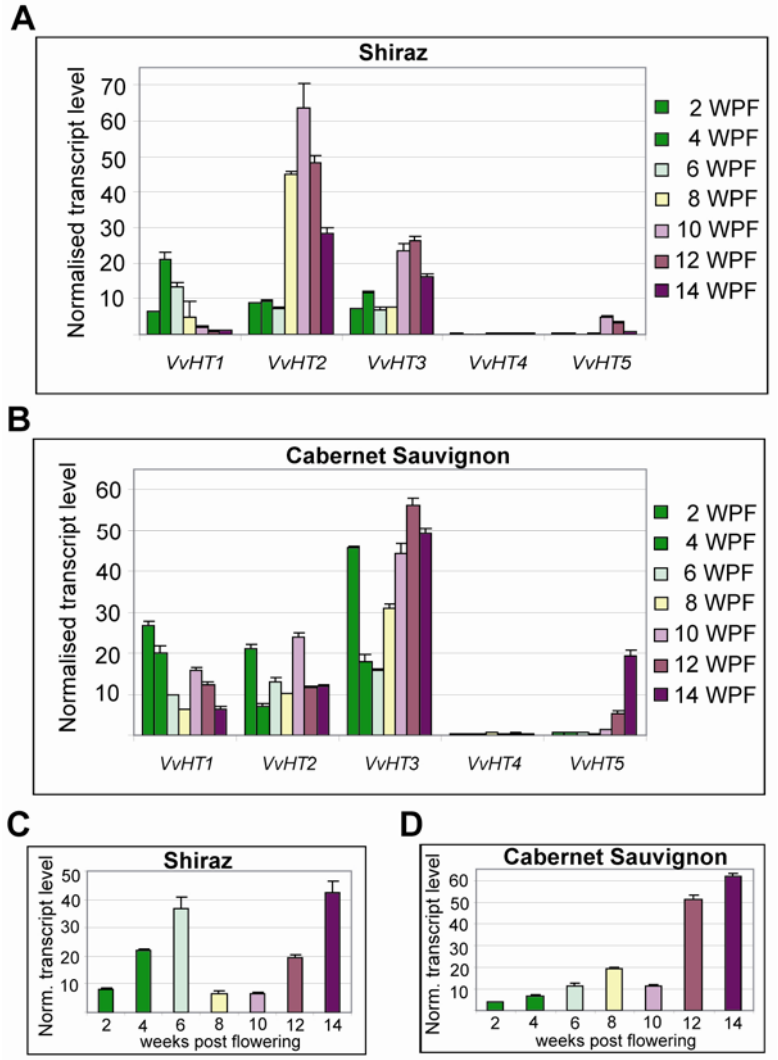


Figure 6.3. Quantitative RT-PCR analysis of VvHTs (A and B) and *VvcwINV* (C and D) during Shiraz (A and C) and Cabernet Sauvignon (B and D) berry ripening. All values were normalised to the expression of ubiquitin and each is the average of three replicates. Analysis was performed using the method of (Muller et al., 2002) which allows comparison of expression level between the genes in each figure. Error bars represent the standard error, primer sequences are described in Table 2.3.

In the initial stages of Shiraz berry development, the level of *VvHT2* expression was low before an approximate 10 fold increase between 6 and 10 weeks after flowering (Fig. 6.3 A). *VvHT2* was the most highly expressed HT post-véraison in Shiraz. In contrast, there was no clear trend in *VvHT2* expression in Cabernet Sauvignon berries.

VvHT3 expression in Shiraz also appeared to increase during the period of sugar accumulation post-véraison (Fig. 6.3 A), but did not reach the expression level of *VvHT2*. In contrast, *VvHT3* was by far the most highly expressed VvHT in post-véraison Cabernet Sauvignon berries with transcript levels increasing significantly in the 8, 10 and 12 week samples, before declining slightly in the 14 week sample.

Relative to the other VvHTs, *VvHT4* and *VvHT5* were only expressed at relatively low levels in both Shiraz and Cabernet Sauvignon berries (Fig. 6.3 A and B). *VvHT4* expression was barely detectable throughout berry development in both cultivars whereas *VvHT5* transcript levels increased in post-véraison berries of both cultivars. In Shiraz, *VvHT5* expression increased 10 fold between the 8 - 10 week samples before declining in subsequent samples. *VvHT5* expression in Cabernet Sauvignon berries increased strongly during the final 4 weeks of berry development.

In general, the expression profile of *VvcwINV* in both cultivars was reasonably similar (Fig. 6.3 C and D). Significantly, *VvcwINV* expression increased markedly during the period of sugar accumulation following véraison at week 8.

6.4 Discussion

6.4.1 Expression of VvHTs and *VvcwINV* in grapevine carbohydrate sink tissues during normal growth and development

Roots represent one of many heterotrophic tissues in plants reliant on carbohydrate import to support normal function and growth. Studies on plasmodesmata frequency and dye tracer experiments in roots indicate that phloem unloading and subsequent distribution via the symplasm can deliver carbohydrate to most root zones (Ma and Peterson, 2001). However, cwINV and HT genes are

expressed in roots (Truernit et al., 1996; Tymowska-Lalanne et al., 1998; Meyer et al., 2004), indicating an apoplasmic supply may also be active. The importance of apoplasmic carbohydrate supply in roots was previously well demonstrated in carrot roots where antisense repression of cwINV expression drastically reduced tap root size (Tang et al., 1999).

In grapevine roots, *VvHT5* and *VvcwINV* were relatively highly expressed suggesting these genes may be preferentially expressed in sink tissues (Fig. 6.1). Previous studies have shown that vacuolar invertase expression in grapevine roots is low (Davies and Robinson, 1996). Taken together, these observations indicate that the apoplasm may be an important carbohydrate supply path to root sink cells, consistent with studies on other plants. For example, in *A. thaliana* roots, the cell wall invertase gene *AtβFRUCT1*, and the sugar transporter genes *AtSTP4* and *AtSUC3* are expressed relatively strongly compared with other members of these particular gene families (Truernit et al., 1996; Tymowska-Lalanne et al., 1998; Meyer et al., 2004). Interestingly, these genes are also induced by wounding and/or pathogen infection, indicating these genes encode proteins that regulate the formation of sink metabolism in response to both developmental and stress-associated cues (Truernit et al., 1996; Chou et al., 2000; Meyer et al., 2004).

Expression of *VvHT5* and *VvcwINV* was also induced in grape berries during the phase of rapid sugar accumulation (Fig. 6.3 A-D) consistent with the idea that these genes are predominantly expressed in sink tissue. In berries, however, other sugar transporter and invertase proteins are likely to play a more significant role in sugar delivery to this particular sink organ (see section 6.4.2 below).

The induction of *VvHT5* and *VvcwINV* at relatively late stages during berry ripening may be mediated by stress-associated signals rather than developmental

cues. Differential screening and northern analysis has previously shown that genes involved in defence responses are amongst the most highly induced during grape ripening (Davies and Robinson, 2000). Structural modifications to permit changes in cell volume, and induction of proteins to manage increased osmotic potential in the sugar accumulating cells, are proposed explanations of these initial observations which have now been confirmed in subsequent publications (Sarry et al., 2004; Terrier *et al*., 2005; Goes da Silva et al., 2005). Potentially, *VvcwINV* and *VvHT5* may be induced as part of this grape berry stress response.

6.4.2 Role of *VvHT*s and *VvcwINV* in grape berry development

Analysis of *VvHT1-5* and *VvcwINV* expression during grape berry development has also provided new insights into the mechanism of sugar import and storage into berries during ripening. Because of the commercial importance of sugar accumulation into grape berries, there is a significant amount of interest in understanding the biochemistry and genetic regulation of this process. (Davies and Robinson, 2000).

In Shiraz and Cabernet Sauvignon berries, *VvHT1*, *VvHT2* and *VvHT3* transcript levels were generally higher than the levels of *VvHT4* and *VvHT5* transcripts. *VvHT1* was most highly expressed pre-véraison in both cultivars, however a small induction at véraison was observed in Cabernet Sauvignon berries (Fig. 6.3). This expression pattern for *VvHT1* is consistent with the biphasic expression pattern observed during the development of *V. vinifera* cv. Ugni Blanc berries in which there was a decrease in transcript levels during an approximate five week period around véraison (Fillion et al., 1999). Interestingly, there was no similar increase in *VvHT1* transcript levels post-véraison in Shiraz berries, which

may indicate cultivar differences in the expression of this gene during berry ripening. Alternatively, these differences may reflect contrasting environmental conditions or different management practices used in the vineyards from where these berries were sampled.

Recently, *VvHT1* transcript and protein was localized to phloem-associated cells in berries rather than the sugar accumulating cells of the pulp, while expression of *VvHT1* was found to be mainly confined to the pre-véraison period of berry development (Vignault et al., 2005). These observations are consistent with a role for VvHT1 in hexose retrieval by cells of the conducting complex during the early phase of berry development, when sugars are utilized for cell proliferation and growth (Vignault et al., 2005).

The expression pattern of *VvHT2* during Shiraz berry ripening was correlated with the period of rapid sugar accumulation, however in Cabernet Sauvignon this correlation was not evident (Fig. 6.3). This cultivar difference in *VvHT2* expression during berry ripening was also noted in the oligo array analysis of Terrier *et al*. (2005). Their analysis indicated that *VvHT2* expression in Shiraz was strongly induced during berry ripening, while in Chardonnay and Cabernet Sauvignon, the increase in *VvHT2* expression was not significant. *VvHT3* expression profiles in Shiraz and Cabernet Sauvignon were also found to be different. In post-véraison Shiraz berries, *VvHT2* transcript levels were significantly greater than *VvHT3*, whereas in Cabernet Sauvignon, the opposite was observed (Fig. 6.3). *VvHT2* expression did not strictly correlate with the phase of sugar accumulation, while *VvHT3* expression was elevated post-véraison and maintained at the highest level of the VvHTs measured. These results suggest that sugar loading into ripening berries of different *V. vinifera* cultivars may not be mediated by common carriers.

Alternatively, cultivar differences in the efficiency of translation of *VvHT2* and *VvHT3* transcripts, or differences in the activity of the respective proteins, could mean these transcriptional differences might not reflect the level of active protein found in the berry.

The amount of *VvHT4* transcript was consistently low during grape berry development, indicating that this gene is not involved in sugar importation during berry ripening, while as discussed above, VvHT5 was induced during the late stages of ripening.

The transcript levels of *VvcwINV* during berry development exhibited a biphasic profile with two peaks in expression, one preceding or approximately at the time of véraison, and another at the ripe stage (Fig. 6.3). Consistent with this biphasic expression profile, proteomic and immunohistochemistry studies have shown the presence of cwINV peptides in berries at early and late stages of berry development. Famiani *et al*. (2000) reported that cwINV epitopes, identified using a cwINV specific antibody, were associated with berry palisade cells associated with developing seeds and vasculature, and with cells underlying the berry epidermis. As berry development proceeded towards véraison, cwINV epitopes were lost from palisade cells. Unfortunately, due to technical limitations, berries after véraison were not analysed in this study (Famiani et al., 2000). Using a proteomic approach, Sarry *et al*. (2004) identified a cwINV degradation product at relatively high concentrations in extracts isolated from ripe berries, however berries at earlier developmental stages, still rapidly accumulating sugars, were not analysed.

Previous studies in grape indicate that transcripts of two vINVs, *GIN1* and *GIN2*, are found at high levels in grape pulp until ten weeks after flowering, and a high level of soluble acid invertases activity is maintained, at least on a per berry

basis, until berries are ripe (Davies and Robinson, 1996). Immunohistochemistry indicated that high levels of vINV protein is localized throughout the sugar-accumulating pulp cells up to the time of véraison (Famiani et al., 2000), while enzymatic studies suggest that vINV activity accounts for the vast majority of invertase activity in berries and cwINV activity represents only 4% of the total activity (Ruffner et al., 1995). Considered together, these observations suggest that sucrose may not be cleaved in the apoplasm before it is loaded into pulp cells.

The actual path of sugar delivery to grape pulp cells, apoplasmic or symplasmic, is yet to be fully resolved, but an apoplasmic step is commonly observed in fruits and seeds where sugars are accumulated to high concentrations (Patrick et al., 2001). Furthermore, after véraison in grapes, enhanced phloem transport is accompanied by reduced xylem flow (Greenspan et al., 1994). Bondada *et al*. (2005) hypothesized that increased apoplasmic solute concentrations may elevate the hydrostatic potential of this compartment, and thus be responsible for the elimination of xylem inflow to ripening berries.

Although a role for cwINV during berry ripening is not clearly supported by current evidence, sugar transporters are expressed by berry pulp cells, indicating that sugars may be retrieved from the apoplasm. In the current study, the expression profiles of *VvHT2* and *VvHT3* during berry ripening were found to be consistent with this role. Monosaccharide transporters from *A. thaliana* (*AtSTP11*; Schneidereit et al., 2005), tomato (*LeHT3*; Gear et al., 2000) and apple (Zhang et al., 2004) are expressed by sink cells where they are proposed to be important for carbohydrate acquisition. Also, transcript levels of two grapevine sucrose transporters, *VvSUC11* and *VvSUC12*, increase significantly after véraison and remain highly expressed through-out the period of sugar accumulation (Davies et al.,

1999). Sucrose transporters isolated from plants other than grapevine have been localized to phloem cells where they are proposed to contribute to sucrose loading, unloading or re-absorption along the phloem path (Stadler et al., 1995; Barth et al., 2003; Carpaneto et al., 2005). Other sucrose transporters are expressed in sink cells, such as *DcSUT2* which is expressed on storage parenchyma cells of *Daucus carota* L. roots, and *AtSUC3* which is expressed on a range of *A. thaliana* sink cells, for example root tips, trichomes and pollen grains (Shakya and Sturm, 1998; Meyer et al., 2004). Although expression of *VvSUC11* and *VvSUC12* has not been localized at the cellular level, the induction of these genes in berry pulp in coordination with the commencement of sugar loading, suggests they may mediate the import of sucrose into berry pulp cells. Vacuolar compartmentation of sucrose, supported by the high rate of vacuolar invertase activity (Davies and Robinson, 1996), would support retrieval of sucrose from the apoplasm by VvSUC11 and VvSUC12, as the inward activity of these transporters is probably dependant on the sucrose concentration gradient between the apoplasm and the sink cell cytoplasm (Carpaneto et al., 2005). However, it must be acknowledged that the pulp of grapes does represent a heterogenous mixture of cell types at different stages of development (Famiani et al., 2000), therefore alternative roles for VvHT2, VvHT3, VvSUC11 or VvSUC12 cannot be ruled out. Potentially, VvSUC11 or VvSUC12 may be localised to the phloem and mediate phloem unloading, rather than sink cell loading. Similarly, VvHT2 or VvHT3 may be localized to phloem-associated cells and as has been proposed for VvHT1 (Vignault et al., 2005), VvHT2 and VvHT3 may contribute to hexose retrieval in the conducting complex.

Chapter 7 - Hormonal regulation and analysis of promoters of VvHT and invertase genes

7.1 Introduction

Plant hormones such as ethylene, jasmonate and abscisic acid (ABA), are important regulators of stress responsive pathways. Ethylene and jasmonate are commonly associated with defence pathways activated by pathogen infection and wounding (Zimmerli et al., 2004) while ABA is well known to regulate responses to abiotic factors such as salinity and drought (Zhou, 2002). More recently, ABA has also been implicated in the establishment of compatible interactions between fungal pathogens and host plants (McDonald and Cahill, 1999; Mohr and Cahill, 2003). Exogenous application of ethylene (Jacobs et al., 1999), jasmonate (Zimmerli et al., 2004) and ABA can elicit aspects of the host response to stress stimuli.

Genomic DNA upstream of protein coding regions, or promoters, contain short (approximately 6-12 bp) nucleotide motifs, or *cis*-acting regulatory elements, that contribute to the transcriptional regulation of the gene downstream. Many stress-associated *cis*-elements that activate transcription in response to salinity, drought, wounding and pathogen infection have been identified in plants (Korfhage et al., 1994; Mihiri et al., 1997; Choi et al., 2000). Web-based databases such as PLACE DB (Higo et al., 1999) provide a convenient way to search for these previously identified promoter motifs in DNA sequences.

In Chapter 5 expression of *VvHT1*, *VvHT5* and *VvcwINV* was observed to be induced by pathogen infection and wounding, while *VvGIN1* expression was repressed by wounding and powdery mildew infection but induced by downy mildew infection. To investigate the potential regulatory factors that may contribute

to these gene expression changes, ABA, methyl-jasmonate and ethylene were supplied to plants and quantitative RT-PCR used to measure transcript levels. Additionally, more than 1 kb of genomic DNA upstream of the start codons of *VvHT3*, *VvHT4*, *VvHT5* and *VvcwINV* ORFs was isolated and the sequences analysed to identify potential regulatory sequence motifs.

7.2 Materials and Methods

7.2.1 Exogenous application of ABA, ethylene and methyl jasmonate

An abscisic acid (ABA) solution containing 200 mg L^{-1} ABA and 0.05% (v/v) Tween 20 was applied by spray to the upper and lower surfaces of Cabernet Sauvignon grapevine leaves. Control leaves were sprayed with a solution containing 0.05% (v/v) Tween 20 only. Duplicate ABA and control sprayed leaves were collected at 1, 2, 4, and 6 h after spray application, snap frozen and stored at -80°C.

Ethylene was applied to grapevine leaves using a 10 mM ethephon (Ethrel, Bayer Crop Science, Australia) solution. Leaves were sprayed to run off, bagged overnight in zip-lock plastic bags and sampled 2 d post treatment. Control leaves were sprayed with distilled water only; one leaf was bagged like the ethephon sprayed leaf, while a second control leaf was not bagged. Leaves were sampled 2 d post treatment, snap frozen in liquid nitrogen and stored at -80°C.

Grapevine leaves sealed in plastic zip-lock bags were exposed to methyl jasmonate vapours generated from an ethanol bud containing 400 µL of 0.5% (v/v) methyl jasmonate. A control leaf was bagged and exposed to the ethanol bud while a second control leaf was not bagged. Leaves were sampled 2 d post treatment, snap frozen in liquid nitrogen and stored at -80°C.

Total RNA was extracted, cDNA synthesized and quantitative RT-PCR undertaken in the same manner as described in sections 2.2.12 and 2.2.13. Actin was used as the reference gene for these hormone treated comparisons. All primer sequences are described in Table 2.3.

7.2.2 Isolation of BAC DNA and direct sequencing

A *V. vinifera* cv. Cabernet Sauvignon genomic bacterial artificial chromosome (BAC) library (Barker et al., 2005) was screened by PCR with the primers used for quantitative RT-PCR to identify BACs containing the genes *VvHT3*, *VvHT4*, *VvHT5* and *VvcwINV*.

The buffers used in the procedure below were from a QIAprep Spin Miniprep Kit (Qiagen). After confirmation, positive BAC DNA was prepared from 7.5 ml of overnight culture grown in LB containing 34 ng ml^{-1} of chloramphenicol. Cultures were centrifuged for 6 min at 5,000 *g* to pellet bacteria, resuspended in 350 µl buffer P1 (Qiagen) and then 350 µl buffer P2 (Qiagen) was added. The lysate was incubated for 5 min at room temperature before 350 µl buffer P3 (Qiagen) was added, and this mixture was incubated on ice for five min. To remove cell debris and bacterial genomic DNA, the mixture was centrifuged at 15,000 *g* for 15 min, the supernatant collected and transferred to a new tube and one ml isopropanol added to precipitate DNA. After centrifugation at 15,000 *g* for 15 min, the supernatant was discarded and the DNA pellet dried under vacuum before being resuspended in 500 µl TE buffer. The DNA was phenol extracted with an equal volume of (25:24:1) phenol:chloroform:isoamyl alcohol followed by centrifugation at 15,000 rcf for 10 min. The aqueous phase was collected, ethanol precipitated using 50 µl 3 M sodium acetate and 1 ml cold absolute ethanol, and then incubated at -20°C for 1 h. BAC

DNA was pelleted by centrifugation at 15,000 *g* for 15 min, the pellet washed with 1 ml 70% ethanol, air dried under vacuum and then resuspended in 20 µl TE buffer.

BAC DNA was sequenced using 8 µl BigDye terminator V3.1 (Applied Biosystems, Foster City, California), 0.25 µM sequencing primer (Table 2.2) and 4 µl of BAC DNA in a total volume of 20 µl. Thermal cycling was performed using 80 cycles of 94°C for 30 s, 55°C for 30 s, 68°C for 4 min. BAC sequencing primers were designed to produce approximately 100 bp overlap with the previous sequencing run to allow unambiguous alignment of sequences. Each run yielded approximately 500 bp of good quality sequence and each was aligned manually using Genedoc (www.psc.edu/biomed/genedoc).

7.2.3 Promoter analysis

Promoter sequences were submitted to the PLACE database (Higo et al., 1999) to identify and map potential regulatory motifs. The PLACE database is served at: http://www.dna.affrc.go.jp/PLACE/signalscan.html.

7.2.4 Quantitative RT-PCR analysis of ABA biosynthetic genes

Gene specific primers for zeaxanthin epoxidase (*VvZEP*) and 9-cis-epoxycarotenoid dioxygenase (*VvNCED1*) were kindly supplied by Dr Jim Speirs, CSIRO Plant Industry, Adelaide. The expression of these genes was measured in the powdery and downy mildew infected, and wounded samples described in sections 5.3.1 and 5.3.2. Quantitative RT-PCR was carried out as described in section 5.2.6 using actin as the control gene for normalization. The un-normalized expression of actin in ABA-treated leaves is shown in Appenidx 2, Figure A2.7.

7.2.5 Measurement of bulk leaf ABA concentration

ABA analysis was kindly performed by Ms Suzanne Maffei, CSIRO Plant Industry Adelaide, using the method described by Soar et al. (2004). Powdery mildew infected and healthy control Chardonnay leaves were sampled 10 days after inoculation, ground under liquid nitrogen and store at -80°C until analysed.

7.3 Results

7.3.1 Expression of VvHTs and invertases in grapevine leaves exogenously supplied with ethylene and methyl jasmonate

Ethylene and jasmonate dependant pathways regulate many defence genes induced in response to pathogen attack in grapevine and other plants (Jacobs et al., 1999; Zimmerli et al., 2004). These chemicals were exogenously supplied to grapevine leaves to determine if the pathogen and wound induced genes *VvHT5* and *VvcwINV,* or the pathogen repressed genes *VvGIN1*, are regulated by these hormones. Expression of the previously reported ethylene-responsive thaumatin-like gene *VvTL2* (Jacobs et al., 1999; homologous to *VvOSM1*, Loulkakis, 1997) was also monitored in ethylene and methyl jasmonate treated leaves as a positive control.

Leaves were bagged overnight to facilitate hormone treatment and in general, this had no significant effect on the expression of the genes investigated. In both ethylene and methyl jasmonate treated leaves, *VvTl2* transcript levels were more than 3.5 fold higher than levels in control samples (Fig. 7.1). *VvHT5* was slightly induced by both treatments but by less than 2 fold relative to control samples. *VvcwINV* expression increased by approximately 2.5 fold in ethylene treated leaves and by approximately 2 fold in jasmonate supplied samples, while *VvGIN1* expression did not significantly respond to these treatments.

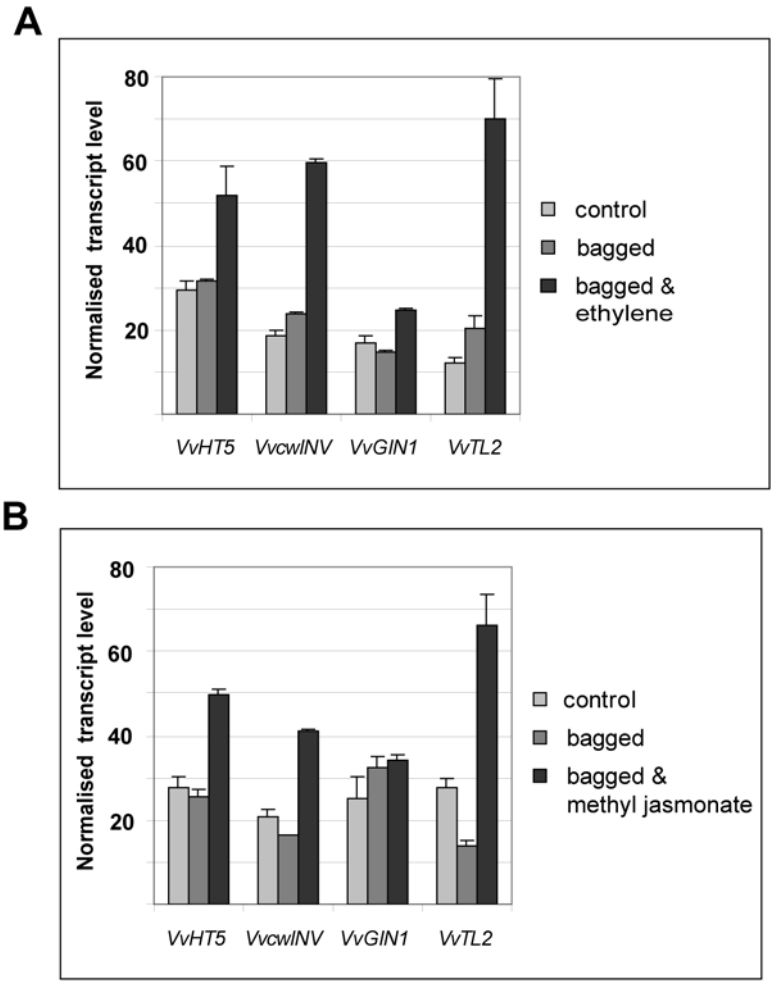


Figure 7.1. Quantitative RT-PCR analysis of *VvHT5*, *VvcwINV*, *VvGIN1* and *VvTL2* expression in leaves treated with ethylene (A) and methyl jasmonate (B). All values are relative to the expression of actin. Data analysed using the method of Muller *et al*. (2002). Data are the mean of a single sample tested in triplicate. Primer sequences are in Table 2.3.

7.3.2 Expression of VvHTs and invertases in grapevine leaves exogenously supplied with ABA

ABA application led to the specific induction of *VvHT1* and *VvHT5* expression in Cabernet Sauvignon leaves (Fig. 7.2 A). *VvHT1* transcript levels increased between 2 and 3 fold in ABA treated leaves relative to control leaves sprayed with the 0.05% Tween solution within 4-6 h after application. Some increase in *VvHT1* transcript levels were also observed in the control samples

suggesting this gene may be diurnally regulated, or alternatively, that the control treatment up-regulated expression of *VvHT1*.

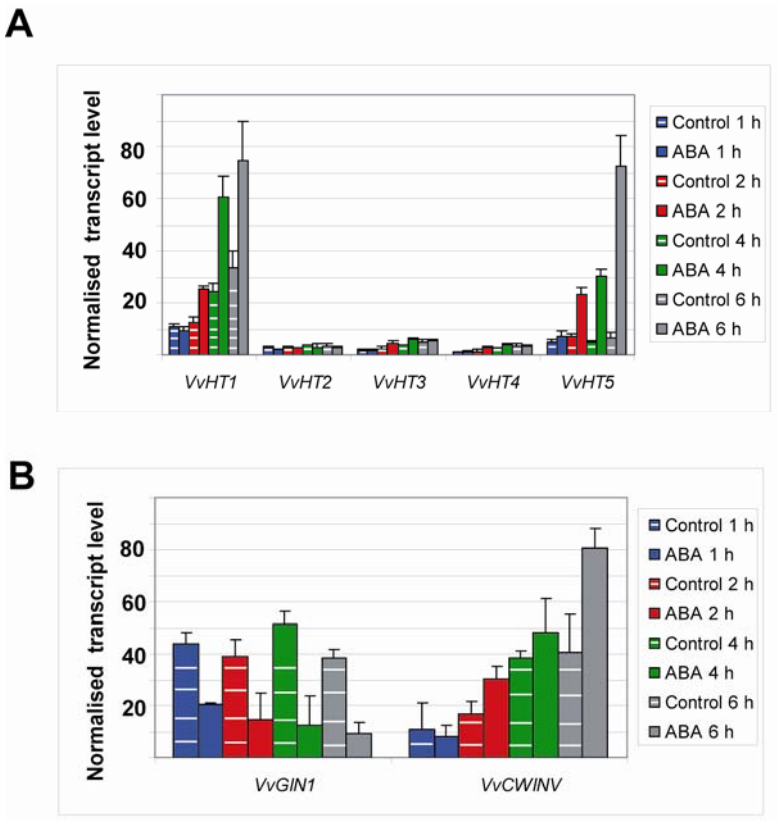


Figure 7.2. Quantitative RT-PCR analysis of VvHTs (A) and invertases (B) in ABA (200 mg/L) sprayed Cabernet Sauvignon leaves. All values are relative to the expression of actin in each sample, and the analysis performed allows comparison of expression level of genes within each figure (Muller et al., 2002). Data are the mean of biological replicates tested in triplicate. Primer sequences are in Table 2.3.

VvHT5 expression was elevated approximately 3 fold within 2 h of ABA treatment, relative to control leaves, and continued to increase until the final sampling point at 6 h where *VvHT5* expression was induced approximately 10 fold, compared to controls. In contrast, no significant induction of *VvHT2*, *VvHT3* and *VvHT4* was observed in response to ABA application (Fig. 7.2 A).

Expression of cytoplasmic invertase *VvGIN1* and the apoplasmic invertase *VvcwINV* were also measured in the ABA treated Cabernet Sauvignon leaves (Fig 7.2 B). *VvGIN1* transcript levels declined to approximately 50% of the control

leaves within 1 h of ABA treatment and continued to decline over the next 5 h. In the 4-6 h ABA treated samples, *VvGIN1* was expressed approximately 4 fold less than the control samples. Like *VvHT1*, *VvcwINV* expression increased in control leaves during the sampling period suggesting this gene may also be diurnally regulated or affected by the control treatment. Relative to the controls, ABA application caused a slight increase in *VvcwINV* expression resulting in a 2 fold increase in expression above the control sample, 6 h after treatment.

7.3.3 Promoter analysis

To identify potential regulatory elements that may mediate the induction of *VvHT5* and *VvcwINV* in response to powdery mildew infection and wounding, promoters of these genes were isolated. Approximately 55,680 clones from a Cabernet Sauvignon genomic BAC library, representing 9.4 copies of the haploid grapevine genome (Barker et al., 2005) were screened, and BACs containing the desired regions were identified. More than 1 kbp of genomic sequence upstream of the ORFs of *VvHT3*, *VvHT4*, *VvHT5* and *VvcwINV* was sequenced from isolated BAC DNA and these sequences were analysed for potential regulatory elements, together with the previously reported promoters of *VvHT1* (AJ001062; Fillion et al., 1999), *AtSTP4* (AB025631; Truernit et al., 1996) and *AtβFRUCT1* (AB028610), using the PLACE database. The promoter analysis identified an abundance of sequence elements commonly found in the 5' non-coding regions of plant genes that are known to be involved in transcriptional regulation.

The upstream genomic sequences of *VvHT3*, *VvHT4*, *VvHT5* and *VvcwINV* all contain motifs characteristic of the various Hogness (TATA) box sequences found in plant promoters (O'Shea-Greenfield and Smale, 1992). The location of the

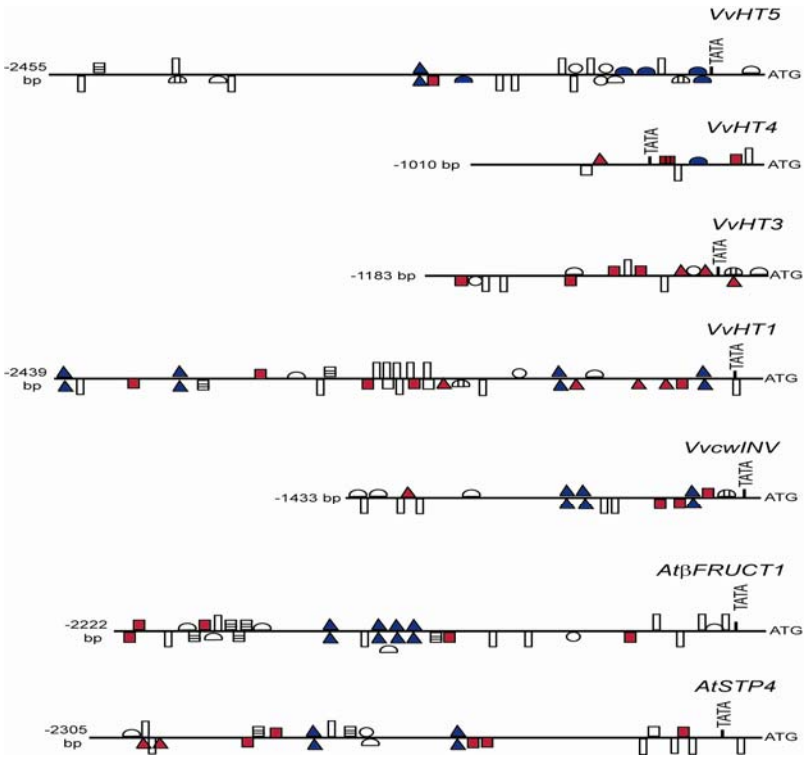


Figure 7.3. Location of regulatory elements found in promoters of grapevine and *A. thaliana* HTs and cwINVs. PLACE database (Higo et al., 1999) was used to identify regulatory motifs. *VvHT5, VvHT4, VvHT3* and *VvcwINV* promoters were isolated and sequenced from a Cabernet Sauvignon genomic BAC library (Barker et al., 2005). Accession numbers of other sequences used are: *VvHT1* (AJ001062), *AtSTP4* (AB025631), *AtβFRUCT1* (AB028610). Explanations of motifs are given below.

- Myc recognition motifs, CATGTG (Tran et al., 2004) or CACATG (Abe et al., 1997). Drought & ABA response.
- ABRE of four types: YACGTGGC (Choi et al., 2000); ACGTSSSC (Marcotte et al., 1989); CCACGTGG (Pla et al., 1993); ACGTGKC (Hatori et al., 2002). ABA response to drought and salinity.
- Pyrimidine box TTTTTTCC, (Cercos and Gomez-Cadenas, 1999). GA & ABA induction.
- EIX motif, TAAAATAT, (Matarasso et al., 2005). Ethylene induction in response to fungal elicitor.
- GARE, TAACAAR (Ogawa et al., 2003). Gibberellin response element.
- ARF, ACTTTA (Baumann et al., 1999) or TGTCTC (Hagen and Guilfoyle, 2002). Auxin regulated expression.
- SURE1 & 2, AATAGAAAA or AATACTAAT (Grierson et al., 1994). Sucrose responsive elements 1 & 2.
- GT1 binding motif, GAAAAA, (Park et al., 2004). Rapid response to pathogen attack and salinity.
- GA-down regulated motif, ACGTGTC (Ogawa et al., 2003). GA negative response element.
- Pyrimidine box, CCTTTT (Morita et al., 1998). Sugar repression.
- S1F box, ATGGTA (Zhou et al., 1992). Negative regulator of transcription.

TATA motif closest to the predicted start codon of each ORF is indicated in Figure 7.3. The TATA motifs and locations were: *VvHT3* (TTATTTT; -260), *VvHT4* (TTATTT;-416), *VvHT5* (TATATAA; -232) and *VvcwINV* (TTATTT; -157).

Numerous motifs associated with stress response and hormonal regulation were identified in the promoters of pathogen and wound responsive grapevine genes. Of particular interest is the observation that the *VvHT5* promoter contained five ABA responsive elements (ABRE) of four closely related types: C/TACGTGGC; ACGTG/CG/CC; CCACGTGG; ACGTGG/TC, whereas ABREs were absent or identified once only in other promoters. A group of drought and salinity induced *trans*-acting factors belonging to the bZIP class of proteins interact with ABREs and mediate the ABA-dependant induction of stress responsive genes (Kang et al., 2002). Numerous MYC (CATGTG) or MYB (CACATG) binding sites were identified in the promoters of *VvHT1* and *VvcwINV*, and also in the promoters of the pathogen induced *A. thaliana* genes *AtSTP4* and *AtβFRUCT1*. Drought, salinity and ABA-induced members of NAC-domain, MYC and MYB classes of transcription factors from *A. thaliana* bind at these sequences and promote expression of downstream genes (Abe et al., 1997; Tran et al., 2004).

A GT1(GAAAAA) motif in the promoter of a calcium calmodulin gene from soybean was recently identified as the *cis*-element that mediates the rapid induction of this gene in response to pathogen attack and salinity (Park et al., 2004) and GT1 *trans*-factors are rapidly induced by pathogen infection and salinity (Park et al., 2004; Wang et al. 2004). Although numerous GT1 *cis*-elements were found within the promoters of the pathogen and wound induced genes, this motif was also identified in the promoter regions of the "non-responsive" genes *VvHT3* and *VvHT4*.

Various other *cis*-elements associated with ethylene, gibberellin and auxin induction were also identified within the promoter regions (Fig. 7.3), but there was no obvious relationship between the presence of these motifs and the response of the downstream gene to pathogen infection. Of these elements, the most interesting in terms of stress induction is a cluster of three EIX sequences (TAAAATAT) found in the *VvHT5* promoter. The EIX sequence is essential for fungal elicitor-induced and ethylene-dependant induction of the tomato *Acs* gene (Matarasso et al., 2005).

Interestingly, the frequency of regulatory elements associated with transcriptional repression was found to be very low in the *VvHT5* promoter relative to the promoter sequences of the others genes examined. A pyrimidine box sequence (CCTTTT) associated with sugar repression occurs more than 3 times within the first 1,400 bp of *VvHT3*, *VvHT1* and *VvcwINV*, but occurs only once in *VvHT5*. Another negative element, S1F (ATGGTA), was not observed in *VvHT5* but is present in most of the other promoters analysed. The S1F sequence is able to repress activity of cauliflower mosaic virus 35 S promoter, and is associated with regulation of a chloroplast associated gene from spinach (Zhou et al., 1992).

7.3.4 Induction of ABA biosynthetic genes in mildew infected and wounded grapevine leaves

The powdery mildew inducible gene *VvHT5* is highly responsive to ABA (Fig. 7.2) and analysis of the *VvHT5* promoter identified the presence of numerous ABRE elements. It was therefore of interest to investigate whether ABA might regulate the powdery mildew/wound response of *VvHT5*. The ABA biosynthetic pathway is generally considered to contain two rate limiting steps (Seo and Koshiba, 2002). The first is the conversion of zeaxanthin to violaxanthin catalysed by

zeaxanthin epoxidase for which a single gene has been isolated from grapevine (*VvZEP1*; Refer to Fig. 7.4). The expression of *VvZEP1* is repressed by water stress (Soar et al., 2004). The second limiting step is the conversion of the epoxy-carotenoids violaxanthin and neoxanthin to xanthoxin, which is a precursor of ABA, catalysed by 9-cis-epoxycarotenoid dioxygenase (NCED). In grapevine, two NCED genes have been isolated: *VvNCED1* is the most highly expressed of the two and its expression is induced by water stress (Soar et al., 2004). *VvNCED2* is not stress induced but may be developmentally regulated as transcript levels tend to increase during leaf development (Soar et al., 2004).

To investigate if ABA biosynthetic genes are induced by mildew infection or wounding, the expression of *VvNCED1* and *VvZEP* was measured in powdery and downy mildew infected samples and wounded leaves. In powdery mildew infected Chardonnay and Cabernet Sauvignon leaves, *VvNCED1* transcript levels were approximately 2-3 fold higher than the appropriate control samples respectively, however *VvZEP* expression was not significantly altered (Fig. 7.5). In the downy mildew infected leaves, *NCED1* expression was induced more than 10 fold relative to controls while *ZEP* expression was repressed approximately 5 fold.

Wounding caused a very rapid, but transient increase in *VvNCED1* expression (Fig. 7.6). Within 1 h after wounding, *VvNCED1* was induced approximately 8 fold relative to unwounded control leaves. This level of expression was sustained until 2 h after wounding, after which time *VvNCED1* transcript levels declined towards control levels. In contrast, *VvZEP* expression tended to decline in response to wounding, but by a smaller amount. *VvZEP* expression remained at approximately half the control level 2-8 h after wounding and returned to normal levels by 24 h.

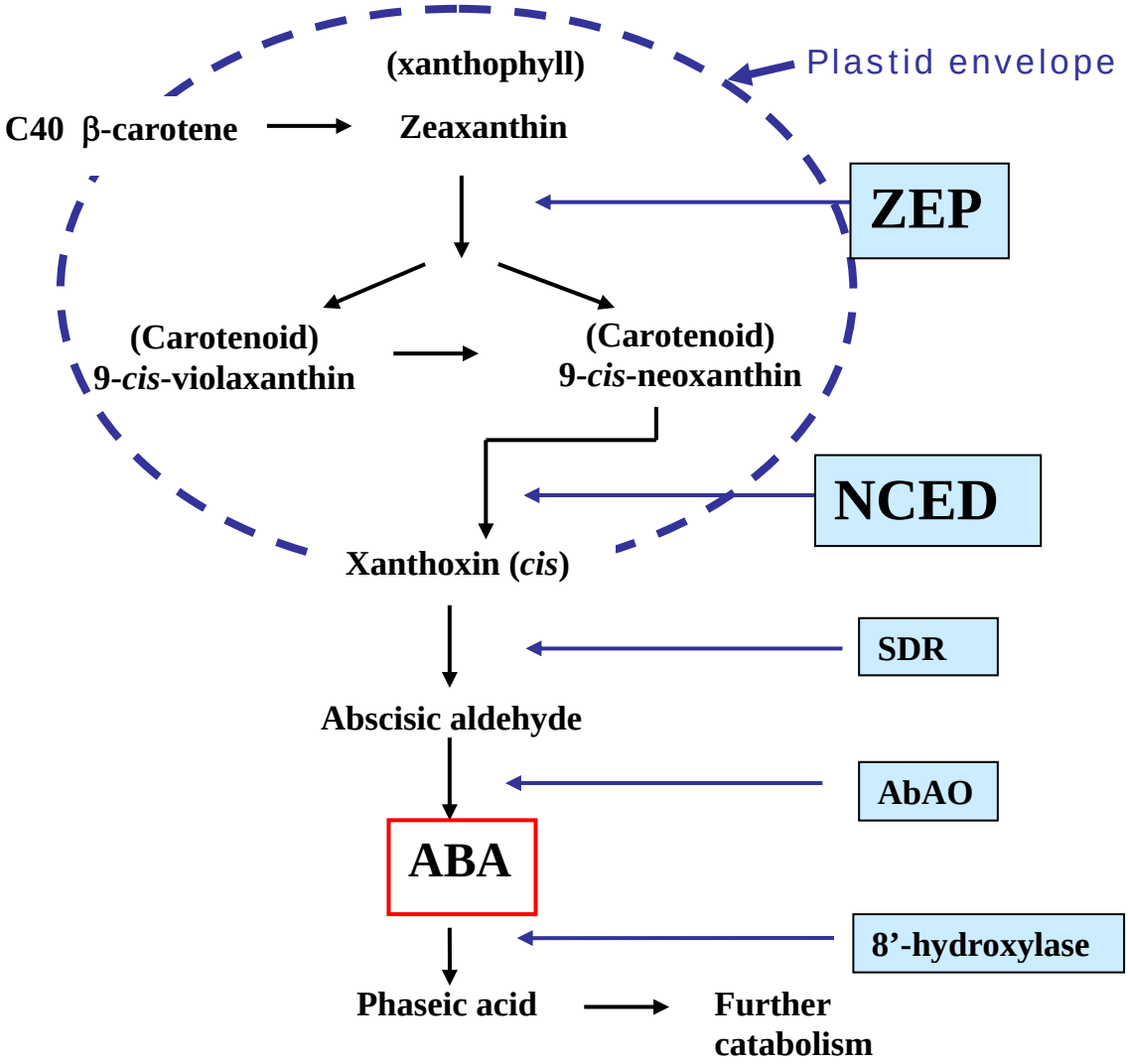


Figure 7.4. Stylised diagram representing a simplified version of the ABA biosynthetic pathway. Enzymes are contained within blue boxes, compound names are given in black text only, ABA is boxed in red. The diagram was produced by Dr Jim Speirs, CSIRO Plant Industry, Adelaide, and modified further. ZEP, zeaxanthin epoxidase; NCED, 9-cis-epoxycarotenoid dioxygenase; SDR, short-chain alcohol dehydrogenase; AbaO, abscisic aldehyde oxidase.

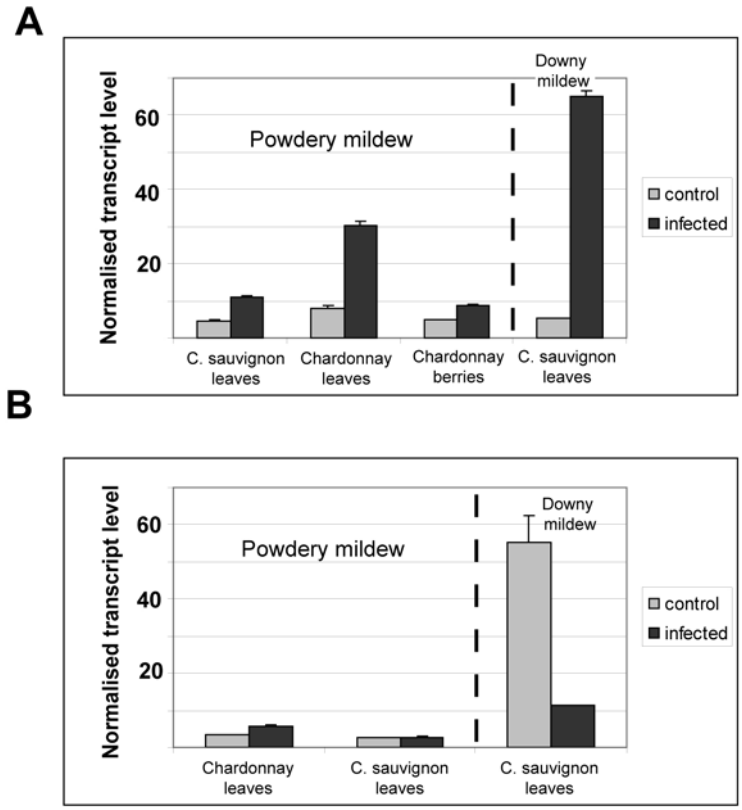


Figure 7.5. Quantitative RT-PCR analysis of VvNCED1 (A) and VvZEP1 (B) expression in powdery mildew and downy mildew infected samples. All values are relative to the expression of actin. Data analysed using the method of Muller et al. (2002). Data are the mean of one sample tested in triplicate. Primer sequences are in Table 2.3.

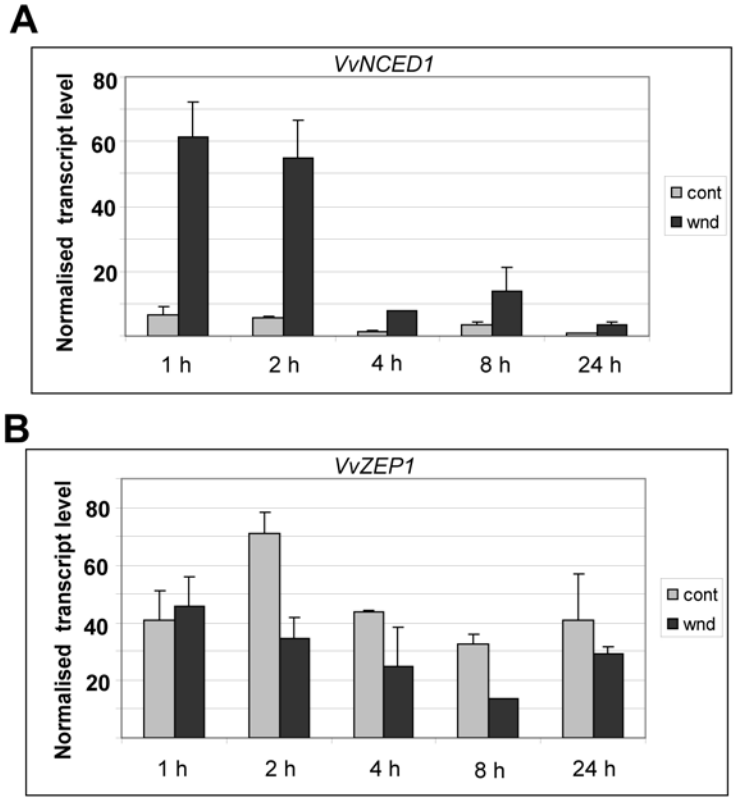


Figure 7.6. Quantitative RT-PCR analysis of *VvNCED1* (A) and *VvZEP1* (B) expression in wounded and control leaves. All values are relative to the expression of actin. Data analysed using the method of Muller et al. (2002). Data are the mean of biological replicates tested in triplicate. cont = control, wnd = wounded. Primer sequences are in Table 2.3.

7.3.5 ABA concentration in powdery mildew infected grapevine leaves

The concentration of ABA in powdery mildew infected (10 days after inoculation) and healthy (control) Chardonnay leaves was measured using gas chromatography and mass spectrometry as described (Soar et al., 2004). There was no statistically significant difference in ABA concentration between infected and healthy leaves although ABA concentration tended to be slightly higher in infected samples (Fig. 7.7)

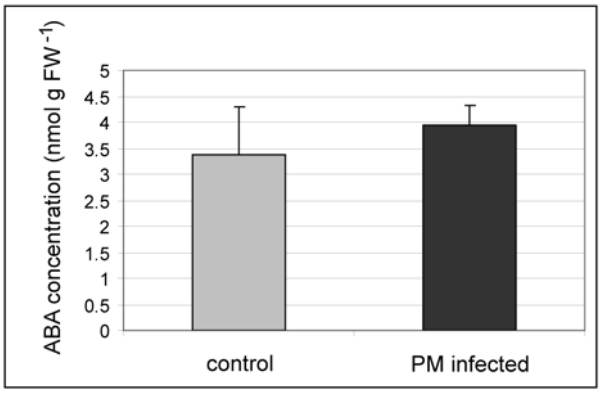


Figure 7.7. Bulk-leaf ABA concentration of glasshouse-grown powdery mildew infected and control Chardonnay leaves. Leaves were collected 10 days after inoculation. Data are means of biological replicates tested in triplicate. Error bars are one standard deviation. ABA concnetration determined using the method of Soar *et al.* (2004).

7.4 Discussion

In addition to regulating various aspects of plant development, plant growth regulators, or hormones, initiate adaptive responses to exogenous cues from both the biotic and abiotic environments. To identify pathways that may be involved in the induction of *VvHT5* and *VvcwINV* in response to powdery mildew infection (Fig. 5.1 and Fig 5.3), downy mildew infection (Fig. 5.6) and wounding (Fig. 5.7), ethylene, methyl jasmonate and ABA were exogenously supplied to grapevine leaves. Ethylene and methyl jasmonate application increased transcript levels of the thaumatin-like gene *VvTl2*, consistent with the observations of Jacobs *et al*. (1999) where expression of grapevine pathogenesis-related proteins *VvTl2*, *VvGlub* and *VvChi4* was elevated by powdery mildew infection and ethylene treatment. These hormones also marginally increased transcript levels of *VvHT5* and *VvcwINV* (Fig. 7.1), however these changes were far smaller than those elicited by pathogen infection (Fig. 5.1 and Fig 5.3) or wounding (Fig. 5.7). Furthermore, *VvGIN1* expression was not changed by either treatment (Fig. 7.1) whereas powder mildew infection strongly down-regulated expression of this gene. Taken together, these

results suggest that ethylene and jasmonate regulated pathways may not be responsible for the induction of *VvHT5* and *VvcwINV* observed during pathogen infection and wounding.

Exogenous application of ABA resulted in elevated transcript levels of *VvHT1* and *VvHT5*, but did not change the levels of *VvHT2*, *VVHT3* and *VvHT4* transcripts (Fig. 7.2 A). Specific induction of *VvHT1* and *VvHT5* was also observed in response to powdery mildew infection (Fig. 5.1) and wounding (Fig. 5.7 A), suggesting ABA-dependant pathways may contribute to the induction of these genes in response to stress stimuli. Transcript levels of *VvHT1* were previously reported to increase in grape cell cultures supplied with ABA (Çakir et al., 2003). The current study supports and extends this observation by showing that *in vivo* expression of *VvHT1* is enhanced by exogenously supplied ABA. Significantly, ABA application also enhanced cell wall invertase *VvcwINV* expression and repressed vacuolar invertase *VvGIN1* expression, again reflecting the changes in transcript levels elicited by powdery mildew infection (Fig 5.2) and wounding (Fig. 5.7 B). VvcwINV enzyme activity in grape berries and avocado is increased by ABA (Richings et al., 2000; Pan et al., 2005), and the promoter of a tomato cwINV *Lin6* is activated by ABA (Roitsch et al., 2003). In contrast to the down regulation of *VvGIN1* in response to ABA, expression of *IVR2*, a vacuolar invertase from maize, was found to be enhanced by water stress and ABA application (Kim et al., 2000; Trouverie et al., 2003). However, it should be noted that expression of other maize invertase genes did not increase in response to ABA application. Furthermore, transcript levels of a vINV from wheat declined in response to drought (Koonjul et al., 2004) indicating that individual invertase family members are differentially regulated by this hormone (Trouverie et al., 2003).

Genetic screens, mainly in *A. thaliana,* have demonstrated that there is significant overlap between sugar and ABA signalling pathways. For example, characterisation of the sugar response mutants *gin1*, *gin5* and *gin6* revealed that they are allelic to ABA response mutants *aba2*, *aba3* and *aba4* respectively (Arenas-Huertero et al., 2000; Cheng et al., 2002). Furthermore, glucose positively regulates the expression of ABA biosynthetic genes such as *ABA2* from *A. thaliana*, suggesting a direct link between sugar signalling and ABA biosynthesis (Cheng et al., 2002). In grapevine, Çakir *et al*. (2003) demonstrated that *VvMSA1*, an ASR (for ABA, stress and ripening-induced) homologue, interacts with the promoter of *VvHT1* and activates transcription of this gene. Additionally, in grape cell cultures, expression of *VvMSA1* is elevated by the addition of sucrose and ABA to the growth media, suggesting *VvMAS1* may be a link between sugar and ABA signalling pathways in grapevine (Çakir et al., 2003).

Consistent with the finding that ABA application elevated transcript levels of *VvHT5*, *VvHT1* and *VvcwINV*, analysis of the promoter regions of these genes identified ABA response motifs. For example, the *VvHT5* promoter contains five ABRE motifs. In *A. thaliana* and maize, ABA and stress-responsive genes are regulated by ABREs which are bound by a specific group of ABA, drought and salinity-induced bZIP transcription factors called ABFs (Busk and Pages, 1998; Choi et al., 2000). Other bZIP proteins closely related to ABFs, such as ABI5, are involved in developmental processes such as seed germination that are also regulated by ABA (Kim et al., 2002). GRIP 55 is a grapevine bZIP homologue that is most highly expressed in post véraison berries between 8 and 14 weeks after flowering, in correlation with maximal grape berry ABA concentrations (Davies and Robinson, 2000; Wheeler and Davies, manuscript in preparation). Consistent with

VvHT5 being ABA-regulated in leaves, transcript levels of *VvHT5* increased in berries at approximately 12 weeks after flowering (Fig. 6.3), when ABA concentration is relatively high, suggesting that GRIP 55 could also regulate *VvHT5* in ripening berries.

In contrast to *VvHT5*, the promoters of *VvHT1* and *VvcwINV* contain MYB and MYC motifs. These sequences are targets of MYB, MYC and NAC-domain transcription factors that regulate stress-induced genes in *A. thaliana* in response to abiotic stimuli, also via ABA-dependant pathways (Abe et al., 1997; Tran et al., 2004). The functional behaviour of *VvHT1* and *VvcwINV* promoters appears significantly different to the *VvHT5* promoter because expression of *VvHT1* and *VvcwINV* was elevated by a lesser amount than *VvHT5* by ABA treatment (Fig. 7.2), by powdery mildew infection (Fig. 5.1) and wounding (Fig. 5.7). This suggests that these genes may be controlled by different regulatory factors and pathways that may all involve the participation of ABA. Additionally, other pathogen and stress-associated motifs such as GT1 (Park et al., 2004; Wang et al. 2004) or EIX (Matarasso et al., 2005) may also contribute to these pathogen and wound-associated responses. Functional investigation of the *VvHT1*, *VvcwINV* and *VvHT5* promoters through promoter deletion experiments would enable the determination of the exact regions that drive gene expression in response to stress stimuli and ABA treatment and therefore establish if common regulatory motifs are in control.

While ABA is an important mediator of responses to abiotic stresses such as drought and salinity (Zhu, 2002), a role in regulating responses to biotic stimuli is also supported. For example, McDonald and Cahill (1999) showed that ABA application mediated the establishment of a compatible interaction between a usually incompatible soybean cultivar and the oomycete *P. sojae*. Furthermore, ABA

addition to *A. thaliana* plants induced susceptibility to a usually avirulent strain of *P. syringae*, while *aba1-1 A. thaliana* lines, which are ABA-deficient, displayed reduced susceptibility to virulent strains of *P. parasitica* (Mohr and Cahill, 2003). These studies provide cogent examples in support of the idea that endogenous ABA concentrations contribute to the formation of compatible interactions between microbial pathogens and plant hosts. This contribution may function by suppression of defence responses (McDonald and Cahill, 1999; Audenaert et al., 2002) or via other as yet unidentified mechanisms. In terms of obligate biotrophic pathogens that derive carbohydrate and other nutrients from plant hosts, the ABA-responsive grapevine genes identified in the current study may contribute to the formation of carbohydrate sink metabolism and subsequently allow pathogens access to additional carbohydrate. Alternatively, supplementary carbohydrate would provide more energy for defence or stress responses. Whether these responses are beneficial or detrimental to pathogen infection has not been demonstrated.

Expression of the ABA biosynthetic gene *VvNCED1* was found to be elevated by pathogen infection (Fig 7.5) and wounding (Fig. 7.6), while consistent with the findings of Soar *et al*. (2004), *VvZEP* expression was unchanged or tended to be repressed by these treatments. However, preliminary attempts to determine bulk leaf ABA levels in powdery mildew infected grape leaves did not indicate any significant differences between infected and control tissues (Fig. 7.7). Soar *et al*. (2004) observed increased transcript levels of *VvNCED1* in water stressed leaves and observed higher bulk leaf ABA concentrations in stressed tissue compared with controls. However, the level of *VvNCED1* expression did not always correlate with bulk leaf ABA concentrations, suggesting other regulatory mechanisms including changes in ABA compartmentation and differential cell-specific concentrations may

be important. Consistent with this idea, apoplasmic ABA concentrations rise rapidly within minutes after drought stress is imposed, indicating that ABA release from stores is more likely than additional biosynthesis via a transcriptionally-regulated enzymatic pathway (Hartung et al., 1997).

Chapter 8 – Summary and concluding remarks

Powdery mildew is the single most important disease of grapevine worldwide and is currently managed via the widespread application of anti-fungal chemicals (Montgomery and Hansen, 2000). Particularly in mild weather conditions where the pathogen tends to grow particularly well, outright crop loss can occur without the use of fungicides (Savocchia et al., 2004). However, liberal use of fungicides has abetted the development of pathogen resistance to these chemicals, which unfortunately no longer offer good control in some viticultural regions (Erickson and Wilcox, 1997; Savocchia et al., 2004).

Traditional plant breeding strategies have used disease resistance loci to develop pathogen resistant cultivars (Larkin et al., 1995). Such an approach is currently being employed to locate and eventually introduce resistance determinants from a North American grapevine into commercially important European species (Barker et al., 2005). However, in the majority of cases, such resistance genes are usually only effective against a single, or at most, a few races of a given pathogen species. Therefore, more recent breeding strategies have attempted to pyramid multiple resistance genes to confer more durable disease resistance (Hulbert et al., 2001).

Alternative sources of powdery mildew resistance could be engineered via identification of host genes that contribute to susceptible pathogen interactions: these genes could be targets for modification to engineer resistance via reduced susceptibility (Vogel and Somerville 2000). In this study, grapevine metabolic genes have been investigated using microarray and quantitative RT-PCR analysis, to determine if any are differentially expressed in powdery mildew infected tissues,

and therefore, may play a role in nutrient, and in particular carbohydrate, delivery to the site of pathogen infection.

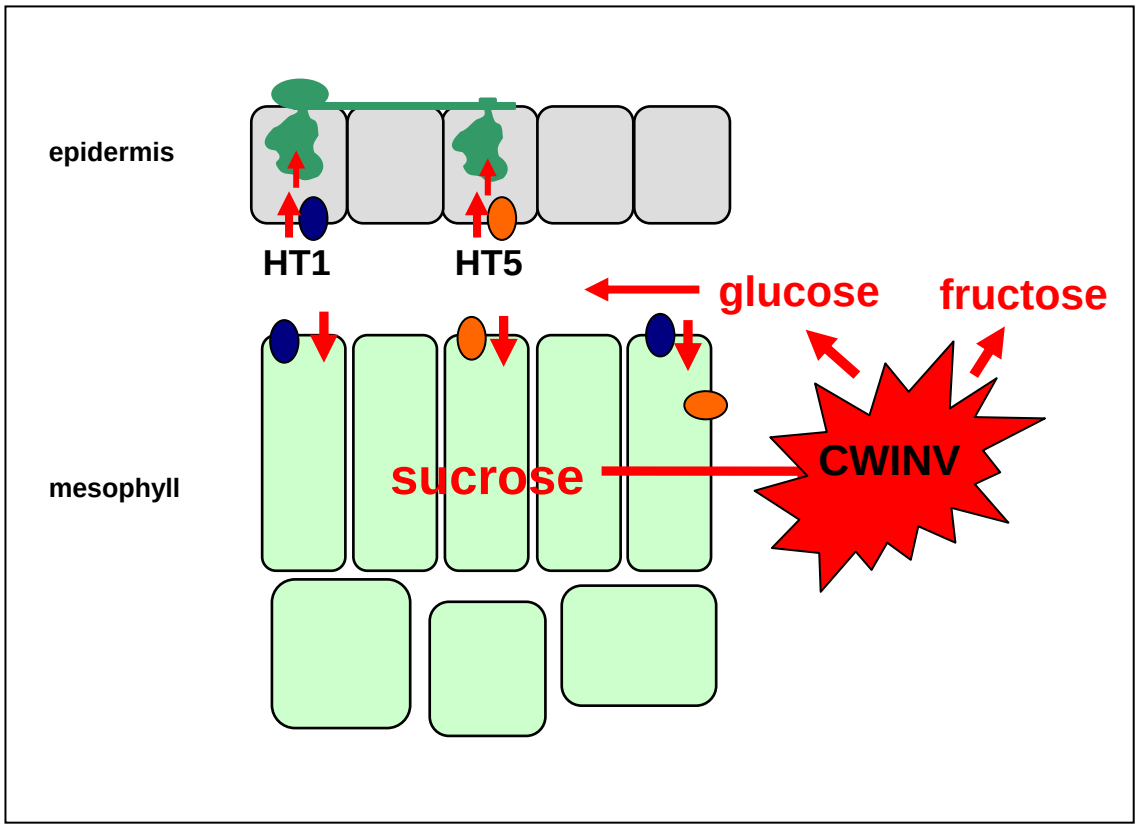


Figure 8.1. Powdery mildew infection induces sink metabolism by elevation of cwINV expression and activity, and by up-regulation of monosaccharide transporter gene expression (HT1 and HT5). Increased cwINV activity will promote apoplasmic phloem unloading and reduce phloem loading, while monosaccharide transporters would provide additional sugar uptake capacity. These genes are not induced specifically in powdery mildew infected cells but may be expressed throughout the mesophyll and in cells outside of infected regions.

The results of this study indicate that powdery mildew infection of grapevine may stimulates the formation of carbohydrate sink metabolism via the induction of cell wall invertase gene *VvcwINV* and specific members of the monosaccharide transporter gene family, *VvHT1* and *VvHT5*, to increase hexose delivery to infected epidermal cells (Refer to Fig. 8.1; Brem et al., 1988). However, this response does not appear to be powdery mildew specific because infection by downy mildew and wounding elicited similar gene expression changes indicating it may be a general response to stress. Putative ABA-responsive regulatory elements were identified in

the promoter regions of these stress-induced genes, and exogenous application of ABA elicited similar gene expression changes to those observed in response to stress. This suggests that ABA may be a participant in the pathways that regulate expression of these genes.

Clearly, an important question in determining the likelihood of success of a powdery mildew resistance strategy based on down-regulation of these host genes is whether the observed induction of sink metabolism is beneficial to the pathogen or the host. The powdery mildew pathogen may enjoy better access to carbohydrate as a result of this host response and may exploit the change in metabolism for its nutritional benefit. If this is the case, then modification of this response may be a potential means to reduce susceptibility to powdery mildew infection. However, it is also possible that the additional carbohydrate supply may be utilised by the host to energise defence and repair mechanisms to cope with infection or wounding (Truernit et al., 1996), which suggests that carbohydrate delivery may be an important aspect of this adaptive response.

Cell wall invertase activity regulates apoplasmic phloem unloading of sucrose (Patrick et al, 2000). Due to elevated *VvcwINV* expression and activity in powdery mildew infected grapevine tissues, this pathway appears to be enhanced, consistent with observations from other pathogen infected plants (Fotopoulos et al., 2003; Roitsch et al., 2003). Thus, could down-regulation of *VvcwINV* lead to increased resistance to powdery mildew without negatively impacting on grapevine growth and development? Antisense inhibition of a pollen-specific cwINV from tobacco induced male sterility, presumably due to a reduction in apoplasmic carbohydrate delivery to this sink organ (Goetz et al., 2001). Furthermore, ectopic expression of an invertase inhibitor reduced hexose concentrations of sweet potato

tubers without detrimental effects on starch content or quality (Greiner et al., 1999). As a novel powdery mildew control strategy, a powdery mildew inducible promoter, such as the *VvHT5* promoter, could be used to drive ectopic expression of an invertase inhibitor or RNA-interference molecule. Initial experiments to determine key powdery mildew responsive regions in the *VvHT5* promoter would be an essential prelude to this approach, and if the responsive sequences are specifically mapped, potential negative traits associated with the transgene may be avoided.

In addition to a reduction in sink metabolism, inhibition of cwINV expression or activity may also induce senescence. Lara *et al*. (2004) elegantly demonstrated that cwINV activity is required for cytokinin-induced delayed senescence, suggesting that apoplasmic carbohydrate delivery may override programmed cell death pathways. If carbohydrate supply to powdery mildew infected regions could be restricted, the apparent stability of the pathogen-host association may be undermined via induction of host programmed cell death pathways.

Modification of metabolic genes, as described above, may reduce susceptibility to powdery mildew infection, however, considering that these genes are not expressed exclusively in powdery mildew infected tissue, new more specific targets should be identified. Microarray analysis using the Affymetrix *V. vinifera* oligo array would allow expression analysis of 14,000 grapevine transcripts, which is 10 times more than screened with the array employed in this study. To increase the likelihood of identifying genes that are induced specifically by powdery mildew infection, microarray comparisons should also be made between powdery mildew infected and wounded tissue.

As described in the General Introduction, Vogel and Somerville (2000) identified *A. thaliana* genes that contribute to powdery mildew susceptibility. Most of these *pmr* loci cloned to date encode genes involved in some aspect of host cell wall synthesis and/or modification (Vogel et al., 2002; Nishimura et al., 2003; Vogel et al., 2004). In light of these observations, identification of grapevine genes that mediate structural changes induced by powdery mildew infection may provide better targets to engineer resistance than the metabolic genes identified in this study. The identification and analysis of grapevine homologues of the *A. thaliana PMR* genes is a direct route to identify putative susceptibility genes that could be down-regulated using RNA interference-techniques to reduce susceptibility to powdery mildew.

The potential of developing novel resistance strategies against powdery mildew through the targeting of "susceptibility" genes is supported by the *A. thaliana pmr* mutants. Furthermore, due to the nature of biotrophic pathogens, susceptibility genes, rather than typical disease resistance determinants, have the added advantage that they are not race-specific and are therefore likely to provide durable resistance in the field.

Reference list

Abe, H., Yamaguchi-Shinozaki, K., Urao, T., Iwasaki, T., Hosokawa, D., and Shinozaki, K. (1997). Role of Arabidopsis MYC and MYB Homologs in Drought- and Abscisic Acid-Regulated Gene Expression. *Plant Cell* **9,** 1859-1868.

Abood, J. K., and Losel, D. M. (2003). Changes in carbohydrate composition of cucumber leaves during the development of powdery mildew infection. *Plant Pathology* **52,** 256-265.

Aked, J., and Hall, J. L. (1993). The uptake of glucose, fructose and sucrose into pea powdery mildew (*Erysiphe pisi* DC) from the apoplast of pea leaves. *New Phytologist* **123,** 277-282.

Angra, R., and Mandahar, C. L. (1991). Pathogenesis of barley leaves by *Helminthosporium teres*I: green island formation and the possible involvement of cytokinins. *Mycopathologia* **114,** 21-27.

Arenas-Huertero, F., Arroyo, A., Zhou, L., Sheen, J., and Leon, P. (2000). Analysis of Arabidopsis glucose insensitive mutants, *gin5* and *gin6*, reveals a central role of the plant hormone ABA in the regulation of plant vegetative development by sugar. *Genes and Development* **14,** 2085-2096.

Audenaert, K., De Meyer, G. B., and Hofte, M. M. (2002). Abscisic Acid Determines Basal Susceptibility of Tomato to Botrytis cinerea and Suppresses Salicylic Acid-Dependent Signaling Mechanisms. *Plant Physiology* **128,** 491-501.

Ayliffe, M. A., Roberts, J. K., Mitchell, H. J., Zhang, R., Lawrence, G. J., Ellis, J. G., and Pryor, T. J. (2002). A Plant Gene Up-Regulated at Rust Infection Sites. *Plant Physiology* **129,** 169-180.

Baiges, I., Schaffner, A. R., and Mas, A. (2001). Eight cDNA encoding putative aquaporins in *Vitis* hybrid Richter-110 and their differential expression. *Journal of Experimental Botany* **52,** 1949-1951.

Balibrea Lara, M. E., Gonzalez Garcia, M.-C., Fatima, T., Ehness, R., Lee, T. K., Proels, R., Tanner, W., and Roitsch, T. (2004). Extracellular Invertase Is an Essential Component of Cytokinin-Mediated Delay of Senescence. *Plant Cell* **16,** 1276-1287.

Bannai, H., Tamada, Y., Maruyama, O., Nakai, K., and Miyano, S. (2002). Extensive feature detection of N-terminal protein sorting signals. *Bioinformatics* **18,** 298-305.

Barker, C. L., Donald, T., Pauquet, J., Ratnaparkhe, M. B., Bouquet, A., Adam-Blondon, A. F., Thomas, M. R., and Dry, I. B. (2005). Genetic and physical mapping of the grapevine powdery mildew resistance gene, Run1, using a bacterial artificial chromosome library. *Theoretical and Applied Genetics* **111,** 370-377.

Barth, I., Meyer, S., and Sauer, N. (2003). PmSUC3: Characterization of a SUT2/SUC3-type sucrose transporter from Plantago major. *Plant Cell* **15,** 1375-1385.

Bendtsen, J. D., Nielsen, H., Heijne, G., and Brunak, S. (2004). Improved prediction of signal peptides: SignalP 3.0. *Journal of Molecular Biology* **340**, 783-795.

Benhamou, N., Grenier, J., and Chrispeels, M. J. (1991). Accumulation of beta - fructosidase in the cell walls of tomato roots following infection by a fungal wilt pathogen. *Plant Physiology* **97,** 739-750.

Bird, D. M. (2004). Signaling between nematodes and plants *Current Opinion in Plant Biology* **7,** 372.

Blackman, L. M., and Overall, R. L. (2001). Structure and function of plasmodesmata. *Australian Journal of Plant Physiology* **28,** 709-727.

Bondada, B. R., Matthews, M. A., and Shackel, K. A. (2005). Functional xylem in the post-veraison grape berry. *Journal of Experimental Botany* **56,** 2949-2957.

Bouarab, K., Melton, R., Peart, J., Baulcombe, D., and Osbourn, A. (2002). A saponin-detoxifying enzyme mediates suppression of plant defences. *Nature* **418,** 889-892.

Boubals, D. (1961) Study of the causes of resistance of vines to powdery mildew of grapevine - *Uncinula necator*, and the mode of hereditary transmission. *Anu. Amélior. Plantes* **11**, 401-500

Boursiac, Y., Chen, S., Luu, D.-T., Sorieul, M., van den Dries, N., and Maurel, C. (2005). Early effects of salinity on water transport in *Arabidopsis* roots. Molecular and Cellular Features of Aquaporin Expression. *Plant Physiology* **139,** 790-805.

Boyd, L. A., Smith, P. H., and Brown, J. K. M. (1994). Molecular and cellular expression of quantitative resistance in barley to powdery mildew. *Physiological and Molecular Plant Pathology* **45,** 47-58.

Brem, S., Rast, D. M., and Ruffner, H. P. (1986). Partitioning of photosynthate in leaves of *Vitis vinifera* infected with *Uncinula necator* or *Plasmopora viticola*. *Physiological and Molecular Plant Pathology* **29,** 285-291.

Bruggmann, R., Abderhalden, O., Reymond, P., and Dudler, R. (2005). Analysis of epidermis- and mesophyll-specific transcript accumulationin powdery mildew-inoculated wheat leaves. *Plant Molecular Biology* **58,** 247.

Burkle, L., Hibberd, J. M., Quick, W. P., Kuhn, C., Hirner, B., and Frommer, W. B. (1998). The H^+-sucrose cotransporter *NtSUT1* is essential for sugar export from tobacco leaves. *Plant Physiology* **118,** 59-68.

Busk, P. K., and Pagès, M. (1998). Regulation of abscisic acid-induced transcription. *Plant Molecular Biology* **37,** 425-435.

Butters, J. A., Burrell, M. M., and Hollomon, S. W. (1985). Purine metabolism in barley powdery mildew and its host. *Physiological Plant Pathology* **27,** 65-74.

Buttner, M., and Sauer, N. (2000). Monosaccharide transporters in plants: structure, function and physiology. *Biochimica et Biophysica Acta* **1465,** 263-274.

Buttner, M., Truernit, E., Baier, K., Scholz-Starke, J., Sontheim, M., Lauterbach, C., Huss, V. A. R., and Sauer, N. (2000). AtSTP3, a green leaf-specific, low affinity monosaccharide -H^+ symporter of *Arabadopsis thaliana*. *Plant Cell and Environment* **23,** 175-184.

Çakir, B., Agasse, A., Gaillard, C., Saumonneau, A., Delrot, S., and Atanassova, R. (2003). A grape ASR protein involved in sugar and abscisic acid signalling. *Plant Cell* **15,** 2165-2180.

Carpaneto, A., Geiger, D., Bamberg, E., Sauer, N., Fromm, J., and Hedrich, R. (2005). Phloem-localized, proton-coupled sucrose carrier ZmSUT1 mediates sucrose efflux under the control of the sucrose gradient and the proton motive force. *Journal of Biological Chemistry* **280,** 21437-21443.

Cheng, W.-H., Endo, A., Zhou, L., Penney, J., Chen, H.-C., Arroyo, A., Leon, P., Nambara, E., Asami, T., Seo, M., Koshiba, T., and Sheen, J. (2002). A unique Short-Chain Dehydrogenase/Reductase in *Arabidopsis* glucose signaling and abscisic acid biosynthesis and functions. *Plant Cell* **14,** 2723-2743.

Cheong, Y. H., Chang, H.-S., Gupta, R., Wang, X., Zhu, T., and Luan, S. (2002). Transcriptional profiling reveals novel interactions between wounding, pathogen, abiotic stress, and hormonal responses in *Arabidopsis*. *Plant Physiology* **129,** 661-677.

Choi, H., Hong, J., Ha, J., Kang, J., and Kim, S. (2000). ABFs, a family of ABA-responsive element binding factors. *Journal of Biological Chemistry* **275,** 1723-1730.

Chou, H.-M., Bundock, N., Rolfe, S. A., and Scholes, J. D. (2000). Infection of *Arabidopsis thaliana* leaves with *Albugo candida* (white blister rust) causes a reprogramming of host metabolism. *Molecular Plant Pathology* **1,** 99-113.

Clark, J. I. M., and Hall, J. L. (1998). Solute transport into healthy and powdery mildew-infected leaves of pea and uptake by powdery mildew mycelium. *New Phytologist* **140,** 261-269.

Coglan, S. E., and Walters, D. R. (1990). Polyamine metabolism in 'green-islands' on powdery mildew-infected barley leaves: possible interactiosn with senescence. *New Phytologist* **116,** 417-424.

Cooper, S. J., and Ashby, A. M. (1998). Comparison of cytokinin and cytokinin-O-glucoside cleaving [beta]-glucosidase production *in vitro* by *Venturia inaequalis* and other phytopathogenic fungi with differing modes of nutrition *in planta*. *Physiological and Molecular Plant Pathology* **53,** 61-72.

Davies, C., Boss, P. K., and Robinson, S. P. (1997). Treatment of grape berries, a nonclimacteric fruit with a synthetic auxin, retards ripening and alters the expression of developmentally regulated genes. *Plant Physiology* **115,** 1155-1161.

Davies, C., and Robinson, S. P. (1996). Sugar accumulation in grape berries. *Plant Physiology* **111,** 275-283.

Davies, C., Wolf, T., and Robinson, S. P. (1999). Three putative sucrose transporters are differentially expressed in grapevine tissue. *Plant Science* **147,** 93-100.

De Coninck, B., Le Roy, K., Francis, I., Clerens, S., Vergauwen, R., Halliday, A. M., Smith, S. M., Van Laere, A., and Van Den Ende, W. I. M. (2005). Arabidopsis AtcwINV3 and 6 are not invertases but are fructan exohydrolases (FEHs) with different substrate specificities. *Plant Cell and Environment* **28,** 432-443.

DiDonato, R. J. J., Roberts, L. A., Sanderson, T., Eisley, R. B., and Walker, E. L. (2004). *Arabidopsis Yellow Stripe-Like2* (YSL2): a metal-regulated gene encoding a plasma membrane transporter of niciotianamine-metal complexes. *Plant Journal* **39,** 403-414.

Doke, N. (1975). Prevention of the hypersensitive reaction of potato cells to infection with an incompatible race of *Phytophthora infestans* by constituents of the zoospores. *Physiological and Molecular Plant Pathology* **7,** 1-7.

Donald, T. M., Pellerone, F., Adam-Blondon, A. F., Bouquet, A., Thomas, M. R., and Dry, I. B. (2002). Identification of resistance gene analogs linked to a powdery mildew resistance locus in grapevine. *Theoretical and Applied Genetics* **104**(4)**,** 610-618.

Dorhout, R., Kollofell, C., and Gommers, F.J. (1992). Alteration of distribution of regions with high net proton extrusion in tomato roots infected with *Meloidogyne incognita. Physiological and Molecular Plant Pathology* **40,** 153-162.

Dreier, L. P., Hunter, J. J., and Ruffner, H. P. (1998). Invertase activity, grape berry development and cell compartmentation. *Plant Physiology and Biochemistry (Paris)* **36,** 865-872.

Ehneß, R., and Roitsch, T. (1997). Co-ordinated induction of mRNAs for extracellular invertase and a glucose transporter in *Chenopodium rubrum* by cytokinins. *The Plant Journal* **11,** 539-548.

Emanuelsson, O., Nielsen, H., and von Heijne, G. (1999). ChloroP, a neural network-based method for predicting chloroplast transit peptides and their cleavage sites. *Protein Science* **8,** 978-984.

Erickson, E. O., and Wilcox, W. F. (1997). Distributions of sensitivities to three sterol demethylation inhibitor fungicides among populations of *Uncinula necator* sensitive and resistant to triadimefon. *Phytopathology* **87,** 784-791.

Famiani, F., Walker, R. P., Tecsi, L., Chen, Z.-H., Proietti, P., and Leegood, R. C. (2000). Am immunohistochemical study of the compartmentation of metabolism

during the development of grape (*Vitis vinifera* L.) berries. *Journal of Experimental Botany* **51,** 675-683.

Felsenstein, J. (1989). PHYLIP - Phylogeny Inference Package (Version 3.2). *Cladistics* **5,** 164-166.

Ficke, A., Gadoury, D.M. & Seem, R.C. (2002). Ontogenic resistance and plant disease management: a case study of grape powdery mildew. *Phytopathology* **92,** 671-675.

Fillion, L., Ageorges, A., Picaud, S., Coutos-Thevenot, P., Lemoine, R., Romieu, C., and Delrot, S. (1999). Cloning and expression of a hexose transporter gene expressed during the ripening of grape berry. *Plant Physiology* **120,** 1083-1093.

Fischer, W. N., Andre, B., Rentsch, D., Krolkiewicz, S., Tegeder, M., Breitkreuz, K., and Frommer, W. B. (1998). Amino acid transport in plants. *Trends in Plant Science* **3,** 188-195.

Fotopoulos, V., Gilbert, M. J., Pittman, J. K., Marvier, A. C., Buchanon, A. J., Sauer, N., Hall, J. L., and Williams, L. E. (2003). The monosaccharide transporter gene, *AtSTP4*, and the cell wall invertase, *AtBfruct1*, are induced in *Arabidopsis* during infection with the fungal biotroph *Erysiphe cichoracearum*. *Plant Physiology* **132,** 821-829.

Fric, F., and Wolf, G. (1994). Hydrolytic enzymes of ungerminated and germinated conidia of *Erysiphe graminis* DC f.sp. hordei Marchal. *Journal of Phytopathology* **140,** 1-10.

Frohman, A., Dush, M. K., and Martin, G. R. (1988). Rapid production of full-length cDNAs from rare transcripts: amplification using a single gene-specific oligonucleotide primer. *Proceedings of the National Academy of Sciences. U.S.A.* **85,** 8998-9002.

Gear, M. L., McPhillips, M.L., Patrick, J.W., and McCurdy, D.W. (2000). Hexose transporters of tomato: molecular cloning, expression analysis and functional characterisation. *Plant Molecular Biology* **44,** 687-697.

Gleave, A. P. (1992). A versatile binary vector system with a T-DNA organisational structure conducive to efficient integration of cloned DNA into the plant genome. *Plant Molecular Biology* **20,** 1203-1207.

Goes da Silva, F., Iandolino, A., Al-Kayal, F., Bohlmann, M. C., Cushman, M. A., Lim, H., Ergul, A., Figueroa, R., Kabuloglu, E. K., Osborne, C., Rowe, J., Tattersall, E., Leslie, A., Xu, J., Baek, J., Cramer, G. R., Cushman, J. C., and Cook, D. R. (2005). Characterizing the Grape Transcriptome. Analysis of expressed sequence tags from multiple *Vitis* species and development of a compendium of gene expression during berry development. *Plant Physiology* **139,** 574-597.

Goetz, M., Godt, D.E., and Roitsch, T. (2000). Tissue-specific induction of the mRNA for an extracellular invertase isoenzyme of tomato by brassinosteroids suggests a role for steroid hormones in assimilate partitioning. *Plant Journal* **22,** 515-522.

Goetz, M., Godt, D. E., Guivarc'h, A., Kahmann, U., Chriqui, D., and Roitsch, T. (2001). Induction of male sterility in plants by metabolic engineering of the carbohydrate supply. *Proceedings of the National Academy of Sciences. U.S.A.* **98,** 6522-6527.

Green, J. R., Carver, T. L. W. and Gurr, S. J. (2002). The formation and function of infection and feeding structures. In: Belanger, R. R., Bushenll, W. R., Dik, A. J., Carver, T. L. W. eds. *The Powdery Mildews. A comprehensive Treatis.* American Phytopathological Society, Minnesota USA, pp. 66-82.

Green, J. R., Pain, N.A., Cannell, M.E., Jones, G.L., Leckie, C.P., McCready, S., Mendgen, K., Mitchell, A.J., Callow, J.A., and O'Connell, R.J. (1994). Analysis of differentiation and development of the specialized infection structures formed by biotrophic fungal plant pathogens using monoclonal antibodies. *Canadian Journal of Botany* **73,** S408-S417.

Greenspan, M. D., Shackel, K. A., and Matthews, M. A. (1994). Developmental changes in the diurnal water budget of the grape berry exposed to water deficits. *Plant Cell and Environment* **17,** 811-820.

Greiner, S., Rausch, T., Sonnewald, U., and Herbers, K. (1999). Ectopic expression of a tobacco invertase inhibitor homolog prevents cold-induced sweetening of potato tubers. *Nature Biotechnology* **17,** 708-711.

Hahn, M., and Mendgen, K. (1997). Characterisation of in planta-induced rust genes isolated from a haustorium-specific cDNA library. *Molecular Plant-Microbe Interactions* **10,** 427-437.

Hahn, M., and Mendgen, K. (2001). Signal and nutrinet exchange at biotrophic plant-fungus interphaces. *Current Opinion in Plant Biology* **4,** 322-327.

Hahn, M., Neef, U., Struck, C., Gottfert, M., and Mendgen, K. (1997). A putative amino acid transporter is specifically expressed in haustoria of the rust fungus *Uromyces fabae*. *Molecular Plant-Microbe Interactions* **10,** 438-445.

Hall, J. L., and Williams, L. E. (2000). Assimilate transport and partitioning in fungal biotrophic interactions. *Australian Journal of Plant Physiology* **27,** 549-560.

Hammond-Kosack, K. E., and Jones, J. D. G. (1996). Resistance Gene-Dependent Plant Defence Responses. *The Plant Cell* **8,** 1773-1791.

Hammes, U. Z., Schachtman, D. P., Berg, R. H., Nielsen, E., Koch, W., McIntyre, L. M., and Taylor, C. G. (2005). Nematode-induced changes of transporter gene expression in Arabidopsis roots. *Molecular Plant-Microbe Interactions* **18**(12)**,** 1247-1257.

Harrison, M. J. (1996). A sugar transporter from *Medicago truncatula:*altered expression pattern in roots during vesicular-arbuscular (VA) mycorrhizal associations. *Plant Journal* **9,** 491-503.

Harrison, M. J. (1999). Biotrophic interfaces and nutrient transport in plant/fungal symbioses. *Journal of Experimental Botany* **50,** 1013-1022.

Harrison, M. J., Dewbre, G.R., and Liu, J. (2002). A phosphate transporter from *Medicago truncatula* involved in the acquisition of phospahte released by Arbuscular Mycorrhizal fungi. *Plant Cell* **14,** 2413-2429.

Hartung, W., Wilkinson, S., and Davies, W. (1998). Factors that regulate abscisic acid concentrations at the primary site of action at the guard cell. *Journal of Experimental Botany* **49,** 361-367.

Haupt, S., Duncan, G. H., Holzberg, S., and Oparka, K. J. (2001). Evidence for symplastic phloem unloading in sink leaves of barley. *Plant Physiology* **125,** 209-218.

Heath, M. C. (1976). Signalling between pathogenic rust fungi and resistant or susceptible host plants. *Annals of Botany* **80,** 713-720.

Heath, M. C. (1994). Signal exchange between higher plants and rust fungi. *Canadian Journal of Botany* **73,** s616-s623.

Heath, M. C. (2000). Nonhost resistance and nonspecific plant defences. *Current Opinion in Plant Biology* **3,** 315.

Hewitt, H. G., and Ayres, P. G. (1976). Effect of infection by *Microsphaera alphitoides* (powdery mildew) on carbohydrate levels and translocation in seedlings of *Quercus robur*. *New Phytologist* **77,** 379-390.

Higo, K., Ugawa, Y., Iwamoto, M., and Korenaga, T. (1999). Plant cis-acting regulatory DNA elements (PLACE) database: 1999. *Nucleic Acids Research* **27,** 297-300.

Holmes, D. S., and Quigley, M. (1981). A rapid boiling method for the preparation of bacterial plasmids. *Analytical Biochemistry* **114,** 193-197.

Hoth, S., Ikeda, Y., Morgante, M., Wang, X., Zuo, J., Hanafey, M. K., Gaasterland, T., Tingey, S. V., and Chua, N.-H. (2003). Monitoring genome-wide changes in gene expression in response to endogenous cytokinin reveals targets in *Arabidopsis thaliana*. *FEBS Letters* **554,** 373-380.

Hoth, S., Schneidereit, A., Lauterbach, C., Scholz-Starke, J., and Sauer, N. (2005). Nematode infection triggers the de novo formation of unloading phloem that allows macromolecular trafficking of green fluorescent protein into syncytia. *Plant Physiology* **138,** 383-392.

Howard, R. J., Ferrari, M. A., Roach, D. H., and Money, N. P. (1991). Penetration of hard substrates by a fungus employing enormous turgor pressures. *Proceedings of the National Academy of Sciences. U.S.A.* **88,** 11281-11284.

Hulbert, S. H., Webb, C. A., Smith, S. M., and Sun, Q. (2001). Resistance Gene Complexes : Evolution and Utilization. *Annual Review of Phytopathology* **39,** 285-312.

Hwang, B. K., and Heitefuss, R. (1986). Sugar composition and acid invertase activity in spring barley plants in relation to adult-plant resistance to powdery mildew. *Phytopathology* **76,** 365-369.

Jackson, S. A., Walters, D. R., and Baldwin, B. C. (1995). Lysine biosynthesis in powdery mildew-infected barley. *Aspects of Applied Biology* **42,** 169-176.

Jacobs, A. K., Dry, I. B. and Robinson, S. P. (1999). Induction of different pathogenesis-related cDNAs in grapevine infected with powdery mildew and treated with ethephon. *Plant Pathology* **48,** 325-336.

Jameson, P. (2000). Cytokinins and auxins in plant-pathogen interactions- an overview. *Plant Growth Regulation* **32,** 369-380.

Jang, J. Y., Kim, D. G., Kim, Y. O., Kim, J. S., and Kang, H. (2004). An expression analysis of a gene family encoding plasma membrane aquaporins in response to abiotic stresses in *Arabidopsis thaliana*. *Plant Molecular Biology* **54,** 713.

Jansen, C., Korell, M., Eckey, C., Biedenkopf, D., and Kogel, K.-H. (2005). Identification and transcriptional analysis of powdery mildew-induced barley genes. *Plant Scie*nce **168,** 373.

Jindal, S., Arora, Y. K., and Bajaj, K. L. (1979). Effect of infection by *Sphaerotheca fuliginea* (powdery mildew) on amino acids and sugars in leaves of muskmelon (*Cucumis melo* L.). *Plant Biochemical Journal* **6,** 115-123.

Kamoun, S., van West, P., Vleeshouwers, V. G. A. A., de Groot, K. E., and Govers, F. (1998). Resistance of *Nicotiana benthamiana* to *Phytophthora infestans* is mediated by the recognition of the elicitor protein INF1. *Plant Cell* **10,** 1413-1426.

Kang, J., Choi, H., Im, M., and Kim, S. (2002). *Arabidopsis* basic leucine zipper proteins that mediate stress-responsive abscisic acid signaling. *Plant Cell* **14,** 343-357.

Kim, J.-Y., Mahe, A., Brangeon, J., and Prioul, J.-L. (2000). A Maize Vacuolar Invertase, IVR2, Is Induced by Water Stress. Organ/Tissue Specificity and Diurnal Modulation of Expression. *Plant Physiology* **124,** 71-84.

Kim, S. Y., Ma, J., Perret, P., Li, Z., and Thomas, T. L. (2002). *Arabidopsis* ABI5 subfamily members have distinct DNA-binding and transcriptional activities. *Plant Physiology* **130,** 688-697.

Koch, K. (2004). Sucrose metabolism: regulatory mechanisms and pivotal roles in sugar sensing and development. *Current Opinion in Plant Biology* **7,** 235-246.

Koh, S., Andre, A., Edwards, H., Ehrhardt, D., and Somerville, S. (2005). *Arabidopsis thaliana* subcellular responses to compatible *Erysiphe cichoracearum* infections. *Plant Journal* **44,** 516-529.

Koltai, H., Dhandaydham, M., Opperman, C., Thomas, J., and Bird, D. (2001). Overlapping plant signal transduction pathways induced by a parasitic nematode and a rhizobial endosymbiont. *Molecular Plant-Microbe Interactions* **10,** 1168-1177.

Koonjul, P. K., Minhas, J. S., Nunes, C., Sheoran, I. S., and Saini, H. S. (2005). Selective transcriptional down-regulation of anther invertases precedes the failure of pollen development in water-stressed wheat. *Journal of Experimental Botany* **56,** 179-190.

Krogh, A., Larsson, B., von Heijne, G., and Sonnhammer, E. L. L. (2001). Predicting transmembrane protein topology with a hidden markov model: application to complete genomes. *Journal of Molecular Biology* **305,** 567-580.

Laloi, C., Mestres-Ortega, D., Marco, Y., Meyer, Y., and Reichheld, J.-P. (2004). The *Arabidopsis* cytosolic Thioredoxin H5 gene induction by Oxidative Stress and its W-Box-mediated response to pathogen elicitor. *Plant Physiology* **134,** 1006-1016.

Lalonde, S., Boles, E., Hellmann, H., Barker, L., Patrick, J.W., Frommer, W.B., and Ward, J.M. (1999). The dual function of sugar carriers: transport and sugar sensing. *Plant Cell* **11,** 707-726.

Lara, M. E. B., Garcia, M.-C. G., Fatima, T., Ehneb, R., Lee, T. K., Proels, R., Tanner, W., and Roitsch, T. (2004). Extracellualr invertase is an essential component of cytokinin-mediated delay of senescence. *Plant Cell* **16,** 1276-1287.

Larkin, P. J., Banks, P. M., and Chen, X. (1995). Registration of six genetic stocks of wheat with rust and BYDV resistance: Z1, Z2, Z3, Z4, Z5, and Z6 disomic addition lines with *Thinopyrum intermedium* chromosomes. *Crop Science* **35,** 604.

Leckie, C. P., Callow, J.A. and Green, J.R. (1995). Reorganisation of the endoplasmic reticulum in pea leaf epidermal cells infected by the powdery mildew fungus *Erysiphe pisi. New Phytologist* **131,** 211-221.

Lohar, D. P., Schaff, J. E., Laskey, J. G., Kieber, J. J., Bilyeu, K. D., and Bird, D. M. (2004). Cytokinins play opposite roles in lateral root formation, and nematode and Rhizobial symbioses. *Plant Journal* **38,** 203-214.

Long, S. R. (1996). Rhizobium symbiosis: Nod factors in perspective. *Plant Cell* **8,** 1885-1898.

Ma, F., and Peterson, C. A. (2000). Plasmodesmata in onion (Allium cepa L.) roots: a study enabled by improved fixation and embedding techniques. *Protoplasma* **211,** 103-115.

Mackie, A. J., Roberts, A.M., Callow, J.A. and Green, J.R. (1991). Molecular differentiation in pea powdery-mildew haustoria. *Planta* **183,** 399-408.

Manners, J. M., and Gay, J. L. (1982). Accumulation of systemic fungicides and other solutes by haustorial complexes isolated from Pisum sativum infected with *Erysiphe pisi*. *Pesticide Science* **13,** 195-203.

Matarasso, N., Schuster, S., and Avni, A. (2005). A novel plant Cysteine Protease has a dual function as a regulator of 1-Aminocyclopropane-1-Carboxylic Acid Synthase gene expression. *Plant Cell* **17,** 1205-1216.

Mathesius, U., Bayliss, C., Weinman, J. J., Schlaman, H. R. M., Spaink, H. P., Rolfe, B. G., McCully, M. E., and Djordjevic, M. A. (1998). Flavonoids synthesized in cortical cells during nodule initiation are early developmental markers in white clover. *Molecular Plant-Microbe Interactions* **11,** 1223-1232.

McDonald, K. L., and Cahill, D. M. (1999). Influence of Abscisic Acid and the Abscisic Acid Biosynthesis Inhibitor, Norflurazon, on interactions between *Phytophthora sojae* and Soybean (*Glycine max*). *European Journal of Plant Pathology* **105,** 651-658.

Mendgen, K., and Hahn, M. (2002). Plant infection and the establishment of fungal biotrophy. *Trends in Plant Science* **1016,** 1360-1385.

Mendgen, K., and Naas, P. (1988). The activity of powdery-mildew haustoria after feeding the host cells with different sugars, as measured with a potentiometric cyanine dye. *Planta* **174,** 283-288.

Meyer, S., Lauterbach, C., Niedermeier, M., Barth, I., Sjolund, R. D., and Sauer, N. (2004). Wounding enhances expression of *AtSUC3*, a sucrose transporter from *Arabidopsis* sieve elements and sink tissues. *Plant Physiology* **134,** 684-693.

Mhiri, C., Morel, J. B., Vernhettes, S., Casacuberta, J. M., Lucas, H., and Grandbastien, M. A. (1997). The promoter of the tobacco Tnt1 retrotransposon is induced by wounding and by abiotic stress. *Plant Molecular Biology* **33,** 257-266.

Miao, G. H., and Verma, D. P. S. (1993). Soybean nodulin-26 gene encoding a channel protein is expressed only in the infected cells of nodules and is regulated differently in roots of homologous and heterologous plants. *Plant Cell* **5,** 781-794.

Mohr, P. G., and Cahill, D. M. (2003). Abscisic acid influences the susceptibility of *Arabidopsis thaliana* to *Pseudomonas syringae* pv. tomato and *Peronospora parasitica. Functional Plant Biology* **30,** 461-469.

Muller, P. Y., Jarovjak, H., Miserez, A. R., and Dobbie, Z. (2002). Processing of Gene Expression Data Generated by Quantitative Real-time RT-PCR. *Biotechniques* **32,** 1372-1379.

Montgomery, R., and Hansen, J.-P. (2000). Plant protection in the EU - consumption of plant protection products in the European Union: data 1992-1996. *ISBN 92-894-0437-x*.

Mumberg, D., Muller, R., and Funk, M. (1994). Regulatable promoters of *Saccharomyces cerevisiae:* comparison of transcriptional activity and their use for heterologous expresion. *Nucleic Acids Research* **22,** 5767-5788.

Murdoch, L. J., Kobayashi, I. & Hardham, A.R. (1998). Production and characterisation of monoclonal antibodies to cell wall components of the flax rust fungus. *European Journal of Plant Pathology* **104,** 331-346.

Murphy, A. M., Pryce-Jones, E., Johnstone, K., and Ashby, A. M. (1997). Comparison of cytokinin production *in vitro* by *Pyrenopeziza brassicae* with other plant pathogens. *Physiological and Molecular Plant Pathology* **50,** 53-65.

Murray, A. J., and Ayres, P. G. (1986). Infection with powdery mildew can enhance the accumulation of proline and glycinebetaine by salt stressed barley seedlings. *Physiological and Molecular Pathology* **29,** 271-277.

Nakai, K., and Horton, P. (1999). PSORT: a program for detecting the sorting signals of proteins and predicting their subcellular localization. *Trends in Biochemical Science* **24,** 34-35.

Nishimura, M. T., Stein, M., Hou, B. H., Vogel, J. P., Edwards, H., and Somerville, S. C. (2003). Loss of a callose synthase results in salicylic acid-dependent disease resistance. *Science* **301,** 969-972.

Oldroyd, G. E. D. (2001). Dissecting Symbiosis: Developments in Nod Factor Signal Transduction. *Annals of Botony* **87,** 709-718.

Opperman, C. H., Taylor, C. G., and Conkling, M. A. (1994). Root-Knot Nematode-directed expression of a plant root-specific gene. *Science* **263,** 221-223.

O'Shea-Greenfield, A., and Smale, S. T. (1992). Roles of TATA and initiator elements in determining the start site location and direction of RNA polymerase II transcription. *Journal of Biological Chemistry* **267,** 1391-1402.

Ough, C. S., and Berg, H. W. (1979). Powdery mildew sensory effect on wine. *American Journal of Enology and Viticulture* **30,** 321.

Papadopoulou, K., Melton, R. E., Leggett, M., Daniels, M. J., and Osbourn, A. E. (1999). Compromised disease resistance in saponin-deficient plants. *Proceedings of the National Academy of Sciences. U.S.A.* **96,** 12923-12928.

Park, H. C., Kim, M. L., Kang, Y. H., Jeon, J. M., Yoo, J. H., Kim, M. C., Park, C. Y., Jeong, J. C., Moon, B. C., Lee, J. H., Yoon, H. W., Lee, S.-H., Chung, W. S., Lim, C. O., Lee, S. Y., Hong, J. C., and Cho, M. J. (2004). Pathogen- and NaCl-induced expression of the SCaM-4 promoter is mediated in part by a GT-1 Box that interacts with a GT-1-like Transcription factor. *Plant Physiology* **135,** 2150-2161.

Park, K.-J., and Kanehisa, M. (2003). Prediction of protein subcellular locations by support vector machines using compositions of amino acids and amino acid pairs. *Bioinformatics* **19,** 1656-1663.

Patrick, J. W. (1997). Phloem unloading: sieve element unloading and post-sieve element transport. *Annual Review of Plant Physiology and Plant Molecular Biology* **48,** 191-222.

Patrick, J. W., Zhang, W., Tyerman, S.D., Offler, C.E., and Walker, N.A. (2001). Role of membrane transport in phloem translocation of assimilates and water. *Australian Journal of Plant Physiology* **28,** 695-707.

Perfect, S. E., and Green, J. R. (2001). Infection structures of biotrophic and hemibiotrophic fungal plant pathogens. *Molecular Plant Pathology* **2,** 101-108.

Pryce-Jones, E., Carver, T., and Gurr, S. J. (1999). The roles of cellulase enzymes and mechanical force in host penetration by *Erysiphe graminis* f.sp. hordei. *Physiologyogical and Molecular Plant Pathology* **55,** 175-182.

Rae, A. L., Bonfante-Fasolo, P., and Brewin, N. J. (1992). Structure and growth of infection threads in the legume symbiosis with *Rhizobium leguminosarum*. *Plant Journal* **2,** 385-395.

Ramonell, K., Berrocal-Lobo, M., Koh, S., Wan, J. R., Edwards, H., Stacey, G., and Somerville, S. (2005). Loss-of-function mutations in chitin responsive genes show increased susceptibility to the powdery mildew pathogen *Erysiphe cichoracearum*. *Plant Physiology* **138,** 1027-1036.

Rezaian, M. A., and Krake, L. R. (1987). Nucleic acid extraction and virus detection in grapevine. *Journal of Virology Methods* **17,** 277-285.

Richings, E. W., Cripps, R. F., and Cowan, A. K. (2000). Factors affecting 'Hass' avocado fruit size: carbohydrate, abscisic acid and isoprenoid metabolism in normal and phenotypically small fruit. *Physiologia Plantarum* **109,** 81-89.

Roberts, A. M., Mackie, A.J., Hathaway, V., Callow, J.A. and Green, J.R. (1993). Molecular differentiation in the extrahaustorial membrane of pea powdery mildew haustoria at early and late stages of development. *Physiological and Molecular Plant Pathology* **43,** 147-160.

Roberts, J. K., and Pryor, A. (1995). Isolation of a flax (*Linum usitatissimum*) gene induced during susceptible infection by flax rust (*Melampsora lini*). *Plant Journal* **8,** 1-8.

Roitsch, T. (1999). Source-sink regulation by sugar and stress. *Current Opinion in Plant Biology* **2,** 198-206.

Roitsch, T., Balibrea, M. E., Hofmann, M., Proels, R., and Sinha, A. K. (2003). Extracellular invertase: key metabolic enzyme and PR protein. *Journal of Experimental Botany* **54,** 513-524.

Roitsch, T., and Ehneß,.R. (2000). Regulation of source/sink relations by cytokinins. *Plant Growth Regulation* **32,** 359-367.

Rose, T., Schultz, E., Henikoff, J., Pietrokovski, S., and Henikoff, S. (1998). Consensu-degenerate hybrid oligonucleotide primers for amplification of distantly-related sequences. *Nucleic Acids Research* **26,** 1628-1635.

Roussel, H., Bruns, S., Gianinazzi-Pearson, V., Hahlbrock, K. & Franken, P. (1997). Induction of a membrane intrinsic protein-encoding mRNA in arbuscular mycorrhiza and elicitor-stimulated cell suspension cultures of parsley. *Plant Science* **126,** 203-210.

Ruffner, H. P., Adler, S., and Rast, D.M. (1990). Soluble and wall associated forms of invertase in *Vitis vinifera. Phytochemistry* **29,** 2083-2086.

Ruffner, H. P., Hurlimann, M., and Skrivan, R. (1995). Soluble invertase from grape berries: purification, deglycosylation and antibody specificity. *Plant Physiology and Biochemistry (Paris)* **33,** 25-31.

Rumbolz, J., Kassemeyer, H.-H., Steinmetz, V., Deising, H. B., Mendgen, K., Mathys, D., Wirtz, S., and Guggenheim, R. (2000). Differentiation of infection structures of the powdery mildew fungus *Uncinula necator* and adhesion to the host cuticle. *Canadian Journal of botany* **78,** 409-421.

Rushton, P. J., Reinstadler, A., Lipka, V., Lippok, B. and Somssich, I.E. (2002). Synthetic plant promoters containing defined regulatory elements provide novel insights into pathogen- and wound-induced signalling. *The Plant Cell* **14,** 749-762.

Sambrook, J., and Russell, D. W. (2001). Molecular Cloning. A Laboratory Manual. Cold Spring Harbor Laboratory press, Cold Spring Harbor, New York, USA.

Sarr, J.-E., Sommerer, N., Bergoin, A., Rossignol, M., Albagnac, G., and Romieu, C. (2004). Grape berry biochemistry revisited upon proteomic analysis of the mesocarp. *Proteomics* **4,** 201-215.

Sauer, N., Friedlander, K., and Graml-Wicke, U. (1990). Primary structure, genomic organization and heterologous expression of a glucose transporter from *Arabidopsis thaliana*. *EMBO Journal* **9,** 3045-3050.

Sauer, N., and Stadler, R. (1993). A sink-specific H^+/monosaccharide co-transporter from *Nicotiana tabacum*: cloning and heterologous expression in baker's yeast. *Plant journal* **4,** 601-610.

Savocchia, S., Stummer, B. E., Wicks, T. J., Heeswijck, R. v., and Scott, E. S. (2004). Reduced sensitivity of *Uncinula necator* to sterol demethylation inhibiting fungicides in southern Australian vineyards. *Australasian Plant Pathology* **33,** 465-473.

Schenk, P. M., Kazan, K., Wilson, I., Anderson, J.P., Richmond, T., Somerville, S.C. & Manners, J.M. (2000). Coordinated plant defence responses in *Arabidopsis* revealed by microarray analysis. *Proceedings of the National Academy of Sciences. U.S.A.* **97,** 11655-11660.

Schneidereit, A., Scholz-Starke, J., Sauer, N., and Buttner, M. (2005). *AtSTP11*, a pollen tube-specific monosaccharide transporter in *Arabidopsis*. *Planta* **221,** 48-55.

Scholes, J. D., Lee, P. J., Horton, P., and Lewis, D. H. (1994). Invertase: understanding changes in the photosynthetic and carbohydrate metabolism of barley leaves infected with powdery mildew. *New Phytologist* **126,** 213-222.

Scholz-Starke, J., Buttner, M., and Sauer, N. (2003). AtSTP6, a new pollen-specific H+-monosaccharide symporter from Arabidopsis. *Plant Physiology* **131**(1)**,** 70-77.

Scott, E. (1998). Mildews: what they are and how they survive in the vineyard. *Australian Viticulture* **2,** 5-15.

Seo, M., and Koshiba, T. (2002). Complex regulation of ABA biosynthesis in plants. *Trends in Plant Science* **7,** 41.

Shahmuradov, I. A., Gammerman, A. J., Hancock, J. M., Bramley, P. M., and Solovyev, V. V. (2003). PlantProm: a database of plant promoter sequences. *Nucleic Acids Research* **31,** 114-117.

Shakya, R., and Sturm, A. (1998). Characterization of source- and sink-specific sucrose/H^+ symporters from carrot. *Plant Physiology* **118,** 1473-1480.

Sherson, S. M., Hemmann, G., Wallace, G., Forbes, S., Germain, V., Stadler, R., Bechtold, N., Sauer, N., and Smith, S. M. (2000). Monosaccharide/proton symporter *AtSTP1* plays a major role in uptake and response of *Arabidopsis* seeds and seedlings to sugars. *Plant Journal* **24,** 849-857.

Soar, C. J., Speirs, J., Maffei, S. M., and Loveys, B. R. (2004). Gradients in stomatal conductance, xylem sap ABA and bulk leaf ABA along canes of *Vitis vinifera* cv. Shiraz: molecular and physiological studies investigating their source. *Functional Plant Biology* **31,** 659-669.

Sohn, J., Voegele, R.T., Mendgen, K., and Hahn, M. (2000). High level activation of Vitamin B1 biosynthesis genes in haustoria of the rust fungus *Uromyces fabae*. *Molecular Plant-Microbe Interactions* **13,** 629-636.

Storr, T., and Hall, J. L. (1992). The effect of infection by *Erysiphe pisi* DC on acid and alkaline invertase activities and aspects of starch biochemistry in leaves of *Pisum sativum* L. *New Phytologist* **121,** 535-543.

Struck, C., Hahn, M., and Mendgen, K. (1996). Plasma membrane H^+-ATPase activity in spores, germ tubes, and haustoria of the rust fungus *Uromyces viciae-fabae*. *Fungal Genetics and Biology* **20,** 30-35.

Stummer, B. E., Francis, I. L., Zanker, T., Lattey, K. A., and Scott, E. S. (2005). Effects of powdery mildew on the sensory properties and composition of Chardonnay juice and wine when grape sugar ripeness is standardised. *Australian Journal of Grape and Wine Research* **11,** 66-76.

Sturm, A., and Chrispeels, M. J. (1990). cDNA cloning of carrot extracellular *β*-fructosidase and its expression in response to wounding and bacterial infection. *Plant Cell* **2,** 1107-1119.

Sutton, P. N., Henry, M. J., and Hall, J. L. (1999). Glucose, not sucrose, is transported from wheat to wheat powdery mildew. *Planta* **208,** 426-430.

Tang, G.-Q., Luscher, M., and Sturm, A. (1999). Antisense repression of vacuolar and cell wall invertase in transgenic carrot alters early plant development and sucrose partitioning. *Plant Cell* **11,** 177-189.

Tang, X., Rolfe, S. A., and Scholes, J. D. (1996). The effect of *Albugo candida* (white blister rust) on the photosynthetic and carbohydrate metabolism of leaves of *Arabidopsis thaliana*. *Plant Cell and Environment* **19,** 967-975.

Terrier, N., Glissant, D., Grimplet, J., Barrieu, F., Abbal, P., Couture, C., Ageorges, A., Atanassova, R., Léon, C. l., Renaudin, J.-P., Dédaldéchamp, F., Romieu, C., Delrot, S., and Hamdi, S. (2005). Isogene specific oligo arrays reveal multifaceted changes in gene expression during grape berry (*Vitis vinifera*) development. *Planta* **222,** 832-847.

Thompson J.D., Higgins, D.G., and Gibson, T.J. (1994). CLUSTAL W: improving the sensitivity of progressive multiple sequence alignment through sequence weighting, position-specific gap penalties and weight matrix choice. *Nucleic Acids Research* **22,** 4673-4680.

Toyofuku, K., Kasahara, M., and Yamaguchi, J. (2000). Characterization and expression of monosaccharide transporters (*OsMSTs*) in Rice. *Plant and Cell Physiology.* **41,** 940-947.

Tran, L.-S. P., Nakashima, K., Sakuma, Y., Simpson, S. D., Fujita, Y., Maruyama, K., Fujita, M., Seki, M., Shinozaki, K., and Yamaguchi-Shinozaki, K. (2004). Isolation and functional analysis of *Arabidopsis* stress-inducible NAC transcription factors that bind to a Drought-responsive cis-element in the early responsive to dehydration stress 1 promoter. *Plant Cell* **16,** 2481-2498.

Trouverie, J., Thevenot, C., Rocher, J.-P., Sotta, B., and Prioul, J.-L. (2003). The role of abscisic acid in the response of a specific vacuolar invertase to water stress in the adult maize leaf. *Journal of Experimental Botany* **54,** 2177-2186.

Truernit, E., Schmid, J., Epple, P., Illig, J., and Sauer, N. (1996). The sink-specific and stress-regulated *Arabadopsis STP4* gene: enhanced expression of a gene encodinga monosaccharide transporter by wounding, elicitors and pathogen challenge. *Plant Cell* **8,** 2169-2182.

Tsiamis, G., Mansfield, J. W., Hockenhull, R., Jackson, R. W., Sesma, A., Athanassopoulos, E., Bennett, M. A., Stevens, C., Vivian, A., Taylor, J. D., and Murillo, J. (2000). Cultivar-specific avirulence and virulence functions assigned to avrPphF in *Pseudomonas syringae* pv. phaseolicola, the cause of bean halo-blight disease. *EMBO Journal* **19,** 3204-3214.

Tsuba, M., Katagiri, C., Takeuchi, Y., Takada, Y., and Yamaoka, N. (2002). Chemical factors of the leaf surface involved in the morphogenesis of *Blumeria graminis. Physiological and Molecular Plant Pathology* **60,** 51-57.

Tymowska-Lalanne, Z. K., M. (1998). Expression of the *Arabadopsis thaliana* invertase gene family. *Planta* **207,** 259-265.

Vasil'ev, A. E. (1999). Primary and secondary plasmodesmata: Their frequencies in shoot apical meristem and leaf. *Izvestiya Akademii Nauk Seriya Biologicheskaya* **4,** 497-500.

Vasse, J., Billy, F., and Truchet, G. (1993). Abortion of infection during the *Rhizobium meliloti*-alfalfa symbiotic interaction is accompanied by a hypersensitive reaction. *Plant Journal* **4,** 555-566.

Vignault, C., Vachaud, M., Cakir, B., Glissant, D., Dedaldechamp, F., Buttner, M., Atanassova, R., Fleurat-Lessard, P., Lemoine, R., and Delrot, S. (2005). *VvHT1* encodes a monosaccharide transporter expressed in the conducting complex of the grape berry phloem. *Journal of Experimental Botony* **56,** 1409-1418.

Voegele, R. T., Hahn, M., Lohaus, G., Link, T., Heiser, I., and Mendgen, K. (2005). Possible roles for mannitol and mannitol dehydrogenase in the biotrophic plant pathogen *Uromyces fabae*. *Plant Physiology* **137,** 190-198.

Voegele, R. T., Struck, C., Hahn, M. and Mendgen, K. (2001). The role of haustoria in sugar supply during infection of broad bean by the rust fungus *Uromyces fabae*. *Proceedings of the National Academy of Sciences. U.S.A.* **98,** 8133-8138.

Vogel, J., and Somerville, S. (2000). Isolation and characterisation of powdery mildew-resistant *Arabidopsis* mutants. *Proceedings of the National Academy of Sciences. U.S.A.* **97,** 1897-1902.

Vogel, J. P., Raab, T. K., Schiff, C., and Somerville, S. C. (2002). *PMR6*, a pectate lyase-like gene required for powdery mildew susceptibility in *Arabidopsis*. *Plant Cell* **14,** 2095-2106.

Vogel, J. P., Raab, T. K., Somerville, C. R., and Somerville, S. C. (2004). Mutations in *PMR5* result in powdery mildew resistance and altered cell wall composition. *Plant Journal* **40,** 968-978.

Walters, D. R., and Wylie, M. A. (1986). Polyamines in discreet regions of barley leaves infected with the powdery mildew fungus, *Erysiphe graminis. Physiologia Plantarum* **67,** 630-633.

Wang, R., Hong, G., and Han, B. (2004). Transcript abundance of rml1, encoding a putative GT1-like factor in rice, is up-regulated by *Magnaporthe grisea* and down-regulated by light. *Gene* **324,** 105-115.

Waters, B. M., Blevins, D. G., and Eide, D. J. (2002). Characterisation of *FRO1*, a pea ferric-chelate reductase invovled in root iron acquisition. *Plant Physiology* **129,** 85-94.

Wei, Y. D., Zhang, Z.G., Anderson, C.H., Schmelzer, E., Gregersen, P.L., Collinge, D.B., Smedegarrd-Petersen, V., Thordal-Christensen, H., Wei, Y.D., and Zhang, Z.G. (1998). An epidermal/papillae-specific oxalate oxidase-like protein in the defence response of barley attacked by the powdery mildew fungus. *Plant Molecular Biology* **36,** 101-112.

Weig, A., Franz, J., Sauer, N., and Komor, E. (1994). Isolation of a family of cDNA clones from *Ricinus communis* L. with close homology to the hexose carriers. *Journal of Plant Physiologyy* **143,** 178-183.

Werner, M., Uehlein, N., Proksch, P., and Kaldenhoff, R. (2001). Characterisation of two tomato aquaporins and expression during the incompatible interaction of tomato with the plant parasite *Cuscuta reflexa*. *Planta* **213,** 550-555.

Wieczorke, R., Krampe, S., Weierstall, T., Freidel, K., Hollenberg, C. P., and Boles, E. (1999). Concurrent knock-out of at least 20 transporter genes is required to block uptake of hexoses in *Saccharomyces cerevisiae*. *FEBS Letters* **464,** 123-128.

Will, A., Caspari, T., and Tanner, W. (1994). KM Mutants of the *Chlorella* Monosaccharide/H^+ Cotransporter randomly generated by PCR. *Proceedings of the National Academy of Sciences. U.S.A.* **91,** 10163-10167.

Wirsel, S. G., Voegele, R. T., and Mengen, K. W. (2001). Differential regulation of gene expression in the obligate biotrphic interaction of *Uromyces fabae* with its host *Vicia faba*. *Molecular Plant-Microbe Interactions* **14,** 1319-1326.

Woods, A. M., and Gay, J.L. (1983). Evidence for a neckband deliminating structural and physiological regions of the host plasma membrane associated with haustoria of *Albugo candida. Physiological Plant Pathology* **23,** 73-88.

Wright, D. P., Baldwin, B. C., Shephard, M. C., and Scholes, J. D. (1995). Source-sink relationships in wheat leaves infected with powdery mildew. I. Alterations in carbohydrate metabolism. *Physiological and Molecular Plant Pathology* **47,** 237-253.

Zhang, L.-Y., Peng, Y.-B., Pelleschi-Travier, S., Fan, Y., Lu, Y.-F., Lu, Y.-M., Gao, X.-P., Shen, Y.-Y., Delrot, S., and Zhang, D.-P. (2004). Evidence for apoplasmic phloem unloading in developing Apple fruit. *Plant Physiology* **135,** 574-586.

Zhou, D. X., Li, Y. F., Rocipon, M., and Mache, R. (1992). Sequence-specific interaction between S1F, a spinach nuclear factor, and a negative cis-element conserved in plastid-related genes. *Journal of Biological Chemistry* **267,** 23515-23519.

Zhu, C., Schraut, D., Hartung, W., and Schaffner, A. R. (2005). Differential responses of maize *MIP* genes to salt stress and ABA. *Journal of Experimental Botony* **56,** 2971-2981.

Zhu, J. K. (2002). Salt and drought stress signal transduction in plants. *Annual Review of Plant Biology* **53,** 247-273.

Zimmerli, L., Stein, M., Lipka, V., Schulze-Lefert, P., and Somerville, S. (2004). Host and non-host pathogens elicit different jasmonate/ethylene responses in *Arabidopsis*. *Plant Journal* **40,** 633-646.

Appendix 1- sequences isolated during this project

Novel sequences amplified from powdery mildew infected leaf cDNA, using degenerate and subsequent RACE PCR, are listed below, along with promoter sequences isolated from a Cabernet Sauvignon BAC library. cDNA sequences are given first, followed by the predicted amino acid and promoter sequences. Putative start and stop codons are indicated in green and red type, respectively.

VvHT3 (Genbank accession number AY538259)

Full length cDNA

AAGGAGAAGAAGGTCTTAGTCATTTTCCTTGGTGTCTCAACTGTGTTGGGAGAGGAGGAAGAAGAGGA
ACTATGGAGGTGGGAGATGGGTCTTTTGCTCCTGTAGGTGTGTCCAAGCAGAGGGCAGACCAGTACAA
AGGCAGGCTCACTACTTATGTGGTCGTTGCTTGCCTTGTTGCTGCTGTTGGGGGTGCAATTTTCGGCT
ATGACATTGGGGTTTCAGGAGGCGTGACATCAATGGATACATTTCTTGAAAAATTCTTCCACACAGTC
TATTTAAAGAAGAGGCGGGCCGAAGAAGACCACTACTGCAAGTACAATGACCAAGGCCTTGCAGCATT
TACCTCTTCCCTCTACCTTGCTGGTTTGGTTGCGTCCATTGTGGCATCGCCTATTACAAGGAAGTATG
GGCGTCGAGCAAGTATAGTATGTGGTGGGATCAGCTTTCTTATTGGAGCTGCCCTAAATGCTGCAGCT
GTGAACTTGGCGATGCTTCTTTCGGGTCGGATCATGCTTGGTATTGGCATTGGATTTGGCGATCAGGC
AGTGCCACTATATTTGTCAGAGATGGCGCCGGCCCATCTCCGAGGAGCCCTGAACATGATGTTTCAGT
TAGCAACTACGACGGGGATCTTCACAGCAAACATGATCAATTACGGAACTGCAAAGCTCCCCTCATGG
GGATGGAGGCTGTCATTGGGCCTGGCTGCATTACCAACTATCTTAATGACAGTGGGAGGCCTATTTCT
TCCTGAGACTCCCAACAGTCTAATCGAACGGGGATCAAGGGAGAAAGGGAGACGAGTCCTAGAAAGAA
TCAGAGGTACCAACGAAGTTGATGCAGAGTTTGAAGACATTGTGGATGCTAGTGAGCCTGCAAACTCA
ATCAAGCATCCTTTCAGAAACATCCTTGAGAGAAGGAACAGGCCACAGCTGGTTATGGCAATCTGCAT
GCCAGCTTTCCAGATCCTCAACGGCATCAATTCTATTCTCTTCTATGCCCCAGTTCTGTTTCAGACCA
TGGGATTTGGAAATGCTACTCTCTACTCGTCCGCTTTGACAGGGGCCGTTCTTGTTTTATCCACAGTG
GTTTCAATCGGATTGGTGGATAGATTGGGTAGAAGAGTTTTATTGATTTCTGGGGGAATCCAAATGGT
CTTATGTCAGGTGACAGTTGCCATAATCCTGGGGGTCAAGTTCGGAAGCAATGACGAGCTCTCGAAAG
GCTACTCAGTATTGGTGGTGATTGTGATCTGCCTCTTTGTTATAGCATTCGGATGGTCGTGGGGGCCA
CTTGGGTGGACAGTTCCAAGTGAGATATTCCCACTGGAGACCCGATCAGCAGGACAGAGCATAACAGT
GGCTGTGAACCTCCTGTTCACCTTCATAATAGCTCAGTGTTTCCTTTCCATGCTTTGTTCTTTCAAGC
ATGGAATTTTCCTCTTTTTTGCTGGGTGGATTGTTATCATGACCCTCTTCGTATACTTCTTCCTACCT
GAAACAAAGGGAGTTCCCATTGAAGAAATGATATTCGTGTGGAAGAAGCATTGGTTCTGGAAGAGGAT
GGTGCCTGGGACTCCAGATGTTGACGACATCGACGGCCTGGGAAGCCATTCAATGGAGTCAGGTGAAA
AGACAAAGCTAGGCAGCTGAGCTTAATTCTTCCGATTTCGGTGAACTTCAAATAATCCATGTAGCATA
TGGCAAGCCAGGCTCCTATCATGAGCCAATAATTAGT

Predicted amino acid sequence

MEVGDGSFAPVGVSKQRADQYKGRLTTYVVVACLVAAVGGAIFGYDIGVSGGVTSMDTFLEKFFHTVY
LKKRRAEEDHYCKYNDQGLAAFTSSLYLAGLVASIVASPITRKYGRRASIVCGGISFLIGAALNAAAV
NLAMLLSGRIMLGIGIGFGDQAVPLYLSEMAPAHLRGALNMMFQLATTTGIFTANMINYGTAKLPSWG
WRLSLGLAALPTILMTVGGLFLPETPNSLIERGSREKGRRVLERIRGTNEVDAEFEDIVDASEPANSI
KHPFRNILERRNRPQLVMAICMPAFQILNGINSILFYAPVLFQTMGFGATLYSSALTGAVLVLSTVVS
IGLVDRLGRRVLLISGGIQMVLCQVTVAIILGVKFGSNDELSKGYSVLVVIVICLFVIAFGWSWGPLG
WTVPSEIFPLETRSAGQSITVAVNLLFTFIIAQCFLSMLCSFKHGIFLFFAGWIVIMTLFVYFFLPET
KGVPIEEMIFVWKKHWFWKRMVPGTPDVDDIDGLGSHSMESGEKTKLGS

Promoter

GATCTTCTCATACCCCCATTATAGCCACAAGATAAAATACCAAAATTTTCAAATACAATATCATCTCT
TTACCACTGCATTGGTGATGGGGCTGAGTGATGATAGTGAATTATTTGGCTTCAATGTAGAGAGTGGG
GCCTGATAAAAGGACTCTGTTTTTGTTTTTGATTTGGCACTGAATTATTTTATGTCTGGAAGATTCAT
TGGTGTTGATGGTGCACAGAGATGGTGACTCTCAACAAGTTGAGGAAAATTACAGCCAAGTACTATAA
AATATTCATACACCTTCATGCATTATATTTGGTTTGGTGACAAAGTCCTCTTGCCTTTCTTTATTAAA
CAAAAAGAGAAAATAAAAATGAAGATTTGGTTGTGGTTAAAATGAAATTATGGGGAGTTTTTCAAAGT
ATTGGTGTCATTCCACTGGGTGTATTTATGGAAGGGAGACTAAGCAAAGTCAATAATAATAAACTGTC
ACTGCGAAAAAAGGGTTGTCTCTGACNATTTCTGAGATGTTTTGGATTATAGGGGGGTGGGACTTNAG
TGTGATGAGCCCACCATCCATGACTACGGAGGAATGCAGACATAGCAGATAAGAAATGGAATCCAGAA
ACTGAAGCAAATCCCANATAAACTTCCAACAGGAAAGAACAAGCCAAGTGGGTGAAGAAAAGACAGAG
GGGGAAAAGCGTTGAAAGGCCCATTAACCTTTTTAAGGGTCTCTCTCTTTCTGTTTNTCTTCTTGCCT
TTTCAAGCGTCTCCAAAACCACCCAAAACCATTTTTTTTTAAATGGAAGTTTTTTCTTGGATGGTAAC
TTTCTTGGGTGCCAAAAACAGAGCAAGCCTTCCGATTGTTTTCATGGTAATTTAATCCCTTCCTTGAT
TTAAAGCAAGGATTTTTTTTCCTTAAATAATTGTTGTCCTGTATCAAATATTTTATCCATTTGTTGTC
GATGAAGACTGGTAACTGATTACGATAGGTCAGCCCCTCATTATTAAAAGCTAATACCATTGTTGATT
TTCTCTTCACTTCAGTTGAGAATTACAAAAACCTTGAGTGGGGAACCTCTCTGTTTCTCCTTGTAAAC
CGCCCTTGGATTGAATTCTCAAGGAGAAGAAGGTCTTAGTCATTTTCCAAGGTGTCTCAACTGTGTTG
GGAGAGGAGGAAGAAGAGGAACTATG

VvHT4 (Genbank accession number AY538260)

Full length cDNA

TCCTCTCTATCCTTTTCTCTCTTCAGAGCCATGGCAGTGGGAATTGCAGTAACAAGCCATGGTGGGCA
CTACAATGGAAGAATAACCCTATTTGTGGTTCTATCTTGTATGATGGCTGGCATGGGAGGAGTCATTT
TTGGATATGATATTGGAATTTCAGGCGGGGTGACCTCAATGGATTCATTTCTAAAGAAATTCTTCCCG
GAGGTGTACAAGAGGATGAAAGAAGACACCAAGATTAGCAACTACTGCAAATTTGACAGTCAATTGTT
GACCTCATTCACATCCTCCCTGTATATTGCTGGCCTTGTTGCTTCCTTTGTTGCTTCTTGGATCACTA
AAAAGTTCGGGCGCAAGCCAACCATCCTTGCTGGAGGGGCTGCCTTTCTCATCGGATCAGCACTAGGT
GGTGCCGCCTTCAATGTCTATATGGTTATATTAGGCCGGATTTTGCTTGGCGTTGGCGTTGGTTTTGC
AAACCAGGCAGTGCCACTTTACCTGTCCGAAATGGCTCCACCAAGATACAGAGGGGCAATCAACAATG
GCTTTCAATTCAGCATTGGCGTTGGGGCTCTATCAGCTAACCTTATTAACTTTGGCACTGAAAAAATC
AAAGGCGGTTGGGGCTGGCGAGTTTCTCTAGCATTGGCTGCAGTTCCGGCTTCAATCCTCACCCTAGG
GGCACTTTTTCTCCCAGAAACCCCCAATAGCTTAATCCAACGAAGCAAAGACTATGGAAAGGCTGAGC
TGATGTTGCAGCGTGTTCGAGGCACAAACGATGTCCAAGCAGAACTTGATGATCTGGTAAAAGCAAGC
TCCCTAGCAAAAACCATCAATGACCCGTTCAAGAAAATCTTGCAAAGGAAATATAGGCCTCAACTTGT
TATGGCAATCGCTATACCATTCTTTCAGCAAGTAACGGGAATCAATGTCATTGCATTTTATGCTCCCG
TACTTTTCCGGGCAATTGGATTAGGTGTGAGTGCATCCCTCCTGTCAGCAGTTGTGACCGGCGTAGTT
GGTATGGCCTCCACCTTCATCTCAATGCTCATAGTAGATAAACTCGGCCGAAGAGTTCTTTTCTTAGT
CGGGGGAATACAAATGCTGGTCTCACAAATTATGGTAGGAGGAATATTGGCAGCTGAGCTTGGTGATC
ATGGTGGGGTGAGCAAAGTGTACGCTTTTCTGGTTCTGCTTTTGATTTGTGTTTATGTCGCTGGGTTC
GGGTGGTCCTGGGGTCCATTGGGATGGTTGGTTCCAAGCGAGATTTTCCCACTCGAGATTCGATCAGC
TGGGCAAAGCATCACAGTGGCAGTCAGCTTTATCTTCACTTTCATTGTAGCTCAAACATTTTTATCTA
TGCTCTGCCATTTCAAGTCTGGGATTTTCTTCTTTTTTGGGGGTTGGGTGGTGTTGATGACTGCATTC
GTGTATTATTTGCTGCCAGAGACTAAGAGCATTCCCATTGAACAGATGGACAGAGTCTGGAAGGAGCA
TTGGTTTTGGAAGAGAATTGTGGTTGAAAAGCTCAGCAACCCTAAAATGGAGACAGCCTAAAGATTCA
ATACAAATCTCAACAGCATCCTCCTCTAAGGAAAAACTGTTAATGCATGCATTCATATACAGTTTCTA
AATTTAGTGGTTGCTAGACCTTAACTGCTTGTTTAGTTCTGTTGAGCCAAAGATCCAGAAGGCAGCCT
TTCATGCACTACAAGAATGAGCTAGCAGTCATAGAAACAATGATCGTAAATTGCCCGAAAAAAAAAAA
AAAAAAAAA

Predicted amino acid sequence

MAVGIAVTSHGGHYNGRITLFVVLSCMMAGMGGVIFGYDIGISGGVTSMDSFLKKFFPEVYKRMKEDT
KISNYCKFDSQLLTSFTSSLYIAGLVASFVASWITKKFGRKPTILAGGAAFLIGSALGGAAFNVYMVI

LGRILLGVGVGFANQAVPLYLSEMAPPRYRGAINNGFQFSIGVGALSANLINFGTEKIKGGWGWRVSL
ALAAVPASILTLGALFLPETPNSLIQRSKDYGKAELMLQRVRGTNDVQAELDDLVKASSLAKTINDPF
KKILQRKYRPQLVMAIAIPFFQQVTGINVIAFYAPVLFRAIGLGVSASLLSAVVTGVVGMASTFISML
IVDKLGRRVLFLVGGIQMLVSQIMVGGILAAELGDHGGVSKVYAFLVLLLICVYVAGFGWSWGPLGWL
VPSEIFPLEIRSAGQSITVAVSFIFTFIVAQTFLSMLCHFKSGIFFFFGGWVVLMTAFVYYLLPETKS
IPIEQMDRVWKEHWFWKRIVVEKLSNPKMETA

Promoter

TGGGATATTTGATGANATATTTTNTAATATAAGGAAAAATAAGGTGGAGAGAAGTAAAAAAATAANGT
CAAGAGAAGGATATTCGGGGAAANAAAAAAATTTATTTANTTANTTATTTTTNCTAATTNACANATTT
CTCTAAATAGTTGTTTTCATATTTCCTTAANTATAAATTGTTCTTTTTAATTAAAAAAATTAAAATAA
TTTTATATTCTAAACTTATTTTTAATTTATTACATATAAATATATATTATATAATATATAACAATAAT
AATAATAATAAAAATATGAAAACAAAAGTTCAAGAATGGGACAGATTAAGGTAATTTCTTTTTTTTTT
TTAAAAAAAAAATTACAAACTAACAATAAAGATTCTTCAAACTTTTACAAGTAGTATAGATTATTGTA
AAAGTTGATCATATAATGACAAAATCTCTTTTTTTTTTTTCTATTTAATTTTAGCAATGGTATAAATG
CGATTTTGTTTCCAAGATTCTATTGAATCACAAATTGGCCGTAACCTTATCATGACCCAATTTAAAGG
GCTTCTCTTTTTTATTTCCATTTTAAAAAATATTTAAGATCTCTTGCTGGTGAAAATTCAAAATTTGG
TCCAATAATTGAGCAAGAGTCAACAAGGATCCCTTCGTTTATTAAATATTCCTTTAACGAGAGATTCT
CTTTCTTTGTTCAGACTTCAGACGGAAGCAATTGATTGGTCCAGTTTGAATCTATCGTATTACGTGTC
TGATAGTGGAAGCCCATGATACTCTAAAGCTCCAACCCCAATGTTCACCTCCACATGCCCCATATAAC
TCCAAATTCACAGCAAAGTACGAAAAGTTTTTATTACTTTTTTATAGTGAACATGTCCTAGCATAGAC
GGCCATATTCACCAGTCAAGAAAGACTGCTTCTCTCTCATCTTCATTTTATCTTCCACTCTTTGTCAT
CATATCTGATTCCACAGGATTTCTCTCCTATCCTTTTCTCTCTTCAGAGCCATG

VvHT5 (Genbank accession number AY538261)

Full length cDNA

TTGAGGCCGAAGCGACATTGATAAGGTTTTTAGGAGTTTGTAGGTGGTGACATCATGCCTGCTGGAGG
ATTCGCGGCCCCGTCGGCCGGTGGCGACTTTGAAGCCAAGATCACTCCTATCGTTATCATTTCTTGCA
TCATGGCCGCCACCGGCGGCCTCATGTTCGGCTACGACGTTGGCGTTTCTGGGGGTGTGACGTCGATG
GACCCATTCTTGAAGAAATTTTTTCCGGTAGTATATAGGAAGCAGCATGAGGAGCTGGAGAGCAATTA
CTGCAAGTACGACAACCAAGGGCTACAGCTGTTCACGTCGTCTCTATATCTTGCGGGCTTGACCTCCA
CTTTCTTCGCATCATACACAACCAGAAGTTTTGGTCGTAAGGCAACCATGCTTATTGCTGGGATTTTC
TTCATTGTGGGAGTGGTGCTTAATACCGCTGCCCAAGATCTAGCTATGCTCATCATTGGGAGGATCCT
TTTGGGCTGTGGCGTCGGTTTCGCTAATCAGGCTGTTCCACTGTTCTTATCGGAGATAGCACCTACAA
GAATACGTGGAGGACTAAACATACTGTTCCAACTTAACGTCACTATTGGCATACTTTTTGCTAACCTC
GTCAATTACGGCACTGCCAAAATCAAAGGGGGATGGGGATGGAGGGTATCATTGGGGTTGGCTGGGAT
TCCTGCGGTCCTCCTAACTGTGGGGTCTCTCTTGGTGGTGGACACCCCTAACAGCCTTATCGAGCGTG
GTCGCTTGGAAGAAGGAAAGGCAGTTCTCAGAAAGATAAGGGGCACTGACAAGATTGAACCAGAATAT
CAGGAGCTTCTTGAGGCAAGTCGTGTGGCTAAATTAGTGAAGCACCCCTTTAGGAATCTAATGCAGCG
CAGAAACCGACCCCAGCTGATCATTGCTGTGGCCTTGCAGATCTTCCAGCAATTCACAGGCATCAATG
CAATCATGTTTTATGCTCCAGTCCTGTTCGACACTTTGGGATTTGGTAGTGATGCGTCCCTCTACTCA
GCTGTCATAACGGGGGCTGTTAATGTTCTCTCAACCCTCGTGTCCGTCTACTCTGTCGACAAAGTAGG
CCGTCGATTGCTCTTGCTGGAAGCTGGCGTCCAGATGTTCTTCTCTCAAGTGGTAATTGCAATCATAC
TAGGCATCAAAGTCAAAGATCACTCCAACAATCTCCACACTGGCTATGCAGTCCTAGTAGTGGTCTTG
GTGTGCACTTTTGTGGCCGGCTTTGCATGGTCTTGGGGGCCACTCGGTTGGCTCATTCCAAGTGAGAC
CTTCCCACTGGAGACCCGATCAGCAGGGCAGAGTGTGACTGTTTGTGTGAACCTGCTCTTCACTTTTG
TCATAGCACAGTCCTTCCTTTCCATGCTTTGCCATTTAAAGTATGGCATCTTCCTTTTCTTCTCCGGC
TGGGTCTTCATCATGTCCTTCTTTGTGCTCTTTTTGCTCCCGGAGACCAAAAACATTCCAATTGAGGA
AATGACAGAGAGGGTGTGGAAGAAGCATTGGTTGTGGAAGAGATTCATGGATGACCATGTGGAGGGCT
TCCCTGTTTTTGGTTATAATGATGAAGAAACTGTTGTTAATGGAAGTGACAAAAAGAGAGATGGGTAC
GGCAATGGATTCGATCCTTCTTCCCAATTATAAGATTAGTGGTGTATGGGGAGGGAAAGAAAAGACAT
CACTAGATAAATGAATAGCTAAAAATAGTTTGATATGCCCCTTGTTGCTTACCATTTGTTTTCACTAG
TTCTATGGTATTTGATACCTTACCCCTATATGATGAATCCCCCTGTATATGTGTTCTTGTGCCCATGT

CGGTCCATGTATGACTCAGAATTATGAAAAAAAATAAAGAGATTATTGGAATTCAAAAAAAAAAAAAA
AAAAA

Predicted amino acid sequence

MPAGGFAAPSAGGDFEAKITPIVIISCIMAATGGLMFGYDVGVSGGVTSMDPFLKKFFPVVYRKQHEE
LESNYCKYDNQGLQLFTSSLYLAGLTSTFFASYTTRSFGRKATMLIAGIFFIVGVVLNTAAQDLAMLI
IGRILLGCGVGFANQAVPLFLSEIAPTRIRGGLNILFQLNVTIGILFANLVNYGTAKIKGGWGWRVSL
GLAGIPAVLLTVGSLLVVDTPNSLIERGRLEEGKAVLRKIRGTDKIEPEYQELLEASRVAKLVKHPFR
NLMQRRNRPQLIIAVALQIFQQFTGINAIMFYAPVLFDTLGFGSDASLYSAVITGAVNVLSTLVSVYS
VDKVGRRLLLLEAGVQMFFSQVVIAIILGIKVKDHSNNLHTGYAVLVVVLVCTFVAGFAWSWGPLGWL
IPSETFPLETRSAGQSVTVCVNLLFTFVIAQSFLSMLCHLKYGIFLFFSGWVFIMSFFVLFLLPETKN
IPIEEMTERVWKKHWLWKRFMDDHVEGFPVFGYNDEETVVNGSDKKRDGYGNGFDPSSQL

Promoter

CATCTTGACCTTGGGTTAGGATTGTNGACGTGGATTAAGAGAGGTCGACTTCTCAATTTCTTCNCCTT
GGAGTGGGCCAAGGAGCAAGGGTTGACCCAAAATGGCTTCACAAAAAACCTACACAACTGTAGGCATG
GTGGGCTGAGGCCTAATCCCATTGTTTACATTTGATACGTGATGGAAAACTCTTAACCAATGTCGGAT
AAACTTACAAGATAACAAAATAACCACCACATCCTGGTGCCAATCAATTCCCAAGAAATAGGACACGA
GCAAAATATTGGATCAATATTCATTAAAAAAATGAAATGTTTTCCAATTTGTAAATTAATTCCCGTGG
TGTTTGTATTTGAAAAGTAATTAATTTTTAATACAGTTTTAAAATAGAAGATTATTGTTATAAGAAAA
AAAGTGAGAGTATTTTAATAAAAAAATTAATATTTTTTAAGCTATAAAATTGTGAAAATTAGATTGAT
AAATTAGGATTGTTTTATCTATTTTAGTTGAATGACCTTAAAATATTTTAAGGTTATGTTTGGTGTTA
GGAAAATATTAAGGAAAAAAAAAATTAAGGGTAGTTTGGCTTAAAAAAGATTTAAAGTTGTTAGAAAA
TTGTTTCCTTATAATTTTTTTTCTTTTTTTTAAAATATTTTCAGGAAACAAAGTATAATATAAGAAAA
ATTATTTTCTTGTATTTGATTGTATTATGAATAAAACTATGAAAGGAAATAAAAATAATTTATTAATT
TTAAATAATTTTTTTTTTTTAAATCTATCTATTTTTTCTGACATTTTTTTCTTCCAGATGCATAGCTG
CCGCCATTTATGATCGAAACCCAAGCTATCACGAGCCCATCTATGAACTCCTAGAAAGTGGAAAGTGG
AAAGTGGAAATTAAGATAAGGTGAAAGGAGTCGACTCAAATCTGTGGCTGCCGGAGTCCAACAACATT
GCTTTTCCTGTGAATGGCGAAAGGTTTTGGGCCAGTAGTACTCTTTTGATTTTCATCCTTATCCATTG
ACGACACGAACTTGGATTTTCCAAACCCTAAATCGAGAGAGTGGTGGTCAAAGTTGGTGTCCCCGATA
TTACAAGCCAACTCACGCCCACACGTTCGTATTGAATGATCTCGCCTCCTAAACCCTCGTTAATTTCT
TAAAAAAATCAAAGTGTTAATTCTCGATGCCATCAACTCTGACTTTGAGGTTGTAAAATACAAAAGCA
TGAGATTCCAAATATAAAGCATTTTTTTTACTAGGATATATACATAGCAGAAGGTCAATCTTTTGACG
TTGAATTTTCCACGGTTGTTGTGGGCCCCTGACTTTCCATGGCAGCCAGTTGATATGATCACATGATT
CAGACGAAAGGCAACAAAAGGTTTTGTTGTTGGATTCTATTCACTTATCAATTTTGCATTGATTTTTA
CTTTTTTTTTTTTTTTTTTTTTTTGTCCATAATTTTTGATGATTGGGTTTGGGTGGAGGAAATGATTT
ATGAGTAGACTAGGAGCATTAGAGGGGCTCCGATTCCGAGTATGGTGGAATTGGGAGTGAAAAGATGG
TCGTAGGCCCAATAATTATCTGCCCACGTCCATTTATGGCCGTCGTGAAATGCATGTTGCAAATGGTC
GTAGGCCCAATAATTATCTGCCCACATCCATTTATAGCCTTCGTGAAATGGATGTTGCAACCAAGCTC
ACTAAAATGATTTCTCATAATTATTTAAATAAATTATTTTTAAAAAAAATTGCAACATCATCAAATCC
CGTAAAATGACAATATTAAGATCTTCGAATCAACTTAAAGTATTCTTGTAACGATAATGATATATGAT
GGTTTTTTTTCTGAGAAAGTTATTTTTTATTTTTTATTTAAATAATAATAATAATAATAGAAGCGTGG
ACTTATACGGTATCAGAACAAAACTCAGTGAAAGTGGGAAAGTTGGCAAGTACTTTCTACTTGGTTTT
GATTACAATAACGAACCTGGAAATGCGCACGTGGCATTATTAGAAGAGGTACAATTGTACAAATAATC
ATCATCCATACACGCCTCTTTGGGTTATGTTCTTACGACGTGGCATTTGGTGAACCCCCTGGCACTGG
CGCACCCACCGTCCATGTTCCCATTTTGCTTCGGAAATGGGCCCCATTATGACGCGAAGGGGGAAAAA
ACGTTGGCTTGACTAAGCAGCCGTCGATGAAGAACATCGGGTTCATGGTTGCCACGTGGATATATCCT
GGTGGTCATCCTATTACATCATCCATTTCGTACTTCGTGCTCCTCTCCCTACTCTCCTCTATATATAC
ACTCGCTCCGGATGGTCTTTTTCCAACTCTCTCTGCCTAGTGTCTCTTCTTCTTCTTCTTCTTCTT
TCTGCTCTTTCTGCTGCTTGAGGCCGAAGCGACATTGATAAGGTTTTTAGGAGTTTGTAGGTGGTGAC
ATCATG

VvcwINV (Genbank accession number AY538262)

Full length cDNA

CACAAAGCCATCATGGCCACCTCTTCTCATGGCCTATTAGGGTTCTTCTTCTCTCGGTTCTTGGGCCA
TGGCTTTGTGCCCCTTGAAGCCTCCCCACCAAGTCTACATCCCACCTCCAAAATCAGTCTCCCCTCTT
CTTTAAAAACCCACCAGCCTTACAGAACTGGATATCATTTCCAGCCTCGCAAGAACTGGATGAATGAT
CCTAATGGGCCTATGATCTACAAGGGGCTCTACCATTTCTTCTATCAATACAATCCCCATGGTGCAGT
TTGGGGAAACATAGTGTGGGCACATTCCACATCAACCGATCTTGTCAACTGGACTCCTCATAAATATG
CCATTTCCCCATCCCAGCCAGCTGATATCAATGGCTGCTGGTCAGGTTCAGCAACCATCCTGCCAAAC
GGCAAGCCAGTGATTCTCTATACTGGTATCGATCCACAGAACAAGCAAGTTCAGAACATGGCTGTGCC
CAAAAATCTCTCTGACCCCTTCCTTCTAGAATGGACTAAGCTCTCTCAGAACCCTCTAATGGAACCTA
CTACCATCAACAGCATCAATGCTAGCTCATTCAGAGACCCTACGACTGCTTGGCAGGGCACTGATGGA
AGATGGAGGGTGATAATTGGAAGCAAAATAAAGCGAAAAGGATTAGCAATTTTGTATAGGAGCAAAGA
TTTTGTCCGCTGGACTAAAGCACAACACCCGTTACATTCAGGGAAGAATACTGGAATGTGGGAGTGTC
CAGACTTTTTTCCAGTATCTATCAACAGCTCTACGGGTGTAGATACATCATCGATAAGTAAAACCCTT
AAATATGTTCTTAAATTGAGCTTGGATGATACTAAGCATGACTACTACACGATTGGAAGCTACAACCG
TGAGAAGGATACCTATGTCCCAGATAAGGGGTCTGTGGATAATGACTCAGGCTTAAGATATGATTATG
GCAAGTTTTATGCTTCAAAAACCTTCTTTGACAACGCTAAGAACCGAAGAATCTTGTGGGGTTGGATC
AACGAATCATCTAGTGTGGAGCACGATATCGAGAAGGGATGGTCTGGAGTTCAGGCAATTCCAAGGAA
TGTTTGGCTGGACAAGTCTGGGAAACAGTTACTGCAATGGCCGATTGCAGAGATTGAAAAACAACGGA
TTAAACCGGGGCATATGTCTAGCAGAGAGCTGAAGGGAGGATCAAAGGTTGAAGTTGGTGGAATAACA
GCATCACAGGCAGATGTGGAGATATCGTTTAAGATATCAGACTTTAAGAAAGCAGAGGTTTTTGACGA
AAGCTGGAGTAATCCACAGCTGCTGTGCAGTCAAAGGGGTGCATCAGTAAAAGGTGGGCTAGGGCCAT
TTGGACTAATGGTGCTGGCTTCAAAGGGCATGGAAGAATACACAGCAGTTTTCTTTAGAATTTTCAAA
CGTCAGACCAAATATGTGGTGCTCATGTGCAGTGACCAAAGCAGGTCGTCTTTAGATAATGATAATGA
TAAGACCACGTATGGGGCATTTTTGGACGTGGATCCTGTCCATGAGAAGCTGTCACTAAGGAGTTTGA
TTGATCACTCAATAGTGGAGAGCTTTGGAGGAGGTGGAAAGGTTTGCATAACAGCTAGGGTTTATCCT
ACATTGGCTATTGACGGTGAAGCCCACTTGTATGCCTTCAACAAAGGAACTGGGAGTGTAGGGATGAC
AACACTGAGAGCTTGGAGCATGAAGAAAGCTAAAATCAATTGAAGGAAACAATCCTAGAGATGTATGT
AGAGTTGTGAGTGAAGAGCCAGGCTTTTGCAAATTTATCTTCTTCTATGGATTTGTACTAGAAGTCTG
CAGCAAATCCTCTTATGTAATTCATGTCAGTTTCTTTTGTTACCTAGCTGGAATCAATTCAAAGTTAG
TACAATATAAGAGAATAATTCCTGAAAAAAAAAA

Predicted amino acid sequence

MATSSHGLLGFFFSRFLGHGFVPLEASPPSLHPTSKISLPSSLKTHQPYRTGYHFQPRKNWMNDPNGP
MIYKGLYHFFYQYNPHGAVWGNIVWAHSTSTDLVNWTPHKYAISPSQPADINGCWSGSATILPNGKPV
ILYTGIDPQNKQVQNMAVPKNLSDPFLLEWTKLSQNPLMEPTTINSINASSFRDPTTAWQGTDGRWRV
IIGSKIKRKGLAILYRSKDFVRWTKAQHPLHSGKNTGMWECPDFFPVSINSSTGVDTSSISKTLKYVL
KLSLDDTKHDYYTIGSYNREKDTYVPDKGSVDNDSGLRYDYGKFYASKTFFDNAKNRRILWGWINESS
SVEHDIEKGWSGVQAIPRNVWLDKSGKQLLQWPIAEIEKQRIKPGHMSSRELKGGSKVEVGGITASQA
DVEISFKISDFKKAEVFDESWSNPQLLCSQRGASVKGGLGPFGLMVLASKGMEEYTAVFFRIFKRQTK
YVVLMCSDQSRSSLDNDNDKTTYGAFLDVDPVHEKLSLRSLIDHSIVESFGGGGKVCITARVYPTLAI
DGEAHLYAFNKGTGSVGMTTLRAWSMKKAKIN

Promoter

AAAANNATNNTGAGAANNCCCCCCNCCCCCTTCCCATTTGTCTCTCTCTCTCTCTCTCTCTCTCTCAT
CTTTTTGGGGGAGAAATCTCAAAGAGACTTTAGTCAAATTTAGAANTCAAATTAGTAATGGTTTTAAA
CAGGACAATTAAGTATTAGGTCAAAGGTATCCAGCCAATCTTTGAGTGTCCATAGTTAGGCTCATTAA
TGTGTTCATTTTTGACGATTAATTGATTCGACAAGTTAATTATTATATCCTCATTAGGGGTTTCAATT
TTCCATATAAATGGTAATCGACATATAACTTTTCATACAATCAAAATTGTATCTATCTTATTTGTCCA
ATACAATTAATGTTTGCATCAAAAGCATTTCTTGACTAATTGTAGATTTTTTTTTTAAAGTCAACAAA
GTTCAAATTTAAATTTTTACGTATTTTCTTAATAAAACTATCATTCTTATAAGATTAGTTTATATTTG
TTGATATCAATATATTCAAAACTGACAAATTTTCCAAGATTCCTCTGTTTCATTCTTTATTTTTTTTT
TCTTCTTATTGTTCAATATGTCATTTTTAGGCATTTTTTTCTTTTTACTTTTATTTCTCGGATCTCTA
ATGAATTAGAGATAAAAATCATATAACACAATGTTAAGATTCCTTATCCATGAATAGAAATAACCCAC

TTGGATTTTGAAATTTAATATCGACAAAACATAATAAATTAAAAAATTATAATCTACATATTAATTTC
TATAAGTAGATTTATTTAAAATCCCATTGCAAATTAAATATTAATTATAAATTGGCCACATCTTATCA
CATGATTCACATGGCACACTTGCAGTCTTTATTTCTAATAAGTAATTATTATAGATGTTTAATTTGCT
ATCATATCAAAATTTTTGTTTGACTCATTTAAAGCATTCAAAAATGAAATTATGACACTAATAAAAGA
GATAAGAAATATAAGATCATAAGACATCAATGCAAAGGAACAGTACCTTATCTATATCTGAGTGGATT
TTCTTTCCATATGATATGGAAAAGGAGCTTTTTGGCCAATCCCAAAATCAACTTTTATTTATTTTATT
ATTATTATTAAAATAAAATTTAGCTAAAGAAAAGGAACCACATGGCCATTGGGGGTGGTCCAAGGGAA
GTTGCCTACACACTTCCCCCGCCTTTTTCTTTGTCTTTTCTAAATATTCAACCATCCCCATATATTGA
CTTCCATTGATACAGAACCCCTCGAATTTTCTATGGCACTTCTCCTCTCCAAAAACACTTTTTTTCCT
GATTTTTTGTGGGGAAAAGAAATAATAAAAAAATGAAAGTAAAAAACCTCATTGGTGACTTTTCCCAT
CACCCAAAATCCTTCACTATAAATAGGACACTCTGGCCTAAGGCTCTCTCCTCATTCCCACAAAGCCA
TCATG

ProT degenerate clone (not submitted to Genbank)

Partial cDNA

TACTCCGGTACCATTATGGTGCCCCTTGGTTGGGCTGGTGGTGTGATTGGTTTTCTTTTAGCCGCAGG
AATATCACTTTATGCAAATTCTCTCGTTGCCAAGCTCCATGAATTTGGTGGAAAGAGACATATTAGAT
ACAGAGATCTTGCAGGATATATATATGGTAAGAAAGCATATACTCTGACTTGGGCTTTGCAATATGTA
AATCTTTTCATGATTAATACTGGATATCTCATTTTGGCAGGTCAGGCTCTGAAGGCTGTCTATGTTCT
TTTTAGGGATGATGGTGGCATGAAGCTCCCATACTTTATTGCGATTGGAGGCTTTGTATGTGCCATCT
TCGCCATAGGAATCCCACACTTGTCAGCTCTAGGGATTTGGCTGGGTTTTTCGACATGCTTGAGTCTA
ATATATATTGTTACAGCATTTGTGCTGTCACTTACAGATGGAATTAAAGCTCCATCTAGGGATTACAG
CATCCCAGGAACAGAAGCAAGCAAGGTCTTCAGTATTATAGGGGCAGCTGCTAATCTTGTTTTTGCAT
TCAACACAGGAATGCTTCCTGAGATACAGGCAACTATTAGACAACCTGTGGTTAAGAATATGATGAAA
GCTCTCTACTTCCAATTTACTGCTGGAATTCTACCACTGTATGCTGTTGTTTTTATGGGGTATTGGGC
TTATGGATCAACAACATCAACCTATTTGCTCAATAGTGTCTCTGGTCCAGTTTGGGGTTAAGACAATG
GCAAATCTTGCTGCCTTCCTGCNAACGGTTATTGCTTTGCATATATTCGCTTCCCCA

Predicted amino acid sequence

YSGTIMVPLGWAGGVIGFLLAAGISLYANSLVAKLHEFGGKRHIRYRDLAGYIYGKKAYTLTWALQYV
NLFMINTGYLILAGQALKAVYVLFRDDGGMKLPYFIAIGGFVCAIFAIGIPHLSALGIWLGFSTCLSL
IYIVTAFVLSLTDGIKAPSRDYSIPGTEASKVFSIIGAAANLVFAFNTGMLPEIQATIRQPVVKNMMK
ALYFQFTAGILPLYAVVFMGYWAYGSTTSTYLLNSVSGPVWG*DNGKSCCLPANGYCFAYIRFP

AAP degenerate clone (not submitted to Genbank)

Partial cDNA

GTTACCGGAAAGAGGAACTATACTTATATGGATGTTGTGAGAGCCAACTTAGGAGGTATGAAGGTTCA
GCTGTGTGGGATCGCTCAATATGGAAATCTCATAGGGGTCACGATCGGATACACAATCACGGCTTCTA
TCAGTATGGTTGCCGTACGACGGTCAAACTGTTACCACAAGCACGGCCATCAGGCGAAGTGCAACCCG
TCAGACTACCCTCACATGATCATCTTCGCTTGCATCCAGATCGTTCTGAGCCAAATACCAAACTTTCA
CAAGCTGTCATGGCTCTCTATTCTCGCAGCTGTCATGTCTTTCAGTTATGCCTCTATAGGCATCGGAC
TCTCCATTGCCAGGGTTGCAGGAGGGGCGCATGCAAGGACAACGTTAACAGGAAGGACAGTTGGAGTG
GACTTGTCAAGCTCAGAGAAGGTTTGGAGAACCTTCGAGTCCATCGGAAATATTGCTTTTGCTTACGC
ATACTCCACCGTCCTCGTC

Predicted amino acid sequence

```
VTGKRNYTYMDVVRANLGGMKVQLCGIAQYGNLIGVTIGYTITASISMVAVRRSNCYHKHGHQAKCNP
SDYPHMIIFACIQIVLSQIPNFHKLSWLSILAAVMSFSYASIGIGLSIARVAGGAHARTTLTGRTVGV
DLSSSEKVWRTFESIGNIAFAYAYSTVLV
```

Appendix 2- Expression of control genes

In Chapters 5, 6 and 7, quantitative RT-PCR was used to measure expression of sugar transport and invertase genes in a range of tissues. To normalise expression between samples, actin and ubiquitin expression was used. The level of actin expression was found to be more stable than ubiquitin in pathogen infected and wounded samples and was the reference gene used in these comparisons, however in the grape developmental series ubiquitin was more stable than actin and was used to normalise these samples. In the following Figures, the "cycling threshold" (CT) of the reference genes is shown. The CT is the cycle number at which the maximal rate of product amplification was observed and therefore, a low CT value represents a highly expressed gene and a high CT value indicates a gene expressed at a low level. In summary, the standard deviation across the samples compared was between 0.1 and 0.66, indicating that expression of the selected reference genes was relatively stable and differed by significantly less than a factor of 2 (ie. a CT difference of 1 would indicate 1 PCR cycle difference which in the exponential phase of amplification is one doubling of PCR product or a two-fold increase).

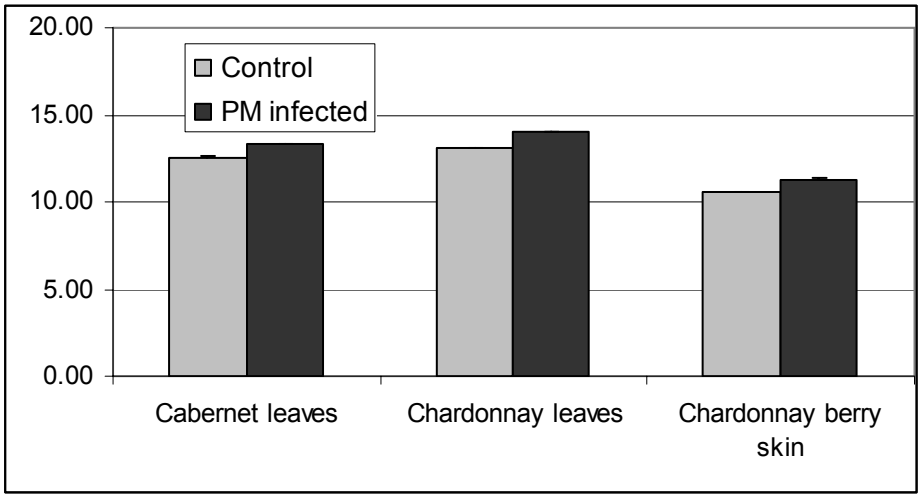


Figure A2.1. Actin expression in control and powdery mildew infected Cabernet Sauvignon and Chardonnay leaves, and Chardonnay berry skins. The standard deviations of the CTs compared was: Cabernet Sauvignon leaves: 0.556, Chardonnay leaves: 0.641, Chardonnay berry skin: 0.542.

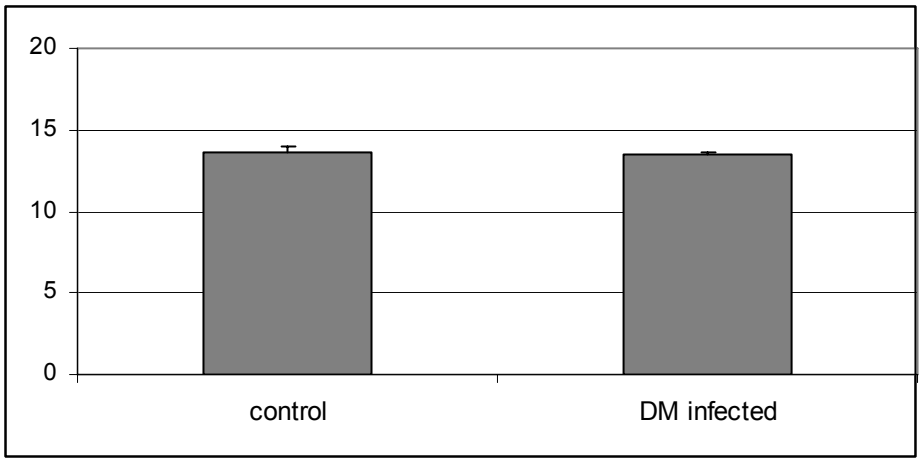


Figure A2.2. Actin expression in healthy control and downy mildew infected Cabernet Sauvignon leaves. The standard deviation of the CTs compared was 0.113.

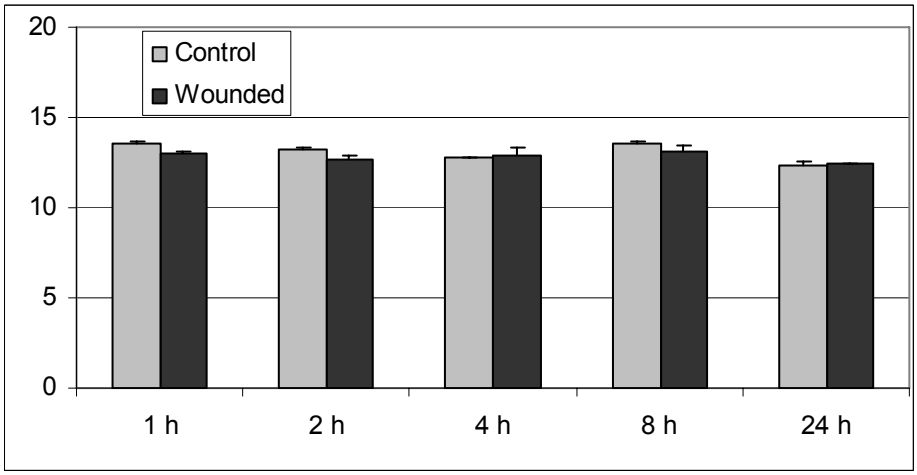


Figure A2.3. Actin expression in healthy control and wounded Cabernet Sauvignon leaves. The standard deviation of the CTs compared was 0.423.

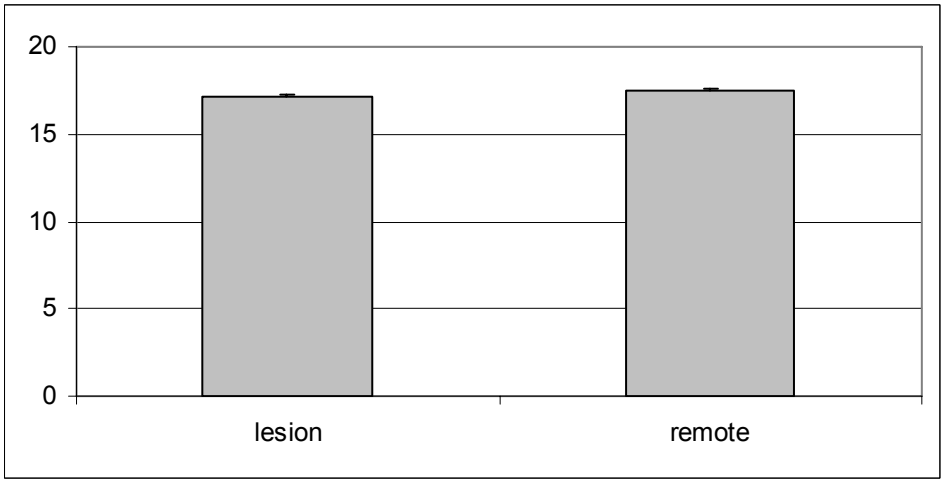


Figure A2.4. Actin expression in discreet powdery mildew infected regions and non-infected areas of the same leaves. The standard deviation of the CTs compared was 0.213.

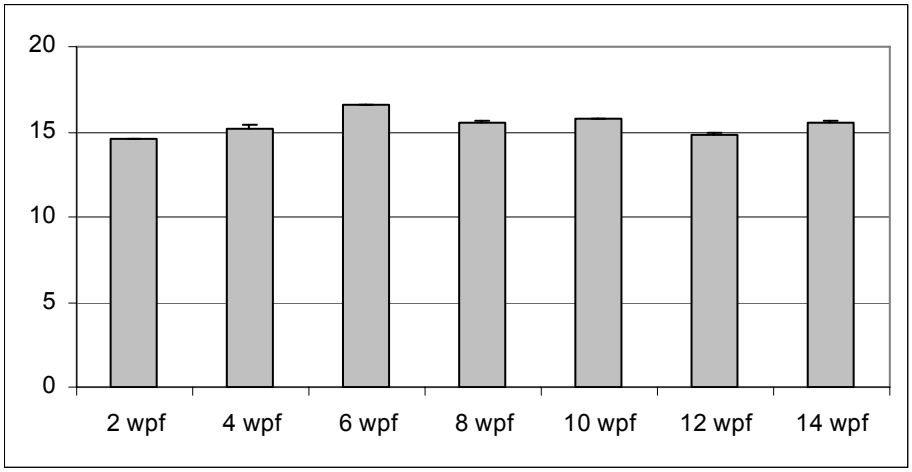


Figure A2.5. Ubiquitin expression in ripening Cabernet Sauvignon berry pulp cells. The standard deviation of the CTs compared was 0.647.

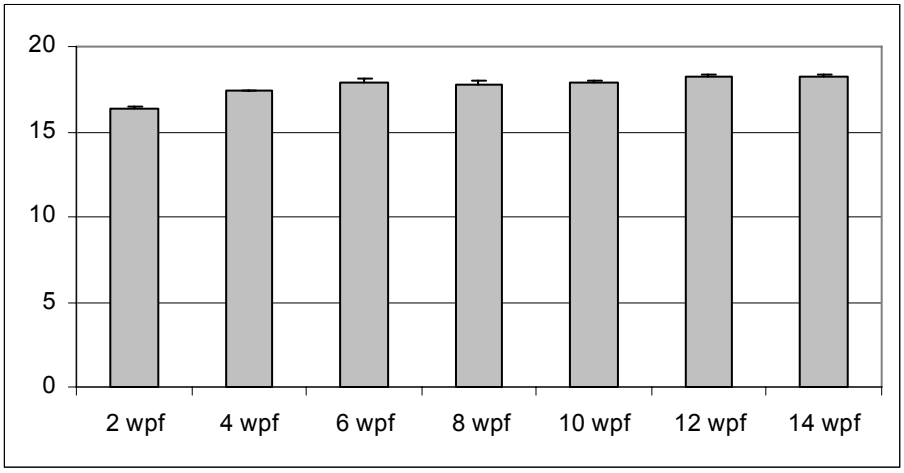


Figure A2.6. Ubiquitin expression in ripening Shiraz berry pulp cells. The standard deviation of the CTs compared was 0.652.

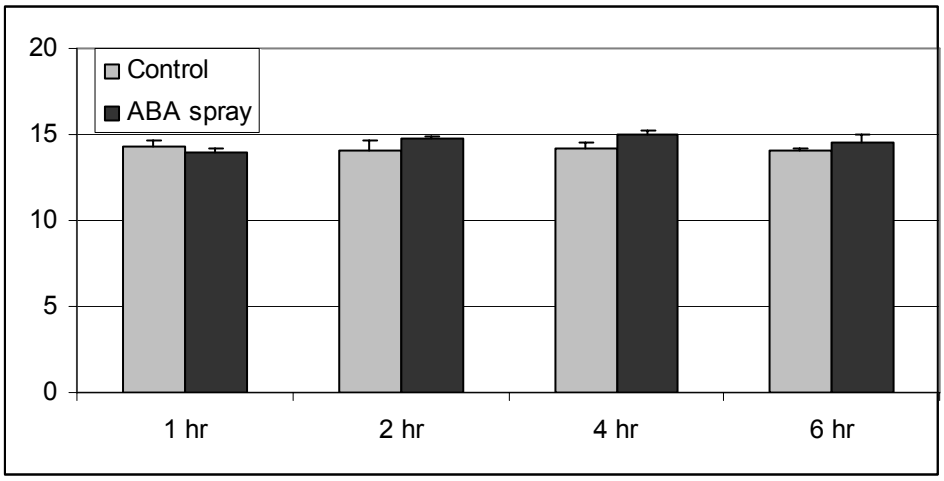


Figure A2.7. Actin expression control and ABA-sparyed leaves. The standard deviation of the CTs compared was 0.471.

Appendix 3- List of cDNAs on grape berry Microarray

Appendix 1: Communication

Scientific Publications

Hayes MA, Davies C. and Dry IB. (200_) Hexose transporters and invertases from grapevine: isolation, functional characterisation and expression analysis during leaf and berry development: role in sink/source relations. *Plant Physiology*, in preparation

Hayes MA. and Dry IB. (200_) Grapevine hexose transporter and invertase genes are regulated by biotic and abiotic stress stimuli, and abscisic acid. *Plant Physiology*, in preparation

Conference Presentations

Hayes MA. and Dry IB. Grapevine powdery mildew: modulation of host gene expression by a biotrophic pathogen. Talk presented at 7th International Symposium on Grapevine Physiology & Biotechnology, Davis, California, June 21-25, 2004.

Hayes MA. and Dry IB. Grapevine powdery mildew: modulation of host gene expression by a biotrophic pathogen. Poster presented 13th International Workshop on Plant Membrane Biology, Montpellier, France, July 6-10, 2004.

Hayes MA., Davies C. and Dry IB. Expression analysis of sugar transporters and invertases during grape berry ripening. Poster presented at 13th International Workshop on Plant Membrane Biology, Montpellier, France, July 6-10, 2004.

Hayes MA, Tyerman SD. and Dry IB. Identification of host genes involved in the biotrophic interaction between grapevine and powdery mildew. Poster presentation at COMBIO, Adelaide, 25-29 September, 2005.

Industry Journal articles

Brochures/Technical Guides

Appendix 2: Intellectual Property

None identified

Appendix 3: References

See thesis

Appendix 4: Staff

Project Staff

Dr Ian Dry	CSIRO Plant Industry, Adelaide.
Matthew Hayes (PhD student)	CSIRO Plant Industry, Adelaide & Dept Horticulture, Viticulture and Oenology, University of Adelaide

Appendix 5:

Appendix 6: Budget reconciliation